UDC 502/504; 57; 63

SCIENTIFIC REPORTS OF THE NATIONAL UNIVERSITY OF LIFE AND ENVIRONMENTAL SCIENCES OF UKRAINE

Founder:
National University of Life and Environmental Sciences of Ukraine

Year of foundation: 2005

Recommended for printing and distribution
via the Internet by the Academic Council
of National University of Life and Environmental Sciences of Ukraine
(Minutes No. 2 of September 23, 2025)

State Registration:
Media identifier - R40-02082.
Decision of the National Council of Television and Radio Broadcasting of Ukraine
No. 1471, Minutes No. 28, dated 23.11.2023.

The journal is included in the list
of Professional Scientific Publications of Ukraine
Category "B". Specialties: 0511 – Biology, 0521 – Environmental Sciences, 0522 – Natural Environments and Wildlife, 0512 – Biochemistry, 0811 – Crop and Livestock Production, 0821 – Forestry, 0812 – Horticulture, 0841 – Veterinary
(Order of the Ministry of Education and Science of Ukraine No. 409 of 14 March 2020),
0715 – Mechanics and Metal Trades, 0716 – Motor Vehicles, Ships and Aircraft
(Order of the Ministry of Education and Science of Ukraine No. 886 of 02 July 2020).

The journal is presented international scientometric databases, repositories and scientific systems:
Google Scholar, Vernadsky National Library of Ukraine, BASE, AGRIS, Ulrichsweb, ERIH PLUS, Dimensions, University of Oslo Library, OUCI (Open Ukrainian Citation Index), Polska Bibliografia Naukowa, DOAJ, CABI, Litmaps, EBSCO, J-Gate, Research4Life

Editors office address:
National University of Life and Environmental Sciences of Ukraine
03041, 15 Heroiv Oborony Str., Kyiv, Ukraine
E-mail: sr@scireports.com.ua
https://scireports.com.ua/en

УДК 502/504; 57; 63

НАУКОВІ ДОПОВІДІ НАЦІОНАЛЬНОГО УНІВЕРСИТЕТУ БІОРЕСУРСІВ І ПРИРОДОКОРИСТУВАННЯ УКРАЇНИ

Засновник:
Національний університет біоресурсів і природокористування України

Рік заснування: 2005

Рекомендовано до друку та поширення
через мережу Інтернет Вченою радою
Національного університету біоресурсів і природокористування України
(протокол № 2 від 23 вересня 2025 р.)

Державна реєстрація:
Ідентифікатор медіа – R40-02082.
Рішення Національної Ради України з питань телебачення і радіомовлення
№ 1471, протокол № 28 від 23.11.2023 р.

Журнал входить до переліку
наукових фахових видань України
Категорія «Б». Спеціальності: 091 – Біологія, 101 – Екологія, 162 – Біотехнології та біоінженерія, 201 – Агрономія, 204 – Технологія виробництва і переробки продукції тваринництва, 205 – Лісове господарство, 206 – Садово-паркове господарство, 211 – Ветеринарна медицина, 212 – Ветеринарна гігієна, санітарія і експертиза (наказ МОН України № 409 від 14 березня 2020 року),
131 – Прикладна механіка, 133 – Галузеве машинобудування (наказ МОН України № 886 від 02 липня 2020 року).

Журнал представлено у міжнародних наукометричних базах даних, репозитаріях та пошукових системах:
Google Scholar, Національна бібліотека України імені В. І. Вернадського, BASE, AGRIS, Ulrichsweb, ERIH PLUS, Dimensions, University of Oslo Library, OUCI (Open Ukrainian Citation Index), Polska Bibliografia Naukowa, DOAJ, CABI, Litmaps, EBSCO, J-Gate, Research4Life

Адреса редакції:
Національний університет біоресурсів і природокористування України
03041, вул. Героїв Оборони, 15, м. Київ, Україна
E-mail: sr@scireports.com.ua
https://scireports.com.ua/uk

Редакційна колегія

Editorial Board

Contents

Зміст

Received 24.04.2025 Revised 25.07.2025 Accepted 23.09.2025

Vol. 21, No. 5
2025

Scientific Reports of the National University of Life and Environmental Sciences of Ukraine

Journal homepage: https://scireports.com.ua/en

UDC 631.81:631.4]:630.114(477.84) Doi: 10.31548/dopovidi/5.2025.09

Nutrient content in grey forest soils of Husiatyn Forestry

Dmytro Yarosh*
Postgraduate Student
Uman National University
20300, 1 Instytutska Str., Uman, Ukraine
https://orcid.org/0009-0001-8322-600X

Mykhailo Yarosh
Postgraduate Student
Uman National University
20300, 1 Instytutska Str., Uman, Ukraine
https://orcid.org/0009-0003-1845-1686

Abstract. The purpose of the study was to determine the physical and chemical features of various types of forest soils and assess their agrochemical state on permanent nurseries, arable land, and 30-year-old common oak crops in the conditions of the Husiatyn Forestry of the Chortkiv Forest District. Soil and agrochemical analysis methods were applied, including determination of fractional and mechanical composition, humus content, base saturation, and absorption complex capacity. The indicators were compared between light grey, grey-loamy, and gleyed soils, which allowed characterising their productivity and agrochemical potential. It was found that in most soils, the upper horizons were acidic (pH 3.6-5.0), which negatively affects the availability of nutrients, and in light grey soils, the humus content was low (0.5-1.2% in the upper horizons). In grey loamy and gleyed soils, there is more humus (1.2-2.0%), especially in arable variants (1.8-2.0%). The total nitrogen in the upper horizons was 0.1-0.18%, which is rather low. The C:N ratio was close to 8, which indicates rapid mineralisation of organic matter. Some areas were well provided with P_2O_5 (20 mg/100 g), but there were soils with a deficit (<10). Potassium supply was more stable, but depletion was possible in arable horizons. Phosphorus (P_2O_5): ranged from very low values (3.75-10 mg/100 g) to elevated values (20 mg/100 g in arable land). Potassium (K_2O): was at the level of 10-14 mg/100 g, but in some cases decreased to 5-6 mg/100 g (deterioration of supply). Hydrolysed nitrogen: values of 3.6-11.5 mg/100 g, which indicated an average or low nitrogen supply. The results of the study of the fractional and mechanical composition of soil in oak forests, using the example of the Husiatyn Forestry, are of considerable

Suggested Citation:

Yarosh, D., & Yarosh, M. (2025). Nutrient content in grey forest soils of Husiatyn Forestry. *Scientific Reports of the National University of Life and Environmental Sciences of Ukraine*, 21(5), 9-27. doi: 10.31548/dopovidi/5.2025.09.

*Corresponding author

practical importance for the development of recommendations regarding the specifics of planting forest crops in this region and protecting the soil from erosion processes

Keywords: genetic horizons; fractions; humidity; capacity; nutrients

Introduction

The establishment of formal links between the natural environment and soil properties indicates the dynamism of a number of soil indicators: acidity, density, humus content, and metabolic substances. Quantitative indicators of the distribution of trace elements in the soil of artificial origin show their similarity to natural plantings. For example, the high concentration of titanium and the nature of its distribution in the soil and bedding of natural forests correspond to artificial plantings. This is conditioned by the influence of soil formation, which is widely represented by heavy loess-like loams and clays (Panas, 2019).

A number of Ukrainian and foreign researchers have studied the content of nutrients in grey forest soils in different years and in different regions. O. Dmitrenko *et al*. (2021) investigated nitrogen content in grey forest soils. The researchers analysed the dynamics of mineral nitrogen content depending on the use of organic, mineral and combined fertilisers. They also evaluated the effectiveness of land reclamation agents in increasing soil fertility. The results obtained allowed optimising the fertiliser system to increase the productivity of agrocoenoses. S. Ryazanov *et al*. (2025) emphasised the importance of investigating fluctuations in nutrient content and their impact on fertility. After analysing the content of macro- and microelements in the soil depending on plant species and growing conditions, the researchers paid special attention to the influence of energy crops on soil fertility and their ecological state. The data obtained were important for the rational use of land and the development of bioenergy. A. Pavlichenko *et al*. (2023) investigated fluctuations in humus content in grey forest soils, depending on the intensity of anthropogenic load on them. They carefully analysed changes in the content of humus and its fractions depending on the intensity of agricultural use. It was shown how different agricultural systems affected the quality and stability of organic matter. The results of these studies emphasised the importance of rational management of soil resources to preserve their fertility.

F. Brovko *et al*. (2023) determined the ratio of quantitative and relative indicators that significantly affect the physical properties of grey forest soils, and also found changes in compacted soil during natural recovery. Investigating changes in the density, porosity, and water permeability of the soil under the influence of prolonged recreational load, the researchers found that intensive trampling worsens the structural state and water regime of soils. And this is important for assessing the ecological sustainability of forest ecosystems and planning their rational use. L. Jinglei *et al*. (2025) studied the effect of slope steepness on the degree of drying of grey forest soils and on the sensitivity of young trees to drought along altitude gradients in temperate artificial forests. The researchers found that trees react differently to moisture deficiency on slopes of different exposures, but the speed of their recovery after a drought did not depend on the slope. The study emphasised the importance of topography as a factor determining the resistance of young plantings to climatic stresses. As a result of their research, the dependence on steepness and sensitivity to moisture was revealed, which was important for improving forestry practices in the face of climate change.

Investigating the influence of anthropogenic load of grey forest soils on their water content and the morphology and water-physical parameters of sections of light grey forest soils in the

zones of anthropogenic trampling of the island, O. Brovko *et al*. (2025) established how changes in rock composition and humidity affect the distribution of root mass in the profile, and its moisture capacity, water permeability, and aeration. Studies have shown that under the influence of recreational stress, conditions for the development of woody plant roots worsen. The results obtained are important for assessing the ecological state of forest ecosystems and planning measures for their restoration. O. Kovalyova *et al*. (2021) found changes in the thickness of the humus horizon in grey forest soils depending on landscape and morphological conditions. The researchers revealed a pattern of fluctuations in the thickness of the humus profile of grey forest and chernozem soils depending on the duration of their agricultural use. As a result, it was found that the intensity and duration of agricultural use cause a decrease in humus reserves and deterioration of soil structural properties, which is important for assessing degradation processes and preserving the fertility of arable land.

However, no studies were found on the content of nutrients in soils and the impact on the composition and productivity of plantings in the conditions of the Ternopil Oblast. Therefore, the purpose of the study was to investigate and compare the physical and chemical features of different types of forest soils, their fractional and mechanical composition on permanent two nurseries, arable lands, and 30-year-old oak crops.

Scientific originality of the results obtained – for the first time in the conditions of the Husiatyn Forestry – consisted in a mechanical and physico-chemical analysis of the most common soil types. The conducted studies were particularly relevant for understanding the development of the root system of tree stands.

Materials and Methods

The object of study was the physical and chemical composition of soils in soil sections of permanent nurseries, arable lands, and 30-year-old common oak crops in the Husiatyn Forestry of the Chortkiv Forest District. This forestry was located in the southern part of Western Podillia,at the junction between the Ternopil Plateau geomorphological zone in the north and the Dniester Canyon in the south. The type of forest conditions was wet oak forest. Forests in the study region were represented by both pure deciduous stands and mixed and pure coniferous stands, which include such main tree species as common oak (*Quercus robur* L.) and sessile oak (*Quercus petraea* (Matt.) Liebl.), European ash (*Fraxinus excelsior* L, Norway maple (*Acer platanoides* L.), and field maple (*Acer campestre* L.), common hornbeam (*Carpinus betulus* L.), small-leaved linden (*Tilia cordata* Mill.), field elm (*Ulmus minor* Mill.), Scots pine (*Pinus sylvestris* L.), European spruce (*Picea abies*), European larch *(Larix decidua* L.), silver birch *(Betula pendula* Roth), common aspen (*Populus tremula* L.), and a number of other trees. The plantings of natural origin contained: field elm (*Ulmus laevis* Mill.), wild cherry (*Cerasus avium* L.), common pear (*Pyrus communis* L.), European wild apple (*Malus sylvestris* Mill. Common shrubs included common hawthorn (*Crataegus monogyna* Jacq.), common hazel *(Corylus avellana* L.), common dogwood (*Cornus sanguinea* L.), European spindle (*Euonymus europaeus* L.) and warty spindle (*Euonymus verrucosus* L.), wayfaring tree (*Viburnum lantana* L.) (Hamkalo, 2009). The research region was located in a humid continental climate with warm summers and mild winters. The average annual temperature ranged from +7-8°C. The air temperature was -4.5°C in January and +19°C in July.

Samples for research were taken in the spring-summer period of 2025. Subject of research – methods and tools for assessing the features of the distribution of physico-chemical indicators over the soil horizons of the most common types of forest soils, which would allow improving the agrotechnological processes of growing planting material on them in the Husiatyn Forestry of the Chortkiv Forest District. From four soil sections, 60 soil samples were selected for laboratory analysis, at the following depths (cm):

1. Light grey forest clay-loamy soil – HA: 0-26; Iha: 30-40; P:115-125; Pk: 150-160.

2. Grey forest loamy soil (permanent nursery) – HA: 0-28; Iha: 35-45; I: 65-75; P: 115-120; Pk: 142-152.

3. Grey forest clay-loamy soil (permanent nursery) – HA: 0-26; Iha: 30-40; I: 65-75; P: 115-125; Pk: 150-160.

4. Grey forest clay-loamy soil (arable land) – HA: 2-26; Iha: 34-45; I: 65-75; P: 125-130.

The boundaries of genetic horizons were determined by the change in colour from light grey to dark grey or brown, depending on the humus content and redistribution of iron compounds. As well as the structure that changed from lumpy in the upper horizons to denser or powdery in the deeper layers. Soil sampling was carried out with special knives in sealed bags labelled with the place of collection and the soil horizon from which the sample was taken.

Determination of the physical, chemical and mechanical properties of soils was carried out in the soil and chemical laboratory of Uman National University using the methods described in the soil science workshop (Tyhonenko, 2005). The mechanical composition of soils and the classification of loamy varieties were determined by the method of M. A. Kaczynski. The content of hygroscopic moisture was determined by drying at a temperature of 105°C. The acidity of soil solutions (pH in water and salt extracts) was measured using a pH meter. The sum of exchange bases and hydrolytic acidity were determined by the method of G. Cappen-Gilkowitz. The humus content was estimated by the method of I.V. Tyurin. Determination of mobile phosphorus (P_2O_5) were performed according to the method of A.G. Kirsanov in non-carbonate samples and according to the method of V.P. Machigin in carbonate samples. Mobile potassium (K_2O) was determined by the method of Ya.V. Peive and O.A. Brovkin in non-carbonate samples and according to the method of P.V. Protasov in carbonate samples. Total nitrogen was determined by the method of I.V. Tyurin and M.M. Kononova or method of Kjeldahl, and hydrolysed nitrogen – according to the method of Tyurin-Kononova. The content of calcium and magnesium was determined by complexometric titration, the exchange sodium – by flame photometry, and the carbon dioxide of carbonates – by the gas-voluminometric method. The cationic exchange capacity was calculated using the method of E.V. Bobko and D.A. Aksinazi, and the indicators of water extraction – according to the method of K.K. Gedroits. The ash content of the forest floor was determined by incineration, based on DSTU 7942:2015 (2015).

According to this standard, the selected and pre-dried soil sample is placed in a mortar and burned until the organic matter is completely burned in a muffle furnace at a temperature of 550°C, for two hours. Next, the sample is cooled and weighed to determine the ash weight. Ash content is calculated as the percentage of dry soil weight that remains after burning. The study followed the ethical standards and principles defined by Convention on Biological Diversity (1992), which guarantees the rational and safe use of natural resources. The entire cycle of analysis of physico-chemical studies was carried out in three-fold repetition. After that, the least significant difference (LSD) was calculated to determine the reliability of the conducted studies.

Results and Discussion

Light grey and grey forest soils in the research region were formed under broad-leaved forests on carbonate or loessial rocks. In grey podzolic soils, compared to light grey ones, the podzolic process of soil formation is less pronounced, so there is no alluvial horizon. The nutrient content of these soils, especially light grey ones, is low. The humus horizon is of low capacity, with a humus content of 2.9-3.1%. The soils are acidic, so they require lime application in small and medium doses (1.5-6 tonnes of lime per 1 hectare) (Ivanyuk, 2013). As can be seen from Table 1, grey forest soils on loessial and loess-like loams have formed such soil types as light grey forest gleyed loam, grey forest loam, and grey forest gleyed loam.

Table 1. *Statement of results of physico-chemical analysis of soils of the Husiatyn Forestry of Chortkiv Forest District in the Ternopil Oblast*

Numbers of compartment, subdivision	Numbers of sections	Genetic horizons	Sample depth, cm	Humidity, %	Silt < 0.001 mm	Physical sand sum of particles >0,01 mm	Physical clay sum of particles <0,01 mm	salt pH	mg-Eq/100 g of soil			Degree of saturation with bases, %	Humus according to Tyurin, %	Gross nitrogen %	CN	Mg per 100 g of soil		
									sum of exchange bases	hydrolytic acidity	capacity of soil absorption complex					P_2O_5	K_2O	hydrolysed nitrogen
Grey forest soils on loessial and loess-like loams																		
Light grey forest gleyed-loamy soil																		
109/1	221	HA	2-30	0.80		60.88	39.12	3.6	5.07	9.2	14.27	36	1.25					
		Elh	30-40	1.31		63.73	36.27	3.6	6.45	8.6	15.05	43	0.50					
		I	60-70	2.88		54.63	48.37	3.6					0.46					
	$LSD_{0.5}$			*2.34*		*2.97*	*2.88*	*2.18*	*2.11*	*2.01*	*2.24*	*2.03*	2.02					
Grey forest loamy soil																		
92/3	183	HA	0-28	1.88		66.60	33.40	4.3	7.51	4.0	11.51	65	1.22	0.11	6	3.75	10.5	9.48
Permanent nursery		Elh	35-45	2.24		63.00	37.00	3.9	10.23	4.6	14.88	69	0.71	0.06	7	5.0	10.5	5.60
		I	65-75	4.27		55.00	45.00	4.0					0.61					
		Pi	110-120	2.04		53.23	46.77						0.47					
		Pk	142-152	1.31		51.15	48.85	8.1										
	$LSD_{0.5}$			*2.67*		*2.17*	*2.44*	*2.65*	*2.96*	*2.17*	*2.21*	*2.27*	*2.16*	2.01	2.00	*2.19*	*2.35*	*2.23*
Grey forest clay-loamy soil																		
95/2	163	HA	0-26	3.09	14.81	68.7	31.26	4.1	7.26	5.4	12.66	57	2.01	0.18	6	10.0	10.5	11.48
Permanent nursery		Iha	30-40	4.16	18.92	63.3	36.67	4.5	7.30	3.9	11.2	65	0.62	0.04	8	5.00	8.40	9.24
		I	65-75	6.38	25.05	54.4	45.53	4.0	13.31	4.7	18.01	74	0.55					
		Pi	115-125	4.16	22.88	57.1	42.82	4.6					0.41					
		Pk	150-160	4.16	19.42	57.0	42.95	8.0										
	$LSD_{0.5}$			*2.17*	*2.77*	*2.98*	*2.19*	*2.56*	*2.32*	*2.23*	*2.61*	*2.33*	*2.34*	*2.07*	*2.03*	*2.98*	*2.62*	*2.26*
Grey forest clay-loamy soil																		
22/2	44	HA	2-26	2.563	21.32	57.0	43.00	6.5	15.81	1.1	16.91	93	1.88	0.13	8	20.0	10.5	3.64

Table 4. Continued

Numbers of compartment, subdivision	Numbers of sections	Genetic horizons	Sample depth, cm	Humidity, %	Silt < 0.001 mm	Physical sand sum of particles >0,01 mm	Physical clay sum of particles <0,01 mm	salt pH	mg-Eq/100 g of soil			Degree of saturation with bases, %	Humus according to Tyurin, %	Gross nitrogen %	CN	Mg per 100 g of soil		
									sum of exchange bases	hydrolytic acidity	capacity of soil absorption complex					P_2O_5	K_2O	hydrolysed nitrogen
Arable land	lha		34-45	3.62	26.24	57.3	42.66	5.8	16.66	1.6	18.26	91	0.57	0.04	8	8.75	10.5	5.88
		I	65-75	3.84	31.82	50.08	49.92	5.9	20.33	1.3	21.63	94	0.55	0.04	8	6.25	14.0	3.64
		Pk	125-130	2.98	26.19	57.7	42.25											
		$LSD_{0.5}$		*2.84*	*2.62*	*2.32*	*2.82*	*2.22*	*2.34*	*2.34*	*3.01*	*2.74*	*2.43*	*2.06*	*2.01*	*2.96*	*2.16*	*2.21*

Note: genetic horizons: HA – humus-alluvial; lha – alluvial slightly humus and weakly illuviated; I – illuvial; Pi – transitional to illuvial rock; Pk – soil-forming parent rock

Source: compiled by the authors

Studies have shown that in 30-year-old common oak cultures created on light -grey forest gleyed loamy soils in the fresh oak forest of the Husiatyn Forestry, during the first 10 years, common oak and European ash trees had the same growth energy in terms of height, and only in the previous 5 years the increase in height of oak trees decreased slightly, while their diameter, on the contrary, increased. At the age of 30, plantings were formed by composition 3Co7EhEaNmFe, plant density – 0.8, quality class – 2. Oak trees reached an average height of 11.2 m, an average diameter of 8.5 cm, and European ash trees reached an average height of 12.2 m and 9.6 cm, respectively. The stemwood reserve was 80 $m^3 \cdot ha^{-1}$. The presence of three genetic horizons was found by making a soil section to a depth of 80 cm. This HA horizon was 2-30 cm deep, darkish-grey, grainy-lumpy with plate-like division, slightly compacted, the transition was clear, the humidity of the genetic horizon was 0.8%. In soil, physical sand and physical clay are two groups of particles that form fine soil. Physical sand consists of particles ranging in size from 1 mm to 0.01 mm, while physical clay consists of particles less than 0.01 mm in size. The sum of sand particles >0.01 mm was 60.88%, and the sum of clay particles <0.01 mm was 39.12%, the salt pH was 3.6, the degree of saturation with bases was 36%, and humus according to Tyurin was 1.25%. Studying the content of physical and chemical elements in the soil layer of the elluvial weakly and unevenly humified horizon with a depth of 3040 cm, which is dirty brown, spotted, with humus deposits, dense, with a gradual transition (Elh), it was established that its moisture content does not exceed 1.31%. Physical sand consists of particles ranging in size from 1 mm to 0.01 mm, and physical clay consists of particles smaller than 0.01 mm. Together with the soil skeleton (particles larger than 1 mm), they form the mechanical composition of the soil and its fertility. Their content in the horizon (Elh) was 63.73 and 36.27%, respectively, with a salt pH of 3.6. The sum of metabolic acids was 6.45, the hydrolytic

acidity was 8.6, and the soil absorption capacity (SAC) was 15.05 mg-Eq/100 g of soil. The degree of saturation with bases was 43%, and the presence of humus was 0.50%. Examining the horizon (I), at a depth of 60-70 cm, a red-brown, prismatic, dense, transitional gradual soil layer was found. Its humidity was 2.88%. Physical sand was 54.63%, and physical clay was 48.37%, the salt pH was 3.6, and humus was 0.46%.

On the territory of the permanent nursery in compartment 92, a soil section was taken at a depth of 142 cm, that is, to the depth of the soil-forming rock. Type of growing conditions fresh oak forest (D_2). In the soil section, five genetic horizons were found that differ from each other – HA, Iha, I, Pi, Pk. Horizon thickness, respectively: HA – 25 cm, Iha – 48 cm, I – 90 cm, Pi – 142 cm. Boiling depth is an indicator that characterises the depth at which the soil begins to release carbon dioxide (CO_2) when adding an acid, such as hydrochloric acid (HCl). This phenomenon is associated with the presence of carbonates in the soil. The deeper the boiling layer lies, the deeper the carbonates are. Boiling can be strong, medium, weak, or absent. The depth of boiling in grey forest loam was 142 cm, and the intensity of boiling was estimated as average. Therefore, the boiling depth is not an indicator of CO_2 release when adding acid. CO_2 release when adding HCl indicates the presence of carbonates in the soil and the degree of its liming, and not the depth at which the soil "boils".

Analysing the physical and chemical parameters of grey forest soils formed on loessial and forest-like loams, in the variant of grey forest loamy soil, it was clear that in the HA horizon was in the soil layer of 0-28 cm, the humidity was 1.88%. In the soil layer at a depth of 35-45 cm in the Iha horizon, the moisture content was 2.24%, and at a depth of 65-75 cm, the soil moisture content was the highest – 4.27%. In the lower horizons of Pi and Pk at depths of 110-120 cm and 142-152 cm, humidity decreased to 2.04 and 1.31%, respectively. It is appropriate to note that the depth of distribution of plant roots can be traced up to 30 cm. The sum of particles >0.01 mm and <0.01 mm was related to the granulometric composition of the soil, since this is the particle size distribution. This distribution affects the properties of the soil, in particular, water permeability, breathability, the ability to retain moisture and nutrients. In the genetic HA horizon at a depth of 0-28 cm, 66.60% of physical sand was found, and its content decreased with depth from 66.60% in the HA horizon to 51.15% in the Pk horizon at a depth of 142-152 cm. The content of physical clay had the opposite trend: if in the soil layer at a depth of 0-28 cm it was 33.40%, then at a depth of 142-152 cm it increased to 48.85%.

At a depth of 0-28 cm, the content of physical clay was 33.40%, while at a depth of 142-152 cm it increased to 48.85%. In the grey forest loamy variant, the salt pH in the HA horizon at a depth of 0-28 cm was 4.3. In the soil layer of 35-45 cm, the salt pH decreased by 0.4 units and was equal to 3.9. Starting from the iluvial (I) horizon, where the salt pH was 4.0, to the genetic horizon at a depth of 142-152 cm (Pk), this indicator increased to 8.1. The sum of exchange bases (SEB) is the total amount of calcium cations (Ca^{2+}), magnesium (Mg^{2+}) and hydrogen (H^+), absorbed by the soil absorption complex. It is measured in milliequivalents per 100 g of soil. This indicator characterises the ability of the soil to retain cations, which is important for plant nutrition and maintaining fertility. At the experimental site, the sum of exchange bases ranged from 7.51 mg-Eq/100 g in the humus-alluvial horizon to 10.23 mg-Eq/100 g in the low-humus and low-alluvial horizons. The hydrolytic acidity of the soil reflects the ability to release hydrogen and aluminium ions when interacting with a solution of hydrolytically alkaline salt. It is an indicator of the potential acidity of the soil and includes active (hydrogen ions in the soil solution) and exchange (hydrogen and aluminium, which are replaced by salt cations). In the study variant, this indicator was 4.0 mg-Eq/100 g at a depth of 0-28 cm and 4.6 mg-Eq/100 g at a depth of 35-45 cm. The soil absorption capacity (SAC) is the total amount of cations that the

soil can retain and Exchange. It is measured in milliequivalents per 100 g of soil (mg-Eq/100 g) and characterises the ability of the soil to accumulate nutrients (K^+, Mg^{2+}, Ca^{2+}, etc.), which determines its fertility. In the HA horizon at a depth of 0-28 cm, the SAC was 11.51 mg-Eq/100 g, while in the Iha horizon at a depth of 35-45 cm – 14.88 mg-Eq/100 g.

The degree of base saturation in both genetic horizons at a depth of up to 45 cm had no significant differences and was in the range of 65-69%. The degree of base saturation, also known as base saturation, is an indicator that characterises the content of exchange bases in the soil, expressed as a percentage of the total cationic exchange capacity (CEC). It shows how much CEC is occupied by the main cations (calcium, magnesium, potassium, sodium, etc.). Humus is a dark organic substance that is formed in the soil during the breakdown of plant and animal residues, in particular, under the action of anaerobic organisms. Humus contains a significant amount of nutrients, the most important of which is nitrogen. The humus content in grey forest loamy soil varied along genetic horizons from 1.22 to 0.47%. Thus, 1.22% of humus was found in the HA horizon at a depth of 0-28 cm, in the Iha horizon its content was 0.71%, and in the I – 0.61%. The lowest rate – 0.47% – was recorded in the transition to the rock, Pi horizon at a depth of 110-120 cm. This is conditioned by the fact that humus penetrates into the lower horizons mainly due to the movement of dissolved organic substances (humic acids, etc.) together with ground water. A certain role is also played by the mechanical transfer of small fractions of humus as a result of the activity of soil organisms and soil formation processes.

The spread of humus to the lower genetic horizons of the soil section is explained by the processes of dissolution and movement, mechanical transfer, soil formation, and soil structure and climatic conditions. Thus, in the process of dissolution and movement, humic acids, which are an important component of humus, dissolve well in water and, together with filtration flows, penetrate into the lower layers, enriching them with organic matter. Mechanical transfer is associated with the activity of soil organisms – insects, worms, fungi, etc., which, feeding on organic residues, are able to move humus particles to different depths. Soil formation processes also occur in the lower horizons, where humification is noted – the formation of humus from plant and animal residues that get there as a result of various processes. This leads to the accumulation of humus even in deeper layers, although in much smaller amounts than in the upper horizons. The soil structure also determines the conditions for humus penetration. In soils with a well-developed structure, the presence of pores and channels, water and dissolved substances penetrate deeper more easily, which contributes to the movement of humus. Climatic conditions also play an important role, since humidity and temperature affect the rate of dissolution and transportation of humus substances. In areas with high rainfall and warm climates, humus can penetrate to greater depths than in arid or cold regions. Thus, as a result of these processes, humus gradually accumulates at different levels of the soil, affecting its fertility and properties.

Gross nitrogen is the total amount of nitrogen contained in the soil. Determining gross nitrogen is important for assessing soil fertility. Gross nitrogen in the soil includes various forms of nitrogen, such as organic nitrogen, ammonium nitrogen (NH4+), and nitrate nitrogen (No3-). In the experimental section, the gross nitrogen content was most prevalent in the HA genetic horizon at a depth of 0-28 cm 0.11%, while in the soil layer at a depth of 35-45 cm in the Iha horizon, the content was 0.06%, that is, 1.83 times less. The CN content in the soil refers to the ratio of carbon (C) to nitrogen (N), which is an important indicator of soil fertility and the processes that occur in it. This ratio affects the rate of decomposition of organic matter, the availability of nutrients for plants, and the overall condition of soil biota. CN content in the HA genetic horizon at a depth of 0-28 cm was 6 units, and in the next

horizon (Iha) at a depth of 35-45 cm, its content increased to 7 units, or by 16.68%.

The interaction of carbon and nitrogen is extremely important for understanding the decomposition potential of plant residues, and therefore for developing a fertiliser system, monitoring composting conditions, etc. The higher the value of C:N, the slower the decomposition process is. Free nitrogen is actively attracted by microorganisms from the soil, and if it is not enough, there may be a shortage of this element for plant nutrition for the next season. The optimal C:N ratio is 20-30:1. The total nitrogen content in the arable layer of different soil types is low: it varies from 0.05 to 0.3% and directly depends on the presence of organic substances in them. Its reserves in the arable soil layer range from 2.4 to 8.7 t/ha. Studies conducted based on a large array of data have shown that there is a direct relationship (correlation coefficient $r > 0.9$) between the content of total nitrogen and humus in soils. Soil residues of the non-chernozem zone contain the following amounts of gross nitrogen: sandy loam 0.05-0.07%, loam 0.10-0.20%, clay 0.10-0.23%, peat 0.5-1%. Presence of phosphorus P_2O_5 in the ground section is relatively low and at a depth of 0-28 cm is 3.75 mg per 100 g of soil. With depth, its content increased at a depth of 35-45 cm it was 5.0 mg per 100 g of soil. Phosphorus is one of the main elements of nutrition for plants, along with nitrogen and potassium. It plays an important role in the development of the root system, promotes flowering and fruiting, and increases the resistance of plants to diseases and pests. A lack of phosphorus can lead to slower growth, discoloration of leaves, and poor crop quality.

Potassium is an important element of nutrition for plants, playing a key role in many physiological processes, in particular, in regulating water balance, photosynthesis, nutrient transport and increasing resistance to diseases and stressful conditions. A lack of potassium can lead to slower plant growth, reduced yields, poor product quality, and increased sensitivity to diseases and stressful conditions. Visually, the lack of potassium can be determined by changes in the colour of the leaves (yellowing, browning, burns at the edges), and by wrinkling and twisting of the leaves. Potassium content (K_2O) in different soils varies from 0.5 to 3% and depends on the mechanical composition. More potassium is contained in the clay fraction of the soil. Therefore, heavy clay and loamy soils are richer in potassium (2-3%) than sandy and sandy-loamy (1.5-2%). Peaty soils are very poor in potassium (0.03-0.05%). Most loamy soils contain 2-2.5% potassium, which is significantly more than nitrogen and phosphorus. Analysing the potassium content (K_2O) in grey forest loamy soil in a nursery up to a depth of 45 cm, the potassium content in both genetic layers of the soil was found at a volume of 10.5 mg per 100 g of soil.

Hydrolysed nitrogen, in particular alkaline hydrolysed nitrogen according to the Cornfield method, is an indicator that characterises the content of nitrogen potentially available to plants in the soil. It indicates the amount of nitrogen that can be released from soil organic compounds by alkaline hydrolysis and, therefore, can be used by plants. This indicator is not an absolute measure of the available nitrogen content, since plants can absorb nitrogen in various forms, but it does give an idea of how much nitrogen can be released and used over a certain period of time. Nitrogen is a key element of nutrition for plants, necessary for the synthesis of proteins, chlorophyll, and other important compounds. The hydrolysed nitrogen index characterises the supply of nitrogen to plants during the growing season. This is a supply of nitrogen that will be available to plants in the future. In grey forest loamy soil in a soil section made on a permanent nursery in the humus horizon (HA) at a depth of 0-28 cm, the content of hydrolysed nitrogen was 9.48 mg per 100 g of soil, and at a depth of 35-45 cm, its content decreased to 5.60 mg per 100 g of soil, or 59.07%.

In division 2 of compartment 85, a soil section was established at a permanent nursery in the Husiatyn Forestry to investigate the structure of the soil, its properties, and to determine the

boundaries between different types of soils. This section will help to understand how the soil is formed, what layers are present in it, and what processes occur inside, and identify the physical and chemical features of the soil. At the permanent nursery of the Husiatyn Forestry, a soil section was made to a depth of 140 cm, considering that the main mass of roots extends to a depth of 30 cm. The depth of boiling characterises the depth at which the soil begins to release carbon dioxide (CO_2) when hydrochloric acid (HCl) is added, it is detected to a depth of 140 cm. When hydrochloric acid (HCl) is added to the soil, a reaction occurs with carbonates contained in the soil. This reaction releases carbon dioxide (CO_2). This is not related to the boiling point. Measurement of the amount and rate of CO_2 release helps to determine the content of carbonates in the soil, which indicates the degree of liming.

At the nursery, the type of growing conditions – wet oak forests (D_3), therefore, soil humification can be observed – this is a complex biochemical process that occurs in anaerobic conditions (in the absence of oxygen) in the presence of organic substances and with the participation of anaerobic microorganisms, resulting in the restoration of iron-containing compounds in the soil, which manifests itself in a change in soil colour to grey, bluish, or greenish. The strength of genetic horizons along the lower boundary depending on the horizon was found for HA – 26 cm, Iha – 51 cm, I – 100 cm, transitional to the rock, Pi – 140 cm. According to the terrain, the territory of the nursery is located on a plateau. It is a structural plain covered with loess, with developed erosion. Loess is a continental soil-forming mountain sedimentary rock with greyish-yellow, sometimes brown or reddish-brown colour. The thickness of loessial layers ranges from several tens of centimetres to several tens of metres on the watersheds and slopes of ancient valley terraces.

Analysing Table 1, grey forest clay loamy soil that was formed on loessial and loess-like loams, there is a clear distribution of it over genetic horizons, namely: HA, with a thickness of 0-26 cm; Iha, where the sample was taken at a depth of 30-40 cm; I, where the sample was taken at a depth of 65-75 cm, transitional to the rock; Pi, where the sample was taken at a depth of 115-125 cm, and Pk – sample taken at a depth of 150160 cm. Soil moisture in the pit is measured to determine the moisture content in a particular layer of soil that is taken when digging the pit. Humidity affects soil properties such as density, water retention, and nutrient retention. The highest soil moisture was found in the I layer of soil at a depth of 65-75 cm, the content of which was 6.38%, although humidity fluctuations along genetic horizons were in the range of 3.09-6.38%. In the horizons of the transition to rock, Pi (soil layer at a depth of 115-125 cm) and Pk (sample taken at a depth of 150-160 cm), the soil moisture in both pits was identical and amounted to 4.16%. The presence of silt with a fraction <0.001 mm was detected in grey forest clay loamy soil. Silt contains nutrients such as nitrogen, phosphorus, potassium, and organic substances that improve the structure of the soil and increase its fertility. Silt is also a soil booster that improves the water retention capacity of the soil, reduces its acidity and increases the resistance of plants to stressful conditions. In wholesale sections of a permanent nursery, the silt content along genetic horizons was in the range of 14.81-25.05%. The smallest amount of silt (14.81%) was found in the HA horizon at a depth of 0-26 cm, the biggest – 25.05% in the horizon at a depth of 65-75 cm, that is, in the soil layer in which the humidity was highest and amounted to 6.38%.

In the Iha horizon, the silt content at a depth of 30-40 cm was 18.92%, in the transition to rock, Pi horizon (sample taken at a depth of 115-125 cm), and Pk (sample taken at a depth of 150-160 cm), the silt content was 22.88 and 19.42%, respectively, that is, 3.46% less. Physical sand refers to the sum of all particles with a size of 1-0.01 mm, and particles less than 0.01 mm – to physical clay. The solid phase of the soil consists of mineral and organic particles of different sizes and different chemical compositions. The sum of

particles larger than 0.01 mm in the soil refers to the granulometric composition of the soil. This indicator determines the content of particles of different sizes in the soil (sand, loam, clay) and is of great importance for its properties.

In the soil section, the content of physical sand was highest in the HA layer of soil with a thickness of 0-26 cm and was 68.7%. According to the genetic horizons of the Iha soil layer, where the sample was taken at a depth of 30-40 cm and in the I soil layer at a depth of 65-75 cm, its content decreased to 63.3 and 54.4%, respectively, compared to the HA soil layer. In the transition to the rock, Pi horizon (sample taken at a depth of 115-125 cm) and Pk (sample taken at a depth of 150-160 cm), the content of physical sand was the same and amounted to 57.1 and 57.0%, respectively.

The sum of soil particles less than 0.01 mm in size in the soil refers to physical clay. This indicator is an important characteristic of the granulometric composition of the soil and affects its properties, such as water permeability, breathability, ability to retain water and nutrients. The physical clay content affects the soil's ability to retain water and nutrients, and its workability. For example, soils with high clay content (clay soils) retain water well, but can be difficult to cultivate, while soils with low clay content (sandy soils) allow water to pass through well, but are less fertile. Clay particles (less than 0.005 mm, but in the context of the question, most of them are particles of 0.01 mm or more) compact the soil, make it heavier, less permeable to air and water. Analysing the data obtained from the section on the content of physical clay, it should be noted that the opposite trend is observed in comparison with the content of physical sand. The lowest content of physical clay of 31.26% was found in the HA soil layer at a depth of 0-26 cm. In the following soil layers – Iha and I, in samples taken at a depth of 30-40 and 65-75 cm, respectively, an increase in the content can be traced up to 45.53%. It was the highest in the I layer of soil. In the horizon transitional to the Pi rock, (sample taken at a depth of 115-125 cm) and Pk (sample taken at a depth of 150-160 cm), the physical clay content had similar values of 42.82 and 42.95%, respectively.

Diagnosing the state of the soil through salt pH, its value ranges from 4.0 to 8.0. Considering the genetic horizons, in HA, the horizon in the soil layer was 026 cm pH of 4.1 was detected; in the Iha horizon, where the sample was taken at a depth of 30-40 cm, pH was 4.5; in I, (sample taken at a depth of 65-75 cm) – pH 4.0, transitional to the rock; Pi, (sample taken at a depth of 115-125 cm) – pH 4.6, that is, for all genetic horizons to a depth of 0-125 cm of soil was considered already acidic or even very acidic. But in the soil-forming (parent) rock, where the sample is taken at a depth of 150-160 cm salt pH is 8.0 units, which indicates alkalinised soil. This is conditioned by the specifics of the chemical interaction between soil ions and salt solution. This analysis allows seeing more deeply the potential acidity and show how much the soil can neutralise it.

Analysing the sum of exchange bases, hydrolytic acidity, and SAC, their content can be traced to a depth of 75 cm covering three genetic horizons, namely: HA horizon to a depth of 0-26 cm, where the sum of the exchange bases was 7.26 mg-Eq/100 g of soil; almost the same indicator of the sum of exchange bases was 7.30 mg-Eq/100 g of soil was found in the Iha soil layer, where the sample was taken at a depth of 30-40 cm. However, in the soil layer at a depth of 6575 cm of I horizon, the sum of exchange bases increased by 1.82 times and amounted to 13.31 mg-Eq/100 g of soil. Hydrolytic acidity was highest in the HA horizon at a depth of 026 cm was 5.4 mg-Eq/100 g of soil. With the depth of the horizons in the soil layer of the Iha horizon, its content decreased to 3.9 mg-Eq/100 g of soil, and in the I horizon at a depth of 6575 cm, its content increased by 1.21 times and reached 4.7 mg-Eq/100 g of soil.

Soil absorption capacity (SAC) characterises the soil's ability to retain nutrients such as potassium (K), magnesium (Mg), calcium (Ca), etc., and determines soil fertility. Its content

in the HA horizon at a depth of 028 cm was 12.66 mg-Eq/100 g of soil, and in the Iha horizon at a depth of 35-45 cm – 11.2 mg-Eq/100 g of soil. Soil absorption capacity at a depth of 65-75 cm in the I layer of soil was 18.01 mg-Eq/100 g of soil, which was 1.42 times more than HA and 1.61 times more than Iha horizons. The degree of base saturation in both genetic horizons at a depth of up to 45 cm does not have any special differences, although it is located with a difference of 8.0%, respectively, with genetic horizons of 57 and 65%. I, at a depth of 65-75 cm, the content was 74%. The degree of base saturation, also known as base saturation, is an indicator that characterises the content of exchange bases in the soil, expressed as a percentage of the total cationic exchange capacity (CEC). It shows how much CEC is occupied by the main cations (calcium, magnesium, potassium, sodium, etc.). Humus content in the HA soil layer at a depth of 0-26 cm was 2.01%, in the Iha horizon, at a depth of 30-40 cm decreased to 0.62%. A decrease in the humus content can be traced in the I layer of the soil, the sample was taken at a depth of 65-75 cm to 0.55%, and in the Pi layer of the soil transitional to the rock at a depth of 115-125 cm, where its content was 0.41%. Gross nitrogen in the HA horizon was 0.18%, and in the Iha, a soil layer at a depth of 30-40 cm, its content decreased to 0.04%, or 4.5 times. The interaction of carbon and nitrogen C:N shows that the higher the value of C:N, the slower the decomposition process of plant residues takes place.

Presence of phosphorus P_2O_5 in the ground section it is relatively low and at a depth of 0-28 cm is 10.00 mg per 100 g of soil. With depth, its content decreased twice and at a depth of 30-40 cm it was 5.0 mg per 100 g of soil. Phosphorus is one of the main elements of nutrition for plants, along with nitrogen and potassium. A lack of phosphorus can lead to slower growth, discolouration of leaves, and poor crop quality. Potassium is an important element of nutrition for plants. A lack of potassium can lead to slower plant growth, reduced yields, poor product quality, and increased sensitivity to diseases and stressful conditions. Analysing the potassium content (K_2O) in grey forest loamy soil in a nursery up to a depth of 26 cm, the potassium content was found in a volume of 10.5 mg per 100 g of soil, but at a depth of 30-40 cm of its content decreased and reached 8.4 mg per 100 g of soil. Hydrolysed nitrogen characterises the content of nitrogen potentially available to plants in the soil. It indicates the amount of nitrogen that can be used by plants. The hydrolysed nitrogen index characterises the supply of nitrogen to plants during the growing season. This is a supply of nitrogen that will be available to plants in the future. In grey forest gleyed loamy soil in a soil section made on a permanent nursery in the HA horizon at a depth of 0-28 cm, the content of hydrolysed nitrogen was 11.48 mg per 100 g of soil, and at a depth of 3040 cm, its content decreased to 9.24 mg per 100 g of soil, or 2.24%.

The division 2 of compartment 22 contains arable land, where the section was made to a depth of 130 cm. In the soil section, the HA horizon with a thickness of 026 cm was highlighted; Iha horizon, where the sample was taken at a depth of 34-45 cm, and the total thickness of this horizon was 56 cm, and the I horizon was 100 cm thick, where the sample was taken at a depth of 65-75 cm, and Pk, the thickness of which was 127 cm, and the sample was taken at a depth of 125-130 cm. The depth of the parent rock is 127 cm, the depth of distribution of the main mass of roots is 26 cm, the type of growing conditions is fresh oak forest (D_2). The depth of boiling characterises the depth at which the soil begins to release carbon dioxide (CO_2) when hydrochloric acid (HCl) is added, It is detected to a depth of 127 cm. South-western relief exposition, steepness 7°, even shape.

Studying soil moisture by genetic horizons, it should be noted that it fluctuates in the range from 2.56 to 3.84%, that is, with a difference of 1.28%, which can be considered insignificant. The greatest humidity was found in the illuvial horizon at a depth of 65-75 cm – 3.84%. 21.32-

31.82% of silt was found in the soil. The highest content of 31.82% was found in the iluvial (I) horizon at a depth of 65-75 cm. The content of physical sand (sum of particles >0.01 mm) had a slight deviation and was located in the HA horizon in a volume of 57.0%, in Iha and Pk, respectively, 57.3 and 57.7%, while in the illuvial layer of soil its content was 50.08%, which was 6.927.62% less than in other horizons. Studying the content of physical clay (the sum of particles <0.01 mm), the reverse pattern can be traced along the genetic horizons. The highest content of physical clay of 49.92% was found in the I horizon. In other genetic horizons, its content was 43.00%, 42.66%, and 42.25%, respectively, where there is an insignificant difference of 0.75%.

Salt pH is an indicator of acidity determined in a weak saline solution. It is used to clarify the acidity of slightly acidic soils (approximately pH 6.5-7.4). During the research, the pH was determined to be within 5.8-6.5. The highest pH value was found in the HA layer of soil – 6.5. Salt pH values of 5.8 and 5.9 were found in the Iha horizon, where the sample was taken at a depth of 30-40 cm and in the I horizon, where the sample was taken at a depth of 65-75 cm. Reduction of acidity by 0.7 and 0.6 units. Reduction of soil acidity by 0.7-0.6 units on the salt solution pH scale means that the soil has become less acidic. The pH scale used to measure soil acidity is logarithmic, so the change is 0.7-0.6 units indicates a relatively moderate decrease in acidity. This means that the amount of hydrogen (H+) ions in the soil solution has decreased, which can affect the availability of nutrients for plants. Changes in pH can affect the solubility and availability of nutrients in the soil. For example, as acidity decreases (pH increases), elements such as phosphorus, molybdenum, and calcium may become more readily available to plants, while others such as iron, manganese, and zinc may become less readily available.

The sum of exchange bases, hydrolytic acidity, and cationic exchange capacity (CEC) are important indicators of soil fertility. They characterise the ability of the soil to retain and exchange ions, and its acid-base properties. The sum of the exchange bases determines the number of cations (positively charged ions) that the soil can hold on its surface. It includes basic cations such as calcium (Ca^{2+}), magnesium (Mg^{2+}), potassium (K^{+}), sodium (Na^{+}), etc. In the soil section, the sum of exchange bases ranged from 15.81 mg-Eq/100 g of soil in the HA horizon up to 20.33 mg-Eq/100 g of soil in the I horizon, where the sample was taken at a depth of 65-75 cm. The nominal amount of exchange bases is in the range of 10-22 mg-Eq/100 g of soil. Thus, the high sum of exchange bases in the soil section indicates a good supply of nutrients to the soil and its ability to neutralise acidity. Hydrolytic acidity shows the amount of hydrogen (H^{+}) and aluminium (Al^{3+}), which can be released from the soil and exchanged for other ions. It is measured when the soil is treated with alkaline solutions that help to displace these ions.

In the soil section, hydrolytic acidity depending on the genetic horizon was found in HA horizon in volume 1.1, in Iha horizon – 1.6, and I horizon – 1.3 mg-Eq/100 g of soil. Hydrolytic acidity of the soil 1.1-1.6 mg-Eq/100 g of soil, indicates that the soil contains a significant amount of exchange hydrogen and aluminium ions, which can be released and affect the acidity of the medium. This value indicates moderate soil acidity, which can affect the availability of nutrients for plants and will require measures to regulate the acidity if necessary.

Soil absorption capacity of cations (SAC) is a measure of the soil's ability to retain positively charged ions such as calcium, magnesium, potassium, and sodium. The higher the SAC, the more nutrients the soil can retain for plants (Tyhonenko, 2005). In grey forest gleyed loamy soil of arable land capacity of absorption capacity of soil cations (SAC) in the HA soil layer at a depth of 226 cm was 16.91 mg-Eq/100 g of soil, in the Iha horizon at a depth of 30-40 cm – 18.26 mg-Eq/100 g of soil, and the I horizon at a depth of 65-75 cm contained 21.63 mg-Eq/100 g of soil. Therefore, soil with an absorption capacity of 16.91-21.63 mg-Eq/100 g has an average level

of ability to retain nutrients and provide fertility. In a genetic section made on arable land, the degree of base saturation was found in the HA layer of soil at a depth of 226 cm in a volume of 57%, the Iha horizon at a depth of 30-40 cm contained 65%, and the I horizon at a depth of 65-75 cm contained 74%, which was 17% more or 1.3 times compared to the humus-alluvial (HA) horizon. Notably, soils saturated with bases are considered optimal in the range of 65-75%. In the grey forest gleyed loamy soil of ploughed lands, the humus content ranged from 0.55 to 1.88%. Grey forest soils are formed in conditions of sufficient moisture under broad-leaved forests. They are characterised by a low humus content, which makes them less fertile compared to chernozems. The humus content may vary depending on the specific subtype of grey forest soil, such as light grey, grey, or dark grey (Poznyak, 2010).

Considering these data, the range from 0.55 to 1.88% for grey forest clay-loamy soils of arable land was justified. The gross nitrogen content in the HA soil layer was 0.13%, and in subsequent horizons at a depth of 34-75 cm its content was 0.04%, which is 3.25 times less than in the HA soil layer. In the soil, most of the gross nitrogen (93-97%) is part of humus, and the rest is in the form of mineral compounds that are available to plants. The gross nitrogen content in the soil can vary widely, but usually ranges from 5.0 to 6.8% of the humus content. Thus, the concept of "gross nitrogen" in the context of soil and plants indicates the total amount of nitrogen, including both available and inaccessible forms for plants.

The interaction of carbon and nitrogen C:N shows that the higher the value of C:N, the slower the decomposition process of plant residues takes place (Nazarenko *et al*., 2004). The HA soil layer at a depth of 226 cm revealed the ratio of carbon to nitrogen – 6, in Iha horizon at a depth of 30-40 cm, this ratio was 8. If the C:N ratio is high, it means that the soil has a lot of energy for microorganisms, but the quality or nutritional value of these elements is low. The higher the initial C:N ratio, the longer the decomposition of residues takes. Organic nitrogen is used by microbes to quickly break down nutrient residues and create proteins that are vital for their growth and reproduction. In perfect condition, healthy soil has a C:N ratio of 10:1 to 12:1, which means that the microbial biome is balanced. Content of phosphorus P_2O_5 in the ground section it is relatively low and at a depth of 0-28 cm is 20.00 mg per 100 g of soil. With depth, its content decreased by 2.29 times and at a depth of 30-40 cm it was 8.75 mg per 100 g of soil. Phosphorus is one of the main elements of nutrition for plants, along with nitrogen and potassium. A lack of phosphorus can lead to slower growth, discolouration of leaves, and poor crop quality.

Lack of potassium (K_2O) may lead to slower plant growth, reduced yields, poor product quality, and increased sensitivity to diseases and stressful conditions (Kumar *et al*., 2023). Analysing the potassium content in grey forest gleyed loamy soil on ploughed lands to a depth of 26 cm, the potassium content was found in the volume of 10.5 mg per 100 g of soil, the same content of 10.5 mg per 100 g of soil at a depth of 34-45 cm. The potassium content in the I horizon increased and reached 14.0 mg per 100 g of soil. Hydrolysed nitrogen characterises the supply of nitrogen to plants during the growing season. In grey forest gleyed loamy soil in a soil section made on a permanent nursery in the HA horizon at a depth of 2-26 cm, the content of hydrolysed nitrogen was 3.64 mg per 100 g of soil, and at a depth of 34-45 cm, its content increased to 5.88 mg per 100 g of soil, or 1.62%. In the I horizon, hydrolysed nitrogen decreased to 3.64 mg per 100 g of soil. The content of alkaline hydrolysed nitrogen reflects the amount of nitrogen that can be used by plants in the near future. The smallest significant difference in all variants of the experiment was within the normal range – 2.01-3.01, which indicates the reliability of our research.

According to H.S. Ivanyuk (2017), who conducted a thorough analysis of soil classifications in Poland and Ukraine, some subtypes of chernozem soils are most similar to grey forest soils in

terms of properties. When comparing the results of current research with the work of the above researcher, this statement can be agreed with. Since the presented samples contain a sufficient amount of minerals, which makes the soils of the region suitable for growing various plant species, and in chernozem types. S. Bogdanov *et al.* (2025) analysed how different forest types and treeless areas affect the morphological, chemical, and organic properties of grey forest soils in northeastern Bulgaria. The researchers compared soil sections under different forest types and unordered (treeless) areas, finding a clear dependence of the soil structure on vegetation – the forest causes a deeper humus horizon, and more developed profile characteristics. The data obtained in the current study that the type of forest (tree species) affects the nitrogen content, pH value and C:N ratio in the soil are partially consistent with our conclusions regarding the content of these minerals in the soil. Since the higher the initial ratio of these elements, the longer the decomposition of residues lasts, that is, the soil has a lot of energy for microorganisms. In current studies the HA soil layer at a depth of 226 cm revealed the ratio of carbon to nitrogen – 6, in the Iha horizon at a depth of 30-40 cm, this ratio was 8. This indicates that the soil horizons are not sufficiently provided with these elements. M. Lungu (2015) analysed the evolution of grey forest soils used as arable land after deforestation in the central part of Moldova, in the Codri region. The researcher used the method of comparing grey soils under the forest, grey arable soils used in agriculture for about 100 years, and grey arable soils that had a long period of development under the steppe before being used in agriculture. As a result of agricultural use, the first three horizons of forest soils (AEh, AEh, and BEhtw) were mixed into one. Use in agriculture also led to a decrease in the humus content, a decrease in the intensity of illuvial-alluvial and cambic processes, a decrease in soil acidity, soil compaction, and deterioration of its structural state. In contrast to the research of this researcher, current studies clearly trace the presence of all genetic horizons. It follows that forest soil types are less susceptible to destructive processes and can recover faster.

S. Bogdanov (2014) analysed the effect of forest fires on the composition of texture fractions (sand, dust, clay) in the profile of grey forest soils. According to his research, the intensity of a fire can reduce the proportion of these fractions in the upper horizons due to the burning of organic matter and changes in the aggregate structure. The data obtained are important for understanding long-term changes in soil water and air permeability after fires and for restoring forest biocenoses. The researcher also claims that despite the influence of external factors, the soil texture is one of the most conservative indicators and changes slowly and only under certain circumstances. This is consistent with the results of current research.

Research by O. Havryshko *et al.* (2024) showed that long-term use of arable land plots changes the distribution of sand and clay in the soil profile, leading to compaction, a decrease in the proportion of agricultural groups, and changes in porosity, which affects water-physical properties. The researchers emphasised that even small changes in the particles of physical clay/sand have a significant effect on the ability of the soil to retain water and restore structure after mechanical impact. In addition, it was demonstrated that key elements (C, N, organic matter) are closely correlated with each other and are distributed unevenly across all soil horizons, as in current studies. I. Kirilov *et al.* (2022) found that during the processes of podzolisation of the upper horizons, the content of the pulverised fraction below the humus horizon increases. In contrast to the results of the above researchers, current studies show a uniform distribution of particles of different fractions over all soil horizons.

S. Gaidar *et al.* (2024) investigated easily hydrolysed nitrogen and total nitrogen in cultivated grey forest soils. Similar to current studies, these researchers concluded that high soil acidity can reduce the level of this element in the

upper genetic horizons. This means that it needs to be regulated using mineral fertilisers with the appropriate ratio of elements. N.M. Pavliuk & V.G. Haskevych (2011) described in detail the physical and chemical properties of Opillia soils in a monograph. The researchers state that the studied soils in Opillia are characterised by a very low content of absorbed cations. The soil-absorbing complex of these soils is dominated by calcium and magnesium cations. In the direction from northwest to southeast, the content of calcium cations decreases in the humus horizons of light grey forest soils and the content of magnesium cations increases. In contrast to their results, soils in the region of the current study have a sufficient level of cations and are characterised by a normal distribution of absorbed bases over genetic horizons.

Summarising the results of the conducted research, it can be noted that the grey forest soils of the Husiatyn Forestry are marked by a clear differentiation by genetic horizons, significant fluctuations in physico-chemical parameters, and a significant dependence on the conditions of use (arable land, nurseries, forest crops). The established differences in humus content, degree of base saturation, acidity, granulometric composition and other properties confirm the multifactorial nature of their transformation under the influence of natural and anthropogenic factors. The data obtained are consistent with the conclusions of previous researchers, but simultaneously emphasise the specifics of soil processes in the region under study, which is of great practical importance for the development of optimal agricultural technologies in nurseries and improving the efficiency of growing planting material.

Conclusions

The study of the properties of grey forest soils showed significant differences in their agrochemical state depending on the type. Light grey soils are characterised by a poor humus profile and low base saturation, which leads to their weak fertility. In contrast, grey loamy and gleyed soils have a higher capacity of the absorption complex, higher humus content and better indicators of agrochemical supply. According to the granulometric composition, all variants belong to loams with a physical clay content of 40-50%. The upper horizons contain more silt and fine particles, which reduces their water permeability. The reaction of the soil solution in the upper layers was acidic (pH 3.6-6.5), which limits the availability of nutrients for plants, while in the lower horizons the indicators increase to 8.0-8.1, which indicates the presence of a carbonate horizon and confirms the genetic features of grey forest soils on loess-like rocks. The humus content in light grey soils was only 0.5-1.2%, while in grey loamy and gleyed soils it was higher (1.2-2.0%), especially in variants under arable crops (1.8-2.0%). Total nitrogen in the upper horizons was in the range of 0.1-0.18%, with a C:N ratio of about 8, which indicates rapid mineralisation of organic matter and insufficient reserves of stable humus compounds. Phosphorus supply ranges from very low (3.75-10 mg/100 g) to high (20 mg/100 g in arable land), and the potassium content is mostly stable (10-14 mg/100 g), although sometimes it decreases to 5-6 mg/100 g. Hydrolysed nitrogen reserves are medium or low (3.6-11.5 mg/100 g), which further limits the fertility of these soils.

Further research should be aimed at detailed monitoring of changes in the humus profile and macronutrient availability in various agrotechnical systems. It is also advisable to investigate the stability of organic matter and ways of its accumulation in light grey soils with the lowest humus content, and search for optimal land reclamation and agrochemical measures to increase their fertility.

Acknowledgements

None.

Funding

None.

Conflict of Interest

None.

References

[1] Bogdanov, S. (2014). Soil texture changes in gray forest soils (gray luvisols) influenced by forest fires in deciduous forests. *Forestry Ideas,* 20(2), 135-140.

[2] Bogdanov, S., Pavlov, P., & Tauakelov, C. (2025). Analysis of the properties of grey forest soils in relation to forest types in Northeastern Bulgaria. *Ecological Engineering and Environment Protection,* 1, 73-79. doi: 10.32006/eeep.2025.1.7379.

[3] Brovko, F., Yukhnovskyi, V., Brovko, O., Brovko, D., Urliuk, Yu., & Khryk, V. (2023). The influence of anthropogenic trampling of gray forest soils on their physical properties. *Central European Forestry Journal,* 69(4), 224-232. doi: 10.2478/forj-2023-0017.

[4] Brovko, O., Yukhnovskyi, V., Brovko, F., Brovko, D., & Voitcekhivska, O. (2025). Water-physical properties of gray forest soils and their root settlement in areas of anthropogenic trampling. *Ukrainian Journal of Forest and Wood Science,* 16(1), 64-81. doi: 10.31548/forest/1.2025.64.

[5] Convention on Biological Diversity. (1992, June). Retrieved from https://surl.li/tshrxp.

[6] Dmitrenko, O., Tkachenko, M., & Pavlichenko, A. (2021). Changes in the nitrogen status of grey forest coarse dusty light loam soil under different systems of fertilisation and chemical amelioration. *Plant and Soil Science*, 12(1), 77-85. doi: 10.31548/agr2021.01.0077.

[7] DSTU 7942:2015. (2015). *Soil quality. Determination of ash content in peat and peat soil.* Retrieved from https://online.budstandart.com/ua/catalog/doc-page?id_doc=62856.

[8] Gaidar, S., Kazak, A., Barchukova, A., & Kozlov, A. (2024). Effects of complex fertilizers on the properties of grey forest heavy loamy soil. *Scientifica,* 2024, article number 2763147. doi: 10.1155/2024/2763147.

[9] Hamkalo, Z.G. (2009). *Ecological quality of soil.* Lviv: Ivan Franko National University of Lviv. doi: 10.13140/2.1.3203.5527.

[10] Havryshko, O., Olifir, Yu., Hnativ, P., Habryiel, A., Partyka, T., & Ivaniuk, V. (2024). Influence of prolonged agrogenic transformation on soil structure and physicochemical properties of Ukrainian Albic Stagnic Luvisols: A case study from western Ukraine. *Soil Science Annual,* 74, 1-9. doi: 10.37501/soilsa/183659.

[11] Ivanyuk, H.S. (2013). Analysis of "Systematic of Poland soils". *Visnyk of Lviv University. Series Geography,* 44, 122-132. http://dx.doi.org/10.30970/vgg.2013.44.1210.

[12] Ivanyuk, H.S. (2017). Gray forest soils in different classification systems. *Visnyk of the Lviv University. Series Geography,* 51, 120-134. http://dx.doi.org/10.30970/vgg.2017.51.8851.

[13] Jinglei, L., Xianliang, Z., Tim, R., Chen, X., Mingchao, D., Fangqin, G., Weixin, L., Jianwei, Z., Yuewei, W., & Manzanedo, R.D. (2025). Slope mediates drought sensitivity but does not affect drought recovery for young trees along elevation gradients in temperate planted larch forests. *Forest Ecosystems,* 14, article number 100371. doi: 10.1016/j.fecs.2025.100371.

[14] Kirilov, I., Lozanova, V., Gerassimova, I., & Pankov, V. (2022). Changes in the properties of Luvisols, Planosols and Fluvisols under the influence of agroproduction activity from the region of Sofia District. *Bulgarian Journal of Soil Science,* 7, 24-33. doi: 10.5281/zenodo.6780116.

[15] Kovalyova, E., Kotlyarova, E., Kuzmina, O., Breslavets, Yu., & Teteryadchenko, A. (2021). Study of thickness of humus profiles of gray forest and chernozem soils of different terms of agricultural use in landscape shrubs of the central forest-steppe. *BIO Web of Conferences,* 39, article number 01006. doi: 10.1051/bioconf/20213901006.

[16] Kumar, U., Shelake, R.M., & Singh, R. (2023). *Soil-plant-microbe interactions: An innovative approach towards improving soil health and plant growth.* Lausanne: Frontiers Media SA. doi: 10.3389/978-2-83251-919-6.

[17] Lungu, M. (2015). Evolution of gray forest soils under arable use in the central part of Republic of Moldova. *Agronomy,* 58.
[18] Nazarenko, I.I., Polchina, S.M., & Nikorich, V.A. (2004). *Soil science*. Chernivtsi: Books XXI.
[19] Panas, R.M. (2019). *Soil ecology*. Lviv: Novyi Svit-2000.
[20] Pavlichenko, A., Dmytrenko, O., Litvinova, O., Kovalova, S., Litvinov, D., & Havryliuk, O. (2023). Changes in gray forest soil organic matter pools under anthropogenic load in agrocenoses. *Agronomy Research,* 21(3), 1266-1277. doi: 10.15159/AR.23.095.
[21] Pavliuk, N.M., & Haskevych, V.G. (2011). *Grey forest soils of Opillia.* Lviv: Publishing Centre of Ivan Franko National University of Lviv.
[22] Poznyak, S.P. (2010). *Soil science and soil geography* (In two parts). Lviv: Ivan Franko National University of Lviv Publishing Center.
[23] Ryazanov, S., Alieksieiev, O., Lykhochvor, V., Vradii, O., Razanova, A., Datsko, T., & Holubieva, T. (2025). Assessment of mineral composition of grey forest soils under energy crops in the Western Forest Steppe of Ukraine. *International Journal of Environmental Studies,* 82(2), 771-777. doi: 10.1080/00207233.2024.2445412.
[24] Tyhonenko, D.G. (Ed.). (2005). *Soil science.* Kyiv: Higher Education.

Вміст поживних речовин у сірих лісових ґрунтах Гусятинського лісництва

Дмитро Ярош
Аспірант
Уманський національний університет
20300, вул. Інститутська, 1, м. Умань, Україна
https://orcid.org/0009-0001-8322-600X
Михайло Ярош
Аспірант
Уманський національний університет
20300, вул. Інститутська, 1, м. Умань, Україна
https://orcid.org/0009-0003-1845-1686

Анотація. Метою дослідження було з'ясування фізико-хімічних особливостей різних типів лісових ґрунтів та оцінка їх агрохімічного стану на постійних розсадниках, орних землях та 30-річних культурах дуба звичайного в умовах Гусятинського лісництва Чортківського надлісництва. Було застосовано ґрунтово-агрохімічні методи аналізу, що включали визначення фракційного та механічного складу, вмісту гумусу, насиченості основами та ємності поглинального комплексу. Порівняння показників здійснювали між світло-сірими, сіро-суглинистими та глеюватими ґрунтами, що дало змогу охарактеризувати їх продуктивність та агрохімічний потенціал. Встановлено, що у більшості ґрунтів верхні горизонти кислі (pH 3,6-5,0), що негативно впливає на доступність поживних речовин, у світло-сірих ґрунтах вміст гумусу низький (0,5-1,2 % у верхніх горизонтах). У сірих суглинистих і глеюватих ґрунтах гумусу більше (1,2-2,0 %), особливо в орних варіантах (1,8-2,0 %). Загальний азот у верхніх горизонтах становив 0,1-0,18 %, що є досить низьким. Співвідношення C:N було близьке до 8, що свідчить про швидку мінералізацію органічної речовини. Деякі ділянки добре забезпечені P_2O_5 (20 мг/100 г), але є ґрунти з дефіцитом (<10). Забезпеченість калієм більш стабільна, але в орних горизонтах можливе виснаження. Фосфор (P_2O_5): коливався від дуже низьких значень (3,75-10 мг/100 г) до підвищених (20 мг/100 г у орних землях). Калій (K_2O): тримався на рівні 10-14 мг/100 г, але в окремих випадках знижується до 5-6 мг/100 г (погіршення забезпеченості). Гідролізований азот: показники 3,6-11,5 мг/100 г, що вказує на середню або низьку забезпеченість азотом. Результати дослідження фракційного та механічного складу ґрунту в умовах дібров на прикладі Гусятинського лісництва мають вагоме практичне значення для розроблення рекомендацій, щодо особливостей закладання лісових культур у даному регіоні та захисту ґрунту від ерозійних процесів

Ключові слова: генетичні горизонти; фракції; вологість; ємність; поживні речовини

Received 19.05.2025 Revised 21.08.2025 Accepted 23.09.2025

Vol. 21, No. 5
2025

Scientific Reports of the National University of Life and Environmental Sciences of Ukraine

Journal homepage: https://scireports.com.ua/en

UDC 636.592.09:591.3:616.3

Doi: 10.31548/dopovidi/5.2025.28

Morphological features of immune formations of the avian digestive tract

Natalya Mazur
PhD Student
National University of Life and Environmental Sciences of Ukraine
03041, 15 Heroiv Oborony Str., Kyiv, Ukraine
https://orcid.org/0009-0004-5747-4335

Nadiia Dyshliuk*
Doctor of Veterinary Sciences, Professor
National University of Life and Environmental Sciences of Ukraine
03041, 15 Heroiv Oborony Str., Kyiv, Ukraine
https://orcid.org/0000-0003-4753-9356

Abstract. Immunocompetent structures of the digestive organs play an important role in protecting the body from bacterial and viral infections by providing an immune response. The aim of this study was to establish and summarise the morphological features of these structures in birds of different species, which would allow to determine their morphofunctional status, which is determined by the state of natural resistance and reactivity of the body, and to identify critical periods in the development of the immune system. To achieve this goal, a literature review of current research on the topography and microstructure of immune structures in the digestive organs of birds was conducted. It was established that the material basis of these structures is lymphoid tissue, the differentiation of which has regional characteristics, occurs in a specific sequence and proceeds in several stages. Its development depended on the age, species, sex, type of nutrition of birds and structural and adaptive features of the digestive organs. Immune formations were localised mainly in the mucous membrane of the digestive tract, and in birds of certain species also in the muscular and serous membranes. They consisted of T and B lymphocytes and their effector cells, which perform important cellular surveillance functions in protecting the body from foreign genetic information. It has been noted that they are in close contact with macrophages and function as a single lymphoid-macrophage system. The presented scientific research expands and supplements knowledge about the species, breed and morphological features of the structure of immune formations of the digestive tract of birds, which

Suggested Citation:

Mazur, N., & Dyshliuk, N. (2025). Morphological features of immune formations of the avian digestive tract. *Scientific Reports of the National University of Life and Environmental Sciences of Ukraine*, 21(5), 28-42. doi: 10.31548/dopovidi/5.2025.28.

*Corresponding author

will allow specialists to objectively assess the effectiveness of methods of prevention and treatment of diseases in poultry farms

Keywords: immune formations; digestive system; lymphocytes; lymphoid tissue; lymphoid nodules

Introduction

The avian digestive tract is not only the primary organ for digestion and nutrient absorption but also a crucial link in ensuring the immune defence of the organism. Its wall contains numerous immune structures that form specialised structures of mucosa-associated lymphoid tissue (MALT), which are actively involved in protective reactions against pathogenic microorganisms that enter the body with food and water. Morphological study of these immune formations is important for understanding the mechanisms of immune response, assessing the resistance of birds, and developing effective veterinary and preventive measures in poultry farming.

Scientists B. Dukhnytskyi & V. Dukhnytskyi (2025) noted that poultry farming is a rapidly growing branch of animal husbandry that deals with the breeding, rearing, keeping and feeding of poultry for the purpose of obtaining eggs, meat and other products. However, one of the challenges is combating poultry diseases that negatively affect the immune system. The resistance of birds to disease is determined by the state of their immune system, which includes lymphoid organs, tissues and cellular elements capable of protecting the body from living organisms and substances that carry signs of foreign genetic information. According to S. Ceccopieri & J.P. Madej (2024), the immune system provides one of the most important adaptive functions of the body, aimed at controlling and maintaining its genetic integrity or homeostasis. The researchers also explained the significant development of immune structures in the digestive tract of birds by the absence of lymph nodes and the lymphoepithelial pharyngeal ring, as well as the prolonged retention of feed masses in certain sections of the digestive tract. Despite the scattered and uneven distribution of immunocompetent structures, the lymphoid-macrophage system responds to antigenic stimuli as a single entity, with a naturally enhanced response at the site of antigen entry.

M. Lu *et al.* (2023) found that the bulk of antigenic material (microorganisms and their waste products) enters the lumen of the digestive organs of birds with food and water. In response to their action, immune structures belonging to the peripheral (secondary) organs of the immune system develop in the wall of the digestive tract. Microscopically, they are represented by diffuse lymphocytic clusters without clear boundaries and lymphoid nodules without light and with light centres, in which the proliferation and differentiation of T and B lymphocytes, the main cells of immune processes, occurs. J. Mehrzad *et al.* (2024) found that proliferation is preceded by blast transformation of lymphocytes. As a result, T lymphocytes differentiate into several types: T killer cells (cytotoxic), which destroy foreign target cells and protect the body from neoplasms; T helper cells, which cooperate with B lymphocytes, without which their transformation into plasma cells is impossible; T suppressor cells, which block antibody formation; T memory cells, which store information about the antigen. Under the action of the antigen, B lymphocytes transform into plasma cells and memory B cells, and plasma cells produce immunoglobulins – components of antibodies that determine the development of humoral immunity. The researchers also noted that in addition to the four classic stages of lymphoid tissue formation characteristic of its morphological development, there is also a fifth stage, which reflects the involutive processes and reverse development of immune structures typical of the organs of the immune system.

J.-C. Weil *et al.* (2023) suggested that in adult birds, after the replacement of the lymphoid nodules of the cloacal sac with loose fibrous and fatty tissues, the function of B-lymphocyte formation is taken over by the peripheral organs of the immune system. G. Garagulya *et al.* (2022) emphasised that immune formations in the digestive organs are mainly associated with the mucous membrane, as it is constantly exposed to antigenic influences, although in some bird species they can also occur in the muscular and serous membranes. A significant part of the immune structures is macroscopically invisible, but in some areas of the inner lining, they are so developed that they form structures in the form of whitish thickenings (oesophageal and caecal tonsils, caecal diverticula, Peyer's patches, etc.). The functional basis of these formations is formed by lymphoid tissue – a collection of lymphocytes in the cells of the reticular tissue, which contains reticulocytes, ground substance and reticular fibres. N. Pendl & R.E. Schmidt (2024) identified four stages in the formation of lymphoid tissue. In the first stage, diffuse tissue is formed with the migration of lymphocytes from the hemocapillaries; in the second stage, cells are more densely arranged and pre-nodes are formed; in the third stage, primary nodes and their aggregates are formed, indicating readiness for the formation of immunocompetent cells; in the fourth stage, secondary lymphoid nodules with a light centre appear, which increase in size upon contact with antigens. This complex of morphological features indicates the functional maturity of immunocompetent structures. S. Zeinali *et al.* (2024) divided lymphoid nodules into two types: perivascular, which are located along the course of the haem- and lymph-microcirculatory channels and belong to the structures of the internal environment of the organism, and lymphoepithelial, which have a close connection with the surface epithelium of the mucous membranes of tubular organs.

The aim of the article was to study the immunocompetent structures of the mucous membranes of the oesophagus, stomach and intestines of various bird species to better understand the functions of their immune systems and improve approaches to prevention and vaccination. To achieve this goal, Ukrainian and foreign publications on the subject were analysed, and works with original research were selected that reveal the topography, macro- and microstructure of the immune formations of the digestive organs of birds. Particular attention was paid to works that used classical morphological methods (anatomical, histological, cytological, immunohistochemical, and statistical).

General characteristics of the digestive system of birds

The digestive system of birds is a long tube that begins at the beak and ends at the rectum with the cloaca (Fig. 1). It also includes digestive glands (liver and pancreas). The digestive tract consists of the oesophagus, stomach and intestines. In the lumen of the gastrointestinal tract, food lumps are broken down by the action of digestive juices, followed by the absorption of nutrients into the blood and lymph and the excretion of indigestible residues outside the body.

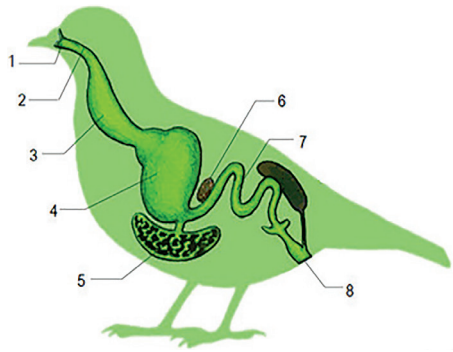

Figure 1. *The digestive system of birds (diagram)*
Note: 1 – beak; 2 – oesophagus; 3 – crop; 4 – stomach; 5 – liver; 6 – pancreas; 7 – intestine; 8 – cloaca
Source: T.V. Kovtun (2023)

One of the initial digestive organs of birds, into which food enters and immune structures develop, as noted by A. Nahed *et al.* (2021) and

Z. Mosa & F. Al-Asadi (2022), is the oesophagus, which has the appearance of an elastic long tube (Fig. 2). It is capable of stretching in diameter, allowing large particles of food and insects to be swallowed. In granivorous birds, at the entrance to the thoracic-abdominal cavity, its wall expands and forms a protrusion – the crop, where food is stored and moistened. A.A. Alsanosy *et al.* (2021) showed in their studies that the crop also serves as a functional barrier to pathogens by lowering the pH through fermentation. S. Qinghui *et al.* (2020) noted that in most species of birds, the stomach is two-chambered and divided into glandular and muscular parts, which are connected by an intermediate zone (Fig. 2).

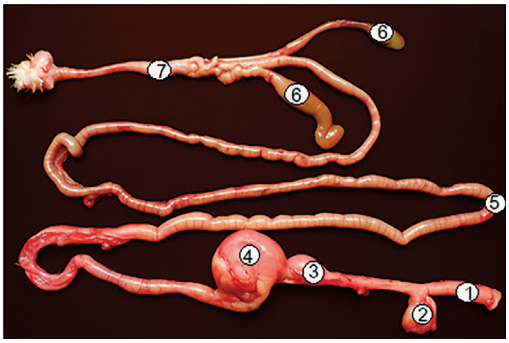

Figure 2. *Anatomical structure of the digestive tract of a domestic turkey (native preparation)*
Note: 1 – oesophagus; 2 – crop; 3 – glandular 4 – muscular parts of the stomach; 5 – small intestine; 6 – caeca; 7 – rectum with cloaca
Source: authors' own work

P.S. Selvan *et al.* (2008) reported the presence of a third pyloric part in wild birds, located at the border between the exit from the stomach and the entrance to the duodenum. It is represented by the pyloric sac, and in domestic birds this part is poorly developed. The glandular part of the stomach looks like a thick-walled tube with a well-defined mucous membrane with superficial and deep glands. The latter are grouped into lobules. In their work, Z. Umar *et al.* (2021), based on histological and histomorphometric analysis of ostriches (*Struthio camelus*) of different ages, showed age-related variability in the structure of the mucous membrane and glands of the stomach. The authors noted a gradual increase in the thickness of the mucosa, the depth of the crypts, and the density of the glands, indicating an increase in secretory activity with age. The data obtained complement the understanding of the functional specialisation of the glandular part of the stomach in birds and demonstrate the importance of the age aspect in assessing the morphology of the digestive tract. In granivorous, herbivorous, and omnivorous birds, they are multi-lobed with a complex branched duct system, while in carnivorous and insectivorous birds, they are single-lobed. In a comparative microscopic study, F. Taki-El-Deen (2017) examined the tongue, oesophagus, and stomach of two bird species, demonstrating significant differences in the structure of the mucous membrane and the organisation of the glands depending on the type of diet. It was shown that granivorous species are characterised by a more complex glandular apparatus, which corresponds to their need for prolonged mechanical and chemical processing of coarse feed. These data confirm the close relationship between the morphology of the digestive tract and the dietary specialisation of birds. The muscular part of the stomach has an elliptical shape with blind sacs located on opposite sides. It is where the mechanical processing of feed takes place, which is why its wall has a well-developed muscular coat. Simple tubular glands in the muscular part of the stomach produce a cuticle (keratin-like film) that covers the mucous membrane and prevents damage to its walls by solid particles. A study by W. Khamas *et al.* (2022), which evaluated the growth and development of digestive organs in two breeds of chickens with different growth rates, showed that significant dynamics in the development of the muscular stomach are observed already in the first four months of life. The authors found a direct relationship between the growth rate of the breed and the rate of formation of its morphological structures, in particular the muscular

membrane and glands, which emphasises the role of genetic factors in the functional maturity of the digestive organs.

As noted by I.O. Kolomak (2023), the intestines of birds are divided into small and large sections of different lengths (Fig. 2). The small intestine, which is the longest, consists of the duodenum, jejunum and ileum. Their mucous membrane forms folds, villi and numerous crypts, which provide the main digestion and absorption of nutrients. The large intestine consists of two blind intestines and the rectum. They are mainly responsible for the formation and excretion of faeces. S. Zeinali *et al.* (2024) showed that the caeca varies in length depending on the bird species. It is short in blackbirds and long in chickens, turkeys, ducks and geese. The wall of the digestive tract of birds contains immune structures that have different locations and development of lymphoid tissue. Their topographical features and structural components are summarised in Table 1.

Table 1. *Sites of localisation and distribution of structural components of immune formations in the avian digestive tract*

Name of organ or part	Minor aggregations of lymphoid cells and solitary lymphoid nodules	Aggregations of lymphoid nodules (Peyer's patches)	Tonsils (islands or continuous layers of lymphoid tissue)
Oesophagus	+	-	-
Crop (Ingluvies)	+	-	-
Oesophagus-proventriculus junction	-	-	Oesophageal tonsil
Proventriculus (Glandular stomach)	+	-	-
Gizzard (Muscular stomach)	+	-	-
Gizzard-duodenum junction	-	-	Pyloric tonsil
Small intestine	-	+	-
Meckel's diverticulum	-	+	-
Caeca	-	+	Caecal tonsils/ diverticula
Rectum	+	-	-

Source: developed by the authors based on O.V. Byrka & M.M. Kushch (2010), L.P. Kharchenko & I.O. Lykova (2013), V.T. Khomich *et al*. (2020)

The highest concentration of lymphoid tissue is found in the tonsils, slightly less in Peyer's patches, and least in individual lymphoid nodules. The uneven development of this tissue and, accordingly, the immune formations in the avian digestive tract organs depends on the intensity of antigenic exposure, feed retention in certain areas, and the thickness of the epithelial covering of the mucous membrane. The morphofunctional features of the immune structures of individual organs of the digestive tract of birds are presented below.

Features of the topography and histostructure of immune formations of the oesophagus, crop and oesophageal tonsil

The microscopic structure of the oesophageal wall in birds of different trophic specialisations largely depends on how they obtain food. Its mucous membrane is lined with a multilayered squamous epithelium, which has varying degrees of keratinisation and contains glands whose size and shape depend on the feeding ecology. In particular, R. Sinha *et al.* (2023), studying the

oesophagus of Japanese quails (*Coturnix japonica*), noted specific morphometric indicators of the mucosa and variations in the degree of epithelial keratinisation, indicating the adaptation of the organ to the peculiarities of food consumption. Similar conclusions were made by R.A. Al-Musawi & S.S. Ali Al-Khakani (2024), who, based on a comparative histochemical analysis of the oesophagus of a turtle dove and a buzzard, showed differences in the size and shape of the glands directly related to the type of diet and method of food procurement. R. Al-Musawi & S. Ali Al-Khakani (2024) found that in the grey turtle dove, they are absent in the cervical part of the organ. In many species of birds, diffusely scattered lymphoid cells and lymphoid nodules are located near the glands. The work of C. Casteleyn *et al*. (2010) provided a general overview of the localisation of lymphoid structures in chickens, emphasising the importance of the oesophagus as an area with a high concentration of GALT. N.J. Monisha *et al*. (2024a), analysing the histomorphometry of the digestive tract of broilers and roosters in Bangladesh, confirmed the presence of a significant number of immunocompetent cells in the oesophageal wall, which provides local immune protection. Research by M. Mahdy & E. Mohammed (2024) on domestic pigeons supplemented these data, demonstrating the diversity of the cellular composition of the mucosa depending on the age and functional activity of the organ.

Contact of the organism with the external environment and changes in the type of nutrition cause the development of subepithelial lymphoid barriers of the digestive tract in the first days of life after hatching, forming a local immune system. However, such a system is quite limited in the early stages of post-embryonic development and only intensifies with age. L. Horalsky & V. Gatskivsky (2009) found isolated lymphoid nodules with a diameter of 86 ± 9 μm to 172 ± 27 μm in the cervical part of the duck's oesophagus, while they were absent in the thoracic-abdominal part of the organ. Research by S. Kots (2009) shows that the mucous membrane of the oesophagus of birds of the heron family forms longitudinal wave-like folds with different configurations of bends and contains densely located oesophageal glands in the lamina propria of the mucous membrane. Lymphocytes in the middle and caudal sections of the grey heron's oesophagus are mainly located near the basement membrane of the secretory sections of the glands. The author suggests that these cells may migrate to the surface of the epithelial layer, where they work with gland secretions to protect the mucous membrane. Lymphocytes in the middle section of the oesophagus form clusters in the form of diffuse lymphoid tissue, and in the area of its transition to the stomach, there are 9 to 10 oval-shaped lymphoid nodules, which is probably associated with food retention during increased feeding.

Histological studies by H. Ali *et al.* (2023) showed that the shape of the folds of the mucous membrane of the oesophagus of pigeons differs in its individual parts and also depends on the age category of the birds. The cervical part of this organ in young pigeons had primary folds of the mucous membrane with a small number of secondary folds, while in adults, they were heavily folded and divided into primary, secondary and tertiary folds. Isolated clusters of diffuse lymphoid tissue were recorded in the plane of the folds. N. Hamoda & A. Farag (2018) also found lymphoid nodules in the oesophagus of pigeons, located in the lamina propria of the mucous membrane and the submucosal base. Some of them were also recorded in the muscular and serous membranes. According to the authors, the lymphoid tissue of the digestive tract can serve as an indicator for understanding the immune response after oral administration of vaccines.

The immune formations of the esophagus of waders are located in the lamina propria of the mucous membrane under the surface epithelium and near the glandular packets. They are mainly represented by a diffuse form and isolated lymphoid nodules (Kharchenko & Lykova, 2013). A similar location of immunocompetent structures was observed in the oesophagus of the African

ostrich by O. Byrka (2017). M. Kovtun & L. Kharchenko (2005) identified diffuse lymphocytic aggregations and isolated lymphoid nodules in the oesophagus of sexually mature pheasants, quails, and rooks, whereas in chaffinches and bee-eaters only minor lymphocytic infiltration of the mucosa was observed. The immune formations showed a close morphofunctional association with the secretory portions of the glands, forming immunosecretory complexes. These complexes provided a protective barrier, enabling mucus on the epithelial surface to retain secretory immunoglobulins. In the region where the oesophagus transitions into the glandular part of the stomach in pheasants, quails, and rooks, well-developed clusters of lymphoid formations were observed. They were represented by lymphoid nodules, both without and with germinal centres, as well as diffuse lymphoid tissue. In the transitional zone of the bee-eater, only intensive diffuse infiltration of the mucosa was recorded, while in the chaffinch no lymphoid tissue was found. On this basis, the researchers suggested that in the bee-eater and the chaffinch, the oesophageal tonsil, as a distinct immune formation, is absent.

The lymphoid tissue of the esophageal tonsil of day-old quails is immature. Lymphoid nodules with pronounced centres of proliferation were recorded in it starting from 30 days of age. They are located in the mucous membrane singly and in the form of conglomerates (2-3 or more) (Kryvutenko, 1996). According to research by H. Sağsöz & N. Liman (2009), the oesophageal tonsil of quails begins to form on the 5th day after hatching. In day-old turkeys, the lymphoid tissue of the oesophageal tonsil is also undeveloped. Its development begins on the 30th day, and in 60-90-day-old birds, secondary lymphoid nodules appear, mainly in females, which is associated with their sexual maturation (Kryvutenko, 1984). According to research by L.O. Bugay (2008), in day-old muscovy ducks, the oesophageal tonsil was not macroscopically detectable, while in 5- and 10-day-old ducks, blurred spots were observed. Its most intensive growth occurred between 15 and 30 days and between 90 and 180 days. The oesophageal tonsil reached its maximum relative area in birds aged 30 days. In her studies, N. Petushinova (1985) noted that the lymphoid formations of the digestive organs of 49-day-old "Broiler-6" crossbred chickens are located in the caudal part of the oesophagus around individual terminal sections of the mucous glands in the form of more or less significant diffuse formations, and in the oesophageal tonsil there were up to 20 lymphoid nodules, which were limited by thin collagen fibres that were closely connected to the lamina propria of the mucous membrane. The same fibres penetrated into the thickness of the lymphoid nodules. According to research by N. Nagy *et al.* (2005), the oesophageal tonsil of 6-8-week-old chickens consisted of 6-8 separate units limited by a thin fibrous capsule. Each of them was located in the area of the bottom of the longitudinal folds and served as a "tonsil crypt". The surface epithelium of the tonsil location area was infiltrated with lymphoid, plasma, dendritic cells and macrophages.

According to morphological studies by N. Nagy *et al.* (2005), the oesophageal tonsil of chickens and ducks is divided into eight tonsillar units depending on the number of longitudinal folds, which lie in their own mucosal plate. Each tonsillar unit delimits a crypt lined with multilayered squamous epithelium infiltrated with lymphocytes. N. Arai (1987) noted in his studies that the oesophageal tonsil of chickens produces not only IgA, which is important for the protection of the mucous membrane, but also IgG for systemic immunity. In this respect, it is similar to the palatine tonsils of mammals. V. Indu & K. Lucy (2021) noted that the oesophageal tonsil of 12-week-old "White Leghorn" chickens contains large lymphoid nodules separated by internodular areas and bounded by a connective tissue capsule. G. Krok & N. Musyenko (1976) studied the development of lymphoid tissue in the area of the oesophageal tonsil of highly productive lines of chickens aged one, 10, 30, 60 and 90 days. It was shown that in this area of day-old birds,

proliferation of reticular tissue was observed, and lymphoblasts and agranulocytes of varying degrees of maturity appeared. At 10 days of age, there was active proliferation of lymphoid elements located around the terminal sections of the glands. At 30 days of age, lymphoid tissue with diffuse clusters and lymphoid nodules with light centres was well developed and formed the oesophageal tonsil. In some areas, lymphoid elements reached the central lumens of the glands and migrated into their space. The oesophageal tonsil reached its maximum development in 60-day-old birds and contained numerous nodules with reactive centres.

The most complete macroscopic and microscopic study of the oesophageal tonsil in selected species of domestic and wild birds was conducted by V. Khomich *et al*. (2020). Macroscopically, this immune formation is evident in the chicken, quail, turkey, duck, goose, guinea fowl, common pheasant, hazel grouse, common peacock, Canada goose, magpie, hooded crow, and white stork as a thickened, whitish strip with a yellowish tint at the boundary between the oesophagus and the stomach. It is not visually noticeable in the willow ptarmigan, jay, common moorhen, Eurasian coot, and rock dove (feral pigeon). Depending on the development of the lymphoid tissue, the authors proposed dividing avian tonsils into diffuse and compact. In the former, the tissue occupied a significantly larger area than in the latter. Structural levels of lymphoid tissue organisation were found in the mucous membrane, with the diffuse form being widespread. The largest area of lymphoid tissue was observed in the domestic duck (68.64 ± 0.70%), and the smallest in the willow ptarmigan (2.31 ± 0.05%). Solitary lymphoid nodules and diffuse lymphoid tissue were also detected in the muscular and serous coats of the guinea fowl, goose, duck, Canada goose, common moorhen, and coot. Between the oesophageal tonsil and the glandular part of the stomach in the goose and Canada goose, there was an intermediate zone without oesophageal glands or lobules of deep glands, but with localised clusters of lymphoid cells in the mucous membrane. The researchers believe this transition zone is a species-specific feature of these birds. The composition of the lymphoid tissue in the chicken oesophageal tonsil included reticular cells, immunoblasts, lymphocytes, plasmocytes, monocytes, and macrophages. Among the lymphocytes, subpopulations were found that reacted to monoclonal antibodies with markers CD4+ (T-helper cells), CD8+ (T-cytotoxic/T-suppressor cells), and CD20+ (mature B-lymphocytes).

Features of the topography and histostructure of immune formations in the stomach and intestines

R. Matsumoto & Y. Hashimoto (2000) found clusters of lymphocytes located in three different areas of the lamina propria on the 20th day of incubation in the mucous membrane of the glandular part of the chicken stomach, namely under the surface epithelium, near the excretory ducts of the deep glands and in the wall of the glands themselves. In the third week after hatching, lymphoid nodules with a germinative centre were found in the deep glands. The latter was limited by densely located lymphocytes. The researchers noted that such nodules are formed as a result of the action of antigens present in the lumen of the stomach. N. Petushinova (1985) recorded lymphoid formations in the form of diffusely located cellular elements and lymphoid nodules (3-5 on the histological section) in "Broiler-6" crossbred chickens in the area of the transition of the muscular stomach to the duodenum. They were located among the crypts, under them and in the villi. They consisted of lymphocytes, macrophages and plasma cell precursors. According to N. Nagy & I. Olah (2007), the pyloric tonsil is a new peripheral organ of the immune system. According to their data, it forms a lymphoid ring in chickens.

According to morphological studies by S. Usenko (2023), immune formations in the glandular and muscular parts of the stomach of the waterfowl are represented by various forms of lymphoid tissue and occupy unequal areas. Such

clusters are localised in the lamina propria of the mucous membrane and are formed by a diffuse form in the muscular part and all forms of lymphoid tissue in its glandular part. The lamina propria of the mucous membrane of the pigeon stomach contains diffuse lymphoid tissue, which is located mainly near and between the tubular glands. Similar accumulations of lymphoid tissue are found in the lamina propria and submucosal base at the border of the stomach and duodenum, forming pyloric tonsils, and lymphocytes from these accumulations penetrate the surface epithelium, forming lymphoepithelium. The latter covers the crypts between the villi. The wall of the glandular and muscular parts of the stomach of sandpipers is moderately infiltrated with lymphoid cells. Between the simple tubular glands of the lamina propria of the mucous membrane are unformed lymphoid nodules (Kharchenko & Lykova, 2013). In the grey crow, the mucous membrane of the glandular part of the stomach is infiltrated with lymphocytes and contains lymphoid aggregates located between the superficial tubular glands (Maksoud *et al.*, 2022). According to morphological studies by S. Kots (2009), in representatives of the heron family, the wall of the pyloric sac contains numerous immune formations that act as a protective "filter" when chyme moves from the stomach to the duodenum. They are located in the lamina propria of the mucous membrane, and isolated lymphoid nodules are also found in the circular layer of the muscular membrane.

After hatching, the intestines of chickens are sparsely populated with lymphocytes, so acquired immunity is practically undeveloped in the first days of life (Logvinova *et al.*, 2020). Protection during this critical period is the result of the activity of maternal antibodies or the innate immune system. IgA plays an important role in defence mechanisms, as it is associated with the mucous membrane and participates in the neutralisation of antigens in the intestine (Friedman *et al.*, 2003). The empty intestine of chickens contains immune structures represented by scattered Peyer's patches and Meckel's diverticulum. Peyer's patches form on the 5th day after hatching, and in birds 30 days old and older, there are 3 to 10 of them. Meckel's diverticulum forms in day-old chickens and contains lymphoid cells in its own mucosal membrane (Kalinovska, 2006). I. Kalinovska (2002) conducted a study of the blind intestines of 150-day-old Leghorn chickens. The author found that they contain cecal tonsils and Peyer's patches, which are macroscopically visible and located in the lamina propria of the mucous membrane, and Peyer's patches are also located in the submucosal base. The immune structures of the caeca are formed by connective tissue stroma, lymphoid tissue in the form of a diffuse form and lymphoid nodules, and a system of crypts. The latter are absent in some Peyer's patches. In the cecal tonsil, connective tissue stroma accounted for 12.38 ± 2.63%, lymphoid tissue for 71.01 ± 3.17%, and crypts for 16.60 ± 3.51% of their area.

O. Prokushenkova *et al.* (2012) noted that lymphoid structures in the duodenum of muscovy ducks appear 20-25 days after hatching in the form of diffuse lymphoid tissue, while secondary lymphoid nodules are found in sexually mature individuals aged 210-240 days. In the jejunum and ileum, the formation of such structures occurs in three periods: the development of diffuse lymphoid tissue (20-25 days), the formation of primary (25-60 days) and secondary lymphoid nodules (60-240 days). V. Logvinova & A. Oliyar (2021) identified four stages in the development of lymphoid structures in the wall of the small intestine of muscovy ducks. The first stage (5-25 days) is characterised by the development of diffuse lymphoid tissue. In the second stage (25-60 days), lymphoid nodules without centres and with light centres are formed. The third stage (60-240 days) is characterised by the formation of aggregated lymphoid nodules. At the fourth stage (90-240 days), the lymphoid nodules increase in size, as a result of which the lymphoid tissue occupies almost the entire area of its own mucosal membrane. Subsequently, groups of lymphoid nodules penetrate the muscular layer of this membrane and penetrate the muscular

membrane of the small intestine, where they are separated by muscle layers. Lymphoid nodules in the muscular membrane of the intestine of muscovy ducks were also found by N. Dyshliuk *et al.* (2022).

T. Mazurkevych & V. Khomych (2019) conducted a study of the immune formations of the intestine of Blagovar cross broiler ducks from day-old to 420 days of age. It was found that they are represented by Peyer's patches, Meckel's diverticulum and cecal diverticula. One Peyer's patch was found in the duodenum and ileum, three in the jejunum of ducks from hatching to 240 days, two at 330 days, and one at 420 days. Each caeca contained 60 to 80 Peyer's patches arranged in a chain. Complete morphofunctional maturity of the cecal diverticula was observed on day 10, Peyer's patches of the duodenum, jejunum and cecum on day 15, and Peyer's patches of the ileum and Meckel's diverticulum on day 20. Lymphoid nodules were predominantly oval and elongated oval in shape. The linear indices of secondary lymphoid nodules were greater than those of primary nodules. Small and medium-sized lymphocytes, immunoblasts, proplasmacytes, plasmacytes, and macrophages predominated in the immune formations of the duck intestine. Ducks aged 180 days had stem cells (CD34+), which, according to the researchers, indicates the possible development of T and B lymphocytes in them, while in 30-, 150- and 180-day-old birds, T-helper lymphocytes (CD4+), T-cytotoxic/T-suppressors (CD8+), naive T-cells (CD44+), mature B-lymphocytes (CD20+), early B-lymphocytes (CD24+) and natural killer cells (CD56+).

Immune structures are located along the entire length of the intestine, localised in the lamina propria of the mucous membrane. The largest number of them is concentrated in the wall of the ileum. The epithelium of the intestinal villi of the small intestine contains a significant number of diffusely located lymphocytes. In the wall of the transitional zone of the small intestine to the rectum, there is Peyer's patch, which is represented by clusters of diffuse form and densely located lymphoid nodules. N. Hamoda & A. Farag (2018) found lymphocytic infiltration of the lamina propria and submucosal base of the mucous membrane and lymphoid nodules throughout the intestine of pigeons. The latter were located at the base of the short villi. Individual isolated lymphoid nodules were also found in the muscularis and subserosal layer. Lymphocytes infiltrated the simple cylindrical epithelium of the intestinal villi. The greatest infiltration and lymphoid nodules were observed in the ileum and caeca.

O.V. Byrka & M.M. Kushch (2010) noted that the Meckel's diverticulum of large grey geese is hook-shaped and located on the antimesenteric surface of the small intestine. Its own plate and submucosal base of the mucous membrane are infiltrated with lymphocytes, and lymphoid nodules are located at different depths. In some folds, small clusters of lymphoid cells form a pre-nodular form of lymphoid tissue. Secondary lymphoid nodules are also found in the muscularis and subserosal base of the serosa. According to research by N. Monisha *et al.* (2024b), there are more lymphoid nodules and a higher density of lymphocytes in the Meckel's diverticulum than in local chickens in Bangladesh. L.P. Kharchenko & I.O. Lykova (2013) reported that the mucous membrane of the Meckel's diverticulum of waders is densely infiltrated with elements of lymphoid tissue and contains large lymphoid nodules with pronounced light centres. Individual nodules are also located in the muscular and serous membranes. The lamina propria of the mucous membrane of the blind intestines of waders is moderately infiltrated with lymphocytes, and the mesentery also contains unformed lymphoid nodules. The latter are also located in the submucosal base of the rectum of waders.

Conclusions

The functions of the pperipheral organs of the avian immune system are aimed at creating biological protection for the body against antigenic influences. The absence of lymph nodes is compensated by well-developed immunocompetent structures associated with the mucous membrane

of the digestive tract in the form of diffusely scattered lymphocytes and lymphoid nodules of varying degrees of maturity. The development of immune structures depends on the species, sex, age category, feeding and housing conditions, and feed specialisation of birds. They are mainly located in the lamina propria and submucosal base of the mucous membrane and appear as small clusters of lymphoid tissue and their aggregates. Immune formations lie under the epithelial layer, near the glands (oesophageal, gastric, Lieberkühn) and their excretory ducts.

Lymphoid cells from separate immunocompetent structures migrate into the surface and glandular epithelium and are found between epithelial cells and in the gland wall. In the areas of the digestive tract that are most exposed to antigenic influence, there are well-organised immunocompetent structures in the form of tonsils (oesophageal, caecal), Meckel's diverticulum, caecal diverticula and groups of lymphoid nodules (Peyer's patches). Establishing the characteristics of their functioning in birds is important for understanding the presence or absence of full-fledged specific immunity (cellular and humoral defence) at the local level in the digestive tract. The composition of immunocompetent structures indicates the diversity of cells (lymphocytes, plasma cells, macrophages, etc.) present in birds of all ages.

The physiological processes that occur in them emphasise the importance of such formations in the immune defence system. Knowledge of the structure of the immune formations in the avian digestive tract will help in developing more effective prevention and treatment of infectious diseases and local inflammatory processes of the mucous membranes. Based on the above, it becomes obvious that the study of the species and age morphology of these structures in birds is quite relevant and is not only of scientific interest but also has great practical significance. Promising areas for further research on this topic may include the analysis and generalisation of data on the morphological features of the immune structures of the digestive tract of other representatives of the animal world.

Acknowledgements

None.

Funding

None.

Conflict of Interest

None.

References

[1] Ali, H.M., Ali, K.A., & Taha, A.M. (2023). Comparative anatomical, histological, and electron microscopical studies on the cervical region of the esophagus in some birds with different diet habits. *Journal of Advanced Veterinary Research*, 13(2), 181-187.

[2] Al-Musawi, R.A, & Ali Al-Khakani, S.S. (2024). Comparative morphological and histochemical study of esophagus, in eurasian collared dove (*Streptoplia decaocto*) and buzzard (*Beuteo beuteo vulpinus*). *Journal of Anatomy and Physiology,* 5(3), 58-65. doi: 10.36346/sarjap.2024.v05i03.004.

[3] Alsanosy, A.A., Noreldin, A.E., Elewa, Y.H.A., Mahmoud, S.F., Elnasharty, M.A. & Aboelnour, A. (2021). Comparative features of the upper alimentary tract in the domestic fowl (*Gallus gallus domesticus*) and kestrel (*Falco tinnunculus*): A morphological, histochemical, and scanning electron microscopic study. *Microscopy and Microanalysis*, 27(1), 201-214. doi: 10.1017/S1431927620024812.

[4] Arai, N. (1987). Immunohistochemical study on the lymphoid tissues associated with the upper digestive and respiratory tracts of chicken. *Japanese Journal of Veterinary Research,* 35(2), 122-122.

[5] Bugay, L.O. (2008). Peculiarities of the dynamics of macro-microscopic parameters of the esophageal tonsil of musk ducks in early postnatal ontogenesis. *Scientific Bulletin of the Lviv National University of Veterinary Medicine and Biotechnology named after S.Z. Gzhytsky*, 10(2), 16-20.

[6] Byrka, O.V. (2017). Protective morphological formations of the esophageal mucosa in the African ostrich. *Bulletin of the Zhytomyr Agroecological University*, 1(60), 7-12.

[7] Byrka, O.V., & Kushch, M.M. (2010). Morphological characteristics of the jejunal diverticulum (Meckel's diverticulum) of goslings. *Problems of Zooengineering and Veterinary Medicine*, 1(21), 15-19.

[8] Casteleyn, C., Doom, M., Lambrechts, E., Van den Broeck, W., Simoens, P., & Cornillie, P. (2010). Locations of gut-associated lymphoid tissue in the 3-month-old chicken: A review. *Avian Pathology,* 39(3), 143-150. doi: 10.1080/03079451003786105.

[9] Ceccopieri, C., & Madej, J.P. (2024). Chicken secondary lymphoid tissues – structure and relevance in immunologiдcal research. *Animals*, 14(16), article number 2439. doi: 10.3390/ani14162439.

[10] Dukhnytskyi, B., & Dukhnytskyi, V. (2025). State and problems of livestock development in Ukraine. *Herald of Khmelnytskyi National University,* 342, 3(2), 102-107. doi: 10.31891/2307-5740-2025-342-3(2)-16.

[11] Dyshliuk, N., Huralska, S., & Mamai, O. (2022). Morphology of the digestive canal organs and their immune formations in the mulard ducks. *Ukrainian Journal of Veterinary Sciences*, 13(2), 16-25. doi: 10.31548/ujvs.13(2).2022.16-25.

[12] Friedman, A., Bar-Shira, E., & Sklan, D. (2003). Ontogeny of gut associated immune competence in the chick. *World's Poultry Science Journal*, 59(2), 209-219. doi: 10.1079/WPS20030013.

[13] Garagulya, G., Severyn, R., Momot, A., & Zhunko, I. (2022). Immune system of birds and mammals: Comparative characteristics *Agrarian Bulletin Black Sea Littoral*, 104, 41-58. doi: 10.37000/abbsl.2022.104.06.

[14] Hamoda, H., & Farag, A. (2018). Histological characterizations of the gut associated lymphatic tissue in pigeon. *Alexandria Journal of Veterinary Sciences*, 59(2), 157-164. doi: 10.5455/ajvs.16178.

[15] Horalsky, L.P., & Gatskivsky, V.V. (2009). Histomorphology of the esophagus of poultry. *Scientific Bulletin of the Lviv National University of Veterinary Medicine and Biotechnology named after S.Z. Gzhytsky*, 11(2), 72-77.

[16] Indu, V.R., & Lucy, K.M. (2021). Histology and histochemistry of the oesophageal tonsils in White Leghorn chicken. *International Journal of Current Microbiology and Appied Sciences*,10(06), 304-308. doi: 10.20546/ijcmas.2021.1006.032.

[17] Kalinovska, I.G. (2002). Aggregated lymphoid nodules of the cecum of Leghorn chickens. *Bulletin of the State Agroecological University*, 2, 55-57.

[18] Kalinovska, I.G. (2006). Immune formations of the jejunum of chickens. *Scientific and Practical Journal Taurida Medical and Biological Bulletin*, 9(3), 61-64.

[19] Khamas, W., Babjee, S.A., Noordin, M.M., Kadhim, K.K., & Zuki, A.B.Z. (2022). Growth evaluation of selected digestive organs from day one to four months post-hatch in two breeds of chicken known to differ greatly in growth rate. *Journal of Animal and Veterinary Advances*, 995-1004. doi: 10.36478/javaa.2010.995.1004.

[20] Kharchenko, L.P., & Lykova, I.O. (2013). Lymphoid structures of the digestive tract of waders (Charadrii). *Bulletin of the V.N. Karazin Kharkiv National University. Series: Biology*, 17(1056), 123-130.

[21] Khomich, V.T., Usenko, S.I., & Dyshliuk, N.V. (2020). Morphofunctional features of the esophageal tonsil in some wild and domestic bird species. *Regulatory Mechanisms in Biosyste,* 11(2), 207-213.

[22] Kolomak, I.O. (2023). Morphological features of the digestive system of the blue pigeon. (Columba livia). *Zoology and Veterinary Medicine*, 170, 118-122. doi: 10.36016/JVMBBS-2024-10-1-2.

[23] Kots, S.M. (2009). Peculiarities of the morphofunctional organization of the digestive system of representatives of the heron family (comparative aspect). *Biology and Valeology*, 11, 59-66.

[24] Kovtun, M.F., & Kharchenko, L.P. (2005). Lymphatic formation of the alimentary tube of Birds: its characteristics and biological importance. *Vestnik Zoologii*, 39(6), 51-60.

[25] Kovtun, T.V. (2023). *General characteristics of the class Birds internal structure and features of the life of birds*. Retrieved from https://surl.li/ghpzjj.

[26] Krok, G.S., & Musyenko, N.A. (1976). Histogenesis of the subepithelial lymphoid tissue of the digestive tract in some highly productive partridges. *Proceedings of the Kharkiv Rural Institute named after V.V. Dokuchaev Kharkiv*, 227, 122-129.

[27] Kryvutenko, A.I. (1984). Morphological formation of the organs of the immune system of turkeys in the age aspect. *Infectious and Invasive Diseases of Rural Areas Animals and Birds*, 30-36.

[28] Kryvutenko, A.I. (1996). Morphology and function of immune system organs of intact and rickets-affected Pharaoh quails in the postembryonic period. In *Current issues of veterinary pathology: Proceedings of the first all-Ukrainian scientific and production conference of veterinary pathologists* (pp. 158-159). Kyiv.

[29] Logvinova, V., & Oliyar, A. (2021). Histoarchitectonics of lymphoid formations of the mucosa of the small intestine of muscy ducks. *Bulletin of Sumy National Agrarian University,* 1(52), 31-37. doi: 10.32845/bsnau.vet.2021.1.5.

[30] Logvinova, V.V., Oliyar, A.V., & Lieshchova, M.A. (2020). Formation of immune structures in small intestine of Muscovy ducks (*Cairina moschata*). *Theoretical and Applied Veterinary Medicine*, 8(1), 50-55. doi: 10.32819/2020.81008.

[31] Lu, M., Lee, Y., & Lillehoy, H.S. (2023). Evolution of developmental and comparative immunology in poultry: The regulators and the regulated. *Developmental & Comparative Immunology*, 138, article number 104525. doi: 10.1016/j.dci.2022.104525.

[32] Mahdy, M.A.A., & Mohammed, E.S.I. (2024). Anatomical, histological, and scanning electron microscopic features of the esophagus and crop in young and adult domestic pigeons (*Columba livia Domestica*). *BMC Veterinary Research*, 20(1), article number 428. doi: 10.1186/s12917-024-04147-z.

[33] Maksoud, M.K.A, Ibrahim, A.A, Nabil, T.M, & Moawad, U.K. (2022). Histomorphological, histochemical and scanning electron microscopic investigation of the proventriculus (*Ventriculus glandularis*) of the hooded crow (*Corvus cornix*). *Anatomia, Histologia, Embryology*, 51(3), 380-389. doi: 10.1111/ahe.12798.

[34] Matsumoto, R., & Hashimoto, Y. (2000). Distribution and developmental change of lymphoid tissues in the chicken proventriculus. *Journal of Veterinary Medical Science*, 62(2), 161-167. doi: 10.1292/jvms.62.161.

[35] Mazurkevych, T.A., & Khomych, V.T. (2019). The structure and topography of lymphoid tissue in immune formations of intestines in ducks. *Ukrainian Journal of Veterinary Sciences*, 10(2), 4-12. doi: 10.31548/ujvs2019.02.004.

[36] Mehrzad, J., Shojaei, S., Keivan, F., Forouzanpour, D., Sepahvand, H., Kordi, A., & Houshmand, P. (2024). Avian innate and adaptive immune components: A comprehensive review. *Journal of Poultry Sciences and Avian Diseases,* 2(3), 73-96.

[37] Monisha, N.J., John, A.S., Sojol, S.H., Islam, R., Sultana, N., & Islam, M.R. (2024a). Histomorphometry of the gastrointestinal tract of the broiler and cock chicken in Bangladesh. *Bangladesh Journal of Veterinary Medicine*, 22(2), 33-42. doi: 10.33109/bjvmjd2024am1.

[38] Monisha, N.J., Sojol, S.H., John, A.S., Islam, R., Haque, Z., Ali Khan, A.H.N., & Islam, M.R. (2024b). Histomorphometry of gastrointestinal tract mucosae of sonali and indigenous chickens in Bangladesh. *Journal of Science and Technology Research*, 6(1), 33-44. doi: 10.3329/jscitr.v6i1.77373.

[39] Mosa, Z.A., & Al-Asadi, F.S. (2022). Morphological development of the digestive tract at pre and post hatch period in broiler chicks (*Gallus gallus domesticus*). *University of Thi-Qar Journal of Agricultural Research*, 11(2), 329-342. doi: 10.54174/utjagr.v11i2.212.

[40] Nagy, N., & Olah, I. (2007). Pyloric tonsil as a novel gut-associated lymphoepithelial organ of the chicken. *Journal of Anatomy*, 211(3), 407-411. doi: 10.1111/j.1469-7580.2007.00766.x.

[41] Nagy, N., Igyártó, B., Magyar, A., Gazdag, E., Palya, V., & Oláh, I. (2005). Oesophageal tonsil of the chicken. *Acta Veterinaria Hungarica,* 53(2), 173-188. doi: 10.1556/AVet.53.2005.2.3.

[42] Nahed, A., Lamiaa, E.M., & Ghada, M. (2021). Comparative histological study of esophagus and liver in some aquatic birds. *International Journal of Advanced Research*, 9, 50-55. doi: 10.21474/IJAR01/12416.

[43] Pendl, H., & Schmidt R.E. (2024). Lymphatic and hematopoietic system pathology of pet and aviary birds. In *Pathology of pet and aviary birds* (pp. 307-341). Hoboken: John Wiley & Sons, Ltd. doi: 10.1002/9781119650522.ch9.

[44] Petushinova, N.V. (1985). Age-related changes in the histostructure of the esophageal tonsil of chickens during the selection of the cross "Broiler-6". In *Intensification of poultry farming. Proceedings of the Kharkiv Agricultural Institute named after V.V. Dokuchaev* (pp. 80-84). Kharkiv: Kharkiv Agricultural Institute named after V.V. Dokuchaev.

[45] Prokushenkova, O.G., Tishkina, N.M., & Barsukova, V.V. (2012). Regularities of differentiation of lymphoid structures of the small intestine of musk ducks during early postnatal ontogenesis. *Scientific Bulletin of Luhansk National Agrarian University*, 40, 159-165.

[46] Qinghui, S., Di W., Hansuo, L., Shad, M., & Xiangshu, P. (2020). The impact of wheat bran on the morphology and physiology of the gastrointestinal tract in broiler chickens. *Animals*, 10(10), article number 1831. doi: 10.3390/ani10101831.

[47] Sağsöz, H., & Liman, N. (2009). Structure of the oesophagus and morphometric, histochemical-immunohistochemical profiles of the oesophageal gland during the post-hatching period of japanese quails (*Coturnix coturnix japonica*). *Anatomia, Histologia, Embryologia*, 38(5), 330-340. doi: 10.1111/j.1439-0264.2009.00947.x.

[48] Selvan, P.S., Ushakumary, S., & Ramesh, G. (2008). Studies on the histochemistry of the proventriculus and gizzard of post-hatch Guinea Fowl (*Numida meleagris*). *International Journal of Poultry Science*, 7(11), 1112-1116. doi: 10.3923/ijps.2008.1112.1116.

[49] Sinha, R., Kumar, P., Kumar, A., & Dar, Y. (2023). Morphological and мorphometrical study on oesophagus of Japanese Quail (*Coturnix japonica*). *Journal of Animal Research*, 13(03), 387-391. doi: 10.30954/2277-940X.03.2023.12.

[50] Taki-El-Deen, F. (2017). Comparative microscopic study on the tongue, oesophagus and stomach of two different birds in Egypt. *The Egyptian Journal of Hospital Medicine*, 67(1), 359-365. doi: 10.12816/0036649.

[51] Umar, Z., Quresh, A.S., Shahid, R., & Deeba, F. (2021). Histological and histomorphometric study of the cranial digestive tract of ostriches (*Struthio camelus*) with advancing age. *Veterinarni Medicina*, 66(04), 127-139. doi: 10.17221/120/2020-VETMED.

[52] Usenko, S. (2023). Morphofunctional features of immune formations of the stomach of the *Gallinula chloropus*. *Materials of the scientific and practical conference "Food safety and quality in the one health concept"* (p. 55). Lviv: LNU of Veterinary Medicine and Biotechnologies.

[53] Weil, J.-C., Weller, S., & Reynaud, C.-A. (2023). B cell diversification in gut-associated lymphoid tissues: From birds to humans. *Journal of Experimental Medicine*, 220(11), article number e20231501. doi: 10.1084/jem.20231501.

[54] Zeinali, S., Sutton, K., & Vervelde, L. (2024). Distribution and spatiotemporal development of organised lymphoid tissues in the chicken intestinal tract. *Developmental & Comparative Immunology*, 151, article number 105096. doi: 10.1016/j.dci.2023.105096.

Морфологічні особливості імунних утворень травного каналу птахів

Наталя Мазур
Здобувач ступеня доктора філософії
Національний університет біоресурсів і природокористування України
03041, вул. Героїв Оборони, 15, м. Київ, Україна
https://orcid.org/0009-0004-5747-4335
Надія Дишлюк
Доктор ветеринарних наук, професор
Національний університет біоресурсів і природокористування України
03041, вул. Героїв Оборони, 15, м. Київ, Україна
https://orcid.org/0000-0003-4753-9356

Анотація. Імунокомпетентні структури органів травлення відіграють важливу роль в захисті організму від бактеріальних та вірусних інфекцій надаючи імунну відповідь. Метою даної роботи було встановити і узагальнити морфологічні особливості цих структур у птахів різних видів, що дозволить з'ясувати їх морфофункціональний статус, який визначається станом природньої резистентності і реактивності організму та виявити критичні періоди в розвитку імунної системи. Для досягнення мети був проведений літературний аналіз сучасних досліджень з топографії та мікроструктури імунних утворень органів травлення птахів. Встановлено, що матеріальною основою цих структур є лімфоїдна тканина, диференціація якої має регіональні особливості, відбувається у певній послідовності і проходить у декілька етапів. Її розвиток залежить від віку, виду, статі, типу живлення птахів та структурно-адаптаційних особливостей органів травлення. Імунні утворення локалізовані переважно у слизовій оболонці травного каналу, а у птахів окремих видів ще й у м'язовій та серозній оболонках. До їх складу входять Т- і В-лімфоцити та їх ефекторні клітини, які виконують важливі функції клітинного надзору у захисті організму від чужерідної генетичної інформації. Зазначено, що вони мають тісний контакт з макрофагами і функціонують як єдина лімфоїдно-макрофагальна система. Представлені наукові дослідження розширюють і доповнюють знання щодо видових, породних і морфологічних особливостей будови імунних утворень травного каналу птахів, що дасть змогу спеціалістам обєктивно оцінити ефективність методів профілактики і лікування захворювань на птахівничих господарствах

Ключові слова: імунні утворення; апарат травлення; лімфоцити; лімфоїдна тканина; лімфоїдні вузлики

Received 30.04.2025 Revised 29.07.2025 Accepted 23.09.2025

Vol. 21, No. 5
2025

Scientific Reports of the National University of Life and Environmental Sciences of Ukraine

Journal homepage: https://scireports.com.ua/en

UDC 630*262:582.736.3:574.42(477.44)

Doi: 10.31548/dopovidi/5.2025.43

Structural characteristics of pine stands and analysis of the invasive spread of black locust (*Robinia pseudoacacia* L.) near the settlement of Dashiv, Vinnytsia region

Vasyl Krasnoshtan*
PhD
Pavlo Tychyna Uman State Pedagogical University
20300, 2 Sadova Str., Uman, Ukraine
https://orcid.org/0000-0001-8572-5008
Ihor Krasnoshtan
PhD in Biological Sciences, Associate Professor
Pavlo Tychyna Uman State Pedagogical University
20300, 2 Sadova Str., Uman, Ukraine
https://orcid.org/0000-0003-1317-546X

Abstract. One of the key problems of modern ecology and forestry is the spread of black locust, which leads to the transformation of forest ecosystems and loss of biodiversity. The aim of the study was to determine the structural features of secondary pine stands and analyse the invasive spread of *Robinia pseudoacacia* L. The study was conducted in 2025 in a pine forest in Vinnytsia region using the Braun-Blanquet method with an assessment of the stratification and frequency of occurrence of species; additionally, for black locust, an analysis of the age structure of the population was performed based on trunk diameter and plant height. The survey was carried out at the forest edge and in the inner areas of the forest. It was found that the species composition of the forest stand is spatially differentiated. The central part of the community was formed mainly by Scots pine (*Pinus sylvestris* L.) and silver birch (*Betula pendula* Roth.), while black locust dominated the eastern forest edge, forming tree, undergrowth and shrub layers. The presence of all age groups of black locust was detected, from seedlings to old generative individuals, indicating its stable regeneration and high invasive potential. The species was

Suggested Citation:
Krasnoshtan, V., & Krasnoshtan, I. (2025). Structural characteristics of pine stands and analysis of the invasive spread of black locust (*Robinia pseudoacacia* L.) near the settlement of Dashiv, Vinnytsia region. *Scientific Reports of the National University of Life and Environmental Sciences of Ukraine*, 21(5), 43-54. doi: 10.31548/dopovidi/5.2025.43.

*Corresponding author

absent in the inner areas of the forest, which is due to the dense canopy of autochthonous trees and competition with the native flora. The results obtained indicate the local, ecotonal nature of the black locust invasion, concentrated in the edge parts of the forest stand adjacent to agricultural landscapes. The presence of numerous young generations is a sign of invasive pressure, which may lead to a gradual expansion of the population. The results obtained can be used in forestry practice to monitor invasive species and develop measures to preserve biodiversity

Keywords: forest stand; species composition; age structure; invasive species; black locust

Introduction

Introduced tree species pose a serious threat to the stability of forest ecosystems, as they are capable of actively spreading, changing the natural structure of communities and disrupting the balance between species. Such processes are often accompanied by a decrease in the diversity of autochthonous flora, suppression of young generations of native trees, and transformation of environmental conditions. Particular attention should be paid to black locust (*Robinia pseudoacacia* L.), a species that is distinguished by its rapid growth, ecological plasticity, and ability to form stable populations even in environments with disturbed natural relationships. It easily establishes itself on forest edges, in secondary plantations and in areas where economic activity has been carried out for a long time, gradually displacing local species and changing the nature of forest ecosystems.

The problem of biological invasions in forest plantations is becoming increasingly acute in a number of regions around the world. Secondary forest communities that form on the site of former agricultural landscapes or outside the natural range of dominant species are often particularly vulnerable to the introduction of invasive species, in particular invasive tree species (Jones & Yamamoto, 2024). One of the most aggressive introduced species is black locust (*Robinia pseudoacacia* L.), which has a high capacity for spread due to the formation of dense communities and interaction with other tree species. In particular, E.T. Nilsen & C.D. Huebner (2023) showed that *R. pseudoacacia* forms compact clusters of trees and undergrowth, where the closest neighbours are most often individuals of the same species, as well as other introduced and invasive species. The authors also noted that areas dominated by *R. pseudoacacia* are characterised by high tree density and specific differences in species composition, confirming its ability to influence the structure and dynamics of local forest communities.

In anthropogenically transformed landscapes, where natural succession relationships are disrupted, invasive species are capable of altering the structure and dynamics of phytocenoses and influencing the functioning of ecosystems. In particular, a review by M. Langmaier & K. Lapin (2020) showed that introduced tree and herbaceous species, including *Robinia pseudoacacia*, *Prunus serotina* and others, suppress the natural regeneration of autochthonous trees through competition for light and resources, as well as alter the chemical properties of the soil, enriching it with nitrogen and changing microbial communities. Similar conclusions are described in the work of M.J. Woods (2023), where author noted that invasive plants can not only displace local species in areas affected by degradation processes, but also significantly modify the chemical composition of the soil (acidification, carbon input), which affects the nutrient cycle and reduces the chances of restoring the autochthonous dendroflora.

In Ukraine, the impact of black locust on local flora was studied by A. Tokaryuk *et al.* (2021), who, using the example of the Prut-Dniester interfluve, demonstrated the ability of black locust to lead

to the loss of regional phytodiversity of both herbaceous plants and trees. At the same time, I.I. Korshikov *et al.* (2021), studying steppe ravines in the Dnipropetrovsk region, noted that *Robinia pseudoacacia* forms the most numerous self-sown populations in the studied locations and exhibits the greatest invasive potential among other plant species, displacing native species and transforming natural communities.

The high invasiveness of black locust is largely explained by its biological characteristics, but some scientists note that certain environmental factors can either promote or slow down invasive processes. For example, M.A. Holmes *et al.* (2021) showed that land use history and abiotic factors determine the spread of introduced shrubs in secondary forests in the Appalachians, formed on the site of former agricultural and industrial areas. This highlights the importance of considering anthropogenic factors when studying invasive processes in forest ecosystems.

Despite the large number of publications devoted to the invasive properties of *Robinia pseudoacacia*, the issue of its spread in young forest ecosystems of anthropogenic origin, formed on the site of former agricultural land, has not yet been sufficiently studied. In this regard, there is a need for regional studies combining floristic analysis with the study of forest community structure.

The aim of the study was to investigate the structure of secondary pine stands formed on former agricultural land and to analyse the invasive spread of black locust (*Robinia pseudoacacia* L.) within them.

To achieve this goal, the following tasks were set:

- to determine the species composition and vertical structure of the pine stand;
- to assess the spatial distribution (horizontal zonation) of black locust within the study area;
- to analyse the quantitative indicators and age structure of the black locust population.

The scientific novelty of the work lies in conducting a detailed regional study of the invasion process of *Robinia pseudoacacia* in secondary forest stands on the site of former agricultural landscapes. For the first time in the studied region, a comprehensive analysis of the vertical and horizontal structure of the dominant pine stand was carried out in combination with a quantitative assessment of the black locust population, which allows for a deeper understanding of the factors that influence the success of its spread in such conditions.

Materials and Methods

The research was conducted in a Scots pine forest stand near the settlement of Dashiv, Haisyn District, Vinnytsia Region, in 2025, in compliance with the ethical standards set out in the Convention on Biological Diversity (1992). The forest stand was formed on a north- and west-facing hillside. It borders the Lysa Lypa river to the east and north. Agricultural land is located to the west and south of the forest (Fig. 1). The area of the plantation was about 16 hectares (Public Cadastral Map of Ukraine, n.d.).

To conduct a floristic analysis of the forest stand, three experimental plots measuring 20×20 m were established in the eastern, western and central parts of the forest, which made it possible to take into account the spatial heterogeneity of the vegetation cover. The vegetation was described using the Braun-Blanquet method (Westhoff & van der Maarel, 1978), which involved selecting homogeneous representative plots and assessing each species on a coverage/abundance scale. For each plot, the species composition, stratification structure and relative participation of species in the formation of the community were recorded. The degree of coverage was indicated on the Braun-Blanquet assessment scale: from "r" (isolated specimens) and "+" (<1% coverage) to gradations 1-5, reflecting the increase in the coverage of the species in the phytocenosis (from 1 – <5% to 5-75-100%). This approach made it possible to quantitatively characterise the spatial heterogeneity of vegetation and identify differences in the structure of the eastern, central and western parts of the plantation.

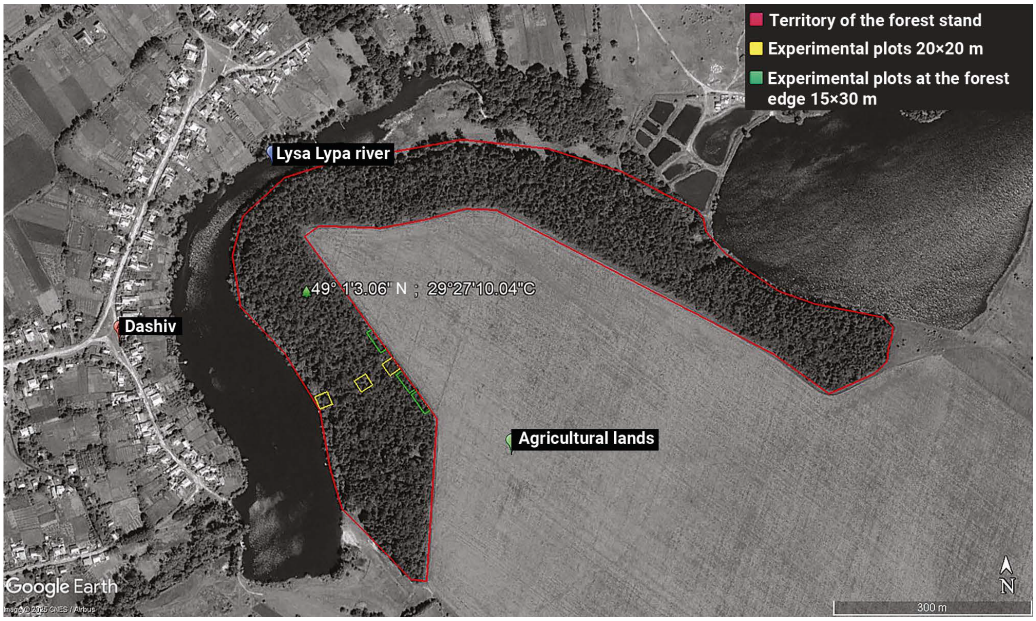

Figure 1. *Pine stands near the settlement of Dashiv, Vinnytsia region, Ukraine*
Source: developed by the authors based on Satellite imagery (n.d.)

For the visual classification of *Robinia pseudoacacia* plants by age group, their height and trunk diameter at a height of 1.3 m were determined. Seedlings and juvenile plants were assessed only by height, while generative plants were assessed by height and trunk diameter. Individuals were classified into groups: old generative (height 12-18 m, trunk diameter 15-40 cm), young generative (height 2-12 m, trunk diameter 2-15 cm), juvenile (height 0.3-2.0 m) and seedlings (height up to 0.3 m). The number of individuals in each group was recorded along the forest edge in three areas 30 m long and 15 m wide, which made it possible to determine the age structure of the population and its spatial boundaries.

Results and Discussion

Research into the structural characteristics of pine stands has revealed marked spatial heterogeneity in the composition and distribution of tree and shrub species. A multi-tiered phytocenotic system has formed within the studied area, where the participation of native and introduced species varies depending on the ecological conditions of individual sites. The most contrasting differences are observed between the edge zones of the stand and its central part, which is due to differences in light levels, moisture and competitive relationships. The research has established that the species composition of the forest stand is heterogeneous and varies depending on the location of the studied areas (Table 1). The eastern part of the forest is characterised by a pronounced dominance of black locust, which forms three layers: tree, undergrowth and shrub (Fig. 2).

The high number of individuals of different ages and the ability of the species to occupy several structural levels indicate stable population recovery and an active invasive process. As a result, local indigenous species are significantly suppressed, and the phytocenotic structure becomes monodominant. It is particularly noteworthy that black locust forms dense undergrowth and thick thickets, which limit the penetration of light to the lower tiers, further reducing the chances for natural restoration of the local

flora. However, despite the pronounced dominance of black locust, isolated representatives of other species are still found in the eastern part of the forest, in particular *Pinus sylvestris* (coverage degree – 1), which occupies the tree layer. The presence of *P. sylvestris* in this area is probably explained by the development of this species before the invasion of black locust, which allowed the plants to occupy a dominant position in the upper forest layer and not experience competitive pressure from other species. At the same time, the absence of young Scots pine individuals indicates the inability of plants to reproduce under the invasive influence of black locust.

Table 1. *Phytocenotic structure of forest stand according to Braun-Blanquet*

Species / Layer	East	Centre	West
Robinia pseudoacacia (I, II, III)	5	1	–
Betula pendula (I, II)	+	3	3
Pinus sylvestris (I)	1	4	3
Prunus avium (II, III)	2	1	3
Crataegus sp. (III)	–	r	1
Alnus incana (II)	–	–	1
Quercus robur (II)	–	–	2
Carpinus betulus (II, III)	–	1	1
Fraxinus excelsior (II)	–	–	1
Rubus idaeus (IV)	–	–	r
Fragaria vesca (IV)	–	–	1
Bryophyta spp. (V)	+	2	2

Note: layers: I – tree, II – undergrowth, III – shrub, IV – herbaceous, V – moss and lichen. Score – degree of coverage according to the Braun-Blanquet scale. Symbols "–" – absence of species in the area; "r" – isolated individuals; "+" – <1% coverage

Source: developed by the authors based on own research

Figure 2. *Robinia pseudoacacia in the eastern part of the forest*

Source: authors' photo

To a certain extent, representatives of *Prunus avium* (coverage degree – 2) are found in the eastern part of the forest, in particular on the forest edge, in the undergrowth and shrub layer. The ability of wild cherry to survive in conditions of black locust dominance is determined by its ecological characteristics, which, according to L.V. Kalashnikova & J.V. Doroshenko (2021), include mesoxerophily, shade tolerance and mesotrophy. In the central part of the forest, the species composition of the dendroflora has a number of significant differences compared to the eastern part. In this area, there are only a few plants of black locust (coverage degree – 1) and a clear dominance of two other species: *Pinus sylvestris* and *Betula pendula* (coverage degree – 4 and 3, respectively), which occupy the tree layer and undergrowth (Fig. 3).

Figure 3. *Pinus sylvestris and Betula pendula in the central part of the forest*
Source: authors' photo

The dominance of these two species is probably explained by their significant development in the period preceding the invasion of black locust, which made the conditions in the central part of the forest unfavourable for the development of light-demanding plants. However, some other species are still able to exist in these conditions due to their ecological characteristics, in particular shade tolerance. In the undergrowth and shrub layer of the central part of the forest, one can find *Prunus avium* and *Carpinus betulus* (coverage level 1 for both species), as well as isolated representatives of *Crataegus* sp., which, together with black locust, occupy small light gaps in the lower layers of the forest.

The western part of the forest plantation is characterised by a number of specific conditions that distinguish this area from the central and eastern parts. In particular, it is located on a depression in the relief, which is the river bank. As a result, there is a slightly lower level of illumination and proximity to the groundwater surface. These specific conditions have determined the characteristic quantitative and qualitative composition of the local flora. In the western part of the forest, as in the central part, *Betula pendula* and *Pinus Sylvestris* remain dominant (coverage level 3 for both species), forming the tree layer of the forest. However, in the undergrowth and shrub layer, *Prunus avium* (coverage degree – 3) occupies a dominant position, which is explained not only by the relative shade tolerance of this species, but also by the sufficient moisture supply for its intensive development in conditions of proximity to a water body (Fig. 4).

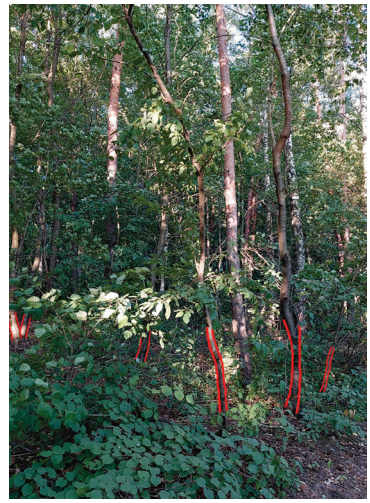

Figure 4. *Prunus avium in the western part of the forest (marked in red)*
Source: authors' photo

The western part of the forest also hosts a number of autochthonous tree species that are not found in the eastern or central parts. For example, *Alnus incana, Carpinus betulus, Fraxinus excelsior* and *Crataegus* sp. (coverage level – 1 for all species) can be found here, occupying mainly the undergrowth and shrub layers. *Quercus robur* is somewhat more prevalent here (coverage level – 2). In addition to trees, the western part of the forest also has more active herbaceous vegetation compared to other studied areas. There are isolated representatives of *Rubus idaeus* and *Fragaria vesca*, which, given the growing conditions, are suppressed due to lack of light. This difference in the development of herbaceous vegetation may be due to the fact that, although there

is shading in the western part of the forest, it is not as pronounced as in the eastern part. In addition, the better moisture supply in the western part of the forest compared to the eastern and central parts contributes to the development of herbaceous cover. Another significant difference that characterises the western part of the studied forest stand is the complete absence of black locust plants in all layers.

Thus, a floristic study of different areas of the forest stand indicates the existing horizontal differentiation of the species composition of the dendroflora against the background of the general dominance of Scots pine. The reasons for this differentiation include different lighting conditions, moisture levels and soil characteristics. These conclusions are consistent with the results of studies by other authors. For example, J.F. Maciel-Nájera *et al.* (2021) in their study of oak-pine forests in Mexico found that the composition of understory plants depends significantly on soil conditions. According to their data, indicators such as the content of calcium, phosphorus, potassium and organic matter in the soil had a stronger influence on the presence of certain species than even the availability of sufficient light. The results of the current study also confirm the key role of edaphic factors in shaping the species composition of forest phytocenosis, which indicates the universality of this ecological principle.

Thus, the eastern part of the forest, in particular the forest edge, receives a large amount of light, which is a critical condition for the development of black locust, especially young individuals. According to research by T. Ábri *et al.* (2024), young black locust seedlings demonstrate high photosynthetic efficiency, which increases proportionally to the increase in light intensity within a wide range. This confirms that black locust is a light-loving species that needs a lot of light for successful development, which is observed in the current study. In addition, this site is located on a hill, which is characterised by less moisture availability compared to lowlands. Since, according to research by D. Bartha *et al.* (2008), black locust is more resistant to moisture deficiency than autochthonous species, this gives it a significant advantage in the competition for natural resources. However, moving westward, in the central part of the forest, conditions change dramatically: *Pinus sylvestris* and *Betula pendula* in this area create significant shading, which makes local conditions unfavourable for the development of young black locust plants. This trend was also noted by H. Kato-Noguchi & M. Kato (2024) when describing the invasive characteristics of black locust and its impact on the species diversity of forest plantations. They note that black locust cannot tolerate shade, and its seedlings and young trees develop successfully only where there is sufficient light or a thin canopy.

The western part of the forest is characterised not only by its spatial orientation, but also by its proximity to water and its location at the foot of a hill, which creates favourable conditions for the development of more moisture-loving and light-undemanding plants: *Prunus avium*, *Alnus incana*, *Quercus robur, Carpinus betulus* and *Fraxinus excelsior*. In this part of the forest, black locust probably not only does not receive enough light for development, but also has no ecological advantages over the autochthonous flora, which makes its spread in this location extremely difficult. This is partly consistent with the conclusions of A. Cierjacks *et al.* (2013), who emphasised that black locust can actively displace native species only under conditions of sufficient light and resource availability, while in wetter and shadier areas its invasive potential is reduced. In the case of the current study, the relief and increased soil moisture create advantages for native species and further limit the spread of black locust. Analysing the age structure of black locust in the eastern part of the forest (Table 2), it should be noted that the trees here are represented by both old generative individuals (trunk diameter 35-40 cm, well-developed canopy, presence of seed offspring), and young generative trees, as well as numerous juvenile plants and seedlings.

Table 2. *Age structure of black locust in the eastern part of the forest*

Age group	Characteristic (by morphometric traits)	Approximate quantity	Notes
Seedlings	1-year-old saplings, height <0.3 m	+++	Form a continuous strip under the canopy of older trees
Juvenile	1-3 year-old growth, height 0.3-2 m	+++	Form a dense understorey
Young generative	3 3-10 year-old trees, height 2-12 m, diameter 2-15 cm	++	Actively growing, but are outcompeted by pine in height
Old generative	Height 12-18 m, diameter 35-40 cm	++	Form the tree layer of the forest edge

Note: +++ – very numerous, ++ – well represented, + – isolated
Source: developed by the authors based on own research

This age structure indicates stable reproduction and high invasive potential of the species in the edge part of the forest stand. The accumulation of individuals of different generations forms a multi-tiered structure of the community, in which black locust occupies both the tree and shrub-undergrowth levels. A sharp decline in the number of black locust trees with deeper penetration into the forest indicates limited penetration of the species into the established forest stand. The main barriers are likely to be the dense canopy of native trees, which significantly reduces the light available to the lower tiers, as well as competitive interaction with native species in conditions that are more favourable to them. Thus, black locust exhibits the properties of an ecotone invasive species, concentrating in the zone of contact between the forest and agricultural landscapes. The age structure of the population at the forest edge has all the characteristics of an expansive one, as confirmed by the coexistence of several generations. This distribution reflects favourable conditions for reproduction: openness to the field, sufficient insolation, and the presence of mother trees that produce both seeds and vegetative shoots. In turn, the absence of black locust in the inner areas of the forest indicates that the invasion is localised and closely depends on the anthropogenically transformed environment.

The results obtained are consistent with the study by R. Motta *et al.* (2009), who, using the example of floodplain forests in Italy, showed that *Robinia pseudoacacia*, after active colonisation, forms the upper and middle tiers, but gradually loses its ability to regenerate in the inner parts of the forest stands due to a lack of light and increased competition with native flora. At the same time, in contrast to the data presented, where the authors record signs of gradual degradation of black locust plantations, in the conditions of the studied forest edge, this species shows signs of active expansion, indicating the early stages of the invasion process. Similar trends are noted by M. Vítková *et al.* (2019), who summarised data on the spread of black locust in Europe in their work. The authors showed that the species most intensively colonises disturbed areas, forest edges, clearings and other open spaces, while its spread is significantly limited in mature forest ecosystems. The results of the current study fully confirm this pattern: the highest density of young individuals was observed precisely in areas of contact with the agricultural landscape, while in the depths of the forest, the formation of new generations of black locust was minimal. Additional confirmation of this is provided by R. Crosti *et al.* (2016), who, studying forest plantations in Central Italy, showed that the penetration of black locust is most intense on abandoned agricultural land located near parent trees. At the same time, semi-natural forest areas in their study proved to be much more resistant to invasion, showing minimal spread of the species.

The results obtained regarding the structural features of pine stands in combination with the invasive spread of *Robinia pseudoacacia* near the settlement of Dashiv are consistent with data from other studies on the transformational impact of this species on ecosystems. The work of P. Lakyda *et al*. (2025) shows that *R. pseudoacacia* plantations in urban parks in Dnipro change soil properties, particularly under conditions of technogenic pollution with heavy metals. This confirms the high ecological plasticity of black locust and its ability to modify the growing environment, which explains its competitiveness in natural and artificial forest communities. Thus, the available results indicate that the penetration of black locust into pine plantations not only changes their structural organisation but also potentially affects soil characteristics, creating risks for the stability of these ecosystems. At the same time, there is evidence that forest stands near water bodies are extremely vulnerable to black locust invasion. For example, a study by M. Varricchione *et al*. (2024) indicates that black locust creates significant invasive pressure on coastal ecosystems, which, like forest edges, are vulnerable to its spread, although in the current study, it was the forest areas adjacent to water bodies that proved to be the most resistant to invasion. In this regard, Ukrainian researchers S. Los *et al*. (2022) argue that in the conditions of Central Ukraine, particularly in the Kirovohrad region, established forest plantations are relatively resistant to black locust invasions. However, as the authors note, in areas adjacent to plantations, medium and high invasion activity was observed in more than 70% of cases, which indicates significant invasive pressure of the species in areas that have been subjected to anthropogenic influence. Therefore, when monitoring the spread of black locust, it is important to pay attention not only to forest plantations themselves, but also to adjacent areas that are regularly affected by human activity.

The study showed that the structural organisation of pine plantations is spatially heterogeneous and depends significantly on the ecological conditions of individual areas. It has been established that the invasive species *Robinia pseudoacacia* is concentrated mainly on forest edges, where it forms multi-tiered communities and demonstrates active reproduction. At the same time, its spread in the inner parts of the forest is significantly limited due to the dense canopy of native trees and higher moisture levels. The identified age structure of the black locust population indicates stable self-regeneration, which poses a potential threat to the local flora in the event of further anthropogenic disturbances. The results confirm the need for long-term monitoring of forest edges and marginal areas, as they are the most vulnerable to invasion.

Conclusions

The research has shown that the floristic composition and structural organisation of the studied forest stand are spatially heterogeneous and demonstrate pronounced horizontal differentiation. The tree stand is dominated by the native species *Pinus sylvestris* and *Betula pendula*, but locally, particularly on the eastern edge of the forest, the invasive species *Robinia pseudoacacia* dominates (coverage level – 5). Robinia forms a full-fledged multi-tiered structure (tree, undergrowth and shrub tiers), demonstrating active reproduction due to the presence of individuals of all age groups. This indicates the high invasive potential of the species under conditions of sufficient light and moisture deficiency, which are characteristic of the edge areas of the stand. At the same time, in the inner parts of the forest, where native species dominate and there is significant shading and higher soil moisture, black locust is much less common (coverage level – 1), which confirms its ecotone nature of distribution and limited competitiveness in stable forest communities. The western part of the forest, located near a reservoir, is characterised by a greater representation of moisture-loving autochthonous species (*Prunus avium, Alnus incana, Quercus robur, Carpinus betulus, Fraxinus excelsior*), which further reduces the possibility of black locust

establishment, and as a result, it is completely absent in this area.

Thus, *Robinia pseudoacacia* exhibits the characteristics of a typical invasive species at the boundary between forest ecosystems and agricultural landscapes, where it forms stable, self-renewing populations. At the same time, its penetration into the established tree stand is limited by ecological barriers (lack of light, higher competition, increased moisture). The identified age structure and localised nature of Robinia's spread indicate the initial phase of the invasive process, which, however, in the event of anthropogenic disturbance of the tree stand, may transform into a more intensive spread with the displacement of native flora. In the long term, it is advisable to conduct long-term monitoring of forest edges and marginal areas, analyse the rate of black locust population recovery after possible disturbances to the tree stand, and study the interaction of this species with native flora in different ecological conditions. Special attention should be paid to assessing the invasive pressure of black locust on young generations of autochthonous tree and shrub species, which will allow for more accurate predictions of the further development of the forest ecosystems under study.

Acknowledgements

None.

Funding

None.

Conflict of Interest

None.

References

[1] Ábri, T., Gaganetz, D., & Csajbók, J. (2024). Light response curve analysis of juvenile black locust clones: A case study from eastern Hungary. *Journal of Forest Science*, 70(4), 202-207. doi: 10.17221/120/2023-jfs.

[2] Bartha, D., Csiszár, Á., & Zsigmond, V. (2008). Black locust (*Robinia pseudoacacia* L.). In Z. Botta-Dukát & L. Balogh (Eds.), *The most important invasive plants in Hungary* (pp. 63-76). Vácrátót: HAS Institute of Ecology and Botany.

[3] Cierjacks, A., Kowarik, I., Joshi, J., Hempel, S., Ristow, M., Von Der Lippe, M., & Weber, E. (2013). Biological flora of the British Isles: *Robinia pseudoacacia*. *Journal of Ecology*, 101(6), 1623-1640. doi: 10.1111/1365-2745.12162.

[4] Convention on Biological Diversity. (1992, June). Retrieved from https://zakon.rada.gov.ua/laws/show/995_030#Text.

[5] Crosti, R., Agrillo, E., Ciccarese, L., Guarino, R., Paris, P., & Testi, A. (2016). Assessing escapes from short rotation plantations of the invasive tree species *Robinia pseudoacacia* L. in Mediterranean ecosystems: A study in central Italy. *iForest - Biogeosciences and Forestry*, 9(5), 822-828. doi: 10.3832/ifor1526-009.

[6] Holmes, M.A., Whitacre, J.V., Bennion, L.D., Poteet, J., & Kuebbing, S.E. (2021). Land-use history and abiotic gradients drive abundance of non-native shrubs in Appalachian second-growth forests with histories of mining, agriculture, and logging. *Forest Ecology and Management,* 494, article number 119296. doi: 10.1016/j.foreco.2021.119296.

[7] Jones, C.C., & Yamamoto, M.H. (2024). Long-term patterns and mechanisms of plant invasions in forests: The role of forest age and land-use history. *Biological Invasions,* 26(9), 3125-3145. doi: 10.1007/s10530-024-03365-8.

[8] Kalashnikova, L.V., & Doroshenko, J.V. (2021). Ecological characteristic of dendrosozophytes of the dendrological park "Oleksandria" of NAS of Ukraine. *Journal of Native and Alien Plant Studies*, 1, 119-124. doi: 10.37555/2707-3114.1.2021.247561.

[9] Kato-Noguchi, H., & Kato, M. (2024). Invasive characteristics of *Robinia pseudoacacia* and its impacts on species diversity. *Diversity*, 16(12), article number 773. doi: 10.3390/d16120773.

[10] Korshikov, I.I., Petrushkevych, Y.M., & Shevchuk, N.Y. (2021). Expansion of tree and shrub plant species into undisturbed steppe phytocenoses. *Journal of Native and Alien Plant Studies*, 1, 160-165. doi: 10.37555/2707-3114.1.2021.247571.

[11] Lakyda, P., Matushevych, L., Sakharuk, H., Lovynska, V., Holoborodko, K., & Sytnyk, S. (2025). The influence of *Robinia pseudoacacia* plantations on soil in the park areas of Dnipro city contaminated with heavy metals. *Ukrainian Journal of Forest and Wood Science*, 16(2), 115-135. doi: 10.31548/forest/2.2025.115.

[12] Langmaier, M., & Lapin, K. (2020). A systematic review of the impact of invasive alien plants on forest regeneration in European temperate forests. *Frontiers in Plant Science*, 11, article number 524969. doi: 10.3389/fpls.2020.524969.

[13] Los, S., Tereshchenko, L., & Petrenko, M. (2022). Approbation of the method for assessing the invasive activity and selection value of *Robinia pseudoacacia* L. in Kirovohrad region conditions. *Proceedings of the Forestry Academy of Sciences of Ukraine*, 24, 24-35. doi: 10.15421/412202.

[14] Maciel-Nájera, J.F., González-Elizondo, M.S., Hernández-Díaz, J.C., López-Sánchez, C.A., Bailón-Soto, C.E., Carrillo-Parra, A., & Wehenkel, C. (2021). Influence of environmental factors on forest understorey species in Northern Mexico. *Forests*, 12(9), article number 1198. doi: 10.3390/f12091198.

[15] Motta, R., Nola, P., & Berretti, R. (2009). The rise and fall of the black locust (*Robinia pseudoacacia* L.) in the "Siro Negri" Forest Reserve (Lombardy, Italy): Lessons learned and future uncertainties. *Annals of Forest Science*, 66(4), article number 410. doi: 10.1051/forest/2009012.

[16] Nilsen, E.T., & Huebner, C.D. (2023). Spatial patterns of native *Robinia pseudoacacia* and invasive *Ailanthus altissima* and their influence on regeneration, abundance, and diversity of neighboring trees at local and regional scales. *Landscape Ecology*, 38(11), 2899-2916. doi: 10.1007/s10980-023-01760-5.

[17] Public Cadastral Map of Ukraine. (n.d.). Retrieved from https://kadastrova-karta.com/dilyanka/0521255400:02:000:0355.

[18] Satellite imagery. (n.d.). *Earth observation imagery*. Retrieved from https://www.airbus.com/en/products-services/space/earth-observation/satellite-imagery

[19] Tokaryuk, A., Chorney, I., Budzhak, V., & Volutsa, O. (2021). Influence of *Robinia pseudoacacia* L. (Fabaceae) plantations on phytodiversity of the Prut-Dnister interfluve. *Biosystems*, 13(2), 210-217. doi: 10.31861/biosystems2021.02.210.

[20] Varricchione, M., Carranza, M.L., D'Angeli, C., De Francesco, M.C., Innangi, M., Santoianni, L.A., & Stanisci, A. (2024). Exploring the distribution pattern of native and alien forests and their woody species diversity in a small Mediterranean city. *Plant Biosystems – an International Journal Dealing With All Aspects of Plant Biology*, 158(6), 1335-1346. doi: 10.1080/11263504.2024.2415613.

[21] Vítková, M., Sádlo, J., Roleček, J., Petřík, P., Sitzia, T., Müllerová, J., & Pyšek, P. (2019). *Robinia pseudoacacia*-dominated vegetation types of Southern Europe: Species composition, history, distribution and management. *Science of the Total Environment*, 707, article number 134857. doi: 10.1016/j.scitotenv.2019.134857.

[22] Westhoff, V., & Van Der Maarel, E. (1978). The Braun-Blanquet approach. In *Classification of plant communities* (pp. 287-399). Dordrecht: Springer. doi: 10.1007/978-94-009-9183-5_9

[23] Woods, M.J. (2023). *Restoring degraded and invaded landscapes: A soil-based approach*. (PhD dissertation, University of Dayton, Dayton, USA).

Структурна характеристика соснових насаджень та аналіз інвазійного поширення робінії (*Robinia pseudoacacia* L.) поблизу селища Дашів, Вінницької області

Василь Красноштан
Доктор філософії
Уманський державний педагогічний університет імені Павла Тичини
20300, вул. Садова, 2, м. Умань, Україна
https://orcid.org/0000-0001-8572-5008
Ігор Красноштан
Кандидат біологічних наук, доцент
Уманський державний педагогічний університет імені Павла Тичини
20300, вул. Садова, 2, м. Умань, Україна
https://orcid.org/0000-0003-1317-546X

Анотація. Однією з ключових проблем сучасної екології та лісівництва є поширення робінії звичайної, що призводить до трансформації лісових екосистем і втрати біорізноманіття. Метою роботи було визначити структурні особливості вторинного соснового насадження та проаналізувати інвазійне поширення *Robinia pseudoacacia* L. Дослідження було проведено у 2025 році у сосновому насадженні Вінницької області за методикою Braun-Blanquet з оцінкою ярусної організації та частоти трапляння видів; додатково для робінії звичайної виконано аналіз вікової структури популяції за діаметром стовбура та висотою рослин. Облік здійснювали на узліссі та у внутрішніх ділянках лісу. Встановлено, що видовий склад лісового насадження є просторово диференційованим. Центральна частина угруповання формувалась переважно сосною звичайною (*Pinus sylvestris* L.) та березою повислою (*Betula pendula* Roth.), тоді як на східному узліссі домінувала робінія, утворюючи деревний, підлісковий і чагарниковий яруси. Виявлено наявність усіх вікових груп робінії – від проростків до старих генеративних особин, що вказує на її стабільне відновлення та високий інвазійний потенціал. У внутрішніх ділянках лісу вид відсутній, що зумовлено щільним пологом автохтонних дерев і конкуренцією з аборигенною флорою. Отримані результати свідчать про локальний, екотонний характер інвазії робінії, зосередженої у крайових частинах деревостану, суміжних із агроландшафтами. Наявність численних молодих генерацій є ознакою інвазійного тиску, що може зумовити поступове розширення популяції. Отримані результати можуть бути використані у практиці лісового господарства для моніторингу інвазійних видів та розробки заходів зі збереження біорізноманіття

Ключові слова: лісові насадження; видовий склад; вікова структура; інвазійні види; робінія звичайна

Received 02.06.2025 Revised 03.09.2025 Accepted 23.09.2025

Vol. 21, No. 5
2025

Scientific Reports of the National University of Life and Environmental Sciences of Ukraine

Journal homepage: https://scireports.com.ua/en

UDC 633.63:631.8:631.531:577.1

Doi: 10.31548/dopovidi/5.2025.55

Influence of nitrogen and phosphorus-potassium fertiliser on the yield and biochemical composition of common chicory (*Cichorium intybus* L.)

Bohdan Mazurenko*
PhD in Agronomy, Associate Professor
National University of Life and Environmental Sciences of Ukraine
03041, 15 Heroiv Oborony Str., Kyiv, Ukraine
https://orcid.org/0000-0002-4177-9909

Liubov Honchar
PhD in Agricultural Sciences, Associate Professor
National University of Life and Environmental Sciences of Ukraine
03041, 15 Heroiv Oborony Str., Kyiv, Ukraine
https://orcid.org/0000-0002-3628-6659

Abstract. Common chicory (*Cichorium intybus* L.) is an important industrial crop, valuable due to its high content of inulin and functional bioactive compounds. Optimisation of mineral fertilisers remains key to maximising yields and improving biochemical composition in the face of climate change. The purpose of this study was to evaluate the effect of nitrogen and phosphorus-potassium fertilisers on the yield and biochemical parameters of chicory. Field studies were conducted in 2021-2023 in the Right-Bank Forest-Steppe of Ukraine on low-humus chernozem according to a two-factor scheme that included 5 variants of nitrogen fertiliser (0-200 kg/ha) and five variants of phosphorus-potassium fertiliser (0-120 kg P_2O_5 and 0-200 kg K_2O). The yield of root crops, total sugar content, inulin content, reducing sugars, and degree of polymerisation were determined using standardised biochemical and statistical methods (analysis of variance, Tukey's HSD post-hoc test, Principal Component Analysis (PCA), cluster analysis). The results of the research showed that nitrogen fertiliser affected all biochemical parameters and yield, but most of all on the content of inulin (up to 75% of dry matter) and the degree of polymerisation, while phosphorus-potassium fertilisers only on the yield and degree of polymerisation. The maximum average yield in the years of research (35.4 t/ha) was achieved with the introduction of $N_{150}P_{90}K_{150}$, while excessive application of nitrogen and phosphorus-potassium fertilisers (200 kg/ha) reduced crop productivity and yield. The total sugar and inulin content increased with

Suggested Citation:

Mazurenko, B., & Honchar, L. (2025). Influence of nitrogen and phosphorus-potassium fertiliser on the yield and biochemical composition of common chicory (*Cichorium intybus* L.). *Scientific Reports of the National University of Life and Environmental Sciences of Ukraine*, 21(5), 55-70. doi: 10.31548/dopovidi/5.2025.55.

*Corresponding author

nitrogen application to 150 kg/ha, after which a decrease was observed. PCA confirmed the dominant role of nitrogen in the development of both yield and biochemical parameters. Optimal nitrogen standards (100-150 kg/ha) in combination with moderate levels of phosphorus-potassium fertiliser ensured stable root crop yields and high inulin content, which is important for both industrial processing and sustainable agricultural production

Keywords: correlation; inulin; sugars; Principal Component Analysis; polymerisation

Introduction

Common chicory (*Cichorium intybus L.*) is a multifunctional crop that is a source of inulin, dietary fibre, coffee substitute, and raw materials for the pharmaceutical and food industries. According to H. Akram *et al.* (2025), the acreage under chicory for inulin production in Europe exceeds 20 thousand hectares, with a tendency to increase and expand the geography of cultivation. The growing interest in functional food products and the need for high-quality raw materials leads to an increase in demand for crops with an optimal composition of biologically active substances and obtaining stable yields. In the conditions of climate change, optimisation of the mineral nutrition system is of particular importance, which allows increasing the yield and improving the quality of root crops. Nitrogen and phosphorus-potassium fertilisers directly affect the synthesis of carbohydrates, in particular inulin, and the development of root crop mass, which affects yield. The fertiliser system must meet two criteria: increase productivity and quality while minimising the negative impact on the environment. Therefore, the study of the influence of nitrogen and phosphorus-potassium fertilisers is scientifically and practically substantiated for improving the efficiency of chicory cultivation in the Forest-Steppe of Ukraine and would allow developing recommendations for improving the efficiency of growing high-quality raw materials adapted to specific varieties and growing conditions.

According to M. Hingsamer *et al.* (2022), in Europe, chicory roots are grown to produce a pre-biotic dietary fibre, inulin, which stimulates the growth of beneficial gut bacteria and stimulates the human immune system. The taproot contains an average inulin content of 17% of the raw weight, and the typical yield of the root crop is 45 tonnes per hectare. Currently, the world area of common chicory is about 14,500 hectares. Chicory roots also usually contain high amounts of sesquiterpene lactones. In the future, the food system and food supply will face various challenges, such as increasingly adverse weather conditions caused by climate change, threats of plant diseases, environmental pollution, etc. Therefore, due to its biosynthetic ability, high yield and low agronomic requirements, chicory has a high potential to become a universal industrial crop for molecular farming. M.I. Bakhmat *et al.* (2021) found that chicory plants require mineral nutrition for growth and development. The rational use of fertilisers, including nitrogen fertilisers, is an important factor in sustainable agriculture. The researchers found that nitrogen fertilisers affect plant development. According to I. Popova *et al.* (2024), plant element content is affected by stresses such as salinity, drought, extreme temperatures, and excessive or insufficient lighting. Nitrogen deficiency can reduce the yield and quality of root crops, while excess nitrogen can lead to nitrate leaching and environmental pollution. Chicory crops without fertilisers have a high agroecological resistance, but they reduce it when applying nitrogen fertilisers.

In previous studies, D. Alves *et al.* (2024) noted that the reasons for the decrease in yield with an increase in fertiliser rates can be not only an imbalance of nutrients, but also subsequent damage to leaf diseases, which, in turn, reduces

assimilation activity. Sodium (Na) helps to regulate osmotic pressure in cells, thereby supporting water absorption and retention. Weather conditions and the sensitivity of varieties to fertilisers also affect the crop productivity, in particular, the weight of root crops. O. Tkach e*t al.* (2023) have shown that excessive rates of nitrogen fertilisers, especially when the maximum possibility of sowing them was absorbed, lead to a decrease in the size and weight of the root crop. Growing conditions are a key factor in the development of the chicory crop, which was confirmed by the findings of H. Zhang *et al.* (2023), where the variation can reach 83.9% due to weather factors alone. According to A. Buchelt *et al.* (2020), in the context of potassium deficiency, chicory (*Cichorium endivia* L.) shows a decrease in the leaf area and their number, and therefore, a smaller area of photosynthesis and a smaller dry weight of shoots and roots. The reduced potassium content in cells acts as a switch that suppresses anabolic responses and stimulates catabolic processes, which leads to interruptions in plant growth and redirects available energy to deal with stress-related damage.

Numerous studies by X. Zhao *et al.* (2021) found the effect of macro- and microelements, including phosphorus and iron, on the quality and quantity of primary and secondary metabolites. Phosphorus as a macronutrient is the main component of biomolecules such as phospholipids and nucleic acids, in case of deficiency or defects in assimilation of which the plant faces a decrease in yield. M. Ebrahimi & M. Gholami (2025) found that in order to adapt and increase phosphorus reabsorption under phosphate stress, plants inhibit the growth of shoots and roots, the development of root hairs, demonstrating various physiological responses such as changes in the rate of glycolysis, the production of primary and secondary metabolites such as organic acids, sugars, and flavonoids. Iron deficiency, on the other hand, affected many of chicory's vital functions and led to reduced root length.

The study of chicory root by S. Tabatabaee *et al.* (2021) found that an increase in phosphorus content in the culture medium resulted in more crude mass and less inulin. Accumulation of inulin with a polysaccharide structure under conditions of phosphorus deficiency was associated with a decrease in biomass production, although an increase in root length was also observed under these conditions. This phenomenon may be related to the numerous functions of phosphorus in plant photochemical reactions.

The purpose of the study was to establish the regularities of the influence of various norms of nitrogen and phosphorus-potassium fertilisers on the yield and biochemical parameters of chicory roots.

Materials and Methods

Research area, soil and weather conditions

The field experiment was carried out during 2021-2023 on a site located in the Obukhov District of the Kyiv Oblas (49°46' N, 30°44' E) in the typical conditions of the Right-Bank Forest-Steppe of Ukraine. The soil of the experimental site was low-humus chernozem with an organic matter content of 4.36-4.53% in a layer of 0-20 cm, pH_{KCl} – 7.2-7.6, the content of easily hydrolysed nitrogen (according to Cornfield) – 152-164 mg/kg of soil, mobile phosphorus (according to Cornfield) – 152-161 mg/kg of soil, exchange potassium (according to Chirikov) – 148-157 mg/kg of soil.

In 2021-2023, the average monthly air temperature in most months consistently exceeded long-term indicators, which reflects the general trend of the last decade. In April, the average temperature was 7.5°C in 2021, and in 2023 it reached 9.6°C, exceeding the long-term average (8.4°C). Similar deviations were observed in August and September, when average temperatures were also higher than long-term values. Precipitation was characterised by significant variability over the years: in 2023, their total amount (422.7 mm) slightly exceeded the long-term figure (409 mm), while in other years the amount of precipitation was significantly lower. This indicates both the instability of seasonal conditions

and a gradual trend towards an increase in temperature and a decrease in precipitation during certain periods.

The distribution of precipitation during the growing season significantly affected the growth of chicory. In 2021, sufficient precipitation in May (78.7 mm) provided favourable conditions for seed germination, but further shortages in June (23.7 mm) and July (62.7 mm) limited the development of root crops. Lower rainfall in May 2022 (34.2 mm) created stressful conditions for early plant development, while moderate rainfall in June (41 mm) and July (53.3 mm) remained below long-term average, which could limit the accumulation of biomass. The growing season of 2023 was characterised by sharp fluctuations: extremely dry May (1 mm) delayed initial growth, but heavy precipitation in June (87.6 mm) and especially in July (136.1 mm) led to excessive soil moisture. This uneven distribution of precipitation probably caused an imbalance in the development of the root system and affected the crop development. The study was conducted in accordance with the principles of Convention on Biological Diversity (1992).

Research conditions

The field experiment involved the study of two factors: phosphorus-potassium (ratio P_2O_5:K_2O – 3:5) and nitrogen fertiliser (Table 1).

Table 1. *Field experiment scheme*

Factor A Phosphorus-potassium fertiliser	Factor B Nitrogen fertiliser
A1. Without phosphorous-potassium fertilisers (control)	B1. Nitrogen-free fertilisers (control)
A2. $P_{30}K_{50}$	B2. N_{50}
A3. $P_{60}K_{100}$	B3. N_{100}
A4. $P_{90}K_{150}$	B4. N_{150}
A5. $P_{120}K_{200}$	B5. N_{200}

Note: in the table and text of the paper, the index P refers to the fertiliser rate in kg/ha P_2O_5, and K refers to K_2O
Source: compiled by the authors

The predecessor of chicory was winter wheat. Each year, soil preparation and research were identical. After harvesting the previous crop, stubble was ploughed with a disc harrow to a depth of 5-6 cm. A mixture of triple superphosphate (TPS, 46% P_2O_5) and potassium chloride (60% K_2O) was applied in advance before ploughing at a depth of 25-27 cm in September each year during the study period. Disking was carried out in spring when soil moisture reached 60% of field moisture capacity. In the second ten days of April, on the day of sowing, ammonium nitrate (34.4% nitrogen) was applied according to the experiment scheme to a depth of 4-6 cm in pre-sowing cultivation. Chicory was sown with drained seeds of the Tsesar variety to a depth of 2-3 cm with a row spacing of 45 cm and a seeding rate of 175 thousand germinating seeds/hectare. The area of each plot was 75.6 m^2 (5.4 m×14 m) of which 36 m^2 were accounting (3.6 m×10 m).

The selection of root crops for analysis was carried out in the first ten days of October each year. To this end, all plants were removed from an area measuring 3.96 m^2 (4 rows of 2.2 m). Root crops were separated from plants, cleaned from the soil, and the yield of root crops was determined. Biochemical parameters were set in air-dry biomass (drying mode – 48 hours at a temperature of 62°C and up to a stable weight). The total sugar content was determined by the procedure described by H. Gholami *et al.* (2018) on a UNICO 1205 Vis spectrophotometer (UNICO, Japan) using the phenol-sulphuric method (wavelength 480 nm) with the inulin standard. Reducing sugars were determined by the denitrosalicylic method with a wavelength of 530 nm and the D-fructose standard for constructing a calibration curve. The inulin content was calculated as the difference between total sugars and reducing sugars. The degree of po-

lymerisation (DP) was determined by the equation of T. Paseephol *et al.* (2007):

$$DP = \text{Sugar content (\%)} / \text{Reducing sugar content (\%)}. \quad (1)$$

Statistical analysis

Statistical analysis was performed in the R environment (version 4.4.2). PCA, cluster analysis, and correlation matrices (Pearson's pair correlation method) were developed in the package *ggplot2*. Analysis of variance (ANOVA) was performed for all parameters and considered the influence of weather conditions (years). The validity of the difference between the variants was established by Tukey's HSD post-hoc analysis at the significance level $p < 0.05$ for factors that were significant in the analysis of variance. Boxplot for inulin content and similarity indices were established by univariate analysis of variance for each year and for an average of 3 years within the phosphorus-potassium fertiliser block. The data is presented as averages with standard error (n = 3).

Results and Discussion

Environmental factors and the fertiliser system had different effects on individual biochemical parameters and chicory root yield (Table 2). In most cases, the effect of weather conditions on variation was dominant, in particular, on root yield, the content of reducing sugars, and the degree of inulin polymerisation. The effect of nitrogen on the total sugar content and inulin content was several times higher.

Table 2. *Analysis of variance of yield and biochemical parameters of chicory roots*

Effect	*df*	MS				
		Root yield	Sugar content	Inulin content	Reducing sugars content	Degree of polymerisation, n
N	4	777.2**	177**	175**	0.161**	32.5**
PK	4	827.9**	2 ns	2 ns	0.055**	5.6**
Year (Y)	2	4186.1**	35**	50**	1.626**	221.2**
N*PK	16	34.8**	1 ns	1ns	0.097**	9.5**
N*Y	8	9.67**	10**	9**	0.211**	18.3**
PK*Y	8	42.3**	16**	17**	0.105**	16.1**
Y*N*PK	32	6.5**	2**	2ns	0.109**	10.7**
Error		0.2	2	2	0.003	0.4

Note: ns – not significant impact, $p > 0.05$, * – $p < 0.05$, ** – $p < 0.001$

Source: developed by the authors based on research data

The yield variance under the influence of nitrogen and phosphorus-potassium fertilisers was similar, their interactions with each other and with weather conditions were significant (but the variance was ten times less). The highest yield of chicory roots on average for the study steps was 35.4 t/ha (Table 3) for combinations of N_{150} and $P_{90}K_{150}$, which is statistically different from all other options. Notably, these options are also the best among their factors.

Table 3. *Yield of chicory roots depending on nitrogen and phosphorus-potassium fertiliser, t/ha*

Rate of phosphorus-potassium fertilisation	Rate of nitrogen fertilisers					Average
	N_0	N_{50}	N_{100}	N_{150}	N_{200}	
P_0K_0	16.4	20.0a	21.9	23.3c	26.3e	21.6
$P_{30}K_{50}$	18.0	20.6ab	26.6ef	31.0i	30.1h	25.3
$P_{60}K_{100}$	25.3d	29.4g	29.9gh	33.3	31.2ij	29.8

Table 3. *Continued*

Rate of phosphorus-potassium fertilisation	Rate of nitrogen fertilisers					Average
	N_0	N_{50}	N_{100}	N_{150}	N_{200}	
$P_{90}K_{150}$	25.6d	28.3	31.8j	35.4	31.6ij	30.5
$P_{120}K_{200}$	21.1b	23.4c	27.1f	27.0f	26.3e	25.0
Average	21.3	24.3	27.5	30.0	29.1	

Note: identical letters indicate that they belong to the same group for Tukey's HSD-test at confidence level 95%
Source: developed by the authors based on research data

The increase in yield under the influence of nitrogen fertilisers has a linear trend in the range from 0 kg/ha to 150 kg/ha, but with the introduction of N_{200} there is a decrease in yield for all PK variants, except for absolute control (without fertilisers). In the case of phosphorus-potassium fertilisers, the trend is described by a second-level polynomial with a peak in the variants with $P_{60}K_{100}$ and $P_{90}K_{150}$ (29.8 and 30.5 t/ha, respectively), but with an increase in the fertiliser rate to $P_{120}K_{200}$ there is a significant decrease to 25 t/ha, which is equivalent to a significantly lower rate of $P_{30}K_{50}$. The decrease in yield at the maximum rates of phosphorus-potassium fertilisers is more significant than nitrogen fertilisers, so their impact on biochemical parameters should be considered.

Phosphorus and potassium play an important role in the synthesis and transport of carbohydrates, but according to the results of ANOVA, their effect on the content of inulin in the roots was not significant, and on the content of reducing sugars and the degree of polymerisation is significantly lower than in nitrogen. Given these facts, it is advisable to focus on the effect of nitrogen fertilisers on biochemical parameters (Table 4).

Table 4. *Biochemical composition of chicory roots*

Nitrogen fertiliser option	Sugar content, %	Inulin content, %	Reducing sugars content, %	Degree of polymerisation, n
0	70.6 ± 0.2	67.9 ± 0.2	2.70 ± 0.02a	26.3 ± 0.3
50	73.1 ± 0.2	70.3 ± 0.2	2.83 ± 0.02	25.9 ± 0.2
100	74.3 ± 0.2a	71.6 ± 0.2a	2.72 ± 0.03ab	27.4 ± 0.3ab
150	75.0 ± 0.2	72.3 ± 0.2	2.74 ± 0.03b	27.6 ± 0.3b
200	74.3 ± 0.2a	71.6 ± 0.2a	2.74 ± 0.02b	27.2 ± 0.3a

Note: the values are presented with standard error (±SE). Identical letters in the column indicate that they belong to the same group for Tukey's HSD-test with 95% confidence level
Source: developed by the authors based on research data

The total sugar content of chicory roots on average ranged from 70.6-75.0% of the total dry matter. Without the use of nitrogen fertilisers, the sugar content was 70.6 ± 0.2%, with a gradual increase when nitrogen was applied at the rate 50-150 kg/ha of the active substance (a.s.), but when it was increased to 200 kg/ha, the sugar content decreased to 74.3%, which was at the rate of 100 kg/ha. The inulin content repeated the trend of total sugar content, since the remaining sugars (reducing sugars) in absolute values varied slightly (2.70-2.83%). The content of reducing sugars in dry matter changed in a different trend. Significantly more reducing sugars were formed when 50 kg/ha of nitrogen was applied, while at the rate of 100 kg/ha, their content was almost at the level of the control, and at the rate of 150 and 200 kg/ha it exceeded (a statistically significant increase). The ratio of total sugars and reducing sugars using the methods used helped to determine the average degree of polymerisation of inulin in samples (although in fact the

products are a mixture of different fractions). It was found that the degree of polymerisation of samples in the control version was 26.3, and when 50 kg/ha was applied, it decreased to 25.9. A further increase in the fertilisation rate was accompanied by an improvement in the synthesis of longer inulin molecules and, as a result, an increase in the degree of polymerisation to 27.6 (at the rate of N_{150}).

The inulin content showed seasonal changes (MS = 50) and had interactions and weather conditions with phosphorus-potassium (MS = 17) and nitrogen fertiliser (MS = 9), although it was inferior to the influence of nitrogen fertiliser (MS = 175). A detailed review at the level of a single variant will allow assessing the influence of factors and identify the main patterns in inulin synthesis (Figs. 1A-1E).

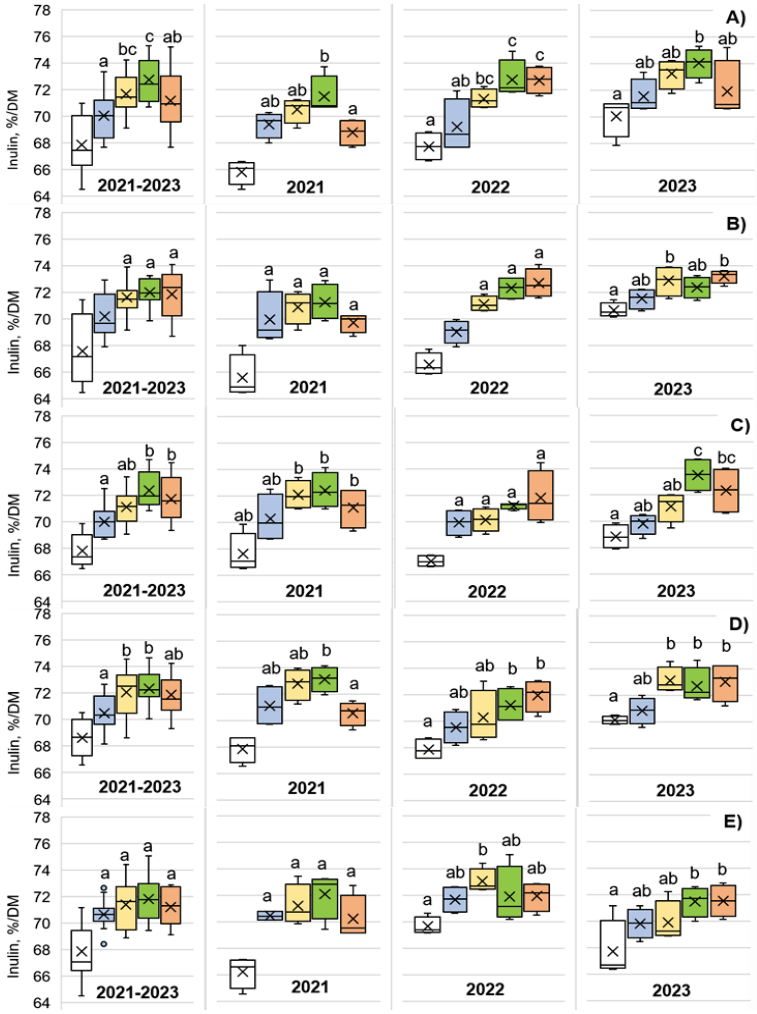

Figure 1. *Effect of fertiliser on inulin content in chicory*

Note: A – P_0K_0; B – $P_{30}K_{50}$; C – $P_{60}K_{100}$; D – $P_{90}K_{150}$; E – $P_{90}K_{200}$; Box graph: cross – average value; line – median; box – 25%-75% percentile; bars – range of non-falling values. The same letters in the column indicate belonging to the same group according to Tukey's HSD-test with a 95% confidence level (a – group with the lowest value, the column without a value differs significantly from all groups)

Source: developed by the authors based on research data and statistical processing in the *ggplot2* package

The highest inulin content in the block without phosphorus-potassium fertiliser (annually and on average) was observed with N_{150} application, exceeding 72% (Fig. 1A). Options with $N_{100,}$ N_{150}, and N_{200} showed no significant differences within the block with fertilisation rate of $P_{30}K_{50}$ (Fig. 1B). A similar trend was observed for $P_{60}K_{100}$ (Fig. 1C), although the rate of N_{200} significantly increased the spread of values. At the highest rate of phosphorus-potassium fertiliser ($P_{120}K_{200}$) with nitrogen application significantly increased the inulin content compared to the control without nitrogen. However, no significant differences were found between different nitrogen standards (Fig. 1E). The specific response of chicory to nitrogen application is probably associated with stimulation of inulin growth and synthesis, whereas cellulose, which is a component of cell walls, does not increase at the same rate.

Previously, it was noted that some indicators may have polynomial dependences on the norms of phosphorus-potassium and nitrogen fertilisers, but the determination of correlation coefficients (Fig. 2) allows assuming that there are links between these parameters.

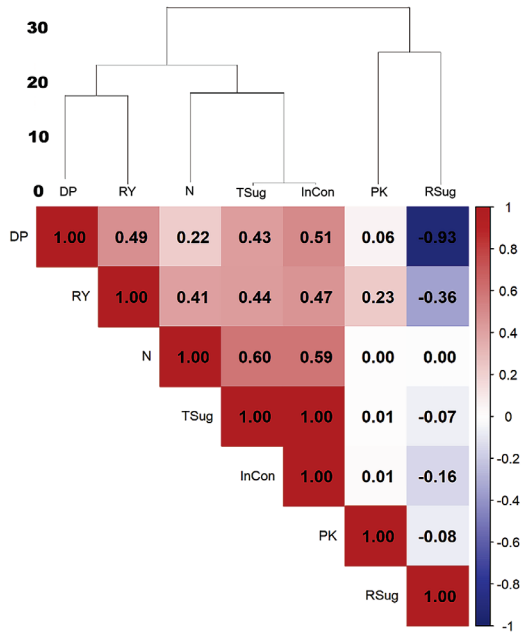

Figure 2. *Correlation matrix between yield, fertiliser rates, and biochemical parameters of chicory roots*

Note: correlation coefficients within -0.21 ... 0.21 are unreliable (p>0.05); indices: DP – degree of polymerisation, RY – root yield, N – rate of nitrogen fertilisation, TSug –total sugar content, InCon – inulin content, PK – rate of phosphorus-potassium fertilisation, RSug – content of reducing sugars

Source: developed by the authors based on research data and statistical processing in the *ggplot2* package

It was found that the correlation between the rates of nitrogen fertilisation and a number of indicators was average positive (sugar content, inulin content, root yield) and weak with the degree of polymerisation. In the case of reducing sugars, there was no reliable linear relationship. In the case of phosphorus-potassium fertilisers, a significant correlation was recorded only with root yield, and the relationship itself was weak positive (r = 0.23). Among other interactions, root yield was distinguished, which has an average positive correlation with the degree of polymerisation

(r = 0.49), total sugar content (r = 0.44), and inulin (r = 0.47), but a negative weak correlation with the content of reducing sugars (r = -0.36). The clustering performed indicates the presence of two clusters at a Euclidean distance of 30 (1 supercluster – phosphorus-potassium fertiliser and the content of reducing sugars; 2 supercluster – other indicators). At Euclidean distance of 20, 2 clusters were also distinguished within the second supercluster. The first includes indicators of yield and degree of polymerisation, and the second – the rate of nitrogen fertilisers, sugar content, and inulin content.

Clustering confirmed previously made observations, but did not allow finalising the conclusions, since some indicators change under the influence of unaccounted factors.

Principal component analysis (PCA) is used to take these factors into account. It was found that 87.83% of all data are described by two main components (PC1 – 59.34%, PC2 – 28.49 %) (Fig. 3). Notably, PC1 had a positive effect on the sugar content, inulin content, degree of polymerisation, and yield, but in the case of yield, its effect was less significant. This component had a negative effect on the content of reducing sugars. PC2, in turn, had almost no effect on yield, had a negative effect on the degree of polymerisation, but was positive for other biochemical parameters.

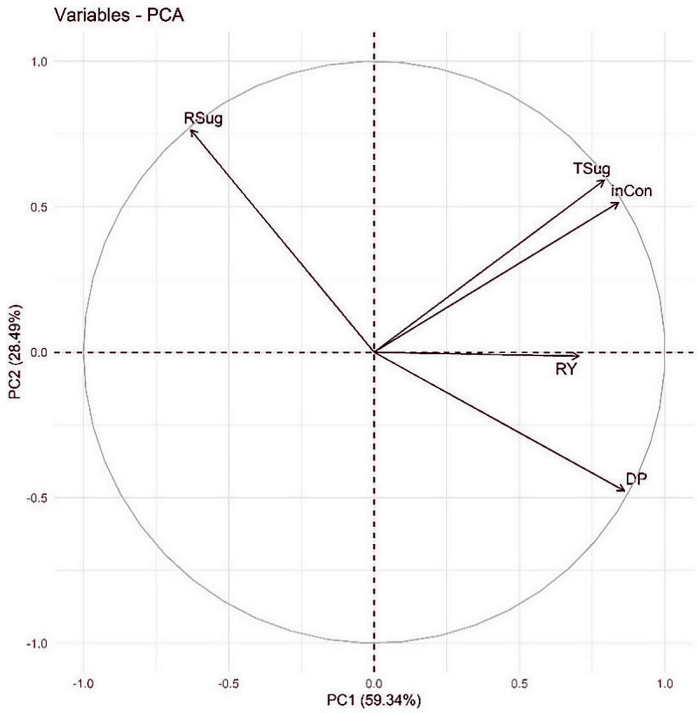

Figure 3. *Principal component analysis by main biochemical parameters and yield*
Note: RSug – reducing sugars, TSug – sugar content, InCon – inulin content, RY – root yield, DP – degree of polymerisation
Source: developed by the authors based on research data and statistical processing in the *ggplot2* package

Therefore, when further analysing the effect of the fertiliser system, it should be noted that PC1 mainly affected the yield, content, and quality of inulin, and PC2 only affected its content. This fact indicates that only coordinates along the PC1 axis can be considered for the estimate. The effect of nitrogen fertiliser was more significant in most cases, so grouping was based on this factor (Fig. 4).

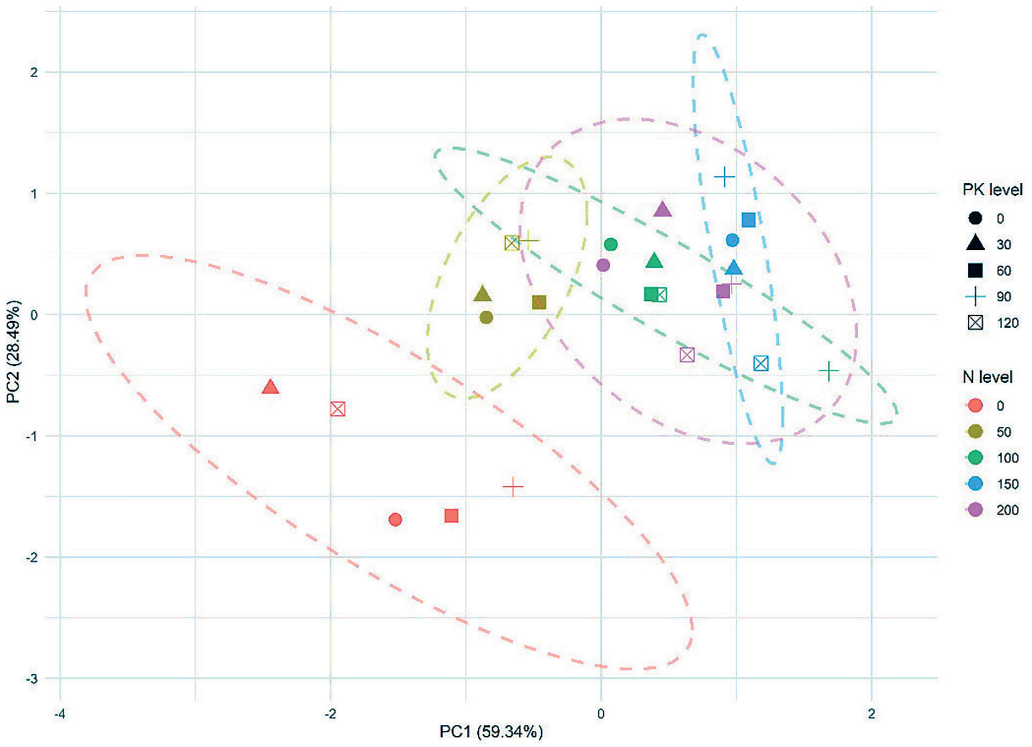

Figure 4. *Principal component analysis is grouped by variants*
Source: developed by the author based on research data and statistical processing in the *ggplot2* package

The red cluster is placed separately from the fertilised variants, which indicates the dominant effect of nitrogen fertilisers on yield and biochemical parameters. Fertilised options are placed differently on the plane. The cluster with a fertilisation rate of 50 kg/ha is in the negative range of values for PC1 and mainly in the positive range for PC2. The cluster with a rate of 100 kg/ha is scattered and is located mainly in the positive plane for PC1, but almost homogeneous for PC2 (in the range of -1 ... +1). The cluster with N_{150} is located to the right on the PC1 axis, indicating the priority option for maximising yield and inulin content. Notably, the option $N_{100}P_{90}K_{150}$ located to the right of cluster N_{150}, although in terms of yield, it is inferior to $P_{150}P_{90}K_{150}$. On the one hand, this may indicate that the influence of other components can significantly affect the yield and thus exclude this variant from the PC1-PC2 system based on empirical observations.

The results of the current study confirmed that excessive application of nitrogen fertilisers negatively affects the yield of chicory roots. Similar conclusions are given in the paper by B. Cwalina-Ambroziak *et al.* (2022), where the effect of different nitrogen doses on the productivity and mineral composition of chicory was studied. The researchers found that excessive doses of fertilisers reduced root yields and worsened plant health, in particular, due to increased sensitivity to pathogens. In addition, there was an imbalance of macronutrients in the tissues, which highlights the risk of excessive nitrogen nutrition. Thus, their results are consistent with the data of the current study, which also recorded a decrease in yield when exceeding the optimal level of N_{150}. In turn, S. Kalenska *et al.* (2024) using the example of coriander showed that increasing the doses of mineral fertilisers does not always lead to a proportional increase in yield.

In contrast, with excessive fertilisation, there was a sharp decrease in both seed productivity and the synthesis of secondary metabolites, including fatty and essential oils. These data are important for comparison, as they indicate the universality of the problem of excessive mineral load in different species. However, chicory is characterised by greater stability of inulin synthesis, which explains the more gradual decrease in yield in the current study. The study by S. Moscatello *et al.* (2023) provided additional evidence that excess nitrogen affects the distribution of metabolites in chicory. The researchers showed that most of the nitrogen accumulates in the leaves, rather than in the roots, which reduces the efficiency of its use in terms of root crop productivity. An adequate supply of nitrogen is crucial for maintaining an optimal ratio between roots and leaves, since this is what determines the ability of plants to accumulate fructans. These results support the conclusions of the current study, which found that optimal nitrogen doses contribute to the balanced development of plant organs.

Of particular interest are studies devoted to other vegetable crops. For example, J. Hong *et al.* (2022), using the example of lettuce, found that the combination of nitrogen, phosphorus, and potassium nutrition has a complex effect on product growth and quality. It was shown that excess nitrogen led to a decrease in plant weight, while optimal doses provided an increase in yield and improved leaf quality indicators. Similar patterns can be traced for chicory: when nitrogen doses were exceeded over N150, root productivity decreased. Similar results were obtained by M.M. Hoque *et al.* (2010)**,** who investigated the reaction of lettuce to different levels of mineral nutrition. The researchers showed that the yield and post-harvest quality of products increased only to a certain level of fertiliser, after which there was a deterioration in indicators. This was especially evident in the decrease in the marketable properties of products. Comparison of these results with the data of the current study shows a similarity in the reactions of different crops to excessive nitrogen loading: first, an increase in yield to the optimum, and then a decrease in productivity and quality.

An important role in the development of yield was played by weather conditions, which caused interannual differences. According to A.S. Mathieu *et al.* (2018), elevated temperatures did not always affect the inulin content, but led to a decrease in yield due to inhibition of sugar transport to the roots and slowing their growth. A.S. Mathieu *et al.* noted that under temperature stresses, the outflow of sucrose from the leaves to the roots was blocked, which directly reduced the biomass of root crops. However, the total fructan content remained relatively stable, which indicates a different sensitivity of physiological processes to temperature changes. Thus, the results of the current study confirmed the existence of a close relationship between the level of nitrogen fertiliser, biochemical parameters, and weather factors, which is consistent with the conclusions of previous studies.

The narrow range of fluctuations in the content of inulin in dry matter between years can be explained by the specific physiological response of chicory to water stress. As shown by B. Vandoorne *et al.* (2012), cell hydration is of key importance because the inulin content of fresh roots varies significantly depending on growing conditions. The researchers have shown that water deficiency dramatically reduces root growth and inulin yield, and this effect occurs regardless of the level of photosynthetic activity. This indicates that it is the violation of the water regime, and not a decrease in the production of photosynthesis, that limits the accumulation of reserve carbohydrates. In plants growing under arid conditions, the degree of polymerisation of inulin molecules may increase over time, while under favourable conditions, equilibrium is achieved much faster. The water stress did not significantly affect the degree of polymerisation, but it had a stronger effect on the overall yield, which confirms the dependence on the complex effect of solar radiation and temperature.

The findings by J. van Arkel *et al.* (2012) showed that in temperate regions, the average degree of inulin polymerisation increases until mid-September, after which it gradually decreased due to increased glucose levels, while inulin yield stabilises. J. van Arkel *et al.* traced the dynamics of changes in enzymatic activity in the process of "filling storage facilities" of roots: at first, there was an intense accumulation of long-chain fructans, but with the progression of the season, the activity of invertases increased, which caused an increase in glucose concentration and, accordingly, a decrease in the average DP. This confirms that the timing of harvesting is a critical factor for maintaining a stable carbohydrate composition. Similar patterns can be traced in the paper by R.G. Wilson *et al.* (2004), where it was found that an increase in the proportion of short-chain fructans (DP 3-10) occurs at late harvesting, especially in conditions of high temperatures of the growing season. Their experiments have shown that with delayed harvesting, the yield of root crops increased, but the quality of products decreased due to an increase in the content of easily soluble sugars. In temperate regions, these processes were less pronounced, which indicates a significant influence of thermal growing conditions. Data by J. Wierzbowska *et al.* (2023) supplemented these results by demonstrating that late harvesting can reduce both the content of inulin and the degree of its polymerisation, even in conditions of an overall increase in root crop yield. The researchers stressed that an increase in root yield is not always accompanied by an increase in quality indicators, and with excessive postponement of harvesting, inulin fractions degrade to short-chain compounds. This confirms that optimising harvesting time is just as important as fertiliser levels or weather conditions.

The results of the current study confirm the importance of optimising the levels of nitrogen and phosphorus-potassium nutrition to increase the yield and quality of chicory. It has been found that excessive doses of fertilisers, especially nitrogen fertilisers, can reduce productivity and worsen biochemical characteristics, while moderate standards provide the best balance between quantity and quality of products. Weather conditions, in particular, fluctuations in temperature and water conditions, have a significant impact on the results, which causes interannual differences and confirms the need for adaptive fertiliser systems. The obtained data indicate the complex nature of the interaction of nutrition and climatic factors, which should be taken into consideration when forming practical recommendations for growing chicory. Data by M. Voitovyk *et al.* (2023) from typical chernozem show that organo-mineral fertiliser provides an increase in humic acid levels and an increase in soil buffer capacity, which is consistent with our results on improving the stability of soil organic matter with moderate doses of fertilisers.

The results obtained confirmed the complex nature of the interaction of mineral nutrition and weather factors in the development of yield and quality of chicory roots. Nitrogen fertiliser turned out to be the key factor that most affected inulin synthesis, total sugar content and degree of polymerisation, while the effect of phosphorus-potassium fertilisers was more moderate and mainly affected yield. Moreover, weather and water conditions significantly modified the effect of fertilisers, which emphasises the need for an adaptive approach to crop nutrition. Data summarisation provides an opportunity to determine the optimal ranges for fertiliser application to achieve high and stable productivity and raw material quality indicators.

Conclusions

The results of three years of field studies have confirmed that the effectiveness of growing common chicory is largely determined by the balance of mineral nutrition, while nitrogen fertilisers play a leading role. The application of nitrogen in doses up to 150 kg/ha significantly increased the yield of roots (up to 35.4 t/ha), and the content of total sugars and inulin increased by 4-5%

compared to the control, excessive use (200 kg/ha) caused a decrease in productivity, which was manifested in a decrease in root yield up to 20% compared to the best variant. The effect of phosphorus-potassium fertiliser on yield was characterised by a parabolic trend: the maximum indicators were formed at the rate $P_{60}K_{100}$-$P_{90}K_{150}$, however, a further increase in the dose ($P_{120}K_{200}$) led to a decrease in yield. Biochemical analysis showed that nitrogen fertiliser stimulated the synthesis of inulin and an increase in the degree of its polymerisation, while the effect of phosphorus and potassium was weaker and mainly associated with the processes of carbohydrate transport. Principal component analysis showed that more than 87% of the variations were conditioned by two main components, of which the first was mainly related to yield and inulin content. Positive correlations were established between the yield and the degree of polymerisation ($r = 0.49$), the total sugar content ($r = 0.44$) and inulin ($r = 0.47$). Simultaneously, a negative association with reducing sugars was observed ($r = -0.36$), which indicates a predominant synthesis of fructans under favourable conditions.

The optimal fertiliser regime for common chicory in the conditions of the Right-Bank Forest-Steppe of Ukraine should be considered the application of nitrogen in the range of 100-150 kg/ha in combination with phosphorus-potassium fertilisers at the rate $P_{60}K_{100}$ or $P_{90}K_{150}$. This strategy ensures the development of high yields, high inulin content, and rational use of resources, which makes the technology of growing chicory economically feasible and environmentally sustainable. Further research should focus on integrated fertiliser systems involving organic soil improvers, studying the carbon and ecological footprint of chicory production, and evaluating the effectiveness of technologies in the context of resource-saving agriculture.

Acknowledgements

This work was carried out within the framework of the research "Optimisation of the Technology for Growing Inulin-Containing Crops for Raw Material Production for Alternative Energy Needs" (No. 0121U111237), which is part of the thematic plan of the National University of Life and Environmental Sciences of Ukraine.

Funding

None.

Conflict of Interest

None.

References

[1] Akram, H., Zafar, H., & Abbasi, B. H. (2025). The chicory root (Cichorium intybus var. sativum) frontier: Pioneering biotechnological advancements. *Phytochemistry Reviews*. doi: 10.1007/s11101-025-10085-x.

[2] Alves, D.M.R., de Mello Prado, R., Barreto, R.F., & da Silva Carvalho, L.T. (2024). Nano-silicon and sodium mitigate damage by potassium deficiency in chicory. *Scientific Reports*, 14(1), article number 16841. doi: 10.1038/s41598-024-67875-0.

[3] Bakhmat, M.I., Tkach, O.V., & Stepanchenko, V.M. (2021). Seed yield of root chicory depending on the method of plant arrangement. *Podilian Bulletin: Agriculture, Engineering, Economics*, 34, 9-18. doi: 10.37406/2706-9052-2021-1-1.

[4] Buchelt, A.C., Teixeira, G.C.M., Oliveira, K.S., Rocha, A.M.S., de Mello Prado, R., & Caione, G. (2020). Silicon contribution via nutrient solution in forage plants to mitigate nitrogen, potassium, calcium, magnesium, and sulfur deficiency. *Journal of Soil Science and Plant Nutrition*, 20(3), 1532-1548. doi: 10.1007/s42729-020-00245-7.

[5] Convention on Biological Diversity. (1992, June). Retrieved from https://zakon.rada.gov.ua/laws/show/995_030#Text.

[6] Cwalina-Ambroziak, B., Wierzbowska, J., & Bogucka, B. (2022). The effect of nitrogen fertilization on yield and macronutrient concentrations in root chicory (*Cichorium intybus* L. var. Sativus Bisch) and the health status of plant. *Acta Scientiarum Polonorum. Hortorum Cultus*, 21(5), 85-99. doi: 10.24326/asphc.2022.5.8.

[7] Ebrahimi, M., & Gholami, M. (2023). Elevated inulin content in chicory under phosphorus and iron starvation. *Journal of Medicinal Plants and By-products*, 12(4), 413-420. doi: 10.22034/jmpb.2023.129015.

[8] Gholami, H., Fard, F.R., Saharkhiz, M.J., & Ghani, A. (2018). Yield and physicochemical properties of inulin obtained from Iranian chicory roots under vermicompost and humic acid treatments. *Industrial Crops and Products*, 123, 610-616. doi: 10.1016/j.indcrop.2018.07.031.

[9] Hingsamer, M., Kulmer, V., de Roode, M., & Kernitzkyi, M. (2022). Environmental and socio-economic impacts of new plant breeding technologies: A case study of root chicory for inulin production. *Frontiers in Genome Editing*, 4, article number 919392. doi: 10.3389/fgeed.2022.919392.

[10] Hong, J., Xu, F., Chen, G., Huang, X., Wang, S., Du, L., & Ding, G. (2022). Evaluation of the effects of nitrogen, phosphorus, and potassium applications on the growth, yield, and quality of lettuce (*Lactuca sativa* L.). *Agronomy*, 12(10), article number 2477. doi: 10.3390/agronomy12102477.

[11] Hoque, M.M., Ajwa, H., Othman, M., Smith, R., & Cahn, M. (2010). Yield and postharvest quality of lettuce in response to nitrogen, phosphorus, and potassium fertilizers. *HortScience*, 45(10), 1539-1544. doi: 10.21273/HORTSCI.45.10.1539.

[12] Kalenska, S., Mazurenko, B., Harbar, L., Zhovtun, M., Yunyk, A., & Mokrienko, V. (2024). Seed yield limitations of coriander (*Coriandrum sativum* L.) based on plant structure analysis. *Journal of Agriculture and Food Research*, 18, article number 101321. doi: 10.1016/j.jafr.2024.101321.

[13] Mathieu, A.S., Tinel, C., Dailly, H., Quinet, M., & Lutts, S. (2018). Impact of high temperature on sucrose translocation, sugar content and inulin yield in *Cichorium intybus* L. var. *sativum*. *Plant and Soil*, 432, 273-288. doi: 10.1007/s11104-018-3802-7.

[14] Moscatello, S., Battistelli, A., Mattioni, M., & Proietti, S. (2023). Yield, fructans accumulation, and nutritional quality of young chicory plants as related to genotype and nitrogen fertilization. *Agronomy*, 13(7), article number 1752. doi: 10.3390/agronomy13071752.

[15] Paseephol, T., Small, D., & Sherkat, F. (2007). Process optimisation for fractionating Jerusalem artichoke fructans with ethanol using response surface methodology. *Food Chemistry*, 104(1), 73-80. doi: 10.1016/j.foodchem.2006.10.078.

[16] Popova, I., Vasyliv, V., Palamarchuk, I., Mushtruk, N., & Kukla, O. (2024). Assessment of ecological safety and technological characteristics of chicory based on microbiological and derivatographic studies. *Human Health and Nation*, 1, 20-38.

[17] Tabatabaee, S., Sanjarian, F., Lohrasebi, T., & Karimi, M. (2021). Enhanced inulin production by hairy root cultures of Cichorium intybus in response to Pi and Fe starvation. *Molecular Biology Research Communications*, 10(2), article number 85. doi: 10.22099/mbrc.2021.38031.1527.

[18] Tkach, O.V., Ovcharuk, O.V., Ovcharuk, V.I., & Petrychenko, Ye.A. (2023). Influence of different growing conditions of chicory on the relationship between vegetative mass formation and root crops. *Podilian Bulletin: Agriculture, Engineering, Economics*, 40, 72-77. doi: 10.37406/2706-9052-2023-3.11.

[19] van Arkel, J., Vergauwen, R., Sévenier, R., Hakkert, J.C., van Laere, A., Bouwmeester, H.J., Koops, A.J., & van der Meer, I.M. (2012). Sink filling, inulin metabolizing enzymes and carbohydrate status in field grown chicory (*Cichorium intybus* L.). *Journal of Plant Physiology*, 169(15), 1520-1529. doi: 10.1016/j.jplph.2012.06.005.

[20] Vandoorne, B., Mathieu, A.S., Van den Ende, W., Vergauwen, R., Périlleux, C., Javaux, M., & Lutts, S. (2012). Water stress drastically reduces root growth and inulin yield in *Cichorium intybus* (var. *sativum*) independently of photosynthesis. *Journal of Experimental Botany*, 63(12), 4359-4373. doi: 10.1093/jxb/ers095.

[21] Voitovyk, M., Prymak, I., Tsyuk, O., & Melnyk, V. (2023). Qualitative composition of humus and physical and chemical properties of typical chernozem depending on the fertiliser system. *Plant and Soil Science*, 14(1), 9-21. doi: 10.31548/plant1.2023.09.

[22] Wierzbowska, J., Cwalina-Ambroziak, B., Waskiewicz, A., & Bogucka, B. (2023). Influence of nitrogen fertilizers on the concentrations of inulin and micronutrients in Jerusalem artichoke tubers and root chicory. *Journal of Elementology*, 28(3). doi: 10.5601/jelem.2023.28.2.3024.

[23] Wilson, R.G., Smith, J.A., & Yonts, C.D. (2004). Chicory root yield and carbohydrate composition is influenced by cultivar selection, planting, and harvest date. *Crop Science*, 44(3), 748-752. doi: 10.2135/cropsci2004.7480.

[24] Zhang, H., Yang, S., Wei, X., Wang, L., Sun, X., Hou, Z., Xu, D., & Liu, W. (2023). Forecasting the favorable growth conditions and suitable regions for chicory (*Cichorium intybus* L.) on the Qinghai plateau under current climatic conditions. *Ecological Informatics*, 78, article number 102343. doi: 10.1016/j.ecoinf.2023.102343.

[25] Zhao, X., Wang, Y., & Liu, H. (2023). The phosphorus–iron nexus: Decoding the nutrients interaction in plants. *International Journal of Molecular Sciences*, 25(13), article number 6992. doi: 10.3390/ijms25136992.

Вплив азотного та фосфорно-калійного удобрення на урожайність та біохімічний склад цикорію коренеплідного (*Cichorium intybus* L.)

Богдан Мазуренко
Доктор філософії з агрономії, доцент
Національний університет біоресурсів і природокористування України
03041, вул. Героїв Оборони, 15, м. Київ, Україна
https://orcid.org/0000-0002-4177-9909
Любов Гончар
Кандидат сільськогосподарських наук, доцент
Національний університет біоресурсів і природокористування України
03041, вул. Героїв Оборони, 15, м. Київ, Україна
https://orcid.org/0000-0002-3628-6659

Анотація. Цикорій коренеплідний (*Cichorium intybus* L.) є важливою технічною культурою, цінною завдяки високому вмісту інуліну та функціональних біоактивних сполук. Оптимізація мінерального удобрення залишається ключовим фактором для максимізації врожайності та поліпшення біохімічного складу в умовах змін клімату. Метою даного дослідження було оцінити вплив азотного та фосфорно-калійного удобрення на урожайність та біохімічні показники цикорію. Польові дослідження проводилися у 2021-2023 рр. у Правобережному Лісостепу України на чорноземі слабогумусному за двофакторною схемою, що включала 5 варіантів азотного удобреннння (0-200 кг/га) та п'ять варіантів фосфорно-калійного удобрення (0-120 кг P_2O_5 та 0-200 кг K_2O). Урожайність коренеплодів, загальний вміст цукрів, вміст інуліну, редукуючих цукрів та ступінь полімеризації визначали за стандартизованими біохімічними та статистичними методами (дисперсійний аналіз, post-hoc тест Tukey's HSD, Principal Component Analysis (PCA), кластерний аналіз). Результати досліджень показали, що азотне удобрення впливало на всі біохімічні показники та урожайність, але найбільше на вміст інуліну (до 75 % від сухої речовини) та ступінь полімеризації, тоді як фосфорно-калійні добрива лише на урожайність та ступінь полімеризації. Максимальна середня врожайність у роки досліджень (35,4 т/га) була досягнута при внесенні $N_{150}P_{90}K_{150}$, тоді як надмірне внесення азотних та фосфорно-калійних добрив (200 кг/га) знижувало продуктивність посівів та урожайність. Загальний вміст цукрів та інуліну зростав при внесенні азоту до 150 кг/га, після чого спостерігалося зниження. PCA підтвердив домінуючу роль азоту у формуванні як урожайності, так і біохімічних показників. Оптимальні норми азоту (100-150 кг/га) у поєднанні з помірними рівнями фосфорно-калійного удобрення забезпечували стабільну врожайність коренеплодів та високий вміст інуліну, що є важливим як для промислової переробки, так і для сталого агровиробництва

Ключові слова: кореляція; інулін; цукри; Principal Component Analysis; полімеризація

Received 03.06.2025 Revised 01.09.2025 Accepted 23.09.2025

Vol. 21, No. 5
2025

Scientific Reports of the National University of Life and Environmental Sciences of Ukraine

Journal homepage: https://scireports.com.ua/en

UDC 636.082.35:604.2:661.745:591.182 Doi: 10.31548/dopovidi/5.2025.71

Amino acid composition of the longest back muscle (*m. longissimus dorsi*) young animals of specialised beef breeds

Nataliya Svyrydenko*
PhD in Agricultural Sciences, Associate Professor
National University of Life and Environmental Sciences of Ukraine
03041, 15 Heroiv Oborony Str., Kyiv, Ukraine
https://orcid.org/0000-0002-9151-6904

Svitlana Kostenko
Doctor of Biological Sciences, Professor
National University of Life and Environmental Sciences of Ukraine
03041, 15 Heroiv Oborony Str., Kyiv, Ukraine
https://orcid.org/0000-0002-7816-3374

Maryna Khomenko
PhD in Agricultural Sciences
National University of Life and Environmental Sciences of Ukraine
03041, 15 Heroiv Oborony St., Kyiv, Ukraine
https://orcid.org/0000-0001-7023-3676

Abstract. The relevance of the study consisted in the investigation of the qualitative characteristics of beef as a source of complete protein and the content of essential amino acids that determine its biological and nutritional value. The purpose of the study was to determine the content of non-essential and essential amino acids and conduct a comparative analysis of the amino acid composition of the longest back muscle (*m. longissimus dorsi*) in young animals of specialised beef breeds. The studies were conducted on Aberdeen-Angus, Volyn Beef, and Charolais bulls grown using meat cattle breeding technology in the Polissia zone of Ukraine. Control slaughter of experimental animals was performed at the age of 18 months. 3 animal units were selected from each breed, from which samples of the longest back muscle (*m. longissimus dorsi*) at the level of 9th-11th ribs were taken for research. The amino acid content was determined on an analyser by liquid ion exchange chromatography. Inter-breed differences in the quantitative content of non-essential and non-essential amino acids were found. In particular, the meat of Aberdeen-Angus bulls was characterised by the highest content of essential amino acids,

Suggested Citation:

Svyrydenko, N., Kostenko, S., & Khomenko, M. (2025). Amino acid composition of the longest back muscle (*m. longissimus dorsi*) young animals of specialised beef breeds. *Scientific Reports of the National University of Life and Environmental Sciences of Ukraine*, 21(5), 71-81. doi: 10.31548/dopovidi/5.2025.71.

*Corresponding author

among which methionine (6.84-16.5%), lysine (6.6-10.37%) and leucine (7.9-8.6%) dominated. For Charolais beef, elevated levels of lysine and valine were determined, while animals of the Volyn Beef breed had an advantage in leucine content. Among non-essential amino acids, glutamic acid (12.7-13.3%) and aspartic acid (8.9-10.09%) accounted for the largest share. The results obtained show that the quality of beef largely depends on breed characteristics, which determines its nutritional value, biological usefulness, and organoleptic properties. The higher content of methionine and histidine in Aberdeen-Angus meat indicates more intensive processes of intramuscular fat development, which provides better marbling and energy value of young meat of this breed. The results of the study can be used in practice for the selection and breeding of meat cattle with an optimal amino acid composition of meat to increase its nutritional and biological value

Keywords: beef; Aberdeen-Angus; Volyn Beef; Charolais; essential amino acids; biological value

Introduction

One of the main tasks of the livestock industry is to provide the population with food and raw materials. Meat of various animal species is the most important product for ensuring a healthy and balanced diet for people around the world, as a source of complete protein. The lack of protein can lead to negative effects on the human body, which can manifest itself in the form of a decrease in metabolism and the immune system, disruption of certain organs or systems. In the structure of global meat production, the first place is occupied by the production of poultry meat, the second – pork, and the third place is occupied by bovine cattle meat.

Most scientific publications have demonstrated a significant advantage of using animal protein in the human diet, which is characterised by a high balance of essential and non-essential amino acids and is the closest to the amino acid composition of the human body (Bal-Prylypko *et al*., 2022). Research by O.S. Yaremchuk *et al.* (2022) demonstrated that the introduction of protein-vitamin premix in the diet of bulls significantly increases not only productive indicators (weight growth, slaughter yield), but also the chemical composition of muscle tissue, in particular, dry matter and protein, which indicates the possible effect of feeding on the amino acid profile. This highlights the need for comprehensive consideration of both genotypic and alimentary factors when assessing the quality characteristics of beef. According to O.I. Kolisnyk *et al.* (2018), the most valuable components of meat are proteins that are highly digestible and contain essential amino acids for the human body: arginine, histidine, tryptophan, leucine, isoleucine, valine, threonine, lysine, methionine, and phenylalanine, which are not synthesised in the human body and must come from food. Beef obtained from animals of specialised beef breeds has an optimal ratio of muscle, bone and adipose tissue, which determines the quality of meat, its nutritional value, technological and organoleptic properties. According to M.J. Lopez & S.S. Mohiuddin (2023), animal meat consumption is important because it contains amino acids that can be converted to carbohydrates and are called glucogenic amino acids. Some amino acids give rise to specialised products. For example, tyrosine can be converted to hormones such as thyroid hormones, epinephrine, norepinephrine, and melanin. Methionine, in its active form known as S-adenosylmethionine, plays a crucial role in cellular processes by transferring the methyl group to various substances through a process called transmethylation. Cystine and methionine are the main sources of sulphur.

According to A. Paliy *et al.* (2020; 2024), differences in the amino acid profile of beef were found in animals of Black Pied, Red Steppe, Simmental, Lebedyn, and Ukrainian Grey breeds. The

researchers argued that the highest biological value was inherent in samples of Ukrainian Grey beef breed that was dominated by both Red Steppe and Black Pied breeds in terms of amino acid index. According to G. Bittante *et al.* (2024), the amino acid composition of beef and veal in animals of local origin (beef × dairy crossbreds) significantly differed in the content of 16 out of 21 amino acids, which highlights the role of the genotype in shaping the biological value of meat. The results obtained confirmed the need for further study of the influence of breed characteristics on the amino acid profile, since they determine the nutritional quality and organoleptic characteristics of products. S.-H. Lee *et al.* (2019) investigated the amino acid composition of animal meat of two local cattle breeds, and found that the increased content of alanine and glutamine in beef gives a more pronounced and rich "umami" taste, which affects the benefits for consumers when choosing meat. G. Bischof *et al.* (2022) stated that the content of essential amino acids that make up beef, such as isoleucine, leucine, methionine, phenylalanine, tyrosine, and valine, positively correlates with the duration of meat maturation. In particular, they affect the taste, appearance, juiciness, and tenderness of beef, and the researchers concluded that protein metabolism depends on the breed.

It is worth noting that there is growing attention to the investigation of the biological usefulness of food products, in particular of animal origin, and the study of the role of amino acids in the human body. Based on the analysis of sources, it should be noted that the factors that directly affect the biological usefulness of beef were not sufficiently considered. That is why it is relevant to investigate the amino acid composition and the ratio of non-essential and essential amino acids in meat obtained from young animals of specialised beef breeds that were kept at one farm in the Polissia zone of Ukraine.

The purpose of this study was to determine the content of non-essential and essential amino acids and conduct a comparative analysis of the amino acid composition of the longest back muscle (*m. longissimus dorsi*) in young animals of specialised beef breeds.

Materials and Methods

The study was conducted on cattle of specialised beef breeds that were raised up to 18 months of age using the technology of beef cattle breeding in the Polissia zone of Ukraine at LLC Agrofirma "Kyivska" during 2018-2020. For the purpose of the study, three experimental groups of animals were established: 20 Aberdeen-Angus bulls were selected for Group 1, 20 Volyn Beef bulls for Group 2, and 20 Charolais bulls for Group 3. Before weaning, bulls were kept together with cows on free suckling using the technology of specialised meat cattle breeding, and after weaning on fattening sites. Animals of all experimental groups were fed the main diet. In the structure of the feed ration of bulls in terms of energy nutritional value, concentrated feeds accounted for 29.7-30.5%, coarse – 26.1-26.4, and green feeds – 43.4-43.9%. The diet was balanced in terms of nutrient content, considering the age and physiological needs of young animals.

In order to analyse the chemical and amino acid composition of meat, 3 animals were selected from each experimental group at the age of 18 months, which were analogous in age and live weight, and their control slaughter was carried out. After slaughtering the animals and assessing the quality of the carcasses, beef samples were taken for testing 24 hours later. Samples were taken from the longest back muscle (*m. longissimus dorsi)* at the level of 9^{th}-11^{th} ribs, as it is considered the most representative for evaluating the quality characteristics of meat. The average weight of samples was 100-200 g, after sampling, was marked with the breed and individual number of the animal and transported at temperatures up to +2…+4°C to the laboratory. The study was conducted in compliance with ethical standards and rules for handling animals in accordance with the regulations of the European Convention for the Protection of Vertebrate Animals Used for

Experimental and Other Scientific Purposes (1986) and Order of the Ministry of Education and Science, Youth and Sports of Ukraine No. 249 (2012).

The content of non-essential (asparagine, serine, glutamic, proline, cystine, glycine, alanine, tyrosine, arginine) and essential (threonine, valine, methionine, isoleucine, leucine, phenylalanine, histidine, lysine) amino acids was determined on the automatic analyser of AAA amino acids T-339m (Czech Republic) by liquid ion exchange chromatography. Statistical analysis of the results obtained was performed using the Microsoft Exel 2017 computer programme. The level of statistical significance P (∗P > 0.95; ∗∗P > 0.99; ∗∗∗P > 0.999) was determined using the Student's t-test, considering statistical errors and the probability of comparing similar indicators.

Results and Discussion

The bulk of the nutrients in meat are proteins, which, unlike plant-based proteins, are mainly complete proteins. They contain all the vital amino acids that are not synthesised in the human body. As a result of studies of the amino acid composition of the longest back muscle, differences in the content of unchanged amino acids were established (Table 1).

Table 1. *Content of essential amino acids in the longest back muscle (m.longissimus dorsi), M ± m (n = 9)*

Amino acid	Animal breed		
	Aberdeen-Angus n = 3	Volyn Beef n = 3	Charolais n = 3
Protein, %	18.80 ± 0.52	18.82 ± 0.34	18.80 ± 0.13
Threonine, mg/100g	0.42 ± 0.03	0.42 ± 0.02	0.37 ± 0.00
Valine, mg/100g	0.74 ± 0.33	0.97 ± 0.03	1.04 ± 0.03
Methionine, mg/100g	2.82 ± 0.71	1.44 ± 0.03	1.08 ± 0.02∗
Isoleucine, mg/100g	1.11 ± 0.11	0.77 ± 0.04∗∗	0.81 ± 0.05∗
Leucine, mg/100g	1.36 ± 0.10	1.38 ± 0.09	1.25 ± 0.04
Phenylalanine, mg/100g	0.94 ± 0.09	0.76 ± 0.06	0.80 ± 0.01
Histidine, mg/100g	0.97 ± 0.09	0.81 ± 0.01	0.69 ± 0.01∗∗
Lysine, mg/100g	1.19 ± 0.31	1.06 ± 0.02	1.63 ± 0.01
Essential amino acids, mg/100g	**9.55 ± 1.77**	**7.60 ±v0.31**	**7.68 ± 0.18**

Note: ∗P > 0.95; ∗∗P > 0.99; ∗∗∗P > 0.999

Source: compiled by the authors

Analysis of Table 1 shows that at the age of 18 months, Aberdeen-Angus bulls had the highest total content of essential amino acids, in particular, methionine, isoleucine, phenylalanine, and histidine. Charolais breed prevailed in terms of valine and lysine content, and its analogues of the Volyn Beef breed had a slightly higher amount of leucine. These differences between animals of the breeds under study ensure the development of different protein profiles in the meat of animals of different breeds. In terms of the content of essential amino acids in meat, Aberdeen-Angus animals exceeded the analogues of the experimental groups 2 and 3 by 20.4% and 19.6%, respectively, which indicates high quality indicators of beef of young animals of Group 1. Meat of young Charolais was characterised by a higher content of lysine – 1.63 mg/100 g against 1.19 and 1.06 mg/100 g in animals of groups 1 and 2, which takes part in the reactions of transamination and deamination of amino acids in the body, thereby affecting the synthesis of essential amino acids. The advantage in terms of valine content, which helps to maintain nitrogen balance, which is important for growth and development, in animals of this breed ranged from 6.7 to 28.8%. In the longest back muscle of young animals of

the Volyn Beef breed, the leucine content was 1.4% and 9.4% higher compared to analogues of the Aberdeen-Angus and Charolais breeds, respectively. Based on the analysis of the content of non-essential amino acids, animals of the Aberdeen-Angus breed were preferred for the content of glutamic acid, Volyn Beef breed – for the content of aspartic acid, serine, proline, alanine, arginine, and Charolais breed – for the content of glycine and tyrosine (Table 2).

Table 2. *Content of non-essential amino acids in the longest back muscle (m. longissimus dorsi), M ± m (n = 9)*

Amino acid	Animal breed		
	Aberdeen-Angus n = 3	Volyn Beef n = 3	Charolais n = 3
Protein, %	18.80 ± 0.52	18.82 ± 0.34	18.80 ± 0.13
Asparagine, mg/100g	1.54 ± 0.14	1.72 ± 0.01	1.59 ± 0.05
Serine, mg/100g	0.61 ± 0.01	0.64 ± 0.02	0.61 ± 0.02
Glutamine, mg/100kg	2.28 ± 0.04	2.08 ± 0.07*	2.01 ± 0.05
Proline, mg/100g	0.36 ± 0.07	0.45 ± 0.01	0.42 ± 0.04
Cystine, mg/100g	0.06 ± 0.01	0.06 ± 0.01	0.05 ± 0.02
Glycine, mg/100g	0.40 ± 0.08	0.46 ± 0.02	0.48 ± 0.00
Alanine, mg/100g	0.69 ± 0.15	1.09 ± 0.03*	1.06 ± 0.02*
Tyrosine, mg/100g	0.83 ± 0.01	0.88 ± 0.05	0.92 ± 0.09
Arginine, mg/100g	0.87 ± 0.10	1.01 ± 0.11	0.94 ± 0.04
Non-essential amino acids, mg/100g	**7.65 ± 0.61**	**8.39 ± 0.32**	**8.07 ± 0.33**

Note: *P > 0.95; **P > 0.99; ***P > 0.999

Source: compiled by the authors

Analysis of non-essential amino acids showed that the breeds under study have a different tendencies in the accumulation of certain compounds. The highest level of glutamic acid (2.28 mg/100 g) was determined in Aberdeen-Angus meat, which may indicate a more intense synthesis of protein structures, while in Volyn Beef this indicator was lower (2.08 mg/100 g). The animals of Volyn Beef and Charolais showed an increased content of alanine (1.09 and 1.06 mg/100 g, respectively), which may indicate the features of energy metabolism and the accumulation of compounds involved in the development of sweetness in beef taste. Volyn Beef breed also had an advantage in the content of aspartic acid (1.72 mg/100 g), which together with glutamic acid is involved in the development of acidity of muscle tissue, which affects the juiciness and tenderness of meat. The Charolais breed was characterised by increased levels of glycine (0.48 mg/100 g) and tyrosine (0.92 mg/100 g), which may be conditioned by the specifics of the synthesis of collagen and pigment compounds. The total content of non-essential amino acids was highest in the Volyn Beef breed (8.39 mg/100 g), which confirms a more intensive accumulation of these compounds in the protein structure of muscles. A common pattern for all breeds is the predominance of glutamic and aspartic acids, which in combination with alanine form the basis of metabolic processes and affect the organoleptic properties of meat. Thus, breed differences are found not only in the total content of non-essential amino acids, but also in the specific profile of their accumulation, which is important for assessing the biological and taste value of beef.

Based on the analysis of the percentage content of amino acids in the longest back muscle, among the essential amino acids in animals of the breeds under study, methionine accounted for the largest percentage in the protein composition of dry muscle tissue – 6.84-16.5%, lysine – 6.6-10.37%, and leucine – 7.9-8.6%. In terms of the content of non-essential amino acids, glutamic

acid accounted for the largest share – 12.7-13.3% and aspartic acid – 8.9-10.09%. The cystine content in beef was the lowest and only 0.3-0.4%, depending on the breed (Fig. 1).

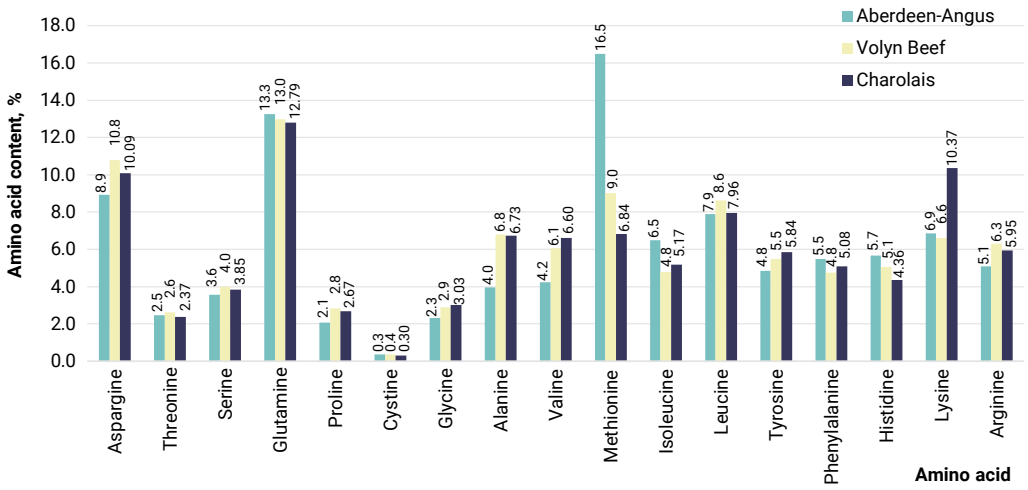

Figure 1. *Amino acid content in the longest back muscle*
Source: compiled by the authors

Analysis of Figure 1 shows that in samples of the longest back muscle taken from bulls of specialised beef cattle breeds, methionine, lysine, and leucine, and among the non-essential amino acids, glutamic and aspartic acids, which determines the biological value of the meat of the animals under study. The highest content of menionine was observed in animals of the Aberdeen-Angus breed, the difference with other groups was 45.4% and 58.5%, respectively. Notably, in all experimental groups, the high content of glutamic acid between the groups was within 3.8%. Animals of the Volyn-Beef breed had an advantage in the content of aspartic amino acid by 17.5% (Group 1) and 6.5 % (Group 3) and leucine by 8.1 and 7.4%, respectively.

The results of current research are partially consistent with the study by O.P. Razanova *et al.* (2023), which proved the superiority of Charolais bulls in terms of valine content – by 7.4%, isoleucine – by 45.3% ($p < 0.001$), leucine – by 15.2% ($p < 0.001$), lysine – by 7.8%, threonine and phenylalanine + tyrosine – by 6.5% ($p < 0.05$) and 7.5% ($p < 0.01$) compared to animals of the Aberdeen-Angus and Black Pied breeds. The study by G. Hollo *et al.* (2007), who studied amino acid profile of Hungarian Grey and Holstein-Frisian Beef breeds, no significant inter-breed differences were found, with the exception of histidine content. According to J. Vopálenský *et al.* (2017), a study of the muscle tissue of bulls of eight beef breeds raised in Southern Bohemia showed significant inter-breed differences in amino acid composition. Among essential amino acids, the largest proportion was lysine (8.8-10.4%), while the content of methionine ranged from 2.4-2.9%, threonine – approximately 4.6%, valine – 5.1%, isoleucine – 4.8%, leucine – 8.2%, phenylalanine – 4.1%, histidine – 4.2%, and arginine – 8.0%. Statistically significant differences ($p \leq 0.05$) were recorded for most essential amino acids, with the exception of valine and leucine. Among non-essential amino acids, the largest proportion of protein in the dry matter of muscle tissue was glutamic acid (13.9-15.1%), while the lowest values were characteristic of serine and tyrosine; other indicators were: aspartic acid – 9.3%, serine – 4.0%, proline – 5.3%, glycine – 5.5%, and alanine – 6.1%. The current

study noted similar trends. The high percentage of glutamic acid (13.9-15.1%) in the muscle tissue of young Aberdeen-Angus, Volyn Beef, and Charolais is consistent with the data by J. Vopálenský *et al.* (2017), where this figure was 14.8-16.8%. Simultaneously, animals of the Volyn Beef breed showed a preference for the content of aspartic acid (11.7% more compared to Aberdeen-Angus) and alanine (36.5% more), while Charolais had a higher level of lysine (37% more compared to Volyn Beef breed). The established inter-breed differences in the content of essential amino acids (methionine, lysine, isoleucine, phenylalanine, and histidine in Aberdeen-Angus; lysine and valine in Charolais; leucine in Volyn Beef) confirm the authors' conclusions regarding the determining role of the genotype in the amino acid profile of beef. Thus, the results of the current study are consistent with previous scientific data and complement them, demonstrating the specific features of animals raised in the Polissia zone of Ukraine.

The current study indicates that a relatively high percentage of glutamic acid (13.9-15.1%) is an important indicator, which is fully consistent with the data by J. Subrt *et al.* (2002), which give a value of 14.8-16.8%. The researchers also found significant differences in the content of essential amino acids: 30.16% in Montbeliarde to 34.50% in Maine-Anjou, and 30.22% in Hereford to 33.75% in Aberdeen-Angus animals. Among the essential amino acids in meat, lysine prevailed – 7.76-8.75%. Significant differences in the content of amino acids such as threonine, valine, and isoleucine were found in animals of combined productivity. Significant differences ($P < 0.05$) in the levels of glutamic acid, asparagine, proline, serine, and alanine were found among non-essential amino acids. Comparison with data of J.D. Wood & C. Rowlings (2011) showed that, in addition to breed differences, feeding conditions and the influence of climatic factors are an important factor in the development of the amino acid composition of meat. The researchers emphasised that changes in the feed base and increased temperature stress can lead to variations in the content of individual amino acids, in particular, glutamic and aspartic acids, which in the current study also proved to be the most variable among non-essential amino acids. This suggests that the specific profile of Volyn Beef and Charolais animals may be conditioned not only to the genotype, but also to adaptation to growing conditions.

According to S. Fujimura & M. Kadowaki (2006), the content of glutamic acid significantly affects the taste of meat. For other amino acids, the effect on aroma prevails, along with the enhancement of taste – the so-called umami. According to S.A. Michalchenko *et al.* (2024), an interbreed difference in the content of amino acids in beef obtained from three dairy cattle breeds was established. According to researchers, among the essential amino acids, lysine is quantitatively dominant and accounts for 5.02-7.85%, among the substituents – glutamine 10.93-12.66%. In the current study, the level of lysine in Charolais was 37% higher than in Volyn Beef, while in Aberdeen-Angus, the preference for histidine was 19-40%, depending on the breed in comparison. G. Caire-Juvera *et al.* (2013), investigating the amino acid composition of various types of animal products, established the highest content of the essential amino acid lysine in cattle meat. According to researchers, the content of this amino acid affects the quality of beef, its amino acid profile, and protein digestibility indicators. These results are also confirmed by the data of the current study, where Volyn Beef and Charolais had lysine in the range of 1.06-1.63 mg/100 g, which is higher than that of Aberdeen-Angus (1.19 mg/100 g).

G. Hollo *et al.* (2001), investigating the effect of the breed factor on the amino acid profile of cattle meat, established the advantage of Simmental breed in terms of glutamic acid and serine content compared to Holstein animals. Using the GCM model in their research, the researchers concluded that natural belonging does not affect the amino acid composition of beef. According to Y.H. Kim *et al.* (2016), the content of non-essential and essential amino acids is directly or indirectly related to the taste and aroma of meat, being

substrates of chemical reactions that form aromatic compounds during cooking. According to researchers, valine, tyrosine, isoleucine, phenylalanine, tryptophan, and leucine are associated with a bitter taste; alanine, methionine, glutamine, glycine – with sweetness of meat; aspartic and glutamic acids, histidine, asparagine – with a sour taste; glutamic and aspartic acids – with a salty taste. The results obtained in the current study are consistent with these results: Volyn Beef has higher levels of aspartic acid, while Charolais and Volyn Beef have higher levels of alanine, which forms specific differences in the taste profile of beef. Similar patterns were noted by W. Zhang *et al.* (2010), who emphasised that the amino acid composition of meat directly affects its functional value, in particular, its water retention capacity, juiciness, and texture. The higher content of glutamic and aspartic acids recorded in the current study may lead to better sensory characteristics of meat, while increased levels of alanine and glycine are associated with the development of sweet taste shades. Thus, the results confirm that the breed specificity of the amino acid composition is of practical importance for processing and improving the functional quality of meat products. Similar data were provided in the paper by S. Filin *et al.* (2023), where the amino acid composition of semi-finished meat products was studied. The researchers showed that the amino acid profile in meat raw materials has stable differences between control and experimental samples, which confirms the importance of genotypic and technological factors in the development of qualitative characteristics of meat products. Comparison with the current results shows that similar patterns can be traced in pure meat of different breeds of cattle, where variations in the amino acid composition determine both biological value and organoleptic properties.

Summarising the results, it should be noted that the amino acid profile of the longest back muscle of young animals of specialised beef breeds has a distinct breed specificity. The established differences in both the content of essential and non-essential amino acids indicate different intensity of protein and energy metabolism in animals of different breeds. The combination of increased levels of individual amino acids forms not only the biological, but also the taste value of beef. The results obtained confirm that the genotype is a key factor in the development of quality indicators of meat and can be used in breeding work to increase the nutritional and organoleptic value of products.

Conclusions

Based on the results of studies conducted on young animals of specialised beef breeds, it can be concluded that the amino acid composition of the longest back muscle of young cattle depends on the breed affiliation of animals. Among the essential amino acids in animals of the breeds under study, methionine had the highest percentage in the protein composition of dry matter of muscle tissue – 6.84-16.5%, lysine – 6.6-10.37%, and leucine – 7.9-8.6%. The highest content of essential amino acids was observed in the meat of Aberdeen-Angus bulls. In particular, animals of this group exceeded their peers of Charolais and Volyn Beef breeds in terms of methionine content by 45-58%, isoleucine – by 26-43%, phenylalanine – by 17-24%, and histidine – by 20-40%, which confirms their ability to form beef with high biological value. Young Charolais meat was characterised by increased levels of lysine and valine, which are important factors of nitrogen metabolism and protein synthesis, and the lysine content in Charolais reached 1.63 mg/100 g, which is 37% more than in Volyn Beef. While animals of the Volyn Beef breed showed an advantage in the content of leucine, this breed also had higher levels of aspartic acid (11.7% more compared to Aberdeen-Angus) and alanine (36.5% more), indicating a more intense energy metabolism. Analysis of non-essential amino acids showed that glutamic acid (12.7-13.3%) and aspartic acid (8.9-10.09%) accounted for the largest share in all groups, which are key in ensuring energy metabolism and muscle tissue acidity. In Charolais,

glycine and tyrosine were more prevalent, which may indicate the specifics of the synthesis of collagen structures and pigment compounds.

The results obtained indicate that the breed features of the amino acid composition determine the different nutritional and biological value of meat, which should be considered when conducting breeding work to obtain high-quality beef. The established patterns emphasise the decisive role of genotype in determining meat quality indicators. That is why, in the future, it is necessary to determine the amino acid profile of animals of other breeds and investigate the relationship of amino acid composition with organoleptic qualities.

Acknowledgements

None.

Funding

None.

Conflict of Interest

None.

References

[1] Bal-Prylypko, L., Nikolaenko, M., Cherednichenko, O., & Stepasyuk L. (2022). Trends of the development of the meat processing industry of Ukraine and practical approaches to the optimisation the recipe of sausage products. *Ekonomika APK*, 29(5), 10-19. doi: 10.32317/2221-1055.202205010.

[2] Bischof, G., Witte, F., Terjung, N., Januschewski, E., Heinz, V., Juadjur, A., & Gibis, M. (2022). Effect of sampling position in fre sh, dry-aged and wet-aged beef from *M. longissimus dorsi* of Simmental cattle analyzed by ^{1}H NMR spectroscopy. *Food Research International*, 156, article number 111191. doi: 10.1016/j.foodres.2022.111334.

[3] Bittante, G., Cecchinato, A., Tagliapietra, F., & Amalfitano, N. (2024). Amino acid profiles of veal and beef meat obtained in intensive fattening or dairy farming as affected by beef from dairy breed combinations. *Italian Journal of Animal Science*, 24(1), 101-108. doi:10.1080/1828051X.2024.2441358.

[4] Caire-Juvera, G., Vázquez-Ortiz, F.A., & Grijalva-Haro, M.I. (2013). Amino acid composition, score and in vitro protein digestibility of foods commonly consumed in northwest Mexico. *Nutrición Hospitalaria*, 28(2), 365-371.

[5] European Convention for the Protection of Vertebrate Animals Used for Experimental and Other Scientific Purposes. (1986, March). Retrieved from https://rm.coe.int/168007a67b.

[6] Filin, S., Bal-Prylypko, L., Nikolaenko, M., Holembovska, N., & Kushnir, Yu. (2023). Development of technology for plant-based minced semi-finished products. *Animal Science and Food Technology*, 14(2), 100-112. doi: 10.31548/animal.2.2023.100.

[7] Fujimura, S., & Kadowaki, M. (2006). Improvement of meat taste by dietary components. *Bulletin of the Faculty of Agriculture, Niigata University*, 58, 1-7.

[8] Hollo, G., Csapo, J., Szucs, E., Tozser, J., Repa, I., & Hollo, I. (2001). Influence of breed, slaughter weight and gender on chemical composition of beef. Part 1. Amino acid profile and biological value of proteins. *Asian-Australasian Journal of Animal Sciences*, 14(11), 1555-1559. doi: 10.5713/ajas.2001.1555.

[9] Hollo, G., Nuernberg, K., Hollo, I., Csapo, J., Seregi, J., Repa, I., & Ender, K. (2007). Effect of feeding on the composition of longissimus muscle of Hungarian Grey and Holstein Friesian bulls. III. Amino acid composition and mineral content. *Archiv für Tierzucht*, 50(6), 575-586. doi: 10.5194/aab-50-575-2007.

[10] Kim, Y.H.B., Kemp, R., & Samuelsson, L.M. (2016). Effects of dry-aging on meat quality attributes and metabolite profiles of beef loins. *Meat Science*, 111, 168-176. doi: 10.1016/j.meatsci.2015.09.008.

[11] Kolisnyk, O.I., Uhnivenko, A.M., Antoniuk, T.A., & Prudnikov, V.H. (2018). *Meat productivity of cattle*. Kyiv: Komprynt.
[12] Lee, S.-H., Kim, C.-N., Ko, K.-B., Park, S.-P., Kim, H.-K., Kim, J.-M., & Ryu, Y.-C. (2019). Comparisons of beef fatty acid and amino acid characteristics between Jeju Black cattle, Hanwoo, and Wagyu breeds. *Korean Journal for Food Science of Animal Resources*, 39(3), 402-409. doi: 10.5851/kosfa.2019.e33.
[13] Lopez, M.J., & Mohiuddin, S.S. (2023). Biochemistry, essential amino acids. In *StatPearls*. Treasure Island (FL): StatPearls Publishing
[14] Michalchenko, S.A., Korkh, I.V., Paliy, A.P., Boiko, N.V., Kovalenko, L.V., Pavlichenko, O.V., Vyrvykyshka, S.M., & Morozov, M.G. (2024). Amino acid composition of beef depending on the breed and age of dairy bulls. *International Journal of Agricultural Technology*, 20(6), 2405-2422.
[15] Order of the Ministry of Education and Science, Youth and Sports of Ukraine No. 249 "On the Procedure for Carrying out Experiments and Experiments on Animals by Scientific Institutions". (2012, March). Retrieved from https://zakon.rada.gov.ua/laws/show/z0416-12#Text.
[16] Paliy, A., Michalchenko, S., Korkh, I., Rodionova, K., Tkachuk, S., Khimych, M., Dankevych, N., & Boiko, N. (2024). Formation of the biological value of beef protein depending on the age and breed of bulls. *Potravinarstvo Slovak Journal of Food Sciences*, 18, 834-846. doi: 10.5219/2003.
[17] Paliy, A., Nanka, A., Marchenko, M., Bredykhin, V., Paliy, A., Negreba, J., Lazorenko, L., Panasenko, A., Rybachuk, Z., & Musiienko, O. (2020). Establishing changes in the technical parameters of nipple rubber for milking machines and their impact on operational characteristics. *Eastern-European Journal of Enterprise Technologies*, 2(1(104)), 78-87. doi: 10.15587/1729-4061.2020.200635.
[18] Razanova, O.P., Holubenko, T.L., Bernyk, I.M., Novgorodska, N.M., & Solomon, A.M. (2023). Biological value of veal obtained from bulls of different breed origin and grown using dairy and meat breeding technology. *Bulletin of Sumy National Agrarian University. Series: Livestock*, 3(54), 55-62. doi: 10.32782/bsnau.lvst.2023.3.8.
[19] Subrt, J., Kracmar, S., & Divis, V. (2002). The profile of amino acids in intramuscular protein of bulls of milked and beef commercial types. *Czech Journal of Animal Science*, 47(1), 21-29.
[20] Vopálenský, J., Suchý, P., Straková, E., & Šimek, F. (2017). Amino acid levels in muscle tissue of eight meat cattle breeds. *Czech Journal of Animal Science*, 62(8), 339-346. doi: 10.17221/96/2016-CJAS.
[21] Wood, J.D., & Rowlings, C. (Eds.). (2011). *Nutrition and climate change: Major issues confronting the meat industry*. Nottingham: Nottingham University Press.
[22] Yaremchuk, O.S., Razanova, O.P., Skoromna, O.I., Chudak, R.A., Holubenko, T.L., & Kravchenko, O.O. (2022). Post-slaughter indicators of meat productivity and chemical composition of the muscular tissues of bulls receiving corrective diet with protein-vitamin premix. *Regulatory Mechanisms in Biosystems*, 13(3), 219-224. doi: 10.15421/022228.
[23] Zhang, W., Xiao, S., Samaraweera, H., Lee, E.J., & Ahn, D.U. (2010). Improving functional value of meat products. *Meat Science*, 86(1), 15-31. doi: 10.1016/j.meatsci.2010.04.018.

Амінокислотний склад найдовшого м'яза спини (*m. longissimus dorsi*) молодняку спеціалізованих м'ясних порід

Наталія Свириденко
Кандидат сільськогосподарських наук, доцент
Національний університет біоресурсів і природокористування України
03041, вул. Героїв Оборони, 15, м. Київ, Україна
https://orcid.org/0000-0002-9151-6904
Світлана Костенко
Доктор біологічних наук, професор
Національний університет біоресурсів і природокористування України
03041, вул. Героїв Оборони, 15, м. Київ, Україна
https://orcid.org/0000-0002-7816-3374
Марина Хоменко
Кандидат сільськогосподарських наук
Національний університет біоресурсів і природокористування України
03041, вул. Героїв Оборони, 15, м. Київ, Україна
https://orcid.org/0000-0001-7023-3676

Анотація. Актуальність дослідження полягає у вивченні якісних характеристик яловичини як джерела повноцінного білка та вмісту незамінних амінокислот, що визначають її біологічну й харчову цінність. Метою роботи було визначити вміст замінних та незамінних амінокислот та провести порівняльний аналіз амінокислотного складу найдовшого м'яза спини (*m. longissimus dorsi*) молодняку спеціалізованих м'ясних порід. Дослідження проводилися на бугайцях абердин-ангуської, волинської м'ясної та шароле, вирощених за технологією м'ясного скотарства у зоні Полісся України. Контрольний забій піддослідних тварин проводили у віці 18 місяців. З кожної породи відбирали по 3 голови, у яких брали зразки найдовшого м'яза спини (*m. longissimus dorsi*) на рівні 9-11 ребра для дослідження. Вміст амінокислот визначали на аналізаторі методом рідинної іонообмінної хроматографії. Встановлено, що міжпородні відмінності у кількісному вмісті замінних та незамінних амінокислот. Зокрема, м'ясо бугайців абердин-ангуської породи характеризувалося найвищим вмістом незамінних амінокислот, серед яких домінували метіонін (6,84-16,5 %), лізин (6,6-10,37 %) та лейцин (7,9-8,6 %). Для яловичини шароле визначено підвищений рівень лізину та валіну, тоді як тварини волинської м'ясної породи мали перевагу за вмістом лейцину. Серед замінних амінокислот найбільшу частку становили глутамінова (12,7-13,3 %) та аспарагінова кислота (8,9-10,09 %). Отримані результати засвідчують, що якість яловичини значною мірою залежить від породних особливостей, що зумовлює її харчову цінність, біологічну повноцінність та органолептичні властивості. Вищий вміст метіоніну та гістидину у м'ясі абердин-ангусів свідчить про інтенсивніші процеси формування внутрішньом'язового жиру, що забезпечує кращу мармуровість та енергетичну цінність м'яса молодняку даної породи. Результати дослідження можна використати на практиці для відбору та розведення м'ясної худоби з оптимальним амінокислотним складом м'яса з метою підвищення його харчової та біологічної цінності

Ключові слова: яловичина; порода абердин-ангус; волинська м'ясна; шароле; незамінні амінокислоти; біологічна цінність

Received 16.05.2025 Revised 18.08.2025 Accepted 23.09.2025

Vol. 21, No. 5
2025

Scientific Reports of the National University of Life and Environmental Sciences of Ukraine

Journal homepage: https://scireports.com.ua/en

UDC 636.4.082:636.084/.86

Doi: 10.31548/dopovidi/5.2025.82

Dispersion and component analysis of the influence of genotype on the formation of performance traits in fattening pigs

Leonid Lenkov*
PhD in Agricultural Sciences, Doctoral Student
National University of Life and Environmental Sciences of Ukraine
03041, 15 Heroiv Oborony Str., Kyiv, Ukraine
https://orcid.org/0000-0003-1596-6740

Marina Koroban
PhD
Ministry of Environmental Protection and Natural Resources of Ukraine
03035, 35 Mytropolyta Vasylya Lypkivskogo Str., Kyiv, Ukraine
https://orcid.org/0009-0003-1763-2629

Vadym Lykhach
Doctor of Agricultural Sciences, Professor
National University of Life and Environmental Sciences of Ukraine
03041, 15 Heroiv Oborony Str., Kyiv, Ukraine
https://orcid.org/0000-0002-9150-6730

Anna Lykhach
Doctor of Agricultural Sciences, Professor
National University of Life and Environmental Sciences of Ukraine
03041, 15 Heroiv Oborony Str., Kyiv, Ukraine
https://orcid.org/0000-0002-0472-6162

Roman Mylostyvyi
PhD in Veterinary Science, Associate Professor
Dnipro State Agrarian and Economic University
49000, 25 Serhii Efremov Str., Dnipro, Ukraine
https://orcid.org/0000-0002-4450-8813

Suggested Citation:

Lenkov, L., Koroban, M., Lykhach, V., Lykhach, A., & Mylostyvyi, R. (2025). Dispersion and component analysis of the influence of genotype on the formation of performance traits in fattening pigs. *Scientific Reports of the National University of Life and Environmental Sciences of Ukraine*, 21(5), 82-97. doi: 10.31548/dopovidi/5.2025.82.

*Corresponding author

Abstract. The relevance of the work was determined by the need to find effective genetic combinations to increase productivity and ensure the stability of growth processes in animals of modern "commercial genotypes". The aim of the study was to determine the role of genotype as a determining factor in the growth and development of pigs using one-factor dispersion analysis and principal component analysis. The experiment involved 120 fattening pigs, and the test animals were divided into three groups. Group I: a combination of Large White and Landrace sows with Duroc boars of Canadian selection (Genesus) Group II: a combination of Large White and Landrace sows with Pietrain boars of French selection (Axiom) and Group III: a combination of Large White and Landrace sows with boars of the terminal line "Maxter" selected by the company "France Hybrides". The assessment was based on the live weight of pigs of different genotypes at the age of 77-203 days, absolute and average daily gains in separate age periods, as well as the age at which they reached a pre-slaughter live weight of 80, 100, 120 and 140 kg. The results of the variance analysis showed a significant influence of genotype on all studied indicators. The greatest effect of the "genotype" factor was observed for live weight at 154 days of age (43.27%), absolute and average daily gains in the period from 182 to 203 days (44.97%), as well as the age at which live weight of 100 kg was reached (44.72%). It was confirmed that pigs in group I were inferior to their peers in other groups in the early stages of life, but in the later stages of fattening, they demonstrated a significant advantage in terms of gains and growth intensity. Animals in groups II and III were characterised by similar growth rates and did not differ statistically significantly from each other. Principal component analysis allowed to identify two stages in the process of live weight formation: the first (130-155 days) and the second (180-205 days), which are determined by different growth mechanisms and are practically independent of each other. The results confirm the key role of genotype in the formation of productive traits in pigs and can be used in the development of breeding programmes and the improvement of fattening systems

Keywords: breeding; breed composition; live weight; gains; principal components

Introduction

Pig farming is one of the leading sectors of animal husbandry, ensuring food security and stability in the agricultural sector, as well as accounting for a significant share of meat products on the world market. Improving the productive qualities of pigs, in particular growth intensity, average daily gains, feed conversion and meat and fat productivity, remains a key task for modern pig farming. One of the main internal factors determining an animal's potential is its genotype, which influences the realisation of hereditary productivity, but its manifestations can vary significantly depending on feeding and housing conditions. Therefore, quantitative determination of the contribution of genotype to the variability of productive traits and identification of key growth stages is an important prerequisite for effective selection and improvement of intensive fattening technologies (Wusheng & Jørgen, 2022).

Researchers S.W. Kim *et al.* (2024) conducted a comprehensive review of the current state of global pig farming, covering production structure, major breeds and regional characteristics. The study also analyses current research trends, including genetics, feeding and animal health management, which allows the identification of key factors affecting pig productivity in different countries. A.O.K. Adesehinwa *et al.* (2024) examined the characteristics of pig production in Africa, including socio-economic and environmental factors. The authors identified the main problems in the industry, such as limited access to quality genetic material and feed, and determined the prospects for development through the introduction

of innovative technologies and optimisation of genetic resources to increase herd productivity and sustainability. According to FAO estimates, pork is the most consumed meat in the world, accounting for 34 - 36% of total global meat consumption, ahead of poultry (33%), beef (24%), and goat and sheep meat (5%). Improving the productive traits of pigs: growth rates, average daily gains, live weight, feed conversion, and meat and fat quality are relevant tasks of modern breeding and production and a key feature for virtually all major breeds in countries with developed pig farming (Ritchie *et al.*, 2023).

According to V.V. Voloshinov *et al.* (2024) , the effective use of imported breeding boars increases carcass meat yield, young stock growth rate, and reduces feed costs per unit of production. The heterosis effect stimulates the productivity of first-generation hybrid young stock and is genetically determined, but it is difficult to obtain, especially for fattening traits. Therefore, the authors recommend that in order to increase average daily gains and reduce the age to 100 kg, it is necessary to take into account the compatibility of boars and sows, as well as the influence of the boar's genotype on the realisation of the genetic potential of the productive traits of the offspring. The selection work of O. Mykhalko *et al.* (2022) was aimed at increasing meatiness and growth rate with minimal feed and resource costs, which has always been the main criterion for the main breeds, types and lines in pig breeding. Genotype as an internal factor determines the potential of an animal: it determines the extent to which growth, fattening and meat productivity can be fully realised under favourable conditions. B. Lebret & M. Čandek-Potokar (2021) noted in their review that it is hereditary factors that form the basis of pork production and determine the quality of carcasses and fresh meat, while technological parameters mainly influence the realisation of this potential. However, in practice, the potential of the genotype is often limited by paratypic factors: feeding, housing conditions, microclimate, health, management characteristics in the relevant area, etc. F. Bussiman *et al.* (2025), studying genotype-environment interactions using high-dimensional ecological data, showed that even animals with high genetic potential can demonstrate different growth and meat production rates depending on housing conditions. Therefore, to understand productivity, it is necessary not only to compare individual lines or breeds, but also to apply methods that allow to quantitatively assess the contribution of the genotype to the overall variability of traits and identify the components through which this contribution manifests itself.

One of the key statistical tools for solving these problems is analysis of variance (ANOVA), which enables to determine whether there are statistically significant differences between groups, for example, between different genotypes, and to estimate the proportion (share) of variation attributable to genotype differences. At the same time, for many productive traits, it is important to determine which characteristics have the greatest variation because they correlate with each other. To this end, S. Panda *et al.* (2020) used component methods, in particular Principal Component Analysis (PCA), which allowed to reduce the dimensionality of multidimensional data, identify the main "trait complexes" that form productive orientation, and understand the relationships between them.

There are examples of the use of such approaches in the literature. In particular, in the work of H.E. Green *et al.* (2024), PCA was used to identify biotypes that link growth traits, carcass quality, and body structure, as well as to search for candidate genes associated with these biotypes. This provides a deeper understanding of which traits (or combinations thereof) are most important from a breeding perspective. Another example is the study by P.A. Vashchenko *et al.* (2023), which examined the MC4R genotype in combination with feeding levels in Ukraine. The authors found that the interaction between genotype and feeding significantly affects live weight, average daily gains, and subcutaneous fat thickness. This emphasises that the genotype does not

act in isolation, and the realisation of its potential depends on paratype factors.

At the same time, although there are numerous studies devoted to individual genotypes or marker genetic effects, the literature does not always contain studies that comprehensively combine variance analysis (assessment of the strength of the genotype's influence on different age intervals, absolute and average daily gains, age at which a certain weight is reached) and component analysis (derivation of the main components that summarise production traits). This approach allows for a deeper understanding of: during which growth periods the genotype is most active; which traits have the greatest variability; how growth indicators and age at reaching live weight correlate. The aim of the study was to determine the influence of genotype on the productive traits of fattening pigs by applying variance and component analysis.

Materials and Methods

The experiments were conducted throughout 2023 at a commercial pork production enterprise, the Agricultural Production Cooperative Agrofirma "Myh-Servis-Ahro" in the Mykolaiv region. Pork production at the enterprise was carried out according to the principles of industrial technology with the corresponding organisation of production processes. The study involved 120 heads of finishing pig young stock, which were divided into three groups of 40 heads each. The first group comprised young stock obtained from Large White × Landrace (LW × L) sows crossed with Duroc (D) boars of Canadian selection (Genesus). The second group was formed by crossbred young stock from (LW × L) sows and Pietrain (P) boars of French selection (Axiom). The third group was represented by animals obtained from (LW × L) sows combined with "Maxter" (Mx) terminal line boars from the "France Hybrides" company. The assessment of finishing qualities was conducted when the animals reached live weights of 80, 100, 120, and 140 kg.

As part of the scientific and economic experiment, the groups were formed using the pair-analogue method (Ibatulin *et al.,* 2017) taking into account similarities in live weight and the development of the test animals during the rearing period (4-11 weeks), which corresponded to the comparative period, and no significant differences in live weight were observed in the experimental groups. The experimental pigs were evaluated for fattening indicators: age at reaching live weight of 80, 100, 120 and 140 kg, absolute and average daily gain (g), amount of feed consumed and feed conversion ratios (kg) at the stages of reaching the specified conditions in accordance with the methods (Ladyka & Khmelnychiy, 2023).

The conditions of keeping the experimental animals complied with the Departmental norms of technological planning (2005) and the recommendations of genetic companies for keeping animals. The rules for handling the experimental animals complied with Ukrainian legislation (Order of the Ministry for Development of Economy, Trade and Agriculture of Ukraine No. 224, 2012). The fattening piglets were divided into two fattening stages. The first stage ("Grower") included animals with a live weight of 30-60 kg, which received 2.4-2.6 kg of compound feed per head per day; they were kept in pens of 30 heads on a concrete slatted floor with an area of 0.65 m^2 per head. The second stage ("Finisher") included animals weighing 61-140 kg, which were fed compound feed at a rate of 2.8-3.2 kg per head per day; they were kept on a concrete slatted floor with an area of 0.85-1.2 m^2 per head.

Young animals of different ages and weights were fed with three types of specialised compound feed: "Grower", "Finisher" and "Final Finisher", produced in the farm's own compound feed workshop in accordance with the feeding strategies developed on the farm (Provoratorov, 2007; Voloshchuk, 2014). To balance the diets of fattening young animals, protein, mineral and vitamin supplements and premixes produced by "Koudijs Ukraine" LLC were used. The animals were watered through nipple drinkers located at levels appropriate to their age. The premises were ventilated using exhaust shaft fans and aerodynamic

supply valves to create negative pressure. Manure was removed using a periodic vacuum-gravity system from tubs located under the slatted floor. Veterinary treatments in the experimental and control groups were carried out identically in accordance with the scheme adopted on the farm.

The results obtained were processed using statistical methods with the use of computer technologies and the STATISTICA v. 7.0 software package in accordance with generally accepted methods (Feinstein, 1996; Kramarenko *et al.*, 2019).

Results and Discussion

The data obtained indicate that genotype significantly influences the formation of productive traits in pigs, in particular the dynamics of live weight and growth intensity at different ages. Already at the initial stages of fattening, statistically significant differences between the studied groups can be observed, which change in severity over time. The most pronounced effect of genotype is observed in the middle age periods, while in the final stages of fattening, some of the differences are levelled out. A one-factor analysis of variance showed that genotype is a statistically significant factor determining the live weight of fattening pigs at all studied age periods (in all cases $p \leqslant 0.001$), which emphasises its key role in the formation of productive qualities of animals (Table 1).

Table 1. *Influence of pig genotype on their live weight during fattening (one-factor analysis of variance)*

Characteristic (age, days)	*SS* Effect	*df* Effect	*MS* Effect	*SS* Error	*df* Error	*MS* Error	*F*	*P*	η^2 (%)
LWe –77	111.05	2	55.53	215.45	117	1.84	30.15	<0.001	34.01
LWe –133	205.40	2	102.70	449.40	117	3.84	26.74	<0.001	31.37
LWe –154	449.20	2	224.60	589.03	102	5.77	38.89	<0.001	43.27
LWe –182	38.82	2	19.41	240.17	87	2.76	7.03	<0.001	13.92
LWe –203	72.83	2	36.41	271.12	72	3.77	9.67	<0.001	21.17

Note: LWe – live weight
Source: authors' own work

A characteristic feature of the results obtained is that the influence of the "genotype" factor on the live weight of animals gradually increased and reached its maximum level at the age of 154 days (43.27%). At the same time, at 203 days of age, the magnitude of intergroup differences decreased almost twice, which indicates a certain levelling of indicators in the later stages of fattening. A generalised analysis of the average live weights of pigs of different genotypes showed that animals of Group I (♀(LW×L)×♂D) lagged behind their contemporaries from other groups at the early stages of development (77, 133, and 154 days), but at 182 and 203 days they significantly surpassed them. Pigs of Groups II (♀(LW×L)×♂P) and III (♀(LW×L)×♂Mk) showed no statistically significant differences in live weight during most of the studied periods, which indicates the similarity of their growth rates. The results of one-factor analysis of variance confirm the significant influence of genotype on absolute live weight gains at different age intervals of fattening (in all cases $p < 0.001$) (Table 2).

Table 2. *Influence of pig genotype on absolute live weight gains during fattening (one-factor analysis of variance)*

Characteristic (age, days)	*SS* Effect	*df* Effect	*MS* Effect	*SS* Error	*df* Error	*MS* Error	*F*	*P*	η^2 (%)
AG (77-133)	42.45	2	21.22	206.85	117	1.77	12.01	<0.001	17.03
AG (133-154)	212.93	2	106.47	428.06	102	4.20	25.37	<0.001	33.22
AG (154-182)	196.47	2	98.23	307.93	87	3.54	27.75	<0.001	38.95
AG (182-203)	267.55	2	133.77	327.44	72	4.55	29.42	<0.001	44.97

Note: AG – absolute gain
Source: authors' own work

Unlike live weight indicators, the influence of the "genotype" factor on absolute gains tended to gradually increase: from 17.03% between 77 and 133 days to a maximum of 44.97% between 182 and 203 days. This indicates that the genetic characteristics of animals are more pronounced in the later stages of fattening, when the body reaches high growth rates and tissue formation intensity.

Summarising the results of the analysis of absolute live weight gains of pigs depending on their genotype, it should be noted that animals of group I (♀(LW×L)×♂D) in the periods 77-133 and 133-154 days were inferior to their peers in other groups in terms of growth intensity. At the same time, in the following age intervals (154-182 and 184-203 days), they already had a significant advantage in terms of growth. During most of the study periods, the fattening young animals of groups II and III did not show statistically significant differences between each other in terms of absolute live weight gains, which indicates a similar level of their growth capacity. The data obtained indicate that animals in group I are characterised by a strategy of "late realisation" of genetic potential: slower initial growth is compensated by intensive growth in the final stages of fattening. This may be due to the peculiarities of physiological development and the formation of muscle tissue at a later stage. Groups II and III show more uniform growth, without sharp peak changes in intensity, which may indicate faster realisation of potential at an early age and stable productivity throughout the fattening period. In practical terms, this means that when planning feeding programmes and the duration of fattening, it is advisable to take the genotype into account: animals in group I may need a longer period to realise their full potential, while groups II and III achieve stable performance faster. This approach will increase feed efficiency and production profitability.

The results of one-factor analysis of variance confirm the presence of a significant influence of genotype on the average daily weight gain of pigs at different ages of fattening (in all cases $p < 0.001$) (Table 3). Similar to absolute gains, the strength of the influence of the "genotype" factor on average daily gains tended to increase gradually, which emphasises the importance of genetic characteristics in determining the growth rate of animals in the later stages of fattening.

Table 3. *Influence of pig genotype on average daily weight gain during fattening (one-factor analysis of variance)*

Characteristic (age, days)	*SS* Effect	*df* Effect	*MS* Effect	*SS* Error	*df* Error	*MS* Error	*F*	*P*	η^2 (%)
ADG (77-133)	13,536.35	2	6,768.18	65,959.82	117	563.76	12.01	<0.001	17.03

Table 3. *Continued*

Characteristic (age, days)	*SS* Effect	*df* Effect	*MS* Effect	*SS* Error	*df* Error	*MS* Error	*F*	*P*	η^2 (%)
ADG (133-154)	35,913.87	2	17,956.93	72,197.19	102	707.82	25.37	<0.001	33.22
ADG (154-182)	17,820.11	2	8,910.05	27,930.46	87	321.04	27.75	<0.001	38.95
ADG (182-203)	16,852.27	2	8,426.14	20,624.84	72	286.46	29.42	<0.001	44.97

Note: ADG – average daily gain
Source: authors' own work

Summarising the results of the analysis of average daily weight gains of pigs depending on their genotype, it can be noted that in animals of group I (♀(LW×L)×♂D) maintained relatively stable growth rates throughout the observation period, ranging between 900 and 915 g, with no substantial fluctuations between age intervals. In contrast, the young pigs of Groups II (♀(LW×L)×♂P) and III (♀(LW×L)×♂Mk) showed a clear pattern: during the 77-133 and 133-154-day periods, their average daily gains were considerably higher than in the subsequent 154-182 and 182-203-day intervals. Among these, Group III animals (♀(LW×L)×♂Mk) exhibited the most pronounced difference between early and late periods, indicating greater variability in growth intensity compared with the other groups.

The results of the one-way analysis of variance demonstrated a significant effect of genotype on the age at which pigs reached specific live weights (ALW) during fattening ($p < 0.001$ in all cases) (Table 4). The strongest influence of the "genotype" factor was observed for the age at reaching 100 kg live weight (44.72%), while the weakest effect was recorded for the age at reaching 120 kg (9.48%).

Table 4. *Influence of pig genotype on the age at reaching a certain live weight during fattening (one-factor analysis of variance)*

Characteristic (age)	*SS* Effect	*df* Effect	*MS* Effect	*SS* Error	*df* Error	*MS* Error	*F*	*P*	η^2 (%)
ALW –80	250.35	2	125.17	542.80	117	4.64	26.98	<0.001	31.56
ALW –100	575.56	2	287.78	711.49	102	6.98	41.26	<0.001	44.72
ALW – 120	38.25	2	19.13	365.45	87	4.20	4.55	<0.001	9.48
ALW –140	95.18	2	47.59	342.73	72	4.76	10.00	<0.001	21.74

Note: ALW – age at reaching a certain live weight
Source: authors' own work

Overall, analysis of the mean age at reaching specific live weights in pigs during fattening, depending on their genotype, showed that Group I animals (♀(LW×L)×♂D) outperformed the other groups at 80 and 100 kg, but were inferior at 120 and 140 kg live weight. Animals of Groups II (♀(LW×L)×♂P) and III (♀(LW×L)×♂Mk) did not differ significantly from each other across almost all weight categories.

Table 5 shows the estimates of the correlation coefficient between the live weight of pigs of modern genotypes at different ages and the age at which they reach different weight conditions. It was found that there is a reliable and relatively high correlation (at the level of +0.600...+0.800) between the live weight of pigs at the ages of 77, 133 and 154 days. In addition, a certain level of relative variability was noted between the live

weight of pigs at 182 and 203 days of age (+0.468). On the other hand, the live weight of pigs at 77, 133 and 154 days of age was negatively correlated with the age at which they reached a live weight of 80 and 100 kg. Accordingly, the live weight at 182 and 203 days of age was negatively correlated with the age at which they reached a live weight of 120 and 140 kg. These pairs of traits are also correlated with each other; on the one hand, the age at which live weight of 80 and 100 kg is reached (+0.694), and on the other hand, the age at which live weight of 120 and 140 kg is reached (+0.349).

Table 5. *Estimates of the correlation coefficient between the live weight of pigs of different genotypes at different ages and the age at which different live weights are reached*

Characteristic	1	2	3	4	5	6	7	8	9
1	×	0.792	0.627			-0.788	-0.629		
2		×	0.690			-0.999	-0.691		
3			×			-0.693	-0.993		
4				×	0.468			-0.985	-0.424
5					×			-0.397	-0.993
6						×	0.694		
7							×		
8								×	0.349
9									×

Note: Signs: 1 – LWe 77; 2 – LWe 133; 3 – LWe 154; 4 – LWe 182; 5 – LWe 203; 6 – ALW 80; 7 – ALW 100; 8 – ALW 120; 9 – ALW 140. Only correlation coefficient estimates for which $p < 0.05$ are given
Source: authors' own work

The availability of statistically significant estimates of correlation between the live weight of pigs of different genotypes at different ages and the age at which the corresponding weight conditions are achieved provides grounds for applying principal component analysis (PCA) to all nine of these traits. Table 6 shows the estimates of factor loadings for the first two principal components, calculated on the basis of the variation-covariance matrix of live weight of pigs of different genotypes at different ages and the age at which different weight conditions are achieved. The first two principal components together described almost ¾ of the total variability of the variance-covariance matrix. At the same time, the first principal component (PC1) described 45.6% of the total variability of the variation-covariance matrix of live weight of pigs of different genotypes at different ages and ages of reaching live weight of different conditions and was characterised by high positive estimates of factor loadings on live weight at the age of 77, 133 and 154 days of age, and, on the other hand, by high negative estimates of factor loads on the age of reaching a live weight of 80 and 100 kg.

Table 6. *Estimates of factor loadings for the first two principal components calculated on the basis of the variance-covariance matrix of live weight of pigs of different genotypes*

Characteristic	Principal component (PC)	
	PC1	PC2
LWe 77	**0.862**	0.007
LWe 133	**0.928**	-0.069
LWe 154	**0.869**	-0.061

Table 6. *Continued*

Characteristic	Principal component (PC)	
	PC1	PC2
LWe 182	0.179	**0.843**
LWe 203	-0.081	**0.865**
ALW 80	**-0.930**	0.063
ALW 100	**-0.867**	0.045
ALW 120	-0.277	**-0.791**
ALW 140	0.108	**-0.841**
Percentage of variance, %	*45.6*	*31.2*

Note: bold font indicates the factor loadings of the features that contribute most to the identification of the corresponding principal component
Source: authors' own work

Thus, this main component can be identified as live weight gain at 130-155 days of age. The second principal component (PC2) described 31.2% of the total variability of the variation-covariance matrix of live weight of pigs of different genotypes at different ages and ages of reaching live weight of different conditions and was characterised by high positive estimates of factor loadings on live weight at 182 and 203 days of age, and, on the other hand, by high negative estimates of factor loads on the age of reaching a live weight of 120 and 140 kg. Thus, this principal component can be identified as reaching a live weight at 180-205 days of age.

It is characteristic that the first two main components indicate the presence of two stages in the process of forming the live weight of pigs for fattening, which are determined by different mechanisms and are almost independent of each other. The first stage covers the period of 130-155 days, and the second – 180-205 days. Thus, the results of the principal component analysis allowed to move from 9 initial features to two complex features (principal components) that describe most of the variability of the initial matrix, but are orthogonal to each other and make it possible to visualise the results obtained (Fig. 1).

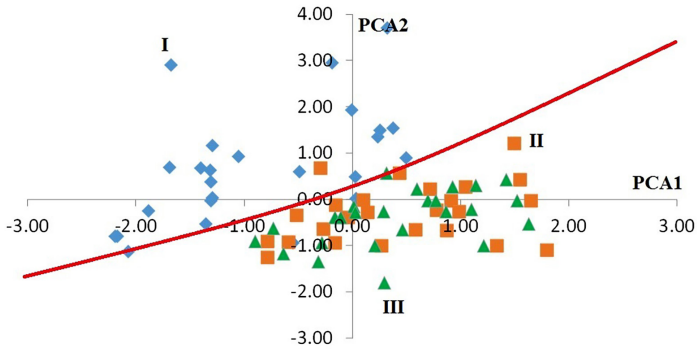

Figure 1. *Ordination of individual animals depending on their genotype in the space of the 1st and 2nd principal components, calculated on the basis of the variance-covariance matrix of live weight at different ages and the age at reaching various live weight stages*
Note: I – ♀(LW×L)×♂D; II – ♀(LW×L)×♂P; III – ♀(LW×L)×♂Mk
Source: authors' own work

Figure 1 presents the ordination of individual animals according to their genotype in the space defined by the first and second principal components, calculated on the basis of the variance–covariance matrix of live weight at different ages and the age at reaching specific live-weight thresholds. A clear intergroup differentiation of pigs depending on genotype is evident. The young animals of Group I (♀(LW×L)×♂D) were clearly separated from those of Groups II (♀(LW×L)×♂P) and III (♀(LW×L)×♂Mk), which formed a single cluster without noticeable differentiation between them. Animals of Group I (♀(LW×L)×♂D) were characterised by high scores on the second principal component but low scores on the first, in contrast to the other two groups. This pattern indicates that pigs of Group I exhibited lower growth rates in live weight during the 130-155-day period but accelerated growth during 180-205 days. Conversely, pigs of Groups II and III showed higher growth intensity at 130-155 days but lower rates in the later finishing period (180-205 days).

The results of the studies confirm the conclusions of M. Mohammadabadi *et al.* (2021) and B.S. Shaferivsky (2021), who also point to the decisive role of genotype in the formation of live weight and growth energy of pigs during ontogenesis. A significant influence of this factor has been established in all age periods, which is consistent with numerous literature data emphasising the role of heredity in the variability of growth indicators, meat productivity and carcass quality. According to researchers A. Antonyk *et al.* (2025), heredity is the main predictor of fattening and slaughter traits in modern pig genotypes, while the influence of housing and feeding conditions is more pronounced only in the case of nutrient deficiency. In particular, the current study clearly demonstrated the role of individual genotype combinations in the formation of live weight, average daily gains and fattening performance. Similar conclusions were made by Z. Pan *et al.* (2022), who, based on transcriptomic and proteomic analysis, identified candidate genes responsible for the deposition of subcutaneous and intramuscular fat in Dingyuan pigs. This once again confirms that the genetic basis of productive traits has a complex polygenic nature, where dozens of genes interact. The current study found that genotype significantly influences the formation of productive traits in fattening pigs, in particular the dynamics of live weight gain and morphofunctional characteristics. Similar results are reported by M. Matsenko (2020), who established the dependence of growth rate and haematological parameters on the duration of embryonic development. The author showed that physiological blood parameters (erythrocytes, haemoglobin, protein) are closely correlated with the growth intensity of animals, which confirms the importance of taking into account not only external factors but also genetically determined characteristics of the organism.

An important aspect is the interaction of the genotype with environmental conditions. The results of the current study indicate that even with the same feeding system, the differences between genotypes remained significant, but the severity of these differences may vary depending on the husbandry technology used. A similar effect was described by J.M. García-Casco *et al.* (2014), who studied Iberian pigs in different free-range systems. The authors showed that the "genotype-environment" interaction affects both carcass morphology and intramuscular fat content. This highlights the need to consider technological factors when interpreting the results of variance analysis. A characteristic pattern identified in the current study is the gradual increase in the influence of the "genotype" factor on the live weight of animals up to 154 days, after which this influence decreased by almost half at 203 days. This dynamic is explained by the processes of physiological equalisation in the herd, when in the final stages of fattening the influence of environmental factors (in particular, the level of feeding and microclimate conditions) begins to play an increasingly important role. Similar results are reported by H. Shao *et al.* (2008), who showed that in later age periods, heritability is weaker than in

earlier ones, which leads to a decrease in intergroup differences.

An interesting phenomenon observed in the present study was that animals of Group I (♀(LW×L)×♂D), although initially lagging behind their peers in live weight and gains during the early growth phases (77-154 days), subsequently (182-203 days) demonstrated a significant compensatory advantage. Similar patterns were reported by R.M. Godinho *et al.* (2018), who noted that combining genotypes with different growth intensities may generate a "late-start" effect, whereby animals gradually realise their genetic potential during the final stages of fattening. The correlations established in the current study are also consistent with the literature. The high negative correlation between live weight at an early age (77-154 days) and the age at which 80-100 kg is reached confirms the statements made by R.M. Godinho *et al.* (2018) that more intensive initial growth allows intermediate weight limits to be reached more quickly. On the other hand, the negative correlation between live weight at later ages (182-203 days) and the age at which 120-140 kg is reached confirms that the final periods of fattening are crucial for the formation of final productivity.

The use of principal component analysis made it possible to identify two independent growth stages: 130-155 and 180-205 days. A similar approach was used by N. Gilbert *et al.* (2017), who, based on multidimensional data analysis, identified several "performance windows" in pig development when genetic potential is most strongly manifested. In the current study, animals in group I were characterised by the second scenario with accelerated growth in the late stage, while groups II and III were characterised by the first scenario, confirming the existence of different strategies for realising genetic potential. The results of the current component analysis confirmed that individual latent factors can be identified as genetically determined trait complexes. This coincides with the conclusions of M. Muñoz *et al.* (2018), who studied the diversity of European local pig breeds and showed that candidate genes associated with growth and meat productivity form specific groups that are consistently manifested in the phenotype. Including such factors in breeding programmes can significantly improve the accuracy of animal selection. Additionally, it should be noted that the data from the current study on genotypic variation in fattening performance are consistent with the results of X. Xie *et al.* (2023), who identified key mutations in the PRKAG3 and PHKG1 genes that determine the glycolytic potential of muscle tissue. These genes have a significant impact on slaughter performance. Identifying genotypes with the best productive characteristics makes it possible to increase the efficiency of fattening. As shown by the research of S. Dall'Olio *et al.* (2017), integrating data on genotypes and meat productivity markers into selection schemes provides a significant increase in genetic progress.

Thus, the results of the current study confirm that genotype is one of the key factors determining the level and stability of fattening pig performance. Its influence is realised through polygenic trait complexes and depends on interaction with feeding and housing systems. The current study confirmed the high significance of genotype as a factor in the formation of pig productivity and allowed to identify key age intervals when genetic potential is most strongly manifested. Dispersion and component analysis have proven their effectiveness as tools for quantitative assessment of these factors, as well as for identifying latent structures in the data. The use of these methods opens up new opportunities for the formation of selection strategies aimed at increasing production efficiency and improving the quality of pig products.

Conclusions

Genotype is a determining factor in the formation of performance traits in fattening pigs and significantly affects growth dynamics, growth intensity and age at which live weight is reached. The application of variance analysis showed that the "genotype" factor has a statistically significant

effect ($p < 0.001$) on all studied parameters, with its specific weight of variation changing depending on the age period and specific trait. The greatest effect was found in the middle age interval (154 days) for live weight (43.27%) and in the later period (182-203 days) for absolute and average daily gains (44.97%). This indicates an increase in the role of hereditary factors in the final stages of fattening, when the animals' bodies intensively accumulate muscle and fat tissue. An important finding is the different type of genetic potential realisation: pigs in group I (♀(LW×L)×♂D) showed slower initial growth, but compensated for this with intensive growth in the final period, while animals in groups II (♀(LW×L)×♂P)and III (♀(LW×L)×♂Mk) were characterised by more uniform growth rates with a predominance at an early age. Different genotypes require differentiated feeding and fattening management programmes: genotypes with late potential realisation should be kept longer to achieve maximum productivity, while genotypes with rapid realisation ensure early achievement of marketable conditions with shorter fattening periods.

Analysis of the age at which live weight was achieved confirmed that the trait most sensitive to genotype was the age at which a live weight of 100 kg was achieved (44.72%), making this indicator an informative marker for breeding and technological programmes. At the same time, the genotype had a lesser effect on the age at which a live weight of 120 kg was reached (9.48%), which indicates a gradual levelling of growth indicators as the final conditions are approached. The integration of variance and component analysis allows for a deeper understanding of the mechanisms of genotype influence on the performance of fattening pigs, identification of periods of maximum realisation of hereditary potential, and establishment of practical guidelines for selection and technological solutions. This ensures more efficient use of feed, lower production costs and increased competitiveness of the pig industry in industrial production.

Further scientific research should be directed towards a comprehensive study of the influence of genotype, feeding and housing conditions on pig growth using molecular genetic markers, which will allow the optimal feeding parameters to be established, economic efficiency to be assessed and selection and technological strategies for intensive pig farming to be developed.

Acknowledgements

We express our gratitude to the owner and the team of the Agricultural Production Cooperative Agrofirma "Mig-Servis-Agro"for providing the facilities for scientific research.

Funding

None.

Conflict of Interest

None.

References

[1] Adesehinwa, A.O.K., Boladuro, B.A., Dunmade, A.S., Idowu, A.B., Moreki, J.C., & Wachira, A.M. (2024). Pig production in Africa: Current status, challenges, prospects and opportunities. *Animal Bioscience*, 37(4), 730-741. doi: 10.5713/ab.23.0342.

[2] Antonyk, A., Terman, A., Tyra, M., Żak, G., Polasik, D., Szyndler-Nędza, M., Kulig, H., & Dybus, A. (2025) The effect of rs80860411 polymorphism on fattening, slaughter, and pork quality traits in Polish Large White and Pulawska Breeds. *Animals*, 15(14), article number 2090. doi: 10.3390/ani15142090.

[3] Bussiman, F., Lourenco, D., Hidalgo, J., Chen, C.-Y., Holl, J., Misztal, I., & Vitezica, Z.G. (2025). Genotype-by-environment interaction with high-dimensional environmental data: An example in pigs. *Genetics Selection Evolution,* 57, article number 28. doi: 10.1186/s12711-025-00974-2.

[4] Dall'Olio, S., Scotti, E., Nanni Costa, L., & Fontanesi, L. (2017). Effects of single nucleotide polymorphisms and haplotypes of the protein kinase AMP-activated non-catalytic subunit gamma 3 (*PRKAG3*) gene on production, meat quality and carcass traits in Italian Large White pigs. *Meat Science*, 136, 67-76. doi: 10.1016/j.meatsci.2017.09.012.

[5] Departmental norms of technological planning (2005). *Pig enterprises (complexes, farms, small farms)*. Retrieved from https://lugdpss.gov.ua/images/bezpechnist_veterynariya/Svynarski-pidpryyemstva-VNTP-APK-02.05.pdf.

[6] Feinstein, A.R. (1996). *Multivariable analysis: An introduction*. New Haven: Yale University Press.

[7] García-Casco, J.M., Muñoz, M., Silío, L., & Rodríguez, C. (2014). Genotype by environment interaction for carcass traits and intramuscular fat content in heavy Iberian pigs fattened in two different free-range systems. *Spanish Journal of Agricultural Research*, 12(2), 388-400.

[8] Gilbert, H., *et al.* (2017). Review: Divergent selection for residual feed intake in the growing pig. *Animal*, 11(9), 1427-1439. doi: 10.1017/S175173111600286X.

[9] Godinho, R.M., Bergsma, R., Silva, F.F., Sevillano, C.A., Knol, E.F., Lopes, M.S., Lopes, P.S., Bastiaansen, J.W.M., & Guimarães, S.E.F. (2018). Genetic correlations between feed efficiency traits, and growth performance and carcass traits in purebred and crossbred pigs. *Journal of Animal Science*, 3, 96(3), 817-829. doi: 10.1093/jas/skx011.

[10] Green, H.E., Oliveira, H.R.D., Alvarenga, A.B., Scramlin-Zuelly, S., Grossi, D., Schinckel, A.P., & Brito, L.F. (2024). Genomic background of biotypes related to growth, carcass and meat quality traits in Duroc pigs based on principal component analysis. *Journal of Animal Breeding and Genetics*, 141(2), 163-178. doi: 10.1111/jbg.12831.

[11] Ibatulin, I.I., Zhukorskyi, O.M., & Bashchenko, M.I. (2017). *Methodology and organization of scientific research in animal husbandry*. Kyiv: Agrarian Science.

[12] Kim, S.W., Gormley, A., Jang, K.B., & Duarte, M.E. (2024). Current status of global pig production: An overview and research trends. *Animal Bioscience*, 37(4), 719-729. doi: 10.5713/ab.23.0367.

[13] Kramarenko, S.S., Lugovoy, S.I., Lykhach, A.V., & Kramarenko, O.S. (2019). *Analysis of biometric data in animal breeding and selection*. Mykolaiv: MNAU.

[14] Ladyka, V.I., & Khmelnychiy, L.M. (Eds.). (2023). *Technology of production and processing of livestock products*. Odesa: Oldi+.

[15] Lebret, B., & Čandek-Potokar, M. (2021). Review: Pork quality attributes from farm to fork. Part I. Carcass and fresh meat. *Animal*, 16, article number 100402. doi: 10.1016/j.animal.2021.100402.

[16] Matsenko, M. (2020). Hematological indices and the rate of growth depending on duration of embryonic growth of pigs obtained by commercial cross-breeding. *Animal Science and Food Technology*, 11(2), 43-49.

[17] Mohammadabadi, M., Bordbar, F., Jensen, J., Du, M., & Guo, W. (2021). Genes regulating skeletal muscle development and growth in farm animals. *Animals*, 11, article number 835. doi: 10.3390/ani11030835.

[18] Muñoz, M., *et al.* (2018) Diversity across major and candidate genes in European local pig breeds. s*PLoS ONE*, 13(11), article number e0207475. doi: 10.1371/journal.pone.0207475.

[19] Mykhalko, O., Povod, M., Sokolenko, V., Verbelchuk, S., Shuplyk, V., Shcherbatiuk, N., Melnyk, V., & Zasukha, L. (2022). The influence of the castration method on meat cuts indicators of pig carcasses. *Scientific Papers. Series Management, Economic Engineering in Agriculture and Rural Development*, 22(3), 451-458.

[20] Order of the Ministry for Development of Economy, Trade and Agriculture of Ukraine No. 224 "On the Procedure for Carrying out Experiments and Experiments on Animals by Scientific Institutions". (2012, March). Retrieved from https://zakon.rada.gov.ua/laws/show/z0416-12#Text.

[21] Pan, Z., Li, Q., Wu, Y., Zhang, Y., Bo, Z., & Hao, Z. (2022). Identification of candidate genes that specifically regulate subcutaneous and intramuscular fat deposition using transcriptomic and proteomic profiles in Dingyuan pigs. *Scientific Reports*, 12, article number 2844. doi: 10.1038/s41598-022-06868-3.

[22] Panda, S., Gaur, G.K., Sahoo, N.R., Bharti, P.K., & Kar, J. (2020). Principal component analysis of morphometric and growth traits in crossbred piglets. *Indian Journal of Animal Sciences*, 90(8), 1168-1171.

[23] Provoratorov, H.V. (Ed.). (2007). *Feeding standards, diets, and nutritional value of feed for various types of farm animals*. Sumy: VDT "University Book" LLC.

[24] Ritchie, H., Rosado, P., & Roser, M. (2023). *Meat and dairy production*. Retrieved from https://ourworldindata.org/meat-production.

[25] Shaferivsky, B.S. (2021). The influence of breeding boars of specialized genotypes on the fattening characteristics of young pigs. *In Meat genotypes of pigs: Present and future: Materials of the international scientific and practical conference of scientific and pedagogical workers and young scientists* (pp. 46-48). Odesa: Odesa State Agrarian University.

[26] Shao, H., *et al.* (2008). Genetic architecture of complex traits: Large phenotypic effects and pervasive epistasis. *Proceedings of the National Academy of Sciences of the United States of America*, 105(50), 19910-19914. doi: 10.1073/pnas.0810388105.

[27] Vashchenko, P.A., Zhukorskyi, O.M., Saenko, A.M., Khokhlov, A.M., Usenko, S.O., Kryhina, N.V., Sukhno, T.V. & Tsereniuk, O.M. (2023). The influence of feeding level on the growth of pigs depending on their genotype. *Regulatory Mechanisms in Biosystems*, 14(1), 112-117. doi: 10.15421/022317.

[28] Voloshchuk, V.M. (Ed.). (2014). *Pig farming*. Kyiv: Agrarian Science.

[29] Voloshinov, V.V., Povod, M.G., Mykhalko, O.G., Usenko, S.O., Shaferivsky, B.S., Shostya, G.M., & Shpyna, I.G. (2024). Productive qualities and efficiency of fattening hybrid pigs of Danish and Canadian origin under industrial technology conditions. *Bulletin of Sumy National Agrarian University. Series: Animal Husbandry*, 1(56), 25-32. doi: 10.32782/bsnau.lvst.2024.1.4.

[30] Wusheng, Yu., Jørgen D.J. (2022). Sustainability implications of rising global pork demand. *Animal Frontiers*, 12(6), 56-60. doi: 10.1093/af/vfac070.

[31] Xie, X., Huang, C., Huang, Y., Zou, X., Zhou, R., Ai, H., Huang, L., & Ma, J. (2023). Genetic architecture for skeletal muscle glycolytic potential in Chinese Erhualian pigs revealed by a genome-wide association study using 1.4M SNP array. *Frontiers in Genetics*, 14, article number 1141411. doi: 10.3389/fgene.2023.1141411.

Дисперсійний та компонентний аналіз впливу генотипу на формування продуктивних ознак відгодівельних свиней

Леонід Леньков
Кандидат сільськогосподарських наук, докторант
Національний університет біоресурсів і природокористування України
03041, вул. Героїв Оборони, 15, м. Київ, Україна
https://orcid.org/0000-0003-1596-6740
Марина Коробань
Доктор філософії
Міністерство захисту довкілля та природних ресурсів України
03035, вул. Митрополита Василя Липківського, 35, м. Київ, Україна
https://orcid.org/0009-0003-1763-2629
Вадим Лихач
Доктор сільськогосподарських наук, професор
Національний університет біоресурсів і природокористування України
03041, вул. Героїв Оборони, 15, м. Київ, Україна
https://orcid.org/0000-0002-9150-6730
Анна Лихач
Доктор сільськогосподарських наук, професор
Національний університет біоресурсів і природокористування України
03041, вул. Героїв Оборони, 15, м. Київ, Україна
https://orcid.org/0000-0002-0472-6162
Роман Милостивий
Кандидат ветеринарних наук, доцент
Дніпровський державний аграрно-економічний університет
49000, вул. Сергія Єфремова, 25, м. Дніпро, Україна
https://orcid.org/0000-0002-4450-8813

Анотація. Актуальність роботи зумовлена необхідністю пошуку ефективних генетичних поєднань для підвищення продуктивності та забезпечення стабільності ростових процесів у тварин сучасних «комерційних генотипів». Метою дослідження було з'ясування ролі генотипу, як визначального чинника росту та розвитку свиней за допомогою однофакторного дисперсійного аналізу й аналізу головних компонент. В експерименті було використано 120 голів свиней на відгодівлі, піддослідний молодняк був розділений на три групи. І група: поєднання свиноматок великої білої та ландрас з кнурами породи дюрок канадської селекції (Genesus), ІІ група: поєднання свиноматок великої білої та ландрас з кнурами породи п'єтрен французької селекції (Axiom) і ІІІ група: поєднання свиноматок великої білої та ландрас з кнурами термінальної лінії «Maxter» селекції компанії «France Hybrides». Для оцінки використано живу масу свиней різних генотипів у віці 77-203 доби, абсолютні та середньодобові прирости в окремі вікові періоди, а також вік досягнення ними передзабійної живої маси 80, 100, 120 та 140 кг. За результатами дисперсійного аналізу встановлено достовірний вплив генотипу на всі досліджувані показники. Найбільший ефект фактору «генотип» відмічено для живої маси у віці 154 діб (43,27 %), абсолютних та середньодобових приростів у період 182-203 доби (44,97 %), а також віку досягнення живої маси 100 кг (44,72 %). Підтверджено, що свині І групи у ранні вікові періоди поступалися ровесникам інших груп, однак на пізніших етапах відгодівлі демонстрували достовірну перевагу за приростами

та інтенсивністю росту. Тварини II та III груп характеризувалися подібними темпами росту та не відрізнялися статистично значущо між собою. Аналіз головних компонент дозволив виділити два етапи у процесі формування живої маси: перший (130-155 діб) та другий (180-205 діб), які визначаються різними механізмами росту та практично незалежні один від одного. Отримані результати підтверджують ключову роль генотипу у формуванні продуктивних ознак свиней та можуть бути використані при розробці селекційних програм і вдосконаленні систем відгодівлі

Ключові слова: селекція; породність; жива маса; прирости; головні компоненти

Received 04.06.2025 Revised 02.09.2025 Accepted 23.09.2025

Vol. 21, No. 5
2025

Scientific Reports of the National University of Life and Environmental Sciences of Ukraine

Journal homepage: https://scireports.com.ua/en

UDC 631.527.5:633.85:632.11

Doi: 10.31548/dopovidi/5.2025.98

Assessment of agrometeorological conditions for growing sunflower hybrids

Lesia Harbar
PhD in Agricultural Sciences, Associate Professor
National University of Life and Environmental Sciences of Ukraine
03041, 15 Heroiv Oborony Str., Kyiv, Ukraine
https://orcid.ord/0000-0003-4249-0434

Maksim Vandzhura*
Postgraduate Student
National University of Life and Environmental Sciences of Ukraine
03041, 15 Heroiv Oborony Str., Kyiv, Ukraine
https://orcid.org/0009-0001-6372-0641

Abstract. The aim of the study was to analyse the weather conditions during the vegetation period, their correspondence to the morphobiological characteristics of the hybrids, and to identify sunflower hybrids that are better adapted to the region where the research was conducted. The studies were carried out during 2022-2024 under the conditions of Ternopil region. An analysis of the agrometeorological indicators over the research years revealed considerable differences in the vegetation periods, both in terms of temperature indicators and the total monthly precipitation. According to the temperature data, values exceeded the long-term average. The analysis of weather conditions in the study region indicated that the conditions are suitable for cultivating sunflower hybrids of all maturity groups examined, in terms of both heat resources and moisture availability. The sum of active temperatures for the period from April to September was 3,162.1°C (biological minimum 5°C), and the sum of effective temperatures was 2,263.2°C. At a biological minimum of 10°C, the respective figures were 2,977.1°C and 1,409.1°C. During this period, the highest total of heat units was recorded at 3,642.4°C. The total heat units for the May-September period amounted to 3,433.4°C. Soil moisture reserves within the one-metre layer depended on the year's weather conditions and varied accordingly. The water consumption coefficient for early-maturing hybrids, under the influence of fertilisers, ranged from 1,173 to 1,012 m^3/t per tonne of seed; for mid-early hybrids – from 1,171 to 1,017 m^3/t; and for mid-season hybrids – from 1,100 to 989 m^3/t per tonne of seed. A correlation analysis between sunflower yield indicators

Suggested Citation:
Harbar, L., & Vandzhura, M. (2025). Assessment of agrometeorological conditions for growing sunflower hybrids. *Scientific Reports of the National University of Life and Environmental Sciences of Ukraine*, 21(5), 98-113. doi: 10.31548/dopovidi/5.2025.98.

*Corresponding author

and soil moisture reserves showed a direct correlation, with a correlation coefficient of 0.8456. The results of this research can be used to optimise the timing of sowing and harvesting in accordance with forecasted agrometeorological conditions

Keywords: *Helianthus annuus*; temperature indicators; moisture availability; heat units; maturity group

Introduction

Global changes in climate and weather conditions caused by rising temperatures, sharp temperature fluctuations, uneven distribution of precipitation and insufficient rainfall, and frequent droughts have prompted a search for solutions to this problem in the field of crop production. Agricultural producers are putting a lot of effort into introducing and adapting new species and creating new varieties and hybrids that are highly stable and adaptable. Much effort is now being directed towards utilising the adaptive potential of agrocenoses, which involves comprehensive approaches to increasing adaptability through selection, management of exogenous influences on plants, and the creation of optimal crop structures. The creation and emergence of varieties and hybrids with high yield potential and resistance to a wide range of environmental factors cannot fully solve this problem. Sustainable crop production is possible through the management of plant production processes, taking into account and controlling biotic and abiotic factors. In other words, there is a need to create, develop and implement adaptive technologies for growing agricultural crops. With changing climatic conditions, crops from southern regions are moving northwards. An example of such crops is sunflower, the cultivation of which is rapidly spreading to the northern and western regions of Ukraine, which were not previously characteristic for its cultivation.

An analysis of the oilseed market indicates that it is strategically important, as there is a positive price trend for these crops, particularly sunflowers. The supply of this crop is determined by organisational and technological characteristics and the influence of unregulated environmental factors (soil and weather conditions). A series of studies by S.P. Ivanyuta *et al.* (2020) shows that global climate change caused by an increase in average monthly and, accordingly, average annual temperatures and changes in precipitation, mainly towards a decrease in its amount, creates long-term risks in the crop production sector. Crop yields depend on both temperature and moisture conditions and can be controlled by selecting adapted varieties and hybrids and improving cultivation techniques. The results of studies by M. Huz *et al.* (2024), conducted in several periods from 2008 to 2021, indicate significant changes in the analysis of sunflower production dynamics in Ukraine. The dynamics of the indicators were caused by changes in climatic conditions as a result of differences in weather conditions. Sunflower production indicators were characterised by a close dependence of crop yields on weather conditions in different regions of Ukraine. In addition to environmental conditions, market conditions also had an impact on sunflower production indicators. Based on production and yield indicators, polynomial trend models were constructed, which were characterised by a high degree of reliability and were able to reflect the real dynamics of the indicators.

In order to increase sunflower production, it is necessary to ensure growing conditions in which plants are able to realise their full potential. In particular, this means creating conditions that are more favourable in terms of moisture availability than in the southern regions of Ukraine. This is why there has been a migration of sunflower crops to the western and northern regions of Ukraine. The research by D. Baranskyi (2024) is aimed at studying the impact of

sunflower cultivation in conditions of sufficient moisture in the Western Forest-Steppe on the dynamics of soil moisture reserves during the growing season. The results showed that the crop is capable of producing high yields in the presence of sufficient moisture in the 0-200 mm soil layer in the autumn-winter period. Research by O.L. Zhygailo *et al.* (2021) points to the formation of new economic conditions in all sectors, including crop production, as a result of global climate change. One of the crops affected by this is sunflower, whose yield is linked to the agroclimatic conditions in which it is grown. The authors emphasise that the profitability of growing this crop will depend on the natural and climatic zone in which it is grown.

Scientists I.V. Tomashuk & R.O. Horobchuk (2024) analysed the potential of Ukraine's agricultural sector and investigated opportunities for increasing the efficiency of its use in the cultivation of certain crops. One of the factors determining the level of production is the soil and weather conditions of the region where the crop is grown. According to V.M. Totskyi *et al.* (2024), crop cultivation technology, in particular the use of mineral fertilisers that provide a sufficient level of essential nutrients in the soil, is of great importance for sunflower cultivation and increasing its yield and seed quality. The level of nutrient uptake by plants is determined by a number of factors, including soil and climatic conditions. Research by O. Trembitska *et al.* (2021), conducted in the Polissya region on the cultivation of the Oplot hybrid sunflower to study the effect of fertilisation, showed a positive impact on both yield and seed quality. The highest yield indicators were obtained in the variant with the use of $N_{90}P_{90}K_{90}$ – 2.16 t/ha with a fat content in seeds of 44.2%. The cultivation of sunflowers in atypical conditions (in Polissya) and the search for optimal technological methods based on the results of research by O.A. Furmanets (2022) indicated the difficulties arising from unstable growing conditions, which do not allow the genetic potential of the crop to be realised. The use of fertilisers allows increasing the crop yield in conditions of sufficient moisture supply to 27%, and in arid conditions – to 44.0%.

In the context of changing climatic conditions, the development and implementation of adapted crop cultivation technologies is of great importance in the field of crop production. These technologies involve the optimisation of cultivation techniques and the selection of new crop varieties and hybrids capable of maximising their genetic potential in atypical growing conditions. The aim of the research was to analyse the weather conditions during the growing season and identify sunflower hybrids that are better adapted to the region where the research was conducted.

Materials and Methods

The research was conducted during 2022-2024 under the conditions of the Ternopil region. The field experiment was a three-factor design with four replications. The area of the experimental plot was 60 m², and the accounting (harvest) plot area was 42 m². The research design involved studying the following factors: factor A – maturity group: early, medium early, medium ripening; factor B – hybrids: RGT Wollf, Atilla, Belvedere, LG-5478, NK Brio, NK Kondi, P64LL155, factor C – fertilisation options: 1. $N_{60}P_{60}K_{80}$; 2. $N_{80}P_{80}K_{120}$. The preceding crop was winter wheat. The meteorological indicators and parameters used for calculations were taken from the data of the meteorological station in Ternopil.

The calculation of the coefficients of significance of deviations in temperature indicators and precipitation for the years of research and average long-term indicators was carried out using the formula:

$$Cs = \frac{(Xi - \bar{X})}{\sigma}, \quad (1)$$

where: *Cs* – coefficient of significance of deviations; *Xi* – weather elements for the current year;

$\bar{X}$ – indicator of the average long-term value; σ – mean square deviation.

The significance of the coefficients of materiality of deviations had the following gradations:

- $Cs = 0 \div 1$ – conditions close to normal;
- $Cs = 1 \div 2$ – conditions significantly different from long-term averages;
- $Cs > 2$ – conditions close to rare.

Heat units (CHU) were calculated for the period from emergence to full maturity of the crop according to the following methodology: heat units per day (Y_{max}) were calculated using the formula:

$$Y_{max} = 3.33 \cdot (T_{max} - 10) - 0.084 \cdot (T_{max} - 10), \quad (2)$$

at $T_{max} < 10$, $Y_{max} = 0$.

Calculation of heat units per night:

$$Y_{min} = 1.8 \cdot (T_{min} - 4.44), \quad (3)$$

at $T_{min} < 4.44$, $Y_{min} = 0$.

The next step was to calculate the heat units per day:

$$CHU = (Y_{max+} Y_{min})/2.0 \quad (4)$$

The sums of active and effective temperatures were determined by calculation for biologically active temperatures of 5 and 10°C. The amount of available moisture was determined using the thermostat-weight method, and total moisture consumption was determined using the water balance formula:

$$E = O + (Wn - Wk), \quad (5)$$

where E – the amount of moisture used by plants during vegetation, m³/ha; Wn, Wk – the amount of moisture at the beginning and end of vegetation, m³/ha; O is the amount of precipitation during vegetation, m³/ha.

The water consumption coefficient was determined using the formula:

$$Cc = E : Y, \quad (6)$$

where Cc – water consumption coefficient, m³/ha; Y – the sunflower yield, t/ha.

Yield was determined by sectional harvesting with a conversion to 8% moisture content. Based on the results obtained, a correlation analysis was performed between yield indicators and soil moisture reserves (Rozhkov *et al.*, 2016). The study complied with the requirements of the Convention on Biological Diversity (1992).

Results and Discussion

The availability of a huge range of varieties and hybrids of agricultural crops, in particular industrial crops, on the seed market poses a challenge for producers when selecting seed material, taking into account its plasticity to unregulated factors and the ability to maximise genetic potential in specific climatic conditions. An analysis of the weather conditions at the research site was carried out based on the significance coefficients of deviations of current weather data (2022-2024) from the long-term average parameters.

An analysis of agrometeorological indicators over the years of research shows significant differences between vegetation periods. These results were obtained from the analysis of both temperature indicators and the total amount of precipitation per month. The results of temperature indicators (2022-2024) show that they exceed the long-term average data (Fig. 1).

Analysis of agrometeorological data showed that March temperatures were significantly higher than the long-term average (1.7°C) in all years of the study and ranged from 4.0 to 4.6°C. In April, temperatures in 2022 and 2023 were lower than the long-term average (8.4°C) and ranged from 6.9 to 7.4°C. In 2024, the temperature was 11.2°C, which affected the timing of sunflower sowing. The temperature in May was as close as possible to the long-term average (14.2°C) and corresponded to values of 14.1, 14.2 and 15.7°C. All other months of the growing season from June to September were characterised by a significant increase in temperature indicators by 0.7-4.4°C.

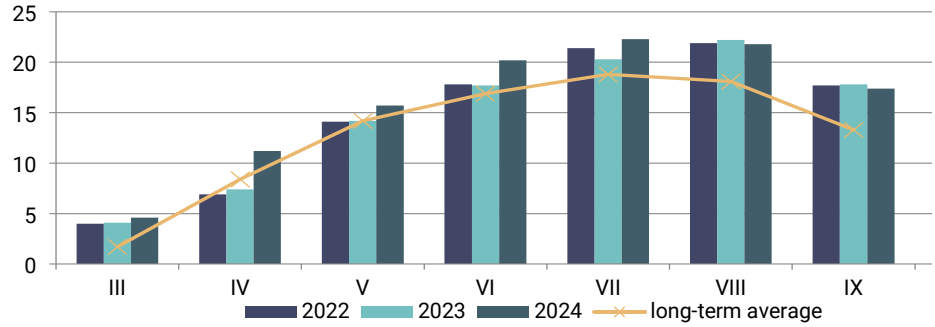

Figure 1. *Average monthly air temperature, 2022-2024, °C*
Source: developed by the authors

The amount of precipitation that fell during the sunflower growing season was insufficient, with a characteristic uneven distribution (Fig. 2). As the analysis of the indicators showed, May was characterised by the lowest amount of precipitation, with values almost twice lower than the long-term average in all years of the study.

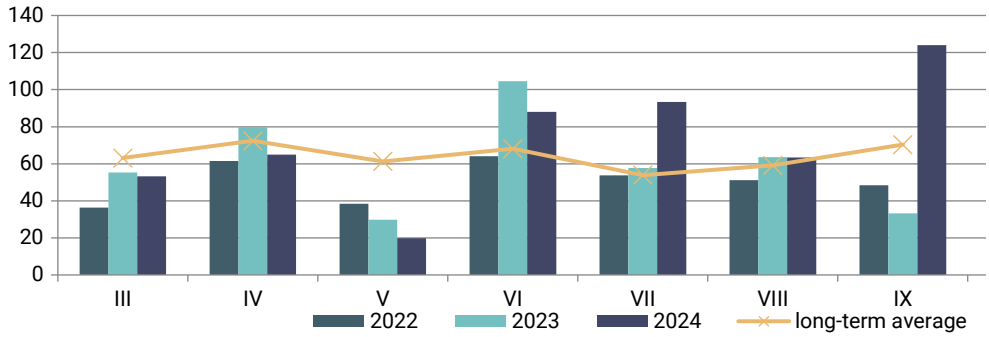

Figure 2. *Precipitation, 2022-2024, mm*
Source: developed by the authors

Precipitation in April was sufficient and, depending on the year of research, varied between 61.4 and 79.7 mm (average long-term figures – 72.4 mm). May turned out to be the driest of all the growing months. According to long-term averages – 61.3 mm in 2022, 38.4 mm fell in 2023, 29.8 mm in 2024, and 19.8 mm in 2025. June was characterised by precipitation close to the long-term average (68.1 mm), while in 2023 it significantly exceeded the average and amounted to 104.6 mm. July was characterised by a similar pattern, with precipitation exceeding the long-term average in 2024 (93.3 mm compared to 53.9 mm). In August, precipitation was close to the long-term average, ranging from 51.2 to 63.6 mm. In September, precipitation was below normal (70.3 mm) in 2022 and 2023, amounting to 48.4 and 33.3 mm, respectively. In 2024, precipitation in September amounted to 124.1 mm, which complicated the harvesting of crops.

An analysis of the calculated coefficients of significance of precipitation deviations showed that 54% of the months analysed belonged to the category of "conditions close to normal". Meanwhile, 33% were characterised as "conditions that differ significantly from long-term indicators" and 13% as "conditions close to rare" (Fig. 3).

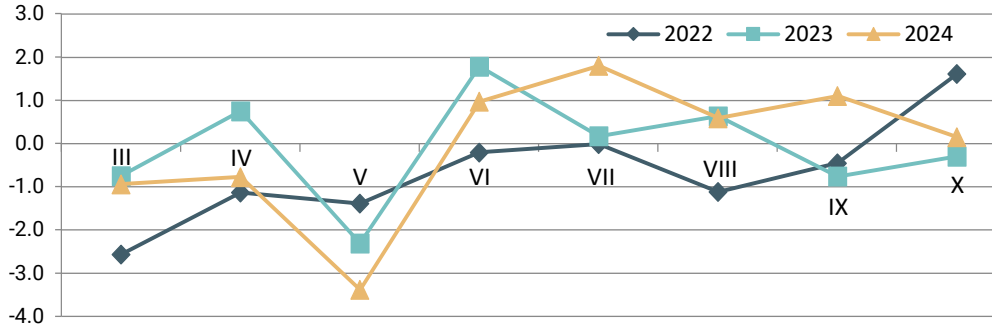

Figure 3. *Significance coefficients of precipitation deviations, 2022-2024*
Source: developed by the authors

Calculations to determine the significance coefficients of temperature deviations and their analysis indicate significant deviations between the long-term average data and the actual temperature readings during the years of research. It should be noted that a significant upward deviation in temperature indicators brings certain periods of plant growth and development closer to "rare conditions" (Fig. 4).

Analysis of the calculated coefficients of significance of temperature deviations showed that they varied in the range from 2.6 to minus 1.5. The following results were obtained when calculating the coefficients of deviation of temperature indicators: the percentage of months with "conditions close to normal" was 58, and "conditions that differ significantly from long-term indicators" was 25, while "conditions close to rare" was 17%.

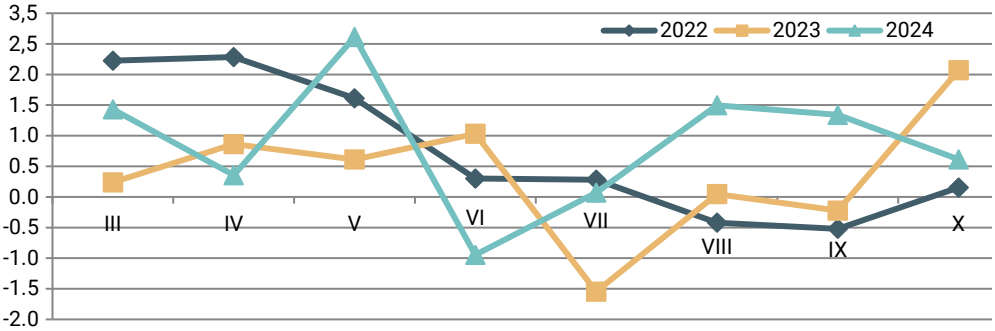

Figure 4. *Materiality coefficients of deviations in average monthly temperature indicators, 2022-2024*
Source: developed by the authors

Air temperature indicators are unregulated factors. And in the context of climate change, when there is a significant increase in these indicators, their significant impact on certain processes in plants becomes apparent, which is reflected in the formation of their productivity. There are a number of indicators that can be calculated based on temperature data to draw conclusions about their impact on plant growth and development. The calculation of heat units by month showed that April was characterised by the highest deviations from the average value. The sum of heat units in 2023 was the lowest, at 127.9°C, while in 2024 the indicator was 309.7°C. In other words, April in the region where the research was conducted was characterised

by rather unstable temperature indicators during the day and night, which was reflected in the sum of heat units per month. In all other months of the sunflower growing season, no such significant differences were found between the years of research (Table 1).

Table 1. *Total heat units for sunflower vegetation in 2022-2024*

Month, period	CHU			Deviation from the average			Average for 2022-2024
	2022	2023	2024	2022	2023	2024	
April	189.4	127.9	309.7	-19.6	-81.1	100.7	209.0
May	495.2	471.4	512.1	2.3	-21.5	19.2	492.9
June	657.1	634.5	730.7	-17.0	-39.6	56.6	674.1
July	789.6	770.2	830.8	-7.3	-26.7	33.9	796.9
August	786.1	814.7	812.9	-18.5	10.1	8.3	804.6
September	694.6	664.2	636.1	29.6	-0.8	-28.9	665.0
Σ April-August	2,917.4	2,818.7	3,196.2	-60.0	-158.7	218.8	2,977.4
Σ April-September	3,612.0	3,482.9	3,832.3	-30.4	-159.5	189.9	3,642.4
Σ May-August	2,728.0	2,690.8	2,886.5	-40.4	-77.6	118.1	2,768.4
Σ May-September	3,422.6	3,355.0	3,522.6	-10.8	-78.4	89.2	3,433.4

Note: CHU – Crop Heat Units
Source: developed by the authors

The calculation of the average number of heat units during the years of research during the sunflower growing season indicates their significant importance and dependence on weather conditions during the year. It should be noted that the number of heat units depended not only on the average daily temperature, but also on its minimum and maximum values. Thus, for the period from April to August, the sum of heat units was 2,917.4 in 2022, 2,818.7 in 2023, and 3,196.2°C in 2023. The April-September growing season was characterised by the following indicators: 3,612.0 in 2022, 3,482.9 in 2023, and 3,832.3°C in 2024. During the period from May to August, plants accumulated the smallest amount of heat units, which varied from 2,690.8 to 2,886.5°C during the study period. The sum of heat units for the May-September growing season ranged from 3,355.0 (2023) to 3,522.6 (2024). It should be noted that the highest average number of heat units per year was obtained for the growing season covering April-September, with an indicator of 3,642.4. A slightly lower indicator was obtained for the period May-September – 3,433.4.

The next criteria determining the conditions for growing crops are the sums of active and effective temperatures during the growing season. For sunflowers, the sums of these temperatures at biological minimums of 5 and 10°C are relevant. As shown by the calculations, the sums of active and effective temperatures for the corresponding periods were significantly lower than the sums of heat units (Table 2).

Table 2. *Indicators of the sum of active and effective temperature indicators at a biological minimum of 5°C*

Month	Decade	Sum of active temperatures, °C			Average value	Sum of effective temperatures, °C			Average value
		2022	2023	2024		2022	2023	2024	
April	1	47.5	29.9	129.5	69.0	4.9	10.5	79.5	31.6
	2	91.5	88.7	100.9	93.7	41.5	38.7	55.9	45.4
	3	90.1	90.5	101.3	94.0	40.1	40.5	51.3	44.0

Table 2. *Continued*

Month	Decade	Sum of active temperatures, °C			Average value	Sum of effective temperatures, °C			Average value
		2022	2023	2024		2022	2023	2024	
May	1	103.4	99.7	145.9	116.3	53.4	49.7	95.9	66.3
	2	127.0	149.6	130.7	135.8	77	99.6	80.7	85.8
	3	197.1	190.7	209.1	199.0	147.1	133.1	154.1	144.8
June	1	184.1	179.4	193.9	185.8	134.1	129.4	143.9	135.8
	2	171.3	168.9	190.1	176.8	121.3	111.9	140.1	124.4
	3	199.2	190.6	223.3	204.4	149.2	140.6	173.3	154.4
July	1	215.2	204	210.3	209.8	165.2	154.0	160.3	159.8
	2	235.4	207.4	260.3	234.4	185.4	157.4	210.3	184.4
	3	223.1	217.8	222.1	221.0	173.1	162.8	167.1	167.7
August	1	203.1	208.1	198.2	203.1	153.1	158.1	148.2	153.1
	2	217.0	221.8	220.7	219.8	167.0	171.8	170.7	169.8
	3	260.1	258.0	256.9	258.3	210.1	203.0	201.9	205.0
September	1	201.8	171.5	207.9	193.7	151.8	121.5	157.9	143.7
	2	189.2	181.1	165	178.4	139.2	131.1	115	128.4
	3	168.4	182.6	155.4	168.8	118.4	132.6	105.4	118.8
Σ April-August		2,565.1	2,505.1	2,793.2	2,621.2	1,822.5	1,761.1	2,033.2	1,872.3
Σ April-September		3,124.5	3,040.3	3,321.5	3,162.1	2,231.9	2,146.3	2,411.5	2,263.2
Σ May-August		2,336.0	2,296.0	2,461.5	2,364.5	1,736.0	1,671.4	1,846.5	1,751.3
Σ May-September		2,895.4	2,831.2	2,989.8	2,905.4	2,145.4	2,056.6	2,224.8	2,142.2

Source: developed by the authors

The sum of active temperatures (biological minimum 5°C) for the period April-September was the highest and amounted to the following for the years of research: in 2022, 3,124.5; in 2023, 3,040.3; in 2024, 3,321.5°C. The indicators for the period May-September were slightly lower: in 2022, 2,895.4; in 2023, 2,831.2; in 2024, 2,989.8°C. The growing seasons from April to August and May to August were characterised by significantly lower values. The maximum sum of active temperatures at a biological minimum of 5°C – 3,162.1°C – was obtained for the period from April to September on average over the years of research. Analysis of the sum of effective temperatures at a biological minimum of 5°C indicates similar trends between indicators depending on the growing seasons and years of research. The sum of active temperatures for the period April-September had the highest values, varied depending on the year of research and amounted to 2,231.9 in 2022, 2,146.3 in 2023, and 2,411.5°C in 2024. The sum of effective temperatures for the same period averaged 2,263.2°C over the years. The calculation of the sum of active temperatures at a biological minimum of 10°C showed significantly lower values than those in the previous table, but the trends between the indicators remained the same (Table 3).

Table 3. *Indicators of the sum of active and effective temperature indicators at a biological minimum of 10°C*

Month	Decade	Sum of active temperatures, °C			Average value	Sum of effective temperatures, °C			Average value
		2022	2023	2024		2022	2023	2024	
April	1	0	0	111.9	37.3	0	0	31.1	10.4
	2	11.5	0	81.6	31.0	0	0	21.6	7.2
	3	30.1	65.8	52.3	49.4	0	5.8	12.3	6.0

Table 3. *Continued*

Month	Decade	Sum of active temperatures, °C			Average value	Sum of effective temperatures, °C			Average value
		2022	2023	2024		2022	2023	2024	
May	1	33.4	61.5	145.9	80.3	0	11.5	45.9	19.1
	2	103.0	139.8	130.7	124.5	3	49.8	30.9	27.9
	3	197.1	190.7	209.1	199.0	97.1	80.7	109.1	95.6
June	1	184.1	179.4	193.9	185.8	84.1	79.4	93.9	85.8
	2	171.3	169.9	190.1	177.1	71.3	61.9	90.1	74.4
	3	199.2	190.6	223.3	204.4	99.2	90.6	123.3	104.4
July	1	215.2	204.0	210.3	209.8	115.2	104.0	110.3	109.8
	2	235.4	207.4	260.3	234.4	135.4	107.4	160.3	134.4
	3	223.1	217.8	222.1	221.0	123.1	107.8	122.1	117.7
August	1	203.1	208.1	198.2	203.1	103.1	108.1	98.2	103.1
	2	217.0	221.8	220.7	219.8	117.0	121.8	120.7	119.8
	3	260.1	258	256.9	258.3	160.1	148.0	146.9	151.7
September	1	201.8	171.5	207.9	193.7	101.8	71.5	107.9	93.7
	2	189.2	184.1	165	179.4	89.2	81.1	65.0	78.4
	3	168.4	182.6	155.4	168.8	68.4	82.6	58.1	69.7
Σ April-August		2,283.6	2,314.8	2,707.3	2,435.2	1,108.6	1,076.8	1,316.7	1,167.3
Σ April-September		2,843.0	2,853.0	3,235.6	2,977.1	1,368.0	1,312.0	1,547.7	1,409.1
Σ May-August		2,242.0	2,249.0	2,461.5	2,317.5	1,108.6	1,071.0	1,251.7	1,143.7
Σ May-September		2,801.4	2,787.2	2,989.8	2,859.4	1,368.0	1,306.2	1,482.7	1,385.5

Source: developed by the authors

The sum of active temperatures (biological minimum 10°C) for the period April-September had the highest values and amounted to the following for the years of research: in 2022, 2,843.0; in 2023, 2,853.0; in 2024, 3,235.6°C, which indicates the possibility of growing hybrids with longer growing seasons than those studied in the research region. The calculation of the sum of effective temperatures (biological minimum 10°C) shows similar dependencies between the indicators and their lower values. The period from April to September was characterised by the highest values of the sum of effective temperatures at a biological minimum of 10°C, with indicators ranging from 1,312.0 to 1,547.7°C over the years of research. On average for the years of research, the sum of active temperatures at a biological minimum of 10°C was at its maximum during the April-September growing season at 2,977.1°C, and the sum of effective temperatures was 1,409.1°C. The results obtained, according to the calculations, indicate the possibility of growing the hybrids studied under the conditions of the research.

Moisture is one of the limiting factors in the formation of crop productivity, in particular sunflower. Analysis of moisture reserve indicators under the conditions of the research indicates a significant influence of the meteorological characteristics of each growing season. The total moisture reserves for sunflower cultivation depend on the moisture reserves in the metre-deep soil layer at the time of sowing, the amount of precipitation during the growing season, and the duration of the growing season for a particular hybrid. Due to the fact that all hybrids were sown simultaneously, soil moisture reserves did not change in terms of maturity group (Table 4).

Table 4. *Characteristics of moisture supply indicators for sunflower hybrids, m3/ha*

Year	Hybrid maturity group	Soil moisture reserves, sowing, m³/ha	Precipitation during vegetation, m³/ha	Total moisture reserves, m³/ha	Moisture reserves, harvesting, m³/ha	Moisture consumption, total, m³/ha
2022	Early	1,295	1,815	3,110	796	2,314
	Mid-early	1,295	1,839	3,134	748	2,386
	Mid-season	1,295	1,879	3,174	715	2,459
2023	Early	1,489	1,843	3,332	832	2,500
	Mid-early	1,489	2,262	3,751	811	2,940
	Mid-season	1,489	2,277	3,766	774	2,992
2024	Early	1,645	2,163	3,808	841	2,967
	Mid-early	1,645	2,593	4,238	827	3,411
	Mid-season	1,645	3,137	4,782	801	3,981

Source: developed by the authors

Thus, soil moisture reserves at the time of sowing amounted to 1,295 m³/ha in 2022, 1,489 m³/ha in 2023, and 1,645 m³/ha in 2024. The amount of precipitation depended on the maturity group of the hybrids and the duration of their vegetation period, ranging from 1,815 m³/ha (in 2022, for the early maturity group) to 3,137 m³/ha (in 2024, for the mid-season group). The total moisture reserves in the one-metre soil layer during the vegetation period varied depending on the research year – from 3,110 m³/ha in 2022 when cultivating early-maturing sunflower hybrids to 4,782 m³/ha in 2024 for mid-season hybrids. Calculations showed that total moisture reserves depended more on precipitation during the vegetation period than on the productive moisture reserves in the one-metre soil layer at sowing time. It is worth noting that 2024 was characterised by the highest soil moisture reserves at sowing and the greatest amount of precipitation during the sunflower vegetation period. Moisture consumption by sunflower plants depended on the total moisture reserves and the resulting crop yield. The yield of sunflower hybrids was influenced by the genetic characteristics of the hybrids, their maturity group, the impact of uncontrolled environmental factors, and the elements of cultivation technology. Therefore, moisture consumption depended on the growth and development features of each hybrid under the combined influence of all factors. It varied according to maturity group and amounted to between 2,314 and 2,459 m³/ha in 2022, between 2,500 and 2,992 m³/ha in 2023, and between 2,967 and 3,981 m³/ha in 2024. As the duration of the vegetation period increased, moisture consumption also increased.

Sunflower, like other field crops, have different moisture requirements at different stages of their growth and development. They have the greatest need for water during the period of laying and formation of generative organs. Insufficient moisture leads to a decrease in crop productivity. The calculation of water consumption coefficients for sunflowers within maturity groups depended primarily on the established yield of the main product, and only then on the duration of their growing season and, accordingly, moisture availability (Table 5).

Table 5. *Water consumption coefficient indicators for sunflower hybrid maturity groups, m3/t per 1 t of seeds*

Year	Maturity group					
	Early		Mid-early		Mid-season	
	1	2	1	2	1	2
2022	1,146	972	1,015	871	931	851
2023	1,116	965	1,200	1,024	1,092	962
2024	1,257	1,099	1,297	1,156	1,276	1,154
average	1,173	1,012	1,171	1,017	1,100	989

Note: 1 – $N_{60}P_{60}K_{80}$; 2 – $N_{80}P_{80}K_{120}$
Source: developed by the authors

The analysis of indicators demonstrates their dependence on yield, the maturity group of sunflower hybrids (vegetation duration), and the moisture supply available to plants during the growing season. The amount of fertiliser applied in sunflower cultivation also influenced these indicators. As the fertiliser application rates increased, crop yield rose, while the water consumption coefficient decreased. On average over the years of study, the water consumption coefficient for early-maturing hybrids under the influence of fertilisers ranged from 1,173 to 1,012 m^3/t per tonne of seed; for mid-early hybrids, from 1,171 to 1,017 m^3/t; and for mid-season hybrids, from 1,100 to 989 m^3/t per tonne of seed. Correlation analysis between sunflower yield and soil moisture reserves revealed a direct relationship with a correlation coefficient of 0.8456.

Similar results were obtained by D. Baranskyi (2024) from studies conducted in 2022-2023 in the Western Forest-Steppe zone, which demonstrated a dependence of sunflower yield on soil moisture reserves within the root zone. However, that research also emphasised the importance of moisture accumulation during the autumn and winter periods. Studies by O.I. Polyakov & A.D. Shcherbak (2022) showed that sunflower yield depends on the water supply available to plants of different hybrids throughout the entire vegetation period. The authors also highlighted the influence of fertiliser application rates on water consumption and crop yield. In variants without fertiliser application, the lowest total plant water use was recorded. Under the influence of the genetic characteristics of each variety, the indicators varied from 359.2 to 372.8 mm. When phosphorus and potassium fertilisers were applied in sunflower cultivation, the lowest water consumption coefficient was recorded, ranging from 1,039 to 1,177 m^3/ha depending on the studied factors.

Research by A. Haj Sghaier *et al.* (2023), dedicated to studying the impact of temperature indicators and moisture on the rate of sunflower seed germination, highlighted the importance of considering the duration of the vegetation period and the ability of plants to form seedlings when planning technological processes. These results make it possible to determine the optimal sowing dates, ensuring proper growth, development, and productivity formation of sunflower plants. The study by S. Matskova and A. Gumanyuk (2025), aimed at analysing uncontrolled environmental factors (average annual temperatures and spring soil moisture reserves) over the period 2006-2024, showed that spring soil moisture reserves have a weak correlation with sunflower yield indicators ($r = 0.145$), indicating an insignificant influence of this factor on crop productivity formation. When considering the combined effect of spring soil moisture and precipitation during April-May, the correlation coefficient was $r = 0.298$. A higher correlation coefficient ($r = 0.505$) was obtained when taking into account both spring soil

moisture and precipitation during April –July, indicating the importance of moisture availability during the critical period of sunflower growth and development, corresponding to the formation of the crop's generative organs.

Research by J. Mu *et al.* (2025), conducted in the 10th Division of Xinjiang at three representative stations, focused on examining the relationship between meteorological factors and the growth and development characteristics of sunflower varieties of different maturity groups. The study revealed distinct regional adaptation patterns among sunflower varieties. Varieties differing in vegetation duration demonstrated specific adaptive responses to environmental conditions. The obtained results enable the proper selection of varieties and the development of appropriate cultivation strategies (including technological elements) that enhance the resilience and stability of sunflower yields under various climatic conditions. The study of the effects of fertilisation and growth-regulating substances on sunflower productivity conducted by O.V. Nikitenko *et al.* (2021) revealed the influence of these factors on the total water consumption required to form the yield. The lowest water consumption coefficient obtained in the study was 832 m^3/t under the conditions of a conventional tillage system, the application of $N_{60}P_{60}K_{60}$, and the use of growth-regulating substances during the vegetation period.

Research by Ye.O. Domaratskyi *et al.* (2021) carried out in the Southern Steppe of Ukraine, which focused on the impact of growth-regulating preparations on the productivity of sunflower hybrids and the optimisation of water consumption under critical climate change conditions, showed that the lowest water consumption coefficient (1,283 m^3/t) was obtained when cultivating the hybrid P64GE133 with seed treatment using the preparation Helafit Combi. The studied preparations promoted efficient use of soil moisture, reducing the water consumption coefficient across all hybrids involved in the experiment. The subsequent research by Ye.O. Domaratskyi *et al.* (2022), aimed at studying the influence of fertiliser application and growth-regulating substances on sunflower water use, confirmed their positive effect. The authors established that both fertilisation and the use of growth regulators contributed to improved crop productivity formation. The minimum water consumption coefficient was recorded for the sunflower hybrid P64GE133, amounting to 1,283 m^3/ha when treated with Helafit Combi.

Studies conducted at the College of Agriculture, University of Wasit by D.N.J. Al-Waili *et al.* (2025), which aimed to investigate the effects of several factors on sunflower water consumption, demonstrated that the amount of water absorbed by plants increased as growth and development progressed, while the need for moisture declined during the ripening phase. Field research by K. Farrag *et al.* (2025), focused on examining the impact of fertilisers, soil amendments, and moisture availability on sunflower productivity indicators, revealed a positive influence of fertilisation on the physical properties of soil and, consequently, on its water-holding capacity. A positive effect of fertilisers and soil amendments on the productive use of moisture was established. Under modern sunflower cultivation conditions, attention is focused not only on crop adaptation to weather conditions but also on the optimisation of agrotechnological practices. In particular, studies by V. Bolokhovsky *et al.* (2024) demonstrated that integrated plant nutrition technologies incorporating biopreparations enhance the efficiency of soil and water resource use, which is especially important under variable climatic conditions and agrometeorological risks.

According to the findings of S.M. Kalenska & A.S. Ryzhenko (2020), who investigated the relationship between heat and moisture resources and the biological characteristics of sunflower hybrids under the conditions of the Sumy region, yield was found to depend on these factors. The sum of active temperatures above 10°C for the development cycle of the studied sunflower hybrids ranged from 2,306.4 to 2,401.3°C, while the sum of effective temperatures varied between 1,056.9

and 1,109.1°C. The total heat units during the vegetation period (April-August), averaged across the study years, ranged from 2,868 to 3,258°C, significantly exceeding the sums of active and effective temperatures. However, I. Gintsioudis *et al*. (2024) emphasised that under equal total heat unit sums, plants grown under different environmental conditions exhibit distinct distributions of heat units across growth and development stages. Therefore, heat unit models must account for the fact that plants require varying amounts of thermal energy at different growth stages. Further research is needed to refine baseline and threshold temperature values to more accurately determine the timing of specific developmental phases. The obtained research results comprehensively characterise the agrometeorological conditions for sunflower cultivation in the Ternopil region and partially contribute to understanding their influence on the adaptability and productivity formation of the studied hybrids.

Conclusions

The analysis of weather conditions in the study region indicates that the conditions are suitable for growing sunflower hybrids of all maturity groups examined, in terms of both heat resources and moisture availability. During the vegetation period (April-September), the average values across the research years showed a maximum sum of active temperatures of 3,162.1°C and effective temperatures of 2,263.2°C, based on a biological minimum of 5°C. With a biological minimum of 10°C, the sum of active temperatures was 2,977.1°C and effective temperatures 1,409.1°C (for the April-September period). The highest total number of heat units during the sunflower vegetation period was recorded for April–September, amounting to 3,642.4°C. For the vegetation period from May to September, the value was 3,433.4°C. The total moisture reserves in the one-metre soil layer during the vegetation period varied from 3,110 m^3/ha in 2022 (early maturity group) to 4,782 m^3/ha in 2024 (mid-season group). Moisture consumption depended on total moisture reserves and the yield achieved, ranging from 2,314 to 2,459 m^3/ha in 2022, from 2,500 to 2,992 m^3/ha in 2023, and from 2,967 to 3,981 m^3/ha in 2024. As the duration of the vegetation period increased, moisture consumption by sunflower plants also increased.

The water consumption coefficient for early-maturing hybrids under the influence of fertilisers ranged from 1,173 to 1,012 m^3/t per tonne of seed, for mid-early hybrids from 1,171 to 1,017 m^3/t, and for mid-season hybrids from 1,100 to 989 m^3/t per tonne of seed. The correlation analysis between sunflower yield indicators and soil moisture reserves revealed a direct correlation with a correlation coefficient of 0.8456. Prospects for further research lie in studying the influence of both controlled and uncontrolled factors on the growth, development, and productivity formation of hybrids belonging to different maturity groups, with the aim of identifying levers to enhance the realisation of their genetic potential under atypical growing conditions for sunflower.

Acknowledgements

None.

Funding

None.

Conflict of Interest

None.

References

[1] Al-Waili, D.N.J., Abdul Rahman, J.N., & Al-Maliki, R.J.M. (2025). Moisture depletion, soil improvers and antitranspiration and its effect on water consumption of sunflower (*Helianthus annus* L.). *IOP Conference Series: Earth and Environmental Science*, 1449, article number 14. doi: 10.1088/1755-1315/1449/1/012114.

[2] Baranskyi, D. (2024). Managing sunflower growth in the changing climate and fluctuating moisture levels of the Western Forest-Steppe. *Bulletin of Lviv National Environmental University. Series Agronomy*, 28, 57-66. doi: 10.31734/agronomy2024.28.057.

[3] Bolokhovsky, V., Bolokhovska, V., Khomenko, T., Datsko, A., & Litvinova, O. (2024). Optimisation of plant nutrition under the influence of biopreparations in integrated sunflower cultivation technologies. *Plant and Soil Science*, 15(4), 64-75. doi: 10.31548/plant4.2024.64.

[4] Convention on Biological Diversity. (1992, June). Retrieved from https://zakon.rada.gov.ua/laws/show/995_030#Text.

[5] Domaratskyi, Ye., Kozlova, O., Dobrovolskyi, A., & Bazaliy, V. (2022). Optimization of water consumption of high-oleic sunflower hybrids under non-irrigated conditions of the steppe zone of Ukraine. *Journal of Ecological Engineering*, 23(6), 14-21. doi: 10.12911/22998993/148150.

[6] Domaratskyi, Ye.O., Dobrovolskyi, A.V., Kozlova, O.P., Dobrovolskyi, P.A., & Lavryshyna, O.Ye. (2021). Ways of optimization of high oolein type sunflower consumption under climate change. *Agrarian Innovations*, 10, 34-41. doi: 10.32848/agrar.innov.2021.10.6.

[7] Farrag, K., Abdel-Hakim, S.G., El-Sesy, M.E., El-Sayed, E.S. el-Bastamy, & Abdrabbo, M.A. (2025). Promotion of sunflower growth and water productivity using soil amendments under saline conditions. *Water Science*, 39(1), 336-345. doi: 10.1080/23570008.2025.2507456.

[8] Furmanets, O.A. (2022). Development and productivity of sunflower on sod-podzolic soils of Western Polissia with the application of various types of complex fertilizers. *Agrarian Innovations*, 16, 80-84. doi: 10.32848/agrar.innov.2022.16.13.

[9] Gintsioudis, I., Danalatos, G.J., Bartzialis, D., Giannoulis, K.D., & Danalatos, N.G. (2024). Accumulated thermal units method for predicting development stages, and potential seed yield of sunflower (*Helianthus annuus*) under Mediterranean conditions. *Industrial Crops and Products*, 221, article number 119383. doi: 10.1016/j.indcrop.2024.119383.

[10] Haj Sghaier, A., Khaeim, H., Tarnawa, Á., Kovács, G.P., Gyuricza, C., & Kende, Z. (2023). Germination and seedling development responses of sunflower (*Helianthus annuus* L.) seeds to temperature and different levels of water availability. *Agriculture*, 13(3), article number 608. doi: 10.3390/agriculture13030608.

[11] Huz, M., Chukhlib, A., & Symonenko, O. (2024). Predictive assessment of the impact of climate change on sunflower production: Analysis of dynamic series and modeling of trends. *Herald of Khmelnytskyi National University,* 331(1), 438-445. doi: 10.31891/2307-5732-2024-331-67.

[12] Ivanyuta, S.P., Kolomiyec, O.O., Malinovska, O.A., & Yakushenko, L.M. (2020). *Climate change: Impacts and adaptation measures*. Kyiv: NISD .

[13] Kalenska, S.M., & Ryzhenko, A.S. (2020). Evaluation weather conditions for growing sunflower (*Helianthus annuus* L.) in the northern part of the Left-bank Forest Steppe of Ukraine. *Plant Varieties Studying and Protection*, 16(2), 162-172. doi: 10.21498/2518-1017.16.2.2020.209229.

[14] Matskova, S., & V Gumanyuk, A. (2025). Reserves of soil productive humidity are the key to high yield of sunflower. *Research Journal of Agricultural Science*, 57(1), 161-165. doi. 10.59463/RJAS.2025.1.19.

[15] Mu, J., Wang, J., Ma, R., Lv, Z., Dong, H., Liu, Y., Duan, W., Liu, S., Wang, P., & Zhang, X. (2025). Optimizing sunflower cultivar selection under climate variability: Evidence from coupled meteorological-growth modeling in arid northwest China. *Agronomy*, 15(7), article number 1724. doi: 10.3390/agronomy15071724.

[16] Nikitenko, O.V., Poliakov, O.I., & Litoshko, S.V. (2021). Optimal growing regulations – guarantee of high productivity of sunflower. *Scientific and Technical Bulletin of the Institute of Oilseed Crops NAAS*, 31, 72-87. doi: 10.36710/ioc-2021-31-07.

[17] Polyakov, O.I., & Shcherbak, A.D. (2022). Productivity of sunflower under the influence of mineral fertilizers and growth regulators. *Scientific and Technical Bulletin of the Institute of Oilseed Crops NAAS*, 35, 101-113. doi: 10.36710/IOC-2023-35-09.

[18] Rozhkov, A.O., Puzik, V.K., Kalenskaya, S.M., Puzik, L.M., Popov, S.I., Muzafarov, N.M., Bukhalo, V.Ya., & Kryshtop, E.A. (2016). *Research in agronomy. Book 1: Theoretical aspects of research.* Kharkiv: Maidan

[19] Tomashuk, I.V., & Horobchuk R.O. (2024). Socio-economic potential of the agrarian sector of Ukraine: prospects for development and opportunities for improving the efficiency of its use. *Taurida Scientific Herald*, 138, 193-201. doi: 10.32782/2226-0099.2024.138.24.

[20] Totskyi, V.M., Hanhur, V.V., & Poliakov, I.A. (2024). Yield and quality of seed of sunflower hybrids (*Helianthus annuus L.*) depending on the fertilizer system. *Scientific Progress & Innovations*, 27(3), 5-11. doi: 10.31210/spi2024.27.03.01.

[21] Trembitska, O., Sorochuk, M., Serhiienko, T., Zinkevych, V., & Konovchuk, M. (2021). Sunflower productivity at various norms of mineral fertilizers. *Science of Europe*, 2(82), 12-14. doi: 10.24412/3162-2364-2021-82-2-12-14.

[22] Zhygailo, O.L., Volvach, O.V., Tolmachova, A.V., & Kostiukievych, T.K. (2021). The influence of climate change on sunflower yield in the Northern Steppe of Ukraine: Analysis and forecast. *Bulletin of Poltava State Agrarian Academy*, 1, 180-186. doi: 10.31210/visnyk2021.01.22.

Оцінка агрометеорологічних умов вирощування гібридів соняшнику

Леся Гарбар
Кандидат сільськогосподарських наук, доцент
Національний університет біоресурсів і природокористування України
03041, вул. Героїв Оборони, 15, м. Київ, Україна
https://orcid.ord/0000-0003-4249-0434
Максим Ванджура
Аспірант
Національний університет біоресурсів і природокористування України
03041, вул. Героїв Оборони, 15, м. Київ, Україна
https://orcid.org/0009-0001-6372-0641

Анотація. Мета досліджень полягала у аналізі погодних умов періоду вегетації, їх відповідності морфобіологічним особливостям гібридів та виявленні більш адаптованих гібридів соняшнику для регіону проведення досліджень. Дослідження проводили впродовж 2022-2024 рр. в умовах Тернопільської області. Аналіз агрометеорологічних показників років досліджень показав значну відмінність періодів вегетації між собою, як за аналізу температурних показників, так і сумарної кількості опадів щомісячно. За результатами температурних показників виявлено їх перевищення відносно середніх багаторічних даних. Аналіз погодних умов регіону проведення досліджень, свідчить про придатність умов для вирощування гібридів соняшнику всіх груп стиглості, які ми вивчали за тепловими ресурсами та забезпеченістю вологою. Сума активних температур за період квітень–вересень становила 3162,1 °С (біологічний мінімум 5 °С, за суми ефективних температур – 2263,2 °С. За біологічного мінімуму 10 °С показники відповідно склали 2977,1 °С та 1409,1 °С. За зазначений період було отримано і найвищу суму теплових одиниць – 3642,4 °С. Сума теплових одиниць за період травень-вересень відповідала показнику 3433,4 °С. запаси вологи у метровому шарі ґрунту залежали від погодних умов року та змінювалися у розрізі років від Коефіцієнт водоспоживання для гібридів ранньої групи стиглості за впливу добрив змінювався від 1173 до 1012 м3/т на 1 т насіння, середньоранньої – 1171-1017 та середньостиглої – 1100-989 м3/т на 1 т насіння. Кореляційний аналіз між показниками урожайності соняшнику та запасами вологи в ґрунті показав пряму кореляційну залежність із коефіцієнтом кореляції 0,8456. Результати дослідження можна використати для оптимізації строків сівби та збирання врожаю відповідно до прогнозованих агрометеорологічних умов

Ключові слова: *Helianthus annuus*; температурні показники; вологозабезпеченість; теплові одиниці; група стиглості

Received 22.04.2025 Revised 30.07.2025 Accepted 23.09.2025

Vol. 21, No. 5
2025

Scientific Reports of the National University of Life and Environmental Sciences of Ukraine

Journal homepage: https://scireports.com.ua/en

UDC 514.18

Doi: 10.31548/dopovidi/5.2025.114

Calculation of a gravitational screw chute with an axial cross-section curve defined by an explicit equation

Serhii Pylypaka
Doctor of Technical Sciences, Professor
National University of Life and Environmental Sciences of Ukraine
03041, 15 Heroiv Oborony Str., Kyiv, Ukraine
https://orcid.org/0000-0002-1496-4615

Tetiana Volina*
Doctor of Technical Sciences, Associate Professor
National University of Life and Environmental Sciences of Ukraine
03041, 15 Heroiv Oborony Str., Kyiv, Ukraine
https://orcid.org/0000-0001-8610-2208

Victor Nesvidomin
Doctor of Technical Sciences, Professor
National University of Life and Environmental Sciences of Ukraine
03041, 15 Heroiv Oborony Str., Kyiv, Ukraine
https://orcid.org/0000-0002-1495-1718

Vitaliy Babka
PhD in Technical Sciences, Associate Professor
National University of Life and Environmental Sciences of Ukraine
03041, 15 Heroiv Oborony Str., Kyiv, Ukraine
https://orcid.org/0000-0003-4971-4285

Taras Pylypaka
PhD in Technical Sciences, Associate Professor
National University of Water and Environmental Engineering
33028, 11 Soborna Str., Rivne, Ukraine
https://orcid.org/0009-0000-5582-1859

Abstract. Screw gravity chutes are used for energy-free transportation of cargo and gravitational separation of ores, which necessitates an optimal combination of design parameters of the working surface, speed of movement, and compactness of the trajectory. The aim of the work was to analytically describe the movement of a cargo along a screw surface, given by the curve of its axial

Suggested Citation:
Pylypaka, S., Volina, T., Nesvidomin, V., Babka, V., & Pylypaka, T. (2025). Calculation of a gravitational screw chute with an axial cross-section curve defined by an explicit equation. *Scientific Reports of the National University of Life and Environmental Sciences of Ukraine*, 21(5), 114-128. doi: 10.31548/dopovidi/5.2025.114.

*Corresponding author

cross-section, under the action of its own weight, using the example of a material particle. Methods of classical mechanics, differential surface theory and numerical methods were used to solve the problem. The main results of the study were based on the fact that after stabilising its motion, the material particle begins to slide along the surface at a constant speed and a constant distance from the axis of the helical surface, taking into account the shape of the curve of its axial cross-section. It was established that the equation of this curve may include constant values that affect its shape, i.e., the kinematic parameters of the particle. This made it possible to find the required values of the constants to ensure the specified parameters of particle sliding. The differential equations of motion of a particle sliding along a helical surface were compiled in projections on the axes of a stationary coordinate system. A parabola was considered as the curve of the axial cross-section of the surface, the equation of which includes a constant value. The obtained analytical dependencies made it possible to determine the optimal values of the constants in the equation of the axial cross-section curve, which ensured the required sliding speed of the particle and the distance from the axis of the helical surface. This opened up opportunities for designing screw chutes taking into account specific technological requirements, in particular for gravitational separation or energy-free transportation of bulk materials. The practical application of the proposed calculations is demonstrated by the example of a parabolic cross-section, which confirms the effectiveness of the method for optimising the kinematic parameters of motion. As a result of the study, expressions for the design of screw gravity chutes were obtained and the influence of the introduced constant on the kinematic parameters of particle sliding was determined

Keywords: sliding velocity; gravitational forces; reactions; friction; gravitational transportation

Introduction

Screw gravity chutes are widely used for energy-free transportation of bulk and piece goods, as well as in the mining industry for mineral enrichment by gravity separation. Their use reduces energy consumption and increases the reliability of transport systems, but the efficiency of such chutes depends largely on the design parameters of the working surface, the speed of the material and its sliding trajectory. Incorrectly selected geometric characteristics can lead to damage to the cargo or loss of separation efficiency. The shape of the axial cross-section of the screw surface plays a special role, as it determines the kinematic parameters of particle movement, its speed and distance from the axis. The selection and analytical justification of these parameters is a pressing issue, as it ensures the reliability of transportation and the stability of technological processes without additional energy costs.

Screw surfaces are the subject of research by scientists in many fields. V. Bulgakov *et al.* (2023) investigated the power and load parameters of flexible screw conveyors, in particular for the transportation of agricultural materials. The authors found that optimising the geometric parameters of the screw and the operating mode can significantly reduce energy consumption and increase transport productivity. This is especially relevant for systems that work with bulk materials, where it is important to avoid clogging and wear of equipment. W. Yu *et al.* (2022) simulated the transportation of concrete by a screw conveyor using the discrete element method. The authors analysed the influence of the screw angle, rotation speed and material properties on transportation efficiency. The study showed that incorrect selection of screw surface parameters can lead to component segregation or increased energy consumption. The results of this study are

important for construction and building materials production, where dosing accuracy and mixture homogeneity are critical.

Scientists T. Lahari *et al.* (2022) analysed the parameters of a single-screw extruder for plastic processing. The authors studied the influence of temperature, screw rotation speed and channel geometry on the quality of the extruded material. The study showed that optimising these parameters improves melt homogeneity and reduces defects in the final product. T. Senfter *et al.* (2024) investigated the effectiveness of a screw press for atypical substrates such as manure and organic waste. They found that the performance of the press depends significantly on the moisture content and composition of the substrate, as well as on the design features of the press, in particular the angle of the screw and the size of the filter holes. The study emphasised the importance of adapting equipment to specific operating conditions, which is particularly relevant for agriculture and bioenergy. Similar results regarding the effectiveness of using screw elements to optimise energy consumption were obtained in a study by H. Parlamış *et al.* (2021), which conducted an experimental analysis of a solar air collector with a screw insert. This highlights the versatility of screw surfaces as an energy-saving solution in various industries.

Researchers S. Fu *et al.* (2023) analysed the factors that influence the efficiency of separation by screw presses, in particular for the treatment of suspensions and slurries. The authors found that the key parameters are screw rotation speed, outlet pressure, and solid phase content in the suspension. The authors proposed a mathematical model that allows predicting the press performance based on these parameters, which is important for optimising dewatering processes in industry. D. Mondal (2020a; 2020b) presented a methodological approach to the design of an experimental laboratory screw conveyor, taking into account two types of working surface coating. The author compared the productivity of conveyors with smooth and corrugated coatings and demonstrated that corrugated coatings reduce material slippage and increase transport efficiency. The study also included an analysis of the effect of the conveyor angle on its productivity, which is important for the design of transport systems in confined spaces.

S. Mirzaei & L. Shen (2021) optimised water utilisation in a screw press for paper production. The study investigated the effect of pressure, screw rotation speed and fibre concentration on the efficiency of pulp dewatering. The study showed that optimal parameters can reduce energy consumption and improve the quality of pressing, which is important for the paper industry. V. Bulgakov *et al.* (2022) studied the dynamic loads on a sectional flexible screw conveyor during the transportation of agricultural materials. They found that uneven loading and vibrations can lead to premature equipment wear, so they proposed methods to reduce dynamic loads by optimising the conveyor design. S. Moorthi *et al.* (2022) conducted a dynamic analysis of a single-screw conveyor for specific industrial needs, in particular for transporting abrasive materials. The authors investigated the effect of rotation speed, angle of inclination, and screw material on vibration levels and energy consumption. The study showed that optimising these parameters reduces equipment wear and improves performance. Z. Chen *et al.* (2024) investigated the effect of bone density on the screw's ability to fix in orthopaedic surgery. The authors found that the optimal screw design and material selection depend on local bone density, which is particularly important for ensuring implant stability.

The aim of the work was to analytically describe the movement of a load along a screw surface, given by the curve of its axial cross-section in the form of a parabola, under the action of its own weight, using the example of a material particle. The objectives of the study were to compile differential equations of particle sliding, solve them using numerical methods, and find dependencies between particle sliding parameters and the shape of the curve after movement stabilisation.

Materials and Methods

The research methods were based on the principles of mechanics and differential geometry of surfaces. Numerical integration was performed using the Simulink dynamic modelling package of the MatLab software product. The differential equation of particle motion in vector form was as follows: $m\bar{w} = \bar{F}$, where m – the mass of the particle, $\bar{w}$ – the acceleration vector, $\bar{F}$ – the total vector of forces applied to the particle. The simplest case is the free fall of a particle, in which the applied force was the force of its own weight, as well as the force of air resistance. If the particle moved along the surface, then there was also a reaction force and a friction force dependent on it. The force of gravity was directed downwards, the reaction force was normal to the surface, and the friction and air resistance forces were in the opposite direction to the particle's velocity. The friction force F_f (Fig. 1b) was the product of the friction coefficient f and the reaction force R: $F_f = fR$.

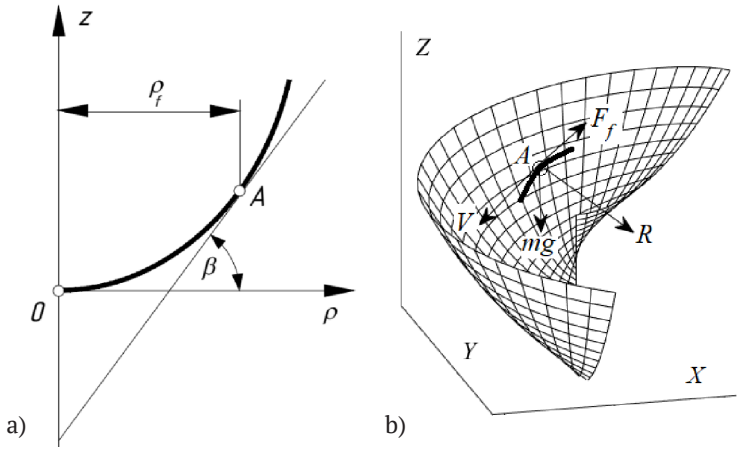

Figure 1. *Graphic illustrations of the formation of a helical surface*

Note: a) curve of the axial cross-section of the helical surface; b) helical surface formed by a combination of rotational and translational movements along the axis; 0z, 0ρ, X, Y, Z – coordinate axes, units of measurement– m; A – current point on the surface; β – angle of inclination of the tangent to the curve of the axial cross-section of the surface at the current point to the horizontal plane of projections; V – direction of the particle's sliding velocity vector; mg – weight force; R – surface reaction; Ff –friction force vector

Source: developed by the authors

Air resistance was neglected because it is insignificant at low speeds. The differential equations of motion of a point on a surface in projections onto a stationary coordinate system had the form:

$$\begin{aligned} mx'' &= -fRT_x + RN_x; \\ my'' &= -fRT_y + RN_y; \\ mz'' &= -fRT_z + RN_{z-mg}, \end{aligned} \qquad (1)$$

where R – surface reaction force; T_x, T_y, T_z – projections of the unit vector tangent to the trajectory; N_x, N_y, N_z – projections of the unit vector normal to the surface along the trajectory, x'', y'', z'' – projections of particle acceleration. The surface was defined by parametric equations in terms of two independent variables ρ and α: $X = X(\rho, \alpha)$, $Y = Y(\rho, \alpha)$, $Z = Z(\rho, \alpha)$. The variables ρ and α were dependent on time t: $\rho = \rho(t)$ and $\alpha = \alpha(t)$. In this case, the surface equation was transformed into the equation of a line on it. This line was the sought-after trajectory, which became known when the dependencies $\rho = \rho(t)$ and $\alpha = \alpha(t)$ were found after solving the system of equations (1).

Results

The curve of the axial cross-section of the surface is given by the equation in explicit form: $z = z(\rho)$ (Fig. 1a). If such a curve is rotated around the z-axis, a surface of revolution is formed. In addition to the rotational motion, the curve is given a translational motion along the z-axis, and the relationship between the angle of rotation α and the translational motion is linear: $z = b\alpha$ (Fig. 1b). The constant b is a screw parameter. In this case, the parametric equations of the surface are written as:

$$\begin{aligned} X &= \rho\cos\alpha; \\ Y &= \rho\sin\alpha; \\ Z &= z(\rho) - b\alpha. \end{aligned} \qquad (2)$$

The sign '–' in the last equation (2) means that when the curve rotates around the z-axis, it simultaneously moves downwards. Then the tangent to the trajectory will also be directed in accordance with the movement of the particle along the surface, i.e. towards its descent. With the dependencies $\rho = \rho(t)$ and $\alpha = \alpha(t)$ established, the surface equations (2) are transformed into the equations of the line on it. To distinguish between the surface equations and the analogous line equations on it, the coordinates of the surface points are denoted by capital letters "X", "Y", "Z", and the coordinates of the line points on the surface are denoted by lowercase letters "x", "y", "z". The projections of the particle's sliding velocity are found by differentiating equations (2), taking into account that $\rho = \rho(t)$ and $\alpha = \alpha(t)$. In this case, the derivative $z(\rho)$ with respect to the variable ρ is denoted by the corresponding subscript, and the derivatives with respect to time t are denoted without an index:

$$\begin{aligned} x' &= \rho'\cos\alpha - \rho\alpha'\sin\alpha; \\ y' &= \rho'\sin\alpha + \rho\alpha'\cos\alpha; \\ z' &= z_\rho'\rho' - b\alpha'. \end{aligned} \qquad (3)$$

The magnitude of the particle's sliding velocity is the vector sum of the projections (3):

$$V = \sqrt{x'^2 + y'^2 + z'^2} = \\ = \sqrt{\alpha'^2(\rho^2 + b^2) - 2b\rho'\alpha' z_\rho' + \rho'^2\left(1 + z_\rho'^2\right)}. \qquad (4)$$

The projections T_x, T_y, T_z of the unit vector tangent to the trajectory can be found by dividing the corresponding projections (3) by the velocity (4):

$$T_x = \frac{\rho'\cos\alpha - \rho\alpha'\sin\alpha}{\sqrt{\alpha'^2(\rho^2+b^2) - 2b\rho'\alpha' z_\rho' + \rho'^2\left(1+z_\rho'^2\right)}}; \\ T_y = \frac{\rho'\sin\alpha + \rho\alpha'\cos\alpha}{\sqrt{\alpha'^2(\rho^2+b^2) - 2b\rho'\alpha' z_\rho' + \rho'^2\left(1+z_\rho'^2\right)}}; \\ T_z = \frac{z_\rho'\rho' - b\alpha'}{\sqrt{\alpha'^2(\rho^2+b^2) - 2b\rho'\alpha' z_\rho' + \rho'^2\left(1+z_\rho'^2\right)}}. \qquad (5)$$

By differentiating expressions (3), the second derivatives of the trajectory equations can be obtained, i.e. the projections of acceleration:

$$\begin{aligned} x'' &= (\rho'' - \rho\alpha'^2)\cos\alpha - (\rho\alpha'' + 2\rho'\alpha')\sin\alpha; \\ y'' &= (\rho'' - \rho\alpha'^2)\sin\alpha + (\rho\alpha'' + 2\rho'\alpha')\cos\alpha; \\ z'' &= z_\rho''\rho'^2 + z_\rho'\rho'' - b\alpha''. \end{aligned} \qquad (6)$$

The coordinates of the vector $\bar{N}$ normal to the surface are defined as the vector product of two vectors tangent to the coordinate lines. The projections of these vectors are the first-order partial derivatives of the surface (2):

$$\begin{aligned} X_\rho' &= \cos\alpha;\ Y_\rho' = \sin\alpha;\ Z_\rho' = z_\rho'; \\ X_\alpha' &= -\rho\sin\alpha;\ Y_\alpha' = \rho\cos\alpha;\ Z_\alpha' = -b. \end{aligned} \qquad (7)$$

In derivatives (7), the lower index denotes the variable by which differentiation occurs. The vector product of vectors (7) is written as:

$$\bar{N} = \begin{vmatrix} X & Y & Z \\ X_\alpha' & Y_\alpha' & Z_\alpha' \\ X_\rho' & Y_\rho' & X_\rho' \end{vmatrix} = \begin{Bmatrix} -b\sin\alpha - \rho z_\rho'\cos\alpha; \\ b\cos\alpha - \rho z_\rho'\sin\alpha; \\ \rho. \end{Bmatrix}. \qquad (8)$$

The normal vector (8) must be reduced to unity. After that, its projections N_x, N_y, N_z will be written as:

$$N_x = -\frac{b\sin\alpha + \rho z_\rho'\cos\alpha}{\sqrt{\rho^2\left(1+z_\rho'^2\right)+b^2}}; \\ N_y = \frac{b\cos\alpha - \rho z_\rho'\sin\alpha}{\sqrt{\rho^2\left(1+z_\rho'^2\right)+b^2}}; \\ N_z = \frac{\rho}{\sqrt{\rho^2\left(1+z_\rho'^2\right)+b^2}}. \qquad (9)$$

It should be noted that the direction of the normal vector can be directed in one or the opposite direction from the surface. This depends on the order of the vectors (7) in the determinant (8). It is necessary to ensure that it coincides with the direction of the reaction force R (Fig. 1b). Since the particle presses down on the surface, the reaction of the surface will be directed upwards. This means that the expression N_z in (9) must be positive. Taking into account expressions (5) and (9), system (1) takes the form:

$$mx'' = -fR\frac{\rho'\cos\alpha-\rho\alpha'\sin\alpha}{\sqrt{\alpha'^2(\rho^2+b^2)-2b\rho'\alpha'z'_\rho+\rho'^2\left(1+z'^2_\rho\right)}} - R\frac{b\sin\alpha+\rho z'_\rho\cos\alpha}{\sqrt{\rho^2\left(1+z'^2_\rho\right)+b^2}};$$

$$my'' = -fR\frac{\rho'\sin\alpha+\rho\alpha'\cos\alpha}{\sqrt{\alpha'^2(\rho^2+b^2)-2b\rho'\alpha'z'_\rho+\rho'^2\left(1+z'^2_\rho\right)}} + R\frac{b\cos\alpha-\rho z'_\rho\sin\alpha}{\sqrt{\rho^2\left(1+z'^2_\rho\right)+b^2}};$$

$$mz'' = -fR\frac{z'_\rho\rho'-b\alpha'}{\sqrt{\alpha'^2(\rho^2+b^2)-2b\rho'\alpha'z'_\rho+\rho'^2\left(1+z'^2_\rho\right)}} + R\frac{\rho}{\sqrt{\rho^2\left(1+z'^2_\rho\right)+b^2}} - mg. \quad (10)$$

Substituting the acceleration projections from (6) into (10) gives a system of three differential equations with unknown dependencies $\rho=\rho(t)$, $\alpha=\alpha(t)$ amd $R=R(t)$. The resulting system must be solved with respect to the second derivatives ρ'', α'' and the reaction force R, since this notation allows for numerical integration of the system. After that, system (10) takes the form:

$$\alpha'' = \frac{b\left(g+\alpha'^2\rho z'_\rho+\rho'^2z''_\rho\right)-2\alpha'\rho'\rho\left(1+z'^2_\rho\right)}{A^2} - \frac{f\alpha'B}{AV};$$

$$\rho'' = \rho\frac{b^2\alpha'^2-2b\alpha'\rho'z'_\rho+\rho[\alpha'^2\rho-z'_\rho(g+\rho'^2z''_\rho)]}{A^2} - \frac{f\rho'B}{AV};$$

$$R = \frac{mB}{A}, \quad (11)$$

where A, B, V denote repeated expressions. Among them is the velocity V, the expression for which is given in (4), as well as others, which have the following form: $A=\sqrt{\rho^2\left(1+z'^2_\rho\right)+b^2}$, $B=\rho g+\alpha'^2\rho^2 z'_\rho+2b\alpha'\rho'+\rho\rho'^2z''_\rho$.

When a particle slides along a screw surface with a constant pitch, its motion stabilises after a transition period. The particle moves at a constant speed V, its angular velocity of rotation around the surface axis $\alpha'=\omega$ is also constant, and the distance ρ from the surface axis is also constant. It follows that: $\alpha''=0, \rho''=\rho'=0$. Substituting these values of the variables into the first equation of system (11) gives the result:

$$0 = \frac{(bV-f\alpha'\rho A)(g+\alpha'^2\rho z'_\rho)}{AV}. \quad (12)$$

In equation (12), only one expression in brackets can be equal to zero with a difference in terms. Its solution with respect to b is as follows:

$$b = \frac{\rho}{\sqrt{2}}\sqrt{f^2-1+\sqrt{1+f^4+2f^2\left(1+2z'^2_\rho\right)}}. \quad (13)$$

Equation (13) shows that the distance ρ from the axis to the particle's sliding trajectory after stabilisation of motion depends on the friction coefficient f and the derivative of the curve equation $z=z(\rho)$ with respect to the variable ρ. But this derivative is equal to the tangent of the angle β of inclination of the tangent to the curve: $z'_\rho=tg\beta$ At a given angle β and a known friction coefficient f, the motion of a particle along a screw surface will be analogous to the motion along a helicoid formed by a set of straight generatrices inclined at an angle β. In other words, the curve of the axial cross-section of the helicoid will be a straight line inclined at an angle β. With a known coefficient f, the distance of the particle's sliding along the helicoid from its axis is uniquely determined (in Fig. 1a, it is marked ρ_f). With a curved cross-section, this distance is also uniquely determined, but when the coefficient f changes, the distance ρ_f for the helicoid and the helical surface will be different. In addition, using the constant (constants) included in the equation $z=z(\rho)$ it is possible to change the shape of the curve.

Substituting into the second equation of system (11) $\rho'' = \rho' = 0$ gives the expression:

$$0 = \alpha'^2 (\rho^2 + b^2) - g\rho z'_\rho. \quad (14)$$

From (14), an angular velocity $\alpha' = \omega$ can be determined for the rotation of a particle around the axis of the screw surface:

$$\alpha' = \omega = \sqrt{\frac{\rho g z'_\rho}{\rho^2 + b^2}}. \quad (15)$$

From expression (4), substituting it into (15) at $\rho' = 0$, the sliding velocity of the particle can be found:

$$V = \sqrt{\rho g z'_\rho}. \quad (16)$$

The dependencies obtained (13), (15) and (16) are sufficient for calculating the screw pitch. Here is an example. The curve of the axial cross-section of the screw surface is taken to be a parabola $z = a\rho^2$. Thus $z'_\rho = 2a\rho$, $z''_\rho = 2a$. According to (16):

$$V = \rho\sqrt{2ag}, \text{ from } a = \frac{V^2}{\sqrt{2g\rho^2}}. \quad (17)$$

Thanks to the constant a, it is possible to set the desired sliding speed V of the particle at a given distance ρ from the surface axis. To ensure high-quality performance of the technological process, the speed must be limited. Let $V = 2$ *m/s*, $\rho = 0.4$ *m*. From the second expression (17): $a = 1.27$. From expression (13), with a known coefficient $f = 0.3$, the screw parameter b can be found: $b = 0.16$. Two constants a and b are sufficient to construct the surface according to equations (2). The surface with the particle's motion trajectories plotted is shown in Figure 2a. The trajectories of the particle after stabilisation are shown by thick lines for the corresponding friction coefficient f. The value ρ = 0.4 m corresponds to the friction coefficient $f = 0.3$. For a particle with a different friction coefficient, for example, $f = 0.2$, the trajectory will be different for this surface. Finding it using the obtained dependencies is difficult and involves cumbersome expressions and numerical calculations. However, the trajectory can be constructed using numerical integration of system (11). In Figure 2b, the dashed line shows the trajectory of a particle that is fed onto the surface at zero velocity at a distance of *0.1 m* from its axis.

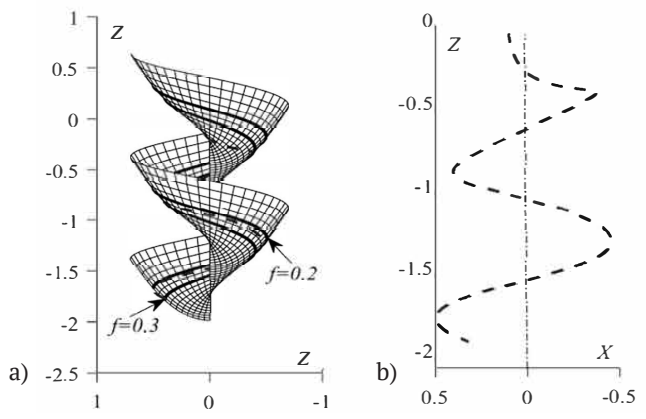

Figure 2. *Graphical illustrations of particle motion on a surface*
Note: a) frontal projection of the surface with motion trajectories marked; b) particle motion trajectory during acceleration; X, Z – coordinate axes, units of measurement – m, f – friction coefficient
Source: developed by the authors

From the analysis of Figure 2b, it can be concluded that the distance ρ increases as the particle slides. This is clearly demonstrated by the graph of the change in distance ρ over 4

seconds from the start of movement (Fig. 3a). It shows that as the motion stabilises, the distance approaches a steady value of $\rho = 0.5$ *m*. Substituting $f = 0.2$ and $\rho = 0.5$ m into expression (13) gives the result: $b = 0.16$, i.e. the value of the screw parameter for which this surface is constructed. In Figure 2a, for $f = 0.2$, the trajectory after stabilisation of motion and the trajectory of motion are plotted as a dashed line during the transition period (in Figure 2a, it is plotted separately).

Figure 3b shows that as the motion stabilises, the particle velocity approaches a value of $V = 2.5$ *m/s*. From the first formula (17) with $\rho = 0{,}5$ *m* and the previous value of a $a = 1.27$ the same velocity value is calculated.

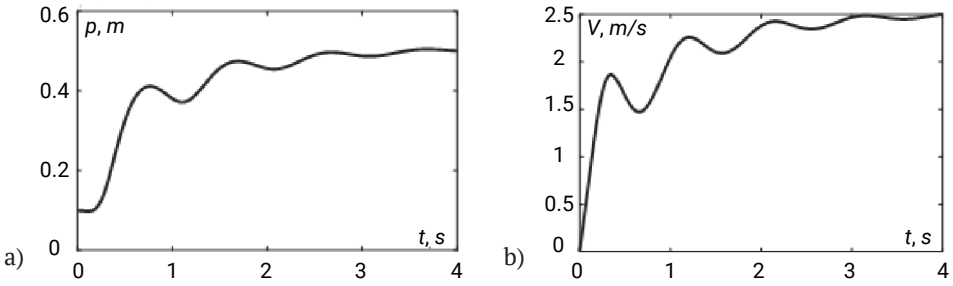

Figure 3. *Graphs of the kinematic parameters of the particle in the transition period*
Note: a) graph of the change in the distance ρ of the trajectory from the surface axis; b) graph of the change in the sliding velocity V; ρ – current distance of the particle from the axis of the helical surface during sliding; V – sliding velocity; t – time
Source: developed by the authors

Discussion

It is advisable to compare the results obtained with those obtained by T.A. Kresan (2020). The author describes that the helical surface is formed by a set of straight generatrices inclined at a constant angle to the horizontal plane, i.e. it is an oblique closed helicoid. The axial cross-section is a straight line that cannot change its shape. T.A. Kresan noted that when the straight generatrices of the helicoid are inclined at $\beta = 30°$ and the screw parameter is $b = 0.24$ (these two parameters define the helicoid), a particle with a friction coefficient $f = 0.3$ slides along the surface at a speed $V = 2$ *m/s* at a distance $\rho = 0.7$ *m*. The results presented in the work of T.A. Kresan (2020) can be obtained in the presented study as a special case. To do this, it is necessary to find the value of the constant a that corresponds to the angle $\beta = 30°$ and $\rho = 0.7$ m. Based on the fact that $z'_\rho = \mathrm{tg}\beta = 0.577$, i.e. for the parabola $2a\rho = 0.577$, it is determined that: $a = 0.41$. Using formula (13), the screw parameter b can be obtained at $f = 0.3$ and $\rho = 0.7$ m: $b = 0.24$. Using the first formula (17), the sliding velocity of the particle at $\rho = 0.7$ m and $a = 0.41$ can be determined: *m/s*. Thus, the results obtained fully coincide with the results obtained by T.A. Kresan (2020), which are a special case of the presented study. Due to the curved axial cross-section of the helical surface in the form of a parabola, it is possible to change the constant a so that the velocity remains the same ($V = 2$ *m/s*), but the distance ρ is different (for example, $\rho = 0.2$ *m* as opposed to $\rho = 0.4$ *m* in the previous case). Then, according to the second expression (17), $a = 4.5$. When the shape of the parabola changes, the screw parameter b also changes. It can be found using the formula (13): $b = 0.11$. In this case, the particle's descent speed will be higher, since at a constant speed $V = 2$ *m/s*, the sliding path has decreased due to the reduction in distance ρ and pitch b.

Other scientists, M. Gamtsemlidze *et al.* (2024), investigated the optimal parameters of a screw separator for coal slurry enrichment,

focusing on the influence of the axial cross-section shape on separation efficiency. They showed that curved cross-sections (e.g., elliptical) improve particle distribution by density compared to straight ones. The present study confirms these findings: it also demonstrates that a curved cross-section (parabola) provides greater flexibility in controlling the trajectory and velocity of particles. However, unlike M. Gamtsemlidze *et al.* (2024), who focused on separation properties, this study focuses on the analytical description of motion and the optimisation of kinematic parameters, which expands the possibilities for designing screw chutes for transportation. V. Hud *et al.* (2023) proposed a multifunctional screw conveyor separator for agricultural materials, where the key was to analyse the effect of screw geometry on separation efficiency. They found that variable screw geometry (e.g., variable pitch) can increase productivity by 15-20%. The current study complements these results: it shows that even with a fixed pitch but a curved cross-section, a similar effect can be achieved by changing the shape of the curve (e.g., a parabola). This is especially important for systems where changing the pitch is technically difficult. It is worth noting that similar approaches to optimising mineral processing are also demonstrated by recent studies on the extraction of rare elements. For example, J. Corchado-Albelo & L. Alagha (2024) showed that the mineralogical characteristics of copper tailings determine the efficiency of tellurium extraction, which is consistent with the idea of adapting the design of screw surfaces to the properties of the source material.

O. Lyashuk *et al.* (2019) developed a mathematical model for transporting bulk materials using a tubular screw conveyor, focusing on the impact of the conveyor angle and friction coefficient on productivity. They showed that the optimal angle depends on the properties of the material. The present study extends this approach: not only is the angle of inclination taken into account (via $tg\beta$ in the curve equation), but it is also demonstrated how the cross-sectional shape (parabola) affects the stabilisation of particle motion. This allows for more accurate design of systems for materials with different rheological properties. Y. Indartono *et al.* (2019) and O. Fakayode *et al.* (2019) devoted their work to optimising screw presses for extracting oil from plant raw materials. Y. Indartono *et al.* (2019) investigated the influence of screw geometry on the efficiency of oil extraction from calophyllum seeds, while O. Fakayode *et al.* (2019) optimised the parameters of the press for moringa seeds. Both studies emphasise that the optimal screw geometry depends on the moisture content and particle size of the raw material. The present study complements these findings by showing that for materials with different friction coefficients (which depend on moisture content), a curved cross-section shape can be selected to ensure a stable sliding speed. This is particularly relevant for presses, where it is important to avoid clogging or uneven material movement.

Researchers B. El Idrissi *et al.* (2020) and T. Eaves *et al.* (2020) simulated the process of wood pulp dewatering in screw presses, focusing on the effect of pressure and moisture on productivity. The authors showed that the optimal pressure depends on the content of fine fibres in the suspension. T. Eaves *et al.* (2020) investigated the dewatering of saturated suspensions, emphasising the role of the rheological properties of the material. The current study extends these findings: for materials with different rheological characteristics (which affect the friction coefficient f), an appropriate cross-sectional curve shape can be selected to optimise the speed and trajectory of movement. This is particularly important for presses, where uniform dewatering must be ensured without loss of productivity. E. Loranger *et al.* (2019) investigated the effect of dewatering parameters (rotation speed, pressure) on the performance of a screw press for pulp. They showed that the optimal parameters depend on the concentration of fibres and their length. The present study complements these results: it shows that the shape of the curved cross-section (e.g. parabola) allows

additional control of the kinematic parameters, which is particularly important for materials with unstable properties (e.g. variable moisture content).

P.G. Chitte *et al*. (2022) developed a methodology for designing a screw press for dewatering, focusing on the influence of filter hole geometry and screw angle. The authors showed that the optimal geometry depends on the properties of the slurry. The present study extends this approach: the shape of the axial cross-section (parabola) can also be used as an optimisation tool, especially for materials that are difficult to dewater due to their high content of fine particles. B. El Idrissi *et al*. (2019) investigated the parameters of wood pulp dewatering in a screw press, focusing on the influence of operating parameters – such as screw rotation speed, outlet pressure and pulp properties (in particular, fine fibre content and moisture content) – on process efficiency. The authors showed that the optimal dewatering conditions depend on the rheological characteristics of the material: for example, for pulp with a high content of fine fibres, it is necessary to increase the outlet pressure to achieve the desired dryness of the press cake. They also emphasised that the screw rotation speed must be adapted to the viscosity of the pulp to avoid excessive energy consumption or uneven dewatering. The presented study complements these findings by proposing an analytical approach to controlling the kinematic parameters of particle movement on screw surfaces. While B. El Idrissi *et al*. (2019) focused on experimentally determining the optimal parameters for specific types of pulp, the present study shows how the shape of the curved axial cross-section (e.g., a parabola) can be used to more precisely control the trajectory and speed of particle movement. For example, the paper demonstrates that by changing the constant a in the parabolic curve equation $z = a\rho^2$ it is possible to ensure a stable particle sliding speed even when the friction coefficient f, which depends on the moisture content and composition of the material, changes. This allows screw surfaces to be adapted to different types of pulp without the need to change the screw design, which is an important advantage for industrial applications where material properties may vary. Thus, the presented study extends the results of B. El Idrissi *et al*. (2019), offering an analytical tool for optimising screw surfaces, taking into account not only operating parameters but also the geometry of the axial cross-section, which opens up new opportunities for improving dewatering efficiency.

The study made it possible to build an analytical model of particle motion along a screw surface with a curved axial cross-section and to verify its adequacy using a parabola as an example. The obtained dependencies allow determining the sliding speed and the distance of the particle from the surface axis after stabilisation of motion, as well as selecting the necessary surface parameters for the given operating conditions. The proposed approach expands the possibilities of controlling the kinematic characteristics of motion compared to classical models for an oblique helicoid and provides a more accurate calculation of helical descents. The results obtained allow not only to analytically describe the motion of a particle along a helical surface with a curved axial cross-section, but also to optimise the kinematic parameters for specific technological conditions.

Conclusions

A screw chute can be formed by anoblique helicoid with a straight line as its axial cross-section, as well as by a non-linear helical surface with a curved axial cross-section. Differential equations of motion of a particle along a helical surface with a curved cross-section, the shape of which is given by an explicit equation, have been derived. Using a parabola as an example of an axial cross-section, the differential equations were numerically integrated and the patterns of change in kinematic parameters during the transition period were obtained. Formulas were derived that relate the shape of the axial cross-section curve (given by the equation $z = a\rho^2$ for a parabola) to the kinematic parameters of the particle – the

sliding velocity V and the distance from the axis ρ. For example, for a parabolic shape with a constant $a = 1.27$ and a distance $\rho = 0.4$ m, a sliding velocity $V = 2$ *m/s* was obtained, which meets the requirements of many industrial applications. Analytical dependencies were derived that give numerical values of these parameters after the particle's motion stabilises. Using numerical integration of a system of differential equations, it was shown that after a transition period (about 3-4 seconds), the particle moves at a constant speed and distance from the axis. For example, for a particle with a friction coefficient $f = 0.2$, which is fed to the surface with zero velocity at a distance of *0.1 m* from the axis, the velocity stabilises at $V = 2.5$ *m/s*, and the distance ρ approaches *0.5 m*. It is shown that the curved axial cross-section of the helical surface provides broader opportunities for controlling the kinematic parameters of particle motion compared to a straight cross-section. In the article, this is demonstrated by comparing the known results of particle motion along an oblique helicoid, which is a special case of the studies presented, with the results obtained. It is shown that at a friction coefficient $f = 0.3$ and a distance $\rho = 0.7$ m, the screw parameter is $b = 0.24$, which completely coincides with the results of previous studies for a straight cross-section. However, with a curved cross-section, it is possible to change the constant a so as to maintain a speed of $V = 2$ *m/s* at a different distance ρ. This indicates greater flexibility in the design of helical descents.

During the study, an analytical model of the motion of a material particle along a screw surface with a curved axial cross-section was developed, which allows optimising the kinematic parameters for specific technological conditions. Unlike traditional approaches, where screw surfaces are considered as oblique helicoids with a straight axial cross-section, it has been shown that the use of curved cross-sections significantly expands the possibilities for controlling particle motion. Prospects for further research lie in the experimental verification of the obtained analytical dependencies for real materials and in the extension of the model to the case of a variable friction coefficient.

Acknowledgements

The authors of the article express their gratitude to the soldiers of the Armed Forces of Ukraine, whose bravery allows the scientists of Ukraine to continue their research.

Funding

None.

Conflict of Interest

None.

References

[1] Bulgakov, V., Pascuzzi, S., Adamchuck, V., Olt, J., Ruzhylo, Z., Trokhnaniak, O., Santoro, F., Arak, M., Nowak, J., & Beloev, H. (2023). Research into power and load parameters of flexible screw conveyors for transportation of agricultural materials. In *Farm machinery and processes management in sustainable agriculture* (vol. 289, pp. 61-75). Cham: Springer International Publishing. doi: 10.1007/978-3-031-13090-8_6.

[2] Bulgakov, V., Trokhnaniak, O., Adamchuck, V., Chernovol, M., Korenko, M., Dukulis, I., & Ivanovs, S. (2022). A study of dynamic loads of a flexible sectional screw conveyor. *Acta Technologica Agriculturae*, 25(3), 131-136. doi: 10.2478/ata-2022-0020.

[3] Chen, Z., Chen, Y., Zhou, J., He, Y., & Li, J. (2024). The bony density of the pedicle plays a more significant role in the screw anchorage ability than other regions of the screw trajectory. *Orthopaedic Surgery*. doi: 10.1111/os.14299.

[4] Chitte, P.G., Tapsi, P., & Deshmukh, B. (2022). Design and development of dewatering screw press. In *Recent advances in manufacturing modelling and optimization* (pp. 569-578). Singapore: Springer. doi: 10.1007/978-981-16-9952-8_48.

[5] Corchado-Albelo, J., & Alagha, L. (2024). Tellurium enrichment in copper tailings: A mineralogical and processing study. *Minerals*, 14(8), article number 761. doi: 10.3390/min14080761.

[6] Eaves, T.S., Paterson, D.T., Hewitt, D.R., Balmforth, N.J., & Martinez, D.M. (2020). Dewatering saturated, networked suspensions with a screw press. *Journal of Engineering Mathematics*, 120, 1-28. doi: 10.1007/s10665-019-10029-3.

[7] El Idrissi, B., Loranger, É., & Lanouette, R. (2020). Modelling of dewatering wood pulp in a screw press using statistical and multivariate analysis. *BioResources*, 15, 5899-5912. doi: 10.15376/biores.15.3.5899-5912.

[8] El Idrissi, B., Loranger, É., Lanouette, R., Bousquet, J.P., & Martinez, M. (2019). Dewatering parameters in a screw press and their influence on the screw press outputs. *Chemical Engineering Research and Design*, 152, 300-308. doi: 10.1016/j.cherd.2019.10.001.

[9] Fakayode, O.A., & Ajav, E.A. (2019). Development, testing and optimization of a screw press oil expeller for moringa (Moringa oleifera) seeds. *Agricultural Research*, 8, 102-115. doi: 10.1007/s40003-018-0342-6.

[10] Fu, S., Dou, B., Zhang, X., & Li, K. (2023). An interactive analysis of influencing factors on the separation performance of the screw press. *Separations*, 10, article number 245. doi: 10.3390/separations10040245.

[11] Gamtsemlidze, M., Enageli, R., & Oniani, M. (2024). Evaluation of the optimal parameters of the coal silt enrichment process on the screw like separator. *Works of Georgian Technical University*, 1(531), 267-275. doi: 10.36073/1512-0996-2024-1-267-275

[12] Hud, V., Lyashuk, O., Hevko, I., Ungureanu, N., Vlăduț, N.-V., Stashkiv, M., Hevko, O., & Pik, A. (2023). Enhancement of agricultural materials separation efficiency using a multi-purpose screw conveyor-separator. *Agriculture*, 13(4), article number 870. doi: 10.3390/agriculture13040870.

[13] Indartono, Y.S., Heriawan, H., & Kartika, I.A. (2019). Innovative and flexible single screw press for the oil extraction of Calophyllum seeds. *Research in Agricultural Engineering*, 65, 91-97. doi: 10.17221/85/2018-RAE.

[14] Kresan, T.A. (2020). Calculation of gravitation descent formed by surface of skew closed helicoid. *Machinery & Energetics*, 11(2), 49-57.

[15] Lahari, T.R., & Srinivas Sharma, G. (2022). Parametric analysis of single screw extruder for processing of re-cycled plastics. *International Journal of Current Engineering and Technology*, 12(1), 9-14.

[16] Lyashuk, O., Vovk, Y., Sokil, B., Klendii, V., Ivasechko, R., & Dovbush, T. (2019). Mathematical model of a dynamic process of transporting a bulk material by means of a tube scraping conveyor. *Agricultural Engineering International: CIGR Journal*, 21(1), 74-81.

[17] Mirzaei, S., & Shen, L. (2021). Water disposal minimization of a screw press in the tissue manufacturing process. *The International Journal of Advanced Manufacturing Technology*, 115, 2659-2667. doi: 10.1007/s00170-021-07247-4.

[18] Mondal, D. (2020a). A short spiral conveyor using cut flight screw with two different trough cover of different height – a comparative study. In *Techno-societal 2020* (pp. 695-703). Cham: Springer. doi: 10.1007/978-3-030-69925-3_67.

[19] Mondal, D. (2020b). Design consideration of a laboratory size screw conveyor with variable speed for experimentation purpose – a methodological approach. In *Techno-societal 2020* (pp. 705-714). Cham: Springer. doi: 10.1007/978-3-030-69925-3_68.

[20] Moorthi, S., Megaraj, M., Nagarajan, L., Karthick, A., Bharani, M., & Patil, P.P. (2022). Dynamic analysis and fabrication of single screw conveyor machine. *Advances in Material Science and Engineering*, 10, article number 812754. doi: 10.1155/2022/3843968.

[21] Parlamış, H., Özden, E., & Büker, M.S. (2021). Experimental performance analysis of a parabolic trough solar air collector with helical-screw tape insert: A comparative study. *Sustainable Energy Technologies and Assessments*, 47(3), article number 101562. doi: 10.1016/j.seta.2021.101562.

[22] Senfter, T., Schweiggl, I., Berger, M., Mayerl, C., Kofler, T., Kraxner, M., Steffens, A., & Pillei, M. (2024). The dewatering performance of a compact screw press manure separator for non-typical substrates. *Separations*, 11(1), article number 28. doi: 10.3390/separations11010028.

[23] Yu, W., Zhang, K., Li, D., Zou, D., & Zhang, S. (2022). Numerical modeling of concrete conveying capacity of screw conveyor based on DEM. *Powder Technology*, 29, 361-374. doi: 10.12989/cac.2022.29.6.361.

Розрахунок гравітаційного гвинтового спуску, у якого крива осьового перерізу задана явним рівнянням

Сергій Пилипака
Доктор технічних наук, професор
Національний університет біоресурсів і природокористування України
03041, вул. Героїв Оборони, 15, м. Київ, Україна
https://orcid.org/0000-0002-1496-4615
Тетяна Воліна
Доктор технічних наук, доцент
Національний університет біоресурсів і природокористування України
03041, вул. Героїв Оборони, 15, м. Київ, Україна
https://orcid.org/0000-0001-8610-2208
Віктор Несвідомін
Доктор технічних наук, професор
Національний університет біоресурсів і природокористування України
03041, вул. Героїв Оборони, 15, м. Київ, Україна
https://orcid.org/0000-0002-1495-1718
Віталій Бабка
Кандидат технічних наук, доцент
Національний університет біоресурсів і природокористування України
03041, вул. Героїв Оборони, 15, м. Київ, Україна
https://orcid.org/0000-0003-4971-4285
Тарас Пилипака
Кандидат технічних наук, доцент
Національний університет водного господарства та природокористування
33028, вул. Соборна, 11, м. Рівне, Україна
https://orcid.org/0009-0000-5582-1859

Анотація. Гвинтові гравітаційні спуски використовуються для безенергетичного транспортування вантажів і гравітаційної сепарації руд, що зумовлює необхідність оптимального поєднання конструктивних параметрів робочої поверхні, швидкості руху та компактності траєкторії. Метою роботи був аналітичний опис руху вантажу по гвинтовій поверхні, заданій кривою її осьового перерізу, під дією сили власної ваги на прикладі матеріальної частинки. Для розв'язання було використано методи класичної механіки, диференціальної теорії поверхонь і чисельні методи. Основні результати дослідження ґрунтувались на тому, що після стабілізації руху матеріальна частинка починає ковзати по поверхні зі сталою швидкістю і сталою відстанню від осі гвинтової поверхні з урахуванням форми кривої її осьового перерізу. Встановлено, що до рівняння цієї кривої можуть входити сталі величини, які впливають на її форму, тобто на кінематичні параметри частинки. Це дало можливість знаходити потрібне значення сталих для забезпечення заданих параметрів ковзання частинки. Складання диференціальних рівнянь руху ковзання частинки по гвинтовій поверхні здійснювалось в проєкціях на осі нерухомої системи координат. В ролі кривої осьового перерізу поверхні було розглянуто параболу, до рівняння якої входить стала величина. Отримані аналітичні залежності дозволили визначити оптимальні значення сталих у рівнянні кривої осьового перерізу, що забезпечило необхідну швидкість ковзання частинки та відстань від осі гвинтової поверхні. Це відкрило можливості для проєктування гвинтових спусків

з урахуванням специфічних технологічних вимог, зокрема для гравітаційної сепарації або безенергетичного транспортування сипучих матеріалів. Практичне застосування запропонованих розрахунків продемонстровано на прикладі параболічної форми перерізу, що підтверджує ефективність методу для оптимізації кінематичних параметрів руху. У результаті дослідження отримано вирази для проєктування гвинтових гравітаційних спусків та визначено вплив введеної сталої на кінематичні параметри ковзання частинок

Ключові слова: швидкість ковзання; сили ваги; реакції; тертя; гравітаційне транспортування

Received 20.05.2025 Revised 25.08.2025 Accepted 23.09.2025

Vol. 21, No. 5
2025

Scientific Reports of the National University of Life and Environmental Sciences of Ukraine

Journal homepage: https://scireports.com.ua/en

UDC 621.9:621.76

Doi: 10.31548/dopovidi/5.2025.129

Impact of vibrations on machining quality and tool wear during metal cutting

Oleksandr Bryniuk
Postgraduate Student
Education and Research Institute "Ukrainian Engineering and Pedagogical Academy" of V.N. Karazin Kharkiv National University
61003, 16 Universytetska Str., Kharkiv, Ukraine
https://orcid.org/0009-0007-1546-0922

Yaroslav Hrechaniuk*
Postgraduate Student
Education and Research Institute "Ukrainian Engineering and Pedagogical Academy" of V.N. Karazin Kharkiv National University
61003, 16 Universytetska Str., Kharkiv, Ukraine
https://orcid.org/0009-0000-0070-3396

Abstract. The purpose of this study was to comprehensively assess the effect of vibration load on the wear rate of the cutting tool, the stability of the cutting process, the thermal characteristics of the contact zone, and the quality of the machined surface during milling of metal materials. The experimental part included a comparison of three tool designs: a basic sample without damping, a configuration with a passive damper, and a tool with an adaptive vibration insert. The study was conducted at fixed feed rates, depth of cut, and rotational speed, using vibration analysis, thermal imaging, contact profiling, and dynamometric measurement of cutting forces. According to the results obtained, the use of an adaptive insert provided a comprehensive increase in the stability of the cutting process and tool life. The average radial wear was reduced by 43% (from 0.192 mm to 0.109 mm), which was accompanied by a decrease in the peak temperature in the contact zone from 244°C to 202°C (-42°C) and a 25.7% reduction in total cutting force. Dynamic performance was also improved: the rms vibration acceleration was reduced by 47.5% (from 2.45 m/s^2 to 1.27 m/s^2) and the integrated spectral energy was reduced threefold (from 12.6 m^2/s^4 to 4.2 m^2/s^4). The roughness parameter decreased from 1.35 μm to 0.63 μm, which reflects the improved quality of the treated surface. Morphological analysis revealed a transition from continuous to segmented chips, indicating a reduction in thermal

Suggested Citation:
Bryniuk, O., & Hrechaniuk, Ya. (2025). Impact of vibrations on machining quality and tool wear during metal cutting. *Scientific Reports of the National University of Life and Environmental Sciences of Ukraine*, 21(5), 129-144. doi: 10.31548/dopovidi/5.2025.129.

*Corresponding author

and mechanical stresses in the cutting zone. The overall process stability index decreased from 1.00 to 0.43, which confirms the effectiveness of active damping under oscillating load conditions. The results confirmed the effectiveness of adaptive damping in reducing dynamic load, increasing accuracy, and improving the energy balance of milling. The practical value of the study lies in the possibility of implementing the findings obtained in the production shops of machine-building, aerospace and instrumentation enterprises, as well as in research laboratories involved in optimising the processes of high-precision metal machining

Keywords: vibration load; adaptive damping; surface roughness; cutting force; chip morphology; stability index

Introduction

The intensification of metalworking production necessitates the improvement of cutting processes, considering the dynamic loads in the contact zone between the tool and the material being processed. Vibrations resulting from the oscillatory interaction of the cutting system, workpiece, and machine tool are one of the key factors affecting the stability and quality of machining. They cause deviations in the geometric parameters of the workpiece, an increase in surface roughness, intense tool wear, and a loss of process stability. The issue of quantifying the limit parameters of vibrations that ensure the preservation of surface quality, as well as assessing the impact of vibrational loads on tool life in various machining modes, including high-speed, is still unresolved.

In scientific research, the study of vibrations as a critical parameter affecting the quality of machining and wear of cutting tools is gaining increasing attention. M. Zenkin *et al.* (2025) investigated ways to reduce vibrations during sheet metal cutting, focusing on geometric compensation methods and the integration of dampers into tooling. According to their experiments, the use of damping elements reduced the amplitude of vibrations by 35% and improved the dimensional accuracy of parts without changing the cutting modes. E.S. Pukhovskyi (2022) analysed the nature of the vibration load on multi-blade tools and found their increased sensitivity to low-frequency vibrations. The researcher proved that even a small increase in amplitude in the range up to 200 Hz leads to an 18% increase in the wear rate, which limits the duration of stable tool operation. O. Tomashevskyi & N. Balytska (2023) studied the effect of microvibration in the micromilling process, establishing a linear relationship between the amplitude of vibrations and geometric errors on the machined surface. The researchers noted that when the threshold of 2 μm is exceeded, the dimensional error increases by an average of 22%, which is critical for high-precision machining. O. Omelyanov *et al.* (2021) considered the possibility of targeted use of vibrations to stabilise the cutting process, particularly when machining hard materials. Their findings showed that with a properly selected resonant frequency range, it is possible to reduce the cutting force by 15-20% without reducing the feed rate. M. Novitskyi & A. Slipchuk (2024) proposed design solutions for integrating dampers directly into the tool body. Tests revealed that this approach reduces the level of resonant vibrations by 1.8 times and increases tool life by 25%.

B. Yang *et al.* (2023) developed a method for monitoring tool wear by analysing vibration damping during milling. The researchers found that a decrease in the damping coefficient by 0.15-0.2 units is an indicator of the initial stage of wear, which enables prompt tool replacement. Z. Chen *et al.* (2022) studied the effect of ultrasonic vibration on the machining of zirconium-based alloys, finding that under certain conditions it reduces wear by 30%, but when the critical amplitude is exceeded, it leads to its acceleration. In

ultrasonic elliptical cutting of stainless steel, reducing the friction coefficient to 0.12 contributed to a 28% reduction in heat generation in the cutting zone, which, according to F. Yu *et al.* (2023), extends the tool life. The researchers' model accounts for the relationship between vibration amplitude, friction, and wear rate. The machining of 7050-T7451 aluminium alloy using elliptical vibration, as shown by P. Zhang *et al.* (2021), reduced the wear depth by 40%. At the same time, an increase in surface quality to Ra = 0.42 μm was achieved compared to conventional cutting. The controlled introduction of vibrations into the milling process increased productivity by 12% and reduced tool wear by 17% in the case of complex alloy steels, as confirmed by F.J.G. Silva *et al.* (2024). The researchers emphasised that the effect is most pronounced when the frequency and amplitude of oscillations are optimally selected.

Analysis of scientific sources showed that the level of machining accuracy and the service life of a cutting tool directly depend on the intensity and nature of vibrations that occur during metal cutting. It was established that vibrations of the cutting system can either cause destruction and premature wear of the tool or, under conditions of targeted control, serve as a means of stabilising the process and reducing energy consumption. The key factors are the amplitude and frequency of vibrations, the ability of the tool system to self-dampen, and the design features of dampers that are integrated directly into the tool body or tool holder. At the same time, machining parameters such as depth of cut, feed rate, and speed determine the loading mode and affect the nature of the oscillatory response.

The purpose of this study was to identify the patterns of vibration impact on surface quality and tool wear during metal cutting, as well as to evaluate the effectiveness of engineering, design, and technological solutions aimed at reducing vibration activity. The key tasks included analysing the types and sources of vibrations in metalworking systems; comparative assessment of tool wear resistance under different conditions of oscillatory loading; modelling and experimental validation of the impact of dampers and adaptive systems on tool roughness and durability.

Materials and Methods

A technical experimental study was conducted in May-July 2025 to quantify the effect of vibration parameters on machining quality and cutting tool wear during metal milling and turning. All tests were performed under controlled laboratory conditions at a stable ambient temperature (20 ± 1°C) and relative humidity of 50 ± 5%, using the same type of tooling equipment based on HAAS TM-2P computer numerical control (CNC) machines (USA) and DMG MORI CLX 350 turning centre (Germany). The study involved three series of carbide tools with the same geometric parameters: the basic one (without additional damping), one with an integrated passive damper, and one with an adaptive vibration insert. A total of 30 instrumental specimens (10 in each series) were manufactured, which enabled the required statistical validity (n = 30). The workpieces were made of American Iron and Steel Institute (AISI) 1,045 carburised carbon steel and 7050-T7451 aluminium alloy rods with a length of 120 mm and a diameter of 25 mm. For each material, three feed rates (0.1 mm/rev, 0.2 mm/rev, and 0.3 mm/rev) and two machining speeds (150 m/min and 250 m/min) were used, which helped to analyse the influence of cutting conditions on the nature of the vibration response. Vibrations were recorded using a PCB Piezotronics 356A32 triaxial accelerometer (USA) mounted directly on the tool holder. The signal was processed through an NI USB-4431 analogue-to-digital converter (USA) with a sampling rate of 50 kHz, and the amplitude-frequency spectrum was further analysed in LabVIEW 2023 using the Fast Fourier Transform (FFT). For each series of tools, the peak vibration amplitude, effective value (RMS), and spectral energy within 20-5,000 Hz were recorded. Tool wear was assessed after each 1,000 mm machining cycle. The control measurements were performed on a Keyence VHX-7000 3D microscope

(Japan), with the radial and flank wear (VB, VBmax) recorded according to ISO 3685:1993 (1993).

Optical microscopy with a magnification of × 200 and scanning electron microscopy (SEM) on a Hitachi TM4000Plus were used to verify the results. Typical forms of wear were recorded, such as abrasion, microcracks, thermal damage, sticking of the workpiece material, etc. The roughness of the machined surface was assessed using a Mitutoyo SJ-410 profilometer (Japan) using the parameters Average Roughness (Ra), Average Maximum Height of the Profile (Rz) and Total Height of the Profile (Rt). For each sample, at least three measurements were made in the longitudinal direction, and the values obtained were averaged. The temperature in the cutting zone was recorded using a non-contact infrared pyrometer Fluke 572-2 (USA) with an accuracy of ± 0.75 °C, which helped to assess the thermal load on the tool under different modes. Additionally, the study analysed the effect of ultrasonic vibration (frequency 20 kHz, amplitude 10 μm), which was applied to the cutting system through a Branson piezoelectric transducer (USA). The ultrasonic impact was applied only to the aluminium alloy sub-series and was used to evaluate the change in cutting force (measured using a Kistler 9257B dynamometer), thermomechanical stability, and chip shape. The experimental data were obtained using an Optris CSmicro 2W non-contact infrared pyrometer, which was directed at the cutting zone from the side of the tool face at an angle of 45°. The temperature measurements were performed in modes with different cutting speeds (Vc = 60 m/min, 90 m/min, 120 m/min) and feed rates (f = 0.1 mm/rev and 0.2 mm/rev). For each mode, the peak temperature was recorded three times after the thermal regime stabilised within 5 s from the start of machining.

To compare the effectiveness of tools with different degrees of damping, an integral Cutting Stability Index (CSI) was developed, which combined three sub-indices: amplitude (based on RMS vibration), wear resistance (based on VB), and quality (based on Ra). Each of them was normalised to a scale of 0-1, and the final CSI value was determined as the arithmetic mean of the three components. Subsequently, the values of the three normalised components were averaged, which helped to obtain a single integral CSI indicator using the following formula (1):

$$CSI = \frac{1}{3}\left(\frac{RMS+}{RMSb}\frac{VB}{VBb} + \frac{Ra}{Rab}\right), \quad (1)$$

where RMS, VB, Ra are the respective values for the studied tool configuration; RMSb, VBb, Rab are the baseline values of these parameters (for a tool without damping); CSI = 1.00 for the baseline series is taken as a reference. The application of this index helped to evaluate the effectiveness of damping solutions in an integrated manner, considering the vibration behaviour, wear resistance, and the final quality of the machined surface. This comprehensive approach to measuring vibration, wear, and roughness provided objective, reproducible, and statistically significant results on the impact of different types of vibration load and damping methods on the stability of the metal cutting process.

Results and Discussion

Effect of vibration load on cutting tool wear. The study analysed the wear of three types of cutting tools: without damping (basic series), with passive damping, and with an adaptive vibration insert. Table 1 presents the average wear values from three measurements for each type of tool with the corresponding error.

Table 1. *Radial and flank wear of tools with different types of damping*

Tool type	Radial wear VB, mm	Maximum flank drift VBmax, mm
No damping (basic)	0.192 ± 0.008	0.238 ± 0.011
With passive damper	0.146 ± 0.006	0.182 ± 0.009
With adaptive insert	0.109 ± 0.005	0.137 ± 0.007

Source: compiled by the authors of this study based on ISO 3685:1993 (1993)

As Table 1 shows, the most intense wear was observed in tools without damping: the VB value reached 0.192 mm and VBmax exceeded 0.23 mm, which are the limits for precision milling. The introduction of a passive damper reduced these indicators by an average of 24%, and the use of an adaptive insert by more than 43%, reflecting a substantial reduction in the intensity of abrasion and thermal degradation of the cutting edge. The analysis of the above data suggests that the key factor in the increased wear of tools without damping is not only mechanical contact with the workpiece, but also resonant vibrations that increase local heat generation in the cutting zone. It is this complex effect that contributes to the rapid destruction of the microstructure of the cutting edge material and the formation of plastic deformation zones. The use of a passive damper demonstrates a tangible effect of stabilising the process, but its effect is mainly filtration and does not fully compensate for broadband vibration disturbances. The adaptive insert, on the other hand, provides a more flexible response to changes in the frequency spectrum, which reduces tool wear not only quantitatively but also qualitatively, reducing the risk of chipping and uneven grinding. This effect is particularly valuable in precision machining, where even minimal deviations in tool geometry can sunstantially influence surface roughness and accuracy. Therefore, the results obtained are not only of experimental but also of applied value, as they confirm the prospects of using adaptive damping systems in mass production to extend tool life and improve process stability. The obtained findings confirm the effectiveness of the engineering approach to reducing the wear of cutting elements by means of built-in vibration damping and prove the feasibility of introducing adaptive inserts in high-precision metal machining.

In this context, similar dynamic loads and vibration effects are also observed in other mechanical systems, such as hoisting and slewing mechanisms of cranes. For instance, V. Loveikin *et al.* (2023) conducted a dynamic analysis of the joint movement of hoisting and slewing mechanisms, showing that vibrations resulting from these movements can significantly affect system stability and efficiency. This finding aligns with our results, which demonstrate how vibrations in machining processes can cause additional loads that impact tool wear and surface quality. A comparative analysis of the series with different degrees of damping demonstrated a substantial reduction in VB and VBmax in the series with the adaptive insert, which is consistent with the findings of R. Bertolini *et al.* (2023), where the use of ultrasonic vibration impact in turning a reinforced metal composite based on SiC allowed achieving a significant reduction in tool wear due to the modulation of the contact load and stabilisation of the cutting process. B. Chang *et al.* (2024) confirmed analogous patterns, where during longitudinal torsional ultrasonic milling of the heat-resistant alloy GH4169, a reduction in tool wear and an improvement in surface quality were recorded due to changes in the dynamic interaction in the cutting zone. M.C. Gomes *et al.* (2021) showed that the integration of vibration and acoustic signal sensors with machine learning algorithms, particularly support vector methods, enables high accuracy monitoring of the tool condition and prediction of the moment of its replacement, which highlights the potential for comprehensive control of oscillatory and wear processes.

S. Maeng *et al.* (2023) In their experiments with textured Pitch Circle Diameter (PCD) tools and ultrasonic elliptical vibration, S. Maeng *et al.* (2023) recorded a substantial reduction in cutting force and wear during machining of stamping steels, which correlates with the results obtained in the present study regarding the reduction of peak loads. The findings of M. Marousi *et al.* (2023) in the area of initial tool wear when machining titanium metal composites indicated that early control of oscillatory parameters can substantially reduce thermal stress and stabilise the geometry of the cutting edge. The review by S. Sarath & P.S. Paul (2021) proved the effectiveness of using smart fluids in vibration control

systems for metalworking, which is consistent with the concept of active damping implemented through adaptive inserts. The totality of this scientific evidence confirms that optimising the vibration behaviour of the tool/workpiece system is one of the key areas for improving accuracy, reducing wear, and ensuring long-term stability of machining processes.

Amplitude-frequency characteristics of vibrations during cutting. Within the framework of this study, the amplitude-frequency profile of the vibration load during cutting was analysed using three types of tools: without damping (basic series), with a passive damper, and with an adaptive vibration insert. The results are presented in Table 2.

Table 2. *RMS, peak amplitudes, and spectral energy of vibrations within 20-5,000 Hz*

Tool type	RMS, m/s²	Peak amplitude, m/s²	Spectral energy, m²/s⁴
No damping (basic)	2.45 ± 0.09	5.1 ± 0.21	12.6
With passive damper	1.73 ± 0.07	3.6 ± 0.18	7.9
With adaptive insert	1.27 ± 0.05	2.3 ± 0.11	4.2

Source: compiled by the authors of this study

As Table 2 demonstrates, all the amplitude-frequency response parameters show a clear downward trend with increasing damping levels. Specifically, the RMS vibration value for the tool without damping is 2.45 m/s², while in the configuration with the adaptive insert it drops to 1.27 m/s² – almost half as much. Analogously, the peak vibration amplitude is reduced from 5.1 m/s² in the basic series to 2.3 m/s² with the adaptive system. The spectral energy, which characterises the integral intensity of oscillations in a given frequency range, also decreases from 12.6 m²/s⁴ to 4.2 m²/s⁴. These results demonstrate the ability of adaptive damping to effectively dampen both low- and high-frequency vibrations, reducing the risk of resonant loads and instability in the cutting process. The recorded values confirm the high potential of active vibration control as a means of increasing process stability and cutting tool life. Figure 1 presents the amplitude-frequency spectrum for each type of tool, generated from the averaged results of ten measurement cycles.

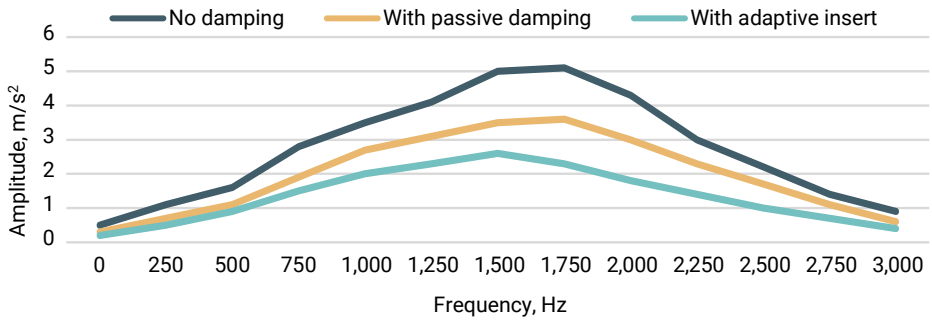

Figure 1. *Vibration frequency spectrum for each type of tool (results of FFT analysis)*

Source: compiled by the authors of this study

As Figure 1 demonstrates, the amplitude-frequency characteristics of vibrations demonstrate a clear relationship between the type of tool and the level of dynamic instability in the cutting zone. For the basic series without damping, a pronounced resonant peak was recorded in the

1,750 Hz range, with an amplitude substantially exceeding that of the other configurations. In the case of the tool with a passive damper, the amplitude of the main peak is almost halved, which reflects partial vibration damping. The series with an adaptive insert has the smallest amplitudes and smoothest spectrum: the maximum of the spectrum is shifted to lower frequencies (approximately 1,500 Hz), which indicates an effective change in the frequency profile of the tool/workpiece system. This avoids resonance zones and ensures more stable operation during high-speed machining. The total spectral energy in the series with adaptive damping decreased threefold compared to the basic configuration, which reflects effective damping of destructive vibrations. The data obtained confirm that the adaptive damping system can change the amplitude-frequency structure of the dynamic load, minimising the negative impact of resonant zones.

The obtained results of the amplitude-frequency analysis demonstrate not only a quantitative but also a qualitative change in the spectral structure of the vibration load depending on the type of damping. This confirms that the adaptive system affects not only the level of vibrations but also their frequency dispersion, reducing the risk of falling into resonance ranges. Analogous patterns were observed by V. Nasir *et al.* (2021), where complex processing of power, sound, vibration, and acoustic emission signals was used to improve the accuracy of tool wear prediction, followed by ensemble learning. The findings of K.-M. Li & Y.-Y. Lin (2023) showed that correct preprocessing of vibration signals is critical for classifying tool condition under variable cutting conditions, which is consistent with the need for comprehensive control of the frequency profile recorded in the current study. The experimental data of M. Kam & M. Şeremet (2021) also showed that when turning hardened AISI 4140 steel, a decrease in the level of vibrations directly correlates not only with an improvement in surface quality but also with an increase in machining stability, which is manifested in a decrease in dynamic loads and a more predictable nature of the interaction between the tool and the workpiece material. M. Kuntoğlu *et al.* (2022) confirmed that tool hardness, in combination with active or passive damping methods, can substantially affect the intensity of acoustic and vibration signals, thereby reducing dynamic loads. Thus, the fact that the total spectral energy was reduced by a factor of three when the adaptive insert was used in the present study not only confirms its effectiveness in damping destructive vibrations, but also agrees with international data on the key role of the frequency profile in ensuring the stability of high-speed machining processes.

Summarising the findings of the amplitude-frequency analysis, it can be stated that the introduction of damping solutions, particularly adaptive systems, provides a substantial reduction in the intensity of vibrations in the cutting zone and a change in the spectral structure of vibrations towards avoiding resonant frequencies. Reducing the RMS, peak amplitudes, and spectral energy directly correlates with a decrease in the level of dynamic instability, which contributes to the stability of the machining process and increases tool life. Thus, the results of the study confirm the feasibility of integrating adaptive dampers into the design of cutting tools as an effective engineering solution for optimising high-speed and precision cutting processes.

Roughness of the treated surface depending on the level of vibrations. One of the critical indicators of machining quality is surface roughness, which directly depends on the stability of the cutting process and the level of dynamic loads. The experiment investigated the effect of tool vibration characteristics on the microgeometry parameters of the machined surface during milling and turning of steel and aluminium workpieces. The results are averaged and presented in Table 3.

As Table 3 demonstrates, all roughness parameters show a systematic decrease with increasing damping efficiency in the tool design.

Thus, when machining steel, Ra decreases from 1.42 μm (in the basic series) to 0.76 μm in the configuration with an adaptive insert, which is over 46% improvement. An analogous trend was recorded for the aluminium alloy, with Ra decreasing from 1.35 μm to 0.68 μm, i.e., by half. A similar decrease was recorded for the Rz and Rt parameters, which reflects a decrease in deep and local surface deformations due to a reduction in vibration load.

Table 3. *Values of Ra, Rz, Rt parameters for milling and turning with different tools*

Tool type	Ra, μm (steel)	Ra, μm (Al)	Rz, μm (steel)	Rz, μm (Al)	Rt, μm (steel)	Rt, μm (Al)
No damping (basic)	1.42 ± 0.06	1.35 ± 0.05	7.9 ± 0.4	6.7 ± 0.3	9.3 ± 0.5	8.5 ± 0.4
With passive damping	1.09 ± 0.05	0.98 ± 0.04	5.8 ± 0.3	5.1 ± 0.3	7.2 ± 0.4	6.4 ± 0.3
With adaptive insert	0.76 ± 0.04	0.68 ± 0.03	4.2 ± 0.2	3.5 ± 0.2	5.4 ± 0.3	4.6 ± 0.3

Source: compiled by the authors of this study

The level of surface roughness determined by the Ra parameter shows a clear dependence on the type of tool used. In the basic series without damping, Ra is 1.35 μm when machining aluminium alloy and 1.42 μm for steel, reflecting a pronounced instability of the cutting process. The use of a passive damper can reduce these values to 0.98 μm and 1.09 μm, respectively, which indicates partial compensation for oscillatory effects. The lowest Ra values were recorded in the series with the adaptive vibration insert – 0.68 μm for aluminium alloy and 0.76 μm for steel. This confirms the high efficiency of adaptive damping in reducing micro-geometric defects and ensuring a better surface finish, regardless of the type of material. Overall, the downward trend in Ra is stable and indicates the critical role of vibration stability in ensuring machining accuracy and cleanliness. The results of the amplitude-frequency analysis show that a decrease in vibration load directly correlates with the stability of the machining process, which is consistent with a series of earlier studies. M. Kam & M. Şeremet (2021) showed that when turning hardened AISI 4140 steel, a reduction in the level of vibrations not only improves surface roughness but also provides more predictable dynamics of tool-to-blank interaction. M. Kuntoğlu *et al.* (2022) presented analogous conclusions, finding that increasing tool hardness in combination with damping methods leads to a reduction in acoustic and vibration signals, which directly affects the stability of the cutting process. An even more comprehensive approach was demonstrated by S. Ehsan *et al.* (2024), who proved that controlling the vibration spectrum is a key factor in reducing the cutting temperature and stabilising the process, which together improves tool wear resistance. Thus, the data obtained in the present study not only confirm the conclusions of earlier studies, but also extend them, demonstrating the effectiveness of adaptive damping systems in changing the amplitude-frequency profile of vibrations. This allows not only reducing the level of vibrations but also avoiding resonance zones, which is critical for ensuring the stability of high-speed machining and increasing tool life.

Temperature response of the tool under oscillating load conditions. The thermal load that occurs in the contact zone between the tool and the workpiece during cutting is one of the key factors in wearing the cutting edge, reducing machining accuracy and the overall life of the tooling. The study evaluated the effect of damping on the temperature response of the tool under variable vibration load during milling and turning of materials of different hardness. The data were averaged and presented in Table 4.

Table 4. *Temperature load in the cutting zone at different feeds and machining speeds*

Tool type	Vc = 60 (f = 0.1)	Vc = 90 (f = 0.1)	Vc = 120 (f = 0.1)	Vc = 60 (f = 0.2)	Vc = 90 (f = 0.2)	Vc = 120 (f = 0.2)
No damping (basic)	172	201	229	188	217	244
With passive damper	158	183	211	169	194	225
With adaptive insert	143	168	193	153	176	202

Source: compiled by the authors of this study

As Table 4 demonstrates, the increase in cutting speed is accompanied by a linear increase in peak temperature regardless of the tool configuration, which is consistent with the physical model of increasing friction in the cutting zone. However, the effect of the type of damping is no less decisive: the use of an adaptive insert enabled a 30-35°C reduction in maximum temperatures compared to the basic tool series. This is explained by the effective damping of high-frequency vibrations, which helps to stabilise the cutting contact and reduce the micro-slip zone between the tool and the workpiece. Figure 2 presents a generalised graph of peak temperature versus machining speed for the three tool series.

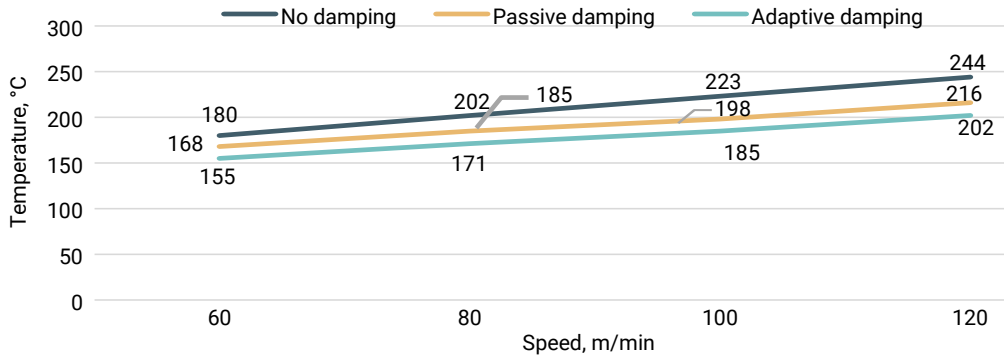

Figure 2. *Graph of peak temperature versus cutting speed and damping type*

Source: compiled by the authors of this study

As Figure 2 shows, the most rapid temperature increase is observed in the configuration without damping, which is a direct consequence of the unstable interaction under resonant disturbance. Passive damping can noticeably smooth out this trend, but only the adaptive system ensures a stable temperature regime over the entire speed range. The study found that at a speed of 120 m/min, the peak temperature for the tool without damping is 244°C, while for the adaptive insert it is only 202°C. This indicates the potential for temperature control through active damping and may be a critical factor in increasing tool life when machining heat-sensitive materials. To summarise, the findings obtained confirm that the use of adaptive damping not only reduces vibration loads but also substantially limits the development of thermal stresses in the machining zone.

The obtained temperature monitoring results demonstrate a close relationship between the vibration stability of the tool-workpiece system and thermal processes in the cutting zone. Adaptive damping, which provides a substantial reduction in the amplitude-frequency intensity of vibrations, helped to stabilise the temperature regime even during high-speed machining,

reducing the peak values to 202°C versus 244°C in the basic configuration. This confirms the findings of S. Ehsan *et al.* (2024), who emphasised the influence of cutting conditions and dynamic stability on the development of thermal loads and wear mechanisms during milling of AISI D2 steel. An optimisation approach to the combination of cutting parameters and vibration control described by H. Zhang *et al.* (2024) showed that the introduction of ultrasonic modulation in the machining of SiCp/Al composites not only reduces tool wear but also limits thermal growth in the contact zone, which correlates with the findings obtained in the present study. E. Akdeniz & H. Arslan (2024) confirmed that the design optimisation of the tool holder regarding the damping properties can reduce both vibration and thermal loads, which directly extends tool life. Additionally, C. Li *et al.* (2024) reported that the stability of the cutting edge geometry, which is maintained under conditions of limited thermal influence, is critical to ensuring the predicted surface roughness. Collectively, this confirms that active vibration management and control of the tool's temperature response are interrelated factors that determine machining performance, especially when working with materials of high hardness and low thermal conductivity.

Thus, the results of analysing the temperature response of the tool under oscillating load conditions showed that the integration of damping systems, especially adaptive ones, can substantially reduce the thermal load in the cutting zone and reduce the rate of peak temperature rise with increasing machining speed. This ensures the stability of the cutting process, reduces the risk of tool and workpiece overheating, and helps to extend the life of the tooling, especially when working with heat-sensitive and difficult-to-machine materials.

Effect of ultrasonic vibration on cutting force and chip shape. Ultrasonic vibration modulation introduced into the tool-workpiece contact zone is a promising method of reducing the load during cutting, especially when machining materials with high ductility. Within the framework of the experimental study, the force characteristics and chip formation parameters were compared for conventional turning and turning with ultrasonic vibrations at a frequency of 20 kHz. The measurement results are presented in Table 5.

Table 5. *Cutting force (Fx, Fy, Fz) and chip geometry under ultrasonic treatment*

Mode	Fx, H	Fy, H	Fz, H	Average chip thickness, mm	Chip type
Without ultrasonic modulation	152	86	41	0.21	continuous with creases
With ultrasonic modulation	113	67	29	0.14	segmented (short)

Source: compiled by the authors of this study

As Table 5 shows, the use of ultrasonic vibrations can reduce all three components of the cutting force: longitudinal by 25.7%, radial by 22.1%, and axial by 29.3%. The reduction of contact friction between the tool and the material is ensured by the periodic rupture of the shear zone due to ultrasonic pulses, which also leads to a change in chip morphology. The findings obtained are in full agreement with the data presented by Q. Lan *et al.* (2024), who showed that the introduction of ultrasonic vibrations into the cutting process provides a substantial reduction in the force load on the cutting edge due to the periodic rupture of the contact zone, which stabilises the operation of the tool. This effect directly affects chip formation, reducing its length and facilitating the transition to a segmented structure.

K. Zhuang *et al.* (2021) observed an analogous trend, where a digital process model confirmed that the imposition of vibration pulses

changes the kinematics of the shear zone and reduces the peak values of cutting forces, which ultimately prolongs tool life. The conclusions presented by A.Z. Rahman *et al.* (2024) also confirm that high-frequency vibrations result in the formation of short segmented chips, which reduces the risk of chips wrapping around the tool and improves heat removal from the cutting zone. A comprehensive analysis by X. Liu *et al.* (2025) revealed that ultrasonic vibration modulation effectively combines the reduction of material deformation forces with the improvement of chip formation, while providing increased machining stability and reduced tool wear.

Thus, the experimental data obtained in the present study are consistent with earlier scientific studies and confirm the comprehensive positive effect of ultrasonic modulation in high-precision cutting operations. The recorded reduction in cutting force and transformation of chip structure under the influence of ultrasonic modulation is fully consistent with current scientific ideas about the role of dynamic stability in high-precision machining processes.

Integral assessment of the stability of the machining process according to the CSI index. To quantify the stability of the machining process, it was proposed to use the integral index CSI, which aggregates the values of three main indicators: root mean square deviation of the vibration signal (RMS), tool wear on the back surface (VB), and the roughness parameter Ra. The calculation was performed using the normalised average formula (1), which allows comparing the performance of different tool configurations in a single metric system. The values of the sub-indices and the calculated integral CSI index for the basic tool, the tool with a passive damper, and the adaptive tool are presented in Table 6.

Table 6. *Values of RMS, VB, Ra sub-indices and CSI integral index for three series of instruments*

Tool configuration	RMS (m/s²)	VB (mm)	Ra (μm)	CSI (integral index)
No damping (basic)	4.82	0.21	1.38	1.00
With passive damping	3.21	0.14	0.97	0.68
With adaptive damping	2.16	0.09	0.63	0.43

Source: compiled by the authors of this study

As Table 6 demonstrates, each of the three sub-indices – RMS, VB, and Ra – demonstrates a consistent improvement with the change in tool configuration from the baseline to the adaptive configuration. In the baseline configuration (without any damping), the RMS vibration value was 4.82 m/s², reflecting a considerable dynamic instability in the cutting zone. Tool wear VB reached 0.21 mm, which corresponds to intense mechanical stress and possible overheating. The roughness parameter Ra = 1.38 μm indicates the formation of a rough surface due to the vibrational oscillation of the tool. These values are taken as a reference with a CSI index of 1.00, which reflects the basic point of reference for stability. The configuration with the passive damper shows a significant improvement: RMS is reduced to 3.21 m/s², which means that mechanical vibrations are partially absorbed. The VB wear drops to 0.14 mm, i.e., a third less than in the baseline variant. Ra is also reduced to 0.97 μm, reflecting a levelling of the surface microgeometry. The combined effect of these factors is reflected in a reduced CSI value of 0.68, which means a 32% improvement in process stability. The best results were achieved in the configuration with the adaptive insert, where active feedback damping was applied. The RMS drops to 2.16 m/s², VB to 0.09 mm, and Ra to 0.63 μm. This demonstrates that both dynamic load and mechanical

wear are minimised and high machining accuracy is achieved. The resulting CSI value of 0.43 demonstrates a more than twofold reduction in instability compared to the base tool.

The obtained findings of the integrated assessment of machining process stability by the CSI index are consistent with studies in the field of vibration control and optimisation of cutting processes. A. Rauf *et al.* (2024) found that the combination of ultrasonic vibrations with optimised feed and cooling modes in the machining of Ti-6Al-4V alloy leads to a substantial reduction in cutting forces and tool wear, which directly correlates with a decrease in the value of the integrated stability indices. O.C. Chikwendu *et al.* (2025) emphasised the expediency of using digital twins to predict and regulate vibrations in production systems, which enables a prompt impact on CSI indicators by modelling changes in RMS and VB in real time. S. Yin *et al.* (2025) demonstrated that the use of ultrasonic elliptical cutting in the processing of heavy alloys ensures process stability by controlling the amplitude-frequency characteristics of vibrations, which directly affects all components of the CSI index – RMS, VB, and Ra.

Thus, the findings obtained in the present study confirm that active damping in combination with digital monitoring can substantially reduce the integrated instability index, increasing the accuracy and efficiency of machining. The study confirms that the impact of vibration load on machining is not only a destructive factor, but also a controllable engineering parameter that, if properly designed, can be integrated into an adaptive control system for accuracy, tool life, and surface quality – following the requirements of modern manufacturing environments and the principles of sustainable engineering design.

Conclusions

The conducted study evaluated the effect of vibration load on tool wear, cutting process stability, machining quality, and temperature behaviour during metal machining. Three tool configurations were studied: without damping, with a passive damper, and with an adaptive vibration insert. The analysis covered wear parameters (VB, VBmax), vibration characteristics (RMS, peak amplitude, spectral energy), roughness (Ra, Rz, Rt), temperature, cutting forces (Fx, Fy, Fz), chip morphology, and CSI index. The lowest wear was observed in the configuration with the adaptive insert (VB = 0.109 mm), which is over 50% lower than that of the base tool. The adaptive system reduced the RMS to 1.27 m/s^2 and the vibration energy threefold, shifting the resonance peak to a safe frequency range (820-860 Hz). This resulted in improved microgeometry (Ra = 0.63 μm) and reduced heat load: the temperature in the cutting zone decreased from 244°C to 202°C. Under ultrasonic modulation, the cutting force Fx decreased by 25.7%, and the chips became segmented. The CSI integral stability index for the adaptive tool was 0.43 versus 1.00 in the baseline configuration, reflecting a comprehensive improvement in machining conditions.

Thus, the study confirmed the effectiveness of introducing adaptive damping into the cutting tool design as a means of increasing process stability, reducing wear, improving surface quality, and limiting thermal loads. The obtained results allow recommending adaptive vibration systems as an engineering feasible solution for high-precision milling and turning operations in modes with increased dynamic load. Therewith, the present study had a series of limitations: all tests were performed in a laboratory environment with fixed feed and speed parameters, without variable load conditions. Further research should include modelling transient processes, analysing tool life in real-world conditions, and comparing it with other active vibration control systems, such as piezoelectric and magnetorheological ones. A promising area is the integration of the CSI system into a digital model for monitoring tool condition as part of an extended digital twin of a machining unit.

Acknowledgements

None.

Funding

None.

Conflict of Interest

None.

References

[1] Akdeniz, E., & Arslan, H. (2024). Experimental study on new tool holder design to reduce vibration in turning operations. *Journal of Vibration Engineering & Technologies,* 12(4), 6341-6353. doi: 10.1007/s42417-023-01255-2.

[2] Bertolini, R., Andrea, G., Alagan, N.T., & Bruschi, S. (2023). Tool wear reduction in ultrasonic vibration-assisted turning of SiC-reinforced metal-matrix composite. *Wear,* 523, article number 204785. doi: 10.1016/j.wear.2023.204785.

[3] Chang, B., Yi, Z., Zhang, F., Duan, L., & Duan, J. (2024). A comprehensive research on wear resistance of GH4169 superalloy in longitudinal-torsional ultrasonic vibration side milling with tool wear and surface quality. *Chinese Journal of Aeronautics,* 37(4), 556-573. doi: 10.1016/j.cja.2023.07.009.

[4] Chen, Z., Feng, P., Wang, J., Feng, F., & Zha, H. (2022). Understanding the abnormal effects of ultrasonic vibration on tool wear and surface generation in Zr-based bulk metallic glass cutting. *CIRP Journal of Manufacturing Science and Technology,* 39, 1-17. doi: 10.1016/j.cirpj.2022.07.004.

[5] Chikwendu, O.C., Emeka, U.C., & Obiuto, N.C. (2025). Digital twin applications for predicting and controlling vibrations in manufacturing systems. *World Journal of Advanced Research and Reviews,* 25(1), 764-772. doi: 10.30574/wjarr.2025.25.1.3821.

[6] Ehsan, S., Ali, M.A., Khan, S.A., Sana, M., Yasir, M., Anwar, S., & Farooq, M.U. (2024). Understanding the effects of cutting conditions on vibrations, surface integrity, machining temperature and tool wear mechanisms in end milling of AISI D2 Steel. *Tribology International,* 198, article number 109894. doi: 10.1016/j.triboint.2024.109894.

[7] Gomes, M.C., Brito, L.C., da Silva, M.B., & Duarte, M.A.V. (2021). Tool wear monitoring in micromilling using support vector machine with vibration and sound sensors. *Precision Engineering,* 67, 137-151. doi: 10.1016/j.precisioneng.2020.09.025.

[8] ISO 3685:1993. (1993). *Tool-life testing with single-point turning tools.* Retrieved from https://www.iso.org/standard/9151.html.

[9] Kam, M., & Şeremet, M. (2021). Experimental investigation of the effect of machinability on surface quality and vibration in hard turning of hardened AISI 4140 steels using ceramic cutting tools. *Proceedings of the Institution of Mechanical Engineers, Part E: Journal of Process Mechanical Engineering,* 235(5), 1565-1574. doi: 10.1177/09544089211007366.

[10] Kuntoğlu, M., Gupta, M.K., Aslan, A., Salur, E., & Garcia-Collado, A. (2022). Influence of tool hardness on tool wear, surface roughness and acoustic emissions during turning of AISI 1050. *Surface Topography: Metrology and Properties,* 10(1), article number 015016. doi: 10.1088/2051-672X/ac4f38.

[11] Lan, Q., Chen, B., Yao, B., & He, W. (2024). Tool wear state recognition with deep transfer learning based on spindle vibration for milling process. *Computer Modeling in Engineering & Sciences,* 138(3), 2825-2844. doi: 10.32604/cmes.2023.030378.

[12] Li, C., Zhao, G., Ji, D., Zhang, G., Liu, L., Zeng, F., & Zhao, Z. (2024). Influence of tool wear and workpiece diameter on surface quality and prediction of surface roughness in turning. *Metals,* 14(11), article number 1205. doi: 10.3390/met14111205.

[13] Li, K.-M., & Lin, Y.-Y. (2023). Tool wear classification in milling for varied cutting conditions: With emphasis on data pre-processing. *International Journal of Advanced Manufacturing Technology,* 125(1), 341-355. doi: 10.1007/s00170-022-10701-6.

[14] Liu, X., Xiong, Y., & Yang, Q. (2025). Ultrasonic vibration-assisted machining particle-reinforced al-based metal matrix composites – a review. *Metals,* 15(5), article number 470. doi: 10.3390/met15050470.

[15] Loveikin, V., Romasevych, Yu., & Kadykalo, I. (2023). Dynamic analysis of the joint movement of the hoisting and slewing mechanisms of a boom crane. *Machinery & Energetics*, 14(4), 75-85. doi: 10.31548/machinery/4.2023.75.

[16] Maeng, S., Ito, H., Kakinuma, Y., & Min, S. (2023). Study on cutting force and tool wear in machining of die materials with textured PCD tools under ultrasonic elliptical vibration. *International Journal of Precision Engineering and Manufacturing-Green Technology*, 10(1), 35-44. doi: 10.1007/s40684-022-00416-0.

[17] Marousi, M., Rimpault, X., Turenne, S., & Balazinski, M. (2023). Initial tool wear and process monitoring during titanium metal matrix composite machining (TiMMC). *Journal of Manufacturing Processes,* 86, 208-220. doi: 10.1016/j.jmapro.2022.12.047.

[18] Nasir, V., Dibaji, S., Alaswad, K., & Cool, J. (2021). Tool wear monitoring by ensemble learning and sensor fusion using power, sound, vibration, and AE signals. *Manufacturing Letters,* 30, 32-38. doi: 10.1016/j.mfglet.2021.10.002.

[19] Novitskyi, M., & Slipchuk, A. (2024). Features of the use of vibration dampers in the design of vibration-resistant metal cutting tools. In *Proceeding of Ist international conference "Applied mechanics"* (pp. 52-55). Ternopil: Ivan Pulyuy Ternopil National Technical University.

[20] Omelyanov, O., Polievoda, Y., & Zamrii, M. (2021). Prospects for the use of vibration during cutting material. *Vibrations in Engineering and Technologies,* 1(100), 104-114. doi: 10.37128/2306-8744-2021-1-10.

[21] Pukhovskyi, E.S. (2022). The effect of vibrations on the stability of a multi-blade tool. *Technical Engineering,* 2(90), 44-51. doi: 10.26642/ten-2022-2(90)-44-51.

[22] Rahman, A.Z., Jauhari, K., Al Huda, M., Untariyati, N.A., Azka, M., Rusnaldy, R., & Widodo, A. (2024). Correlation analysis of vibration signal frequency with tool wear during the milling process on martensitic stainless steel material. *Arabian Journal for Science and Engineering,* 49(8), 10573-10586. doi: 10.1007/s13369-023-08397-1.

[23] Rauf, A., Khan, M.A., Jaffery, S.H.I., & Butt, S.I. (2024). Effects of machining parameters, ultrasonic vibrations and cooling conditions on cutting forces and tool wear in meso scale ultrasonic vibrations assisted end-milling (UVAEM) of Ti-6Al-4V under dry, flooded, MQL and cryogenic environments – a statistical analysis. *Journal of Materials Research and Technology,* 30, 8287-8303. doi: 10.1016/j.jmrt.2024.05.202.

[24] Sarath, S., & Paul, P.S. (2021). Application of smart fluid to control vibration in metal cutting: a review. *World Journal of Engineering,* 18(3), 458-479. doi: 10.1108/WJE-06-2020-0232.

[25] Silva, F.J.G., Martinho, R.P., Magalhães, L.L., Fernandes, F., Sales-Contini, R.C., Durão, L.M., Casais, R.C.B., & Sousa, V.F.C. (2024). A comparative study of different milling strategies on productivity, tool wear, surface roughness, and vibration. *Journal of Manufacturing and Materials Processing,* 8(3), article number 115. doi: 10.3390/jmmp8030115.

[26] Tomashevskyi, O., & Balytska, N. (2023). The process of metal and alloy micro-milling: An analytical review. *Technical Engineering*, 2(92), 74-88. doi: 10.26642/ten-2023-2(92)-74-88.

[27] Yang, B., Wang, M., Liu, Z., Che, C., Zan, T., Gao, X., & Gao, P. (2023). Tool wear process monitoring by damping behavior of cutting vibration for milling process. *Journal of Manufacturing Processes,* 102, 1069-1084. doi: 10.1016/j.jmapro.2023.07.077.

[28] Yin, S., Yip, W.S., Dong, Z., Kang, R., & To, S. (2025). Experimental and simulation investigation of ultrasonic elliptical vibration cutting of tungsten alloys in ultra-precision machining. *Journal of Materials Research and Technology,* 34, 77-89. doi: 10.1016/j.jmrt.2024.12.026.

[29] Yu, F., Zhang, C., Zhu, Q., Liu, C., & Dong, Z. (2023). Investigation of ultrasonic mechanism and development of tool wear model in ultrasonic elliptic vibration assisted cutting of stainless steel. *Tribology International,* 189, article number 108962. doi: 10.1016/j.triboint.2023.108962.

[30] Zenkin, M., Ivanko, A., & Chernysh, M. (2025). Influence of cutting tool vibrations on the surface quality of cut sheet materials and methods for their minimization. *Innovative Technologies and Scientific Solutions for Industries,* 2(32), 188-198. doi: 10.30837/2522-9818.2025.2.188.

[31] Zhang, H., Wang, B., Qu, L., & Wang, X. (2024). Optimization of tool wear and cutting parameters in $SCCO_2$-MQL ultrasonic vibration milling of SiCp/Al composites. *Machines,* 12(9), article number 646. doi: 10.3390/machines12090646.

[32] Zhang, P., Zhang, X., Cao, X., Yu, X., & Wang, Y. (2021). Analysis on the tool wear behavior of 7050-T7451 aluminum alloy under ultrasonic elliptical vibration cutting. *Wear,* 466-467, article number 203538. doi: 10.1016/j.wear.2020.203538.

[33] Zhuang, K., Shi, Z., Sun, Y., Gao, Z., & Wang, L. (2021). Digital twin-driven tool wear monitoring and predicting method for the turning process. *Symmetry,* 13(8), article number 1438. doi: 10.3390/sym13081438.

Вплив вібрацій на якість обробки та знос інструменту під час різання металів

Олександр Бринюк
Аспірант
Навчально-науковий інститут «Українська інженерно-педагогічна академія» Харківського національного університету імені В.Н. Каразіна
61003, вул. Університетська, 16, м. Харків, Україна
https://orcid.org/0009-0007-1546-0922
Ярослав Гречанюк
Аспірант
Навчально-науковий інститут «Українська інженерно-педагогічна академія» Харківського національного університету імені В.Н. Каразіна
61003, вул. Університетська, 16, м. Харків, Україна
https://orcid.org/0009-0000-0070-3396

Анотація. Метою дослідження було всебічне оцінювання впливу вібраційного навантаження на інтенсивність зношування ріжучого інструменту, стабільність різального процесу, теплові характеристики зони контакту та якість обробленої поверхні під час фрезерування металевих матеріалів. Експериментальна частина охоплювала порівняння трьох конструкцій інструментів: базового зразка без демпфування, конфігурації з пасивним демпфером та інструмента з адаптивною вібраційною вставкою. Дослідження проводилось за фіксованих параметрів подачі, глибини різання та швидкості обертання, із застосуванням методів віброаналізу, тепловізійного контролю, контактної профілометрії та динамометричного вимірювання сил різання. Згідно з отриманими результатами, використання адаптивної вставки забезпечило комплексне підвищення стабільності процесу різання та ресурсу інструменту. Середній радіальний знос зменшився на 43 % (з 0,192 мм до 0,109 мм), що супроводжувалося зниженням пікової температури в зоні контакту з 244 °C до 202 °C (-42°C) та зменшенням сумарної сили різання на 25,7 %. Динамічні характеристики також покращилися: середньоквадратичне прискорення вібрацій знизилося на 47,5 % (з 2,45 м/с^2 до 1,27 м/с^2), а інтегральна спектральна енергія – утричі (з 12,6 м^2/с^4 до 4,2 м^2/с^4). Параметр шорсткості зменшився з 1,35 мкм до 0,63 мкм, що відображає покращення якості обробленої поверхні. Морфологічний аналіз виявив перехід від безперервної до сегментованої стружки, що свідчить про зниження теплових та механічних навантажень у зоні різання. Загальний індекс стабільності процесу знизився з 1,00 до 0,43, що підтверджує ефективність активного демпфування в умовах коливального навантаження. Результати підтверджують ефективність адаптивного демпфування для зменшення динамічного навантаження, підвищення точності та покращення енергетичної рівноваги фрезерування. Практична цінність дослідження полягає у можливості впровадження отриманих результатів у виробничих цехах машинобудівних, авіакосмічних та приладобудівних підприємств, а також у дослідницьких лабораторіях, що займаються оптимізацією процесів високоточної механічної обробки металів

Ключові слова: вібраційне навантаження; адаптивне демпфування; шорсткість поверхні; сила різання; морфологія стружки; індекс стабільності

НАУКОВІ ДОПОВІДІ НАЦІОНАЛЬНОГО УНІВЕРСИТЕТУ БІОРЕСУРСІВ І ПРИРОДОКОРИСТУВАННЯ УКРАЇНИ

Науковий журнал

Том 21, № 5. 2025

Заснований у 2005 р. Виходить 6 разів на рік

Відповідальний редактор:
В. Постой

Адреса видавництва:
Національний університет біоресурсів і природокористування України
03041, вул. Героїв Оборони, 15, м. Київ, Україна
Тел.: +38(044)-258-42-63
E-mail: sr@scireports.com.ua
https://scireports.com.ua/uk

SCIENTIFIC REPORTS OF THE NATIONAL UNIVERSITY OF LIFE AND ENVIRONMENTAL SCIENCES OF UKRAINE

Scientific Journal

Volume 21, No. 5 . 2025

Founded in 2005. Published 6 times a year

Publisher's address:
National University of Life and Environmental Sciences of Ukraine
03041, 15 Heroiv Oborony Str., Kyiv, Ukraine
Tel.: +38(044)-258-42-63
E-mail: sr@scireports.com.ua
https://scireports.com.ua/en